Understanding Tamoxifen Resistance In Breast cancer

by

Raie Taye Bekele

A thesis submitted in partial fulfillment of the requirements for the degree of

Doctor of Philosophy

Department of Biochemistry
University of Alberta

ABSTRACT

Tamoxifen is the accepted therapy for patients with estrogen receptor α (ERα)–positive breast cancer. However, clinical resistance to tamoxifen, as demonstrated by recurrence or progression on therapy, is frequent and precedes death from metastases. To improve breast cancer treatment it is vital to understand the mechanisms that result in tamoxifen resistance. The study presented in this thesis shows that concentration of tamoxifen and its metabolites, which accumulate in tumors of patients, killed breast cancer cells by inducing oxidative stress. Breast cancer cells responded to tamoxifen-induced oxidation by increasing Nrf2 expression and subsequent activation of the anti-oxidant response element (ARE). This increased the transcription of anti-oxidant genes and multidrug resistance transporters. As a result, breast cancer cells are able to destroy or export toxic oxidation products leading to increased survival from tamoxifen-induced oxidative damage. These responses in cancer cells also occur in breast tumors of tamoxifen-treated mice. Additionally, high levels of expression of Nrf2 and its downstream targets in breast tumors of patients at the time of diagnosis were prognostic of poor survival after tamoxifen therapy.

The oxidative stress induced by tamoxifen also activated phospholipase D (PLD) and led to the up regulation of the RALBP1 (Ral-binding protein 1). Tamoxifen resistant cells also had a significant increase in both basal and stimulated PLD activity along with increased PLD1 and RALBP1 levels. The activity of PLD provides survival signals to cancer cells, whereas RALBP1

exports chemotherapeutic drugs. Thus both RALBP1 and PLD in concert can lead to development of an aggressive and metastatic breast cancers and also contribute to chemo-resistance.

In our study, cancerous breast tissues from patients have a significantly higher expression of RALBP1 compared to normal breast tissue. Furthermore, cytotoxic chemotherapy combination offered no significant advantage in patient cohorts with high RALBP1 expression as compared to those patients receiving mono or non-cytotoxic chemotherapies. Moreover, patients with high expression of PLD1 also had poor prognostic outcomes to different treatments.

Thus, overcoming adaptive responses to tamoxifen-induced oxidative stress could improve the survival of breast cancer patients.

PREFACE

This thesis is an original work by Raie T. Bekele. Animal procedures were performed in accordance with the Canadian Council of Animal Care as approved by the University of Alberta Animal Welfare Committee (Animal User Protocol 226). Human Breast tumors from patients along with the complete long-term follow up on each of these patients were obtained through Canadian Breast Cancer Foundation Tumor Bank (Edmonton, AB, Canada) with approval from the Health Research Ethics Board of Alberta: Cancer Committee (ID 26195).

All the experimental work in this thesis was designed and conceived by my self under the guidance and mentorship of my supervisor David Brindley. My colleagues, Ganesh Venkatraman, Matthew Benesch, Xiaoyun Tang, Si Mi, Rong-Zong Liu assisted in conducting portions of the experimental procedures and their specific contribution is cited in the appropriate method section. Jay Dewald provided technical help necessary for conducting experiments. Todd. McMullen and John Mackey helped with interpretation of the clinical results. Roseline Godbout helped facilitate the patient prognostic analysis and Jonathan Curtis facilitated mass spectrometric analysis.

Sections of the thesis are partly based on my previously published works:

Bekele RT, Venkatraman G, Liu R, Tang X, Mi S, Benesch MG, Mackey JR, Godbout R, Curtis JM, McMullen TP, Brindley DN. Oxidative stress contributes to the tamoxifen-induced killing of breast cancer cells: implications for tamoxifen therapy and resistance. Nature Sci. Rep. 6, 21164; doi: 10.1038/srep21164 (2016).

Benesch MG, Tang X, Venkatraman G, **Bekele RT**, Brindley DN. Recent advances in targeting the autotaxin-lysophosphatidate-lipid phosphate phosphatase axis in vivo. J Biomed Res. 2015 Aug 28;30. doi: 10.7555/JBR.29.20150058.

Bekele RT, Brindley DN: Role of autotaxin and lysophosphatidate in cancer progression and resistance to chemotherapy and radiotherapy. Clinical Lipidology 7(3), 313-328 (2012). doi:10.2217/clp.12.30

Samadi N, **Bekele RT**, Goping IS, Schang LM, Brindley DN: Lysophosphatidate induces chemo-resistance by releasing breast cancer cells from taxol-induced mitotic arrest. PLoS One 6(5), e20608 (2011). doi: 10.1371/journal.pone.0020608.

Samadi N, **Bekele RT**, Capatos D, Venkatraman G, Sariahmetoglu M, Brindley DN: Regulation of lysophosphatidate signaling by autotaxin and lipid phosphate phosphatases with respect to tumor progression, angiogenesis, metastasis and chemo-resistance. Biochimie 93(1), 61-70 (2011). doi: 10.1016/j.biochi.2010.08.002.

To my father, Dr. Taye Bekele, this is for you!

To my mother, Woubayehu Bekele, for her unconditional love and support

To my uncle, Mogese Girma, for all the amazing Sundays

To my brothers, Beide, Beakal and Amen for cheering me all the way

"And those who were seen dancing were thought to be insane by those who could not hear the music."

-Friedrich Nietzsche

ACKNOWLEDGMENTS

I would like to thank my supervisor, Dr. David Brindley, for all his guidance and mentorship. He has provided me with all the necessary support, encouragement and willingness to freely develop my ideas and bring them to fruition. He has been an excellent supervisor and role model. I would also like to thank my committee members, Dr. Ing Swie Goping and Dr. Zhixiang Wang, for all their supervision and helpful insights that made my project a success. I am also deeply grateful to Dr. Todd McMullen for being involved in the supervision of my project and providing his clinical expertise. I want to thank my external examiners, Dr. Andrew J. Morris and Dr. Richard Fahlman, for their time and commitment.

I would like to thank all former and present lab members of the Brindley lab: Ganesh Venkatraman, Matthew Benesch and Xiaoyun Tang for their help with my experiments. Meltem Sariahmetoglu, Nasser Samadi, Sabina Isgandarova, Bernard Kok, Le Luong, Zelei Yang and Guanmin Meng, for all their support and encouragements. I would like to extend a special thank you to Jay Dewald for providing an excellent technical support and for all the wonderful memories. Thank you also to the McMullen lab members: Ana Lopez-Campistrous and Esther Ekpe, department of Biochemistry chair, Dr. Charles Holmes, graduate program coordinator, Dr. David Stuart, administrative staff and members of Signal Transduction Research Group.

This project would not have been possible if it was not for the generous supply of reagents and cell lines from our collaborators Dr. Roland Wolf, Dr. Pu Xia and Dr. Sylvain Bourgoin. I would like to acknowledge Dr. John Mackey, Dr. Roseline Godbout and Dr. Jonathan Curtis for their continued involvement in my project. I am also deeply indebted to Dr. Rong-Zong Liu and Si Mi for their continued interest and help with my project. I want to thank the funding agencies: Women and Children's Health Research Institute, for providing stipend and travel award and the Canadian Breast Cancer Foundation, for funding my project. I also thank, Faculty of Medicine and Dentistry and the Graduate Student Association for providing additional travel award.

Finally, I would like to thank my friends Wondimagegnehu Teferi, Adam Kebede, Robel Teklebrhan and Melesse Birega for providing the necessary social support during my stay in Edmonton. I am also extremely thankful for the love and support of my parents, brothers, sister, Freya Bekele, and my lovely nephew and niece, Lucas and Maraki.

TABLE OF CONTENTS

LIST OF FIGURES

LIST OF TABLES

LIST OF ABBREVIATIONS

ASMase	Acidic sphingomyelinase
AF-1 and AF-2	Activation function-1 and -2
AP-1	Activator protein 1
Arf	ADP-ribosylation factor
ATCC	American Type Culture Collection
APS	Ammonium persulfate
AIB1	Amplified in breast cancer
ARE	Anti-oxidant response element
AEBS	Anti-estrogen Binding Site
ASK-1	Apoptosis signal regulating kinase
APAF1	Apoptotic protease activating factor 1
ABC	ATP binding cassettes
ATX	Autotaxin
BCL-2	B-cell lymphoma 2
bZip	Basic leucine zipper
BH	BCL-2 homology
BSA	Bovine serum albumin
BCRP1	Breast cancer resistance protein 1
BSO	Buthionine sulphoximine
CREB	cAMP response element binding protein
CIP2A	Cancerous inhibitor of protein phosphatase-2A
CL	Cardiolipin
CR	Conserved region
CBP	CREB binding protein
cul3	Cullin 3
CypA	Cyclophilin A
Cytc	Cytochrome C
DISC	Death inducing signaling complex
DAB	Diaminobenzidine

DsiRNAs	Dicer-substrate siRNA
DHE	Dihydroethidium
DMBA	Dimethylbenzanthracene
DNP	Dinitrobenzene
DBD	DNA binding domain
EBCTCG	Early Breast Cancer Trialists' Collaborative Group
ENPP	Ecto-nucleotide pyrophosphatase/phosphodiesterase
Edg	Endothelial differentiation gene
ERα	Estrogen receptor-α
ERE	Estrogen Response Element
ERK	Extracellular regulated kinase
GPR30	G-protein coupled estrogen receptor
GPCR	G-protein coupled receptor
GCL	Gamma glutamyl ligase
GCS	Glucosylceramide synthase
GSH	Glutathione
GPX	Glutathione peroxidase
GST	Glutathione-s-transferase
GAPDH	Glyceraldehyde 3-phosphate dehydrogenase
GPI	Glycosylphosphatidylinositol
G-CSF	Granulocyte-colony stimulating factor
GDS	Guanine nucleotide dissociation stimulator
GEF	Guanine nucleotide exchange factor
HBSS	Hank's Balanced Salt Solution
HR	Hazard ratio
HSF-1	Heat shock factor 1
HMOX1	Heme oxygenase 1
HBS	HEPES-buffered saline
HEV	High endothelial venules
HER2	Human Epidermal growth factor Receptor 2
HPRT	Hypoxanthine phosphoribosyltransferase

HIF1	Hypoxia-inducible transcription factor 1)
IHC	Immunohistochemistry
IAP	Inhibitor of apoptosis protein
LBD	Ligand binding domain
LPP	Lipid phosphatase phosphatases
LPA	Lysophosphatidate
LPC	Lysophphosphophatidyl choline
MMPs	Matrix metalloproteinases
MOMP	Mitochondria outer membrane permebilization
MAPK	Mitogen-activated protein kinase
MKK	Mitogen-activated protein kinase kinase
MAG	Monoacylglycerols
MEFs	Mouse embryonic fibroblast
MDRT	Multi-drug resistance transporter
MDR	Multi-drug resistance
MRPs	Multidrug resistance associated protein
NAC	N-acetyl cysteine
NDMT	N-desmethyltamoxifen
TEMED	N,N,N′,N′-Tetramethylethane-1,2-diamine
NQO1	NAD(P)H dehydrogenase, quinone 1
NOX	NADPH oxidase
NSMase	Neutral sphingomyelinase
NSLC	Non- small cell like lung cancer
Nrf2	Nuclear factor erythroid 2 related factor 2
NPP	Nucleotide pyrophosphatase and phosphodiesterase
POB1	Partner of RalBP1
PMC	Pentamethyl-6-chromanol
p-glycoproteins	Permeability glycoprotein
PRDX	Peroxiredoxin
PMA	Phorbol-12-myristate-13-acetate
PA	Phosphatidate

PE	Phosphatidylethanolamine
PIP5K	Phosphatidylinositol 4-phosphate 5-kinase
PDK	Phosphoinositide-dependent protein kinase
PLD	Phospholipase D
PX	Phox
PB	Phpsphatidylbutanol
PC-1	Plasma cell glycoprotein-1
PDGF	Platelet-derived growth factor
PH	Pleckstrin homology
PARP	Poly (ADP-ribose) polymerase
PAGE	Polyacrylamide gel electrophoresis
PCD	Programmed cell death
PKB	Protein kinase B
PKC	Protein kinase C
PP2A	Protein phosphatase 2A
PTP	Protein tyrosine phosphatase
qRT-PCR	Quantitative real-time PCR
RALBP1	Ral binding protein 1
ROS	Reactive oxygen species
ROC	Receiver Operating Characteristic
Rf	Retention factor
RPM	Revolutions per minute
SMAC	Second mitochondria-derived activator of caspase
SPT	Serine Palmitoyl Transferase
SNPs	Single nucleotide polymorphisms
SCLC	Small cell like lung cancer
SDS	Sodium dodecyl sulphate
SOS	Son of Sevenless
SMase	Sphingomyelinase
SK	Sphingosine kinases
Spns2	Spinster 2

SH3	Src homology domain 3
SAPK	Stress-activated protein kinases
SOD	Superoxide dismutase
Tm	Temperature of melting
TBHQ	Tert-Butylhydroquinone
TLC	Thin layer chromatography
TXN	Thioredoxin
TXNRD	Thioredoxin-reductase
TMA	Tissue microarray
TRAF-2	TNF-receptor-associated factor 2
TGF	Transforming growth factor
tBid	Truncated-Bid
TNF-α	Tumor necrosis factor-α
VEGF	Vascular endothelial growth factor
4HNE	4-hydroxynonenal
4HT	4-hydroxytamoxifen

1 CHAPTER: INTRODUCTION

1.1 Overview

Breast cancer is one of the most common malignancies among women in western societies [1]. Approximately 75% of all breast tumors are estrogen receptor-α (ERα) positive and these patients are typically prescribed tamoxifen [2-5]. Tamoxifen is thus the most widely used therapy for breast cancer and leads to tumor stabilization in about 50% of previously untreated patients with metastatic breast cancer [3, 6]. Moreover, this widespread use of tamoxifen has been credited with much of the decrease associated with breast cancer mortality over the last decade. Despite being one of the most successful drugs used in the clinics, about 40% patients receiving adjuvant tamoxifen treatment and almost all patient with metastatic tumors relapse and die from their disease [3, 7].

This Chapter will give a background review of the history of tamoxifen and its development as a breast cancer therapy and how the link between the estrogen receptors and tamoxifen was established (*Section 1.2 and 1.3*). As tamoxifen is prescribed to patients based on ERα status, the next section will focus on estrogen and its receptors (*Section 1.4*). One of the thesis objectives impinges on the killing of cancer cells and thus, the general induction of apoptosis will be discussed (*Section 1.5*). Stress pathways that are activated and the mechanisms employed by these pathways to lead to cell killing will also be outlined (*Section 1.5 and 1.6*).

Cancer cells employ several adaptive mechanisms to resist the toxic effects of therapeutic drugs by utilizing anti-oxidant defense system (*Section 1.6.1*),

increasing the expression and/or activity of multidrug resistance transporters (*Section 1.6.2)*, Phospholipase D (*Section 1.7.4*) and RalBP1 (*Section 1.7.5*) and also hijacking the normal physiological roles of enzymes such as autotaxin (*Section 1.7.1-3*) leading to chemo-resistance. All these aspects will be reviewed. Finally, I will end this Chapter by giving a summary of the thesis objectives and goal of the research presented in this thesis (*Section 1.8*).

1.2 A brief history of tamoxifen

By the turn of the twentieth century the Nobel Prize winning scientist Paul Ehrlich had put forward the concept that the structure of a chemical compound was closely tied down to its pharmacological activity. He also developed the current model strategy for drug development, which involved the synthesis of different chemical compounds for generating a library of potential therapeutic drugs that could be tested in the respective disease models for efficacy and toxicities. Using this approach in 1944, Sir Alexander Haddow screened several polycyclic hydrocarbons as potential drugs for treatment of cancer and identified some targets compounds to be effective. Nevertheless, their utility as potential drugs was hindered due to their prior classification as carcinogens for human beings. Hence, Sir Haddow refocused his attention on naturally occurring polycyclic hydrocarbons, such as the triphenylethylene based estrogens and subsequently identified these compounds to be first chemical therapy for treatment of breast and other malignant cancers [8, 9]. His study heralded the emergence of a new era of cytotoxic chemotherapy.

The cancer treatment method from 1960 onwards consequently used cytotoxic chemotherapy approach, which involves using a cocktail of drugs to kill remaining cancer cells following the resection of the primary tumor by surgery [10]. As the specificities of most drugs were largely unidentified at the time, this approach largely relied on fortuitous identification of a combination of drugs that could potentially kill cancer cells. Hence, this approach proved to be unsuccessful [9] and this led to the birth of targeted chemotherapy approach to treat cancer.

Tamoxifen was the first targeted anticancer drug and was pioneered after the collaboration of Arthur L. Walpole, the head of reproductive biology at the then ICI Pharmaceuticals currently now known as Astrazeneca, and V. Craig Jordan dubbed as the "father of tamoxifen" [11]. In the 1960s, the market for developing breast cancer drugs was quite low as opposed to developing contraceptives and so ICI Pharmaceuticals focused all their efforts on developing a drug that counteracts estrogen's effect with the hope that it will lead to an effective birth-control drug.

The project to develop a contraceptive eventually led to the synthesis and discovery of tamoxifen [5]. However, tamoxifen actually did the opposite and promoted ovulation and so the human clinical trail for testing of tamoxifen as contraceptive was deemed to be a failure. Nevertheless, due to Walpole's interest in cancer therapy development, another clinical trial testing the efficacy of tamoxifen in breast cancer was being run simultaneously as the trials for contraceptive development [5]. The result showed that tamoxifen was modestly

effective as breast cancer therapy [9], however, to further its application as a cancer treatment its mechanism of action had to be established and this critical work was later performed by V. Craig Jordan.

At the time when tamoxifen was developed, mammary tumors were generated in animals using DMBA (7,12-Dimethylbenzanthracene) and the prerequisite for this was the presence of estrogen and prolactin. Craig Jordan using this mammary tumors model performed his landmark study that showed tamoxifen treatment led to the inhibition of tumorigenesis. Furthermore, tamoxifen treatment resulted in decreased binding of radiolabeled estrogen to tissues [12]. This study was important in two ways; first it corroborated the previous clinical trials done by ICI. Secondly, the potential mode of action of tamoxifen was identified, as tamoxifen treatment decreased DMBA tumor initiation and also decreased binding of estrogens to tissues.

Thus, tamoxifen nicely fitted into the theme of a targeted therapy, which prompted further clinical trials and studies that culminated in establishing tamoxifen as the current gold standard for ERα-positive breast cancer therapy.

1.3 Tamoxifen and breast cancer therapy

The Clinical Trial Service Unit of Oxford University established in 1983 a group called EBCTCG (Early Breast Cancer Trialists' Collaborative Group) [13]. Every 5 years the EBCTCG undertakes meta-analyses of all randomized clinical trials of any aspect of early breast cancer treatment. The analysis only considers those clinical trails done for women with “early breast cancer” who are patients presenting with breast cancers that are detectable and restricted to

the breast or local lymph nodes and subjected to an adjuvant treatment after tumor resection [2].

Three editions of published work by EBCTCG, since its establishment, conclusively showed that adjuvant tamoxifen treatment significantly improved 10-year survival of women with early breast cancer. However, there was uncertainty over who should receive tamoxifen treatment or for how long treatment should be continued. Hence, on the 4th edition the group obtained and analyzed data from 55 randomized clinical trials done worldwide comprising of 37,000 women who received either no tamoxifen or adjuvant tamoxifen. In analyzed clinical trials, the patient cohort was further subdivided between patients that had ERα-positive tumors, this made up 18,000 patients. The remaining patients, about 8000 of whom had either very low or no ERα expression with an additional 12,000 patients that were not tested for estrogen-receptor expression in their tumors. This stratification of patients based ERα was due to the aforementioned effects of tamoxifen on ERα and also as ERα was the only identified receptor for estrogens at the time of the clinical trails. Thus, most studies and trials were largely focused on elucidating the mechanism of tamoxifen through its ability to block ERα.

In the analysis the EBCTCG unequivocally stated that tamoxifen treatment in ERα positive tumors or patients with unknown ERα status (of which 4000 were predicted to be ERα negative, as one-third of general breast cancers population is ERα negative) provide substantial survival advantage over 10 year period to breast cancer patients [2]. Nevertheless, the group also

reported that tamoxifen had produced some activity in the patients with very low or no ERα. Additionally, another clinical trial done after the analysis by EBCTCG also showed that tamoxifen indeed had some beneficial activity in the patient groups negative for ERα in their breast tumors [14].

The effect of tamoxifen on tumors could either be cytostatic (growth arrest) or cytotoxic (apoptosis and necrosis of tumors leading to shrinkage) or both. It is not difficult to envision tamoxifen-causing cytostasis by preventing the growth of tumors addicted to estrogen through blocking the activity of ERα. On the other hand, the effect of tamoxifen in ERα negative tumors could be due to cytotoxic effects leading to tumor shrinkage caused by the induction of a programmed cell death (PCD) known as apoptosis. As such several groups have noted ERα-independent effects of tamoxifen on several signaling mediators that involve PKC (protein kinase C) [15-17], calmodulin [15, 18], c-myc [19], TGF-β (transforming growth factor-β) [20] and PP2A (protein phosphatase 2A) [21] all of which could potentially contribute to the observed clinical utility of tamoxifen in counteracting the growth of tumors in both ERα-positive and ERα-negative tumors.

1.4 Estrogen and its role in tumorigenesis

Estrogens belong to the class of steroids hormones, which are compounds that are comprised of three six membered and one five membered cyclic hydrocarbons arranged in a characteristic pattern (Fig. 1.1). Naturally occurring estrogens are classified in to three types, estrone (E1), estradiol (E2) and estriol (E3), which is based on the number of hydroxyl groups present (Fig. 1.1), and of the three types 17β estradiol (E2) is the predominant estrogen in women [22].

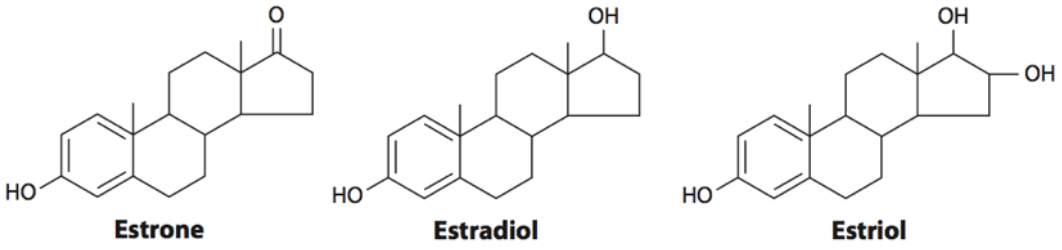

Figure 1.1: Chemical structure of different types of estrogen.

Shown from left to right E1, E2 and E3 with a characteristic phenol group on the A ring of the steroid structure, which is common to all three estrogens. E1 has an aldehyde group on the D-ring; however, E2 and E3 have one and two hydroxyl group respectively. The rings of steroids are identified by IUPAC nomenclature using letters A-D from left to right [23]. The figure is adapted from reference [22].

The ovaries primarily secrete estrogens in preparation for pregnancy and also for modulating the secondary female sexual characteristics. Adipose tissue, adrenal glands, placenta and testes can also secrete estrogens, albeit in much smaller quantities. In addition to their function as sex hormones, estrogens also play a role in cholesterol mobilization, regulation of bone density and also in brain function [22].

Under a pathological context estrogens are known to promote breast cancer development and this conclusion comes from the works showing the requirement of estrogen for tumor initiation by DMBA [12]. Also, this relationship was emphatically shown in the study that had to be discontinued after increased breast cancer incidence from using estrogen as a hormone replacement therapy for postmenopausal women [24]. Hence, estrogens are currently classified as bonafide carcinogens. It is therefore no surprise that microarray analysis studies on the MCF-7 breast cancer cell line revealed that estrogen induced the upregulation of genes involved in cell-cycle progression and cell proliferation while it led to the downregulation of transcriptional repressors, anti-proliferative and pro-apoptotic genes [25].

Estrogens exert their influence in target cells by binding to estrogen receptors and there are three known estrogen receptors, ERα, ERβ and G-protein coupled estrogen receptor (GPR30).

1.4.1 Estrogen receptor-α

The first major receptor identified for estrogen was ERα. Upon binding to estrogen, ERα dissociates from heat shock proteins and undergoes a conformational change, phosphorylation and dimerization after which it translocates to the nucleus, where it binds to the estrogen response element (ERE) to drive the transcription of estrogen-dependent genes [3, 26, 27]. Hence, ERα is known as a ligand-activated transcription factor and it mediates the transcription of its target genes through its two distinct activation domains termed as activation function-1 and -2 (AF-1, and AF-2) [3, 22]. Along with the

DNA binding domain (DBD) that recognizes and binds to ERE, AF-1 and AF-2 make up three major domains of ERα (Fig 1.2).

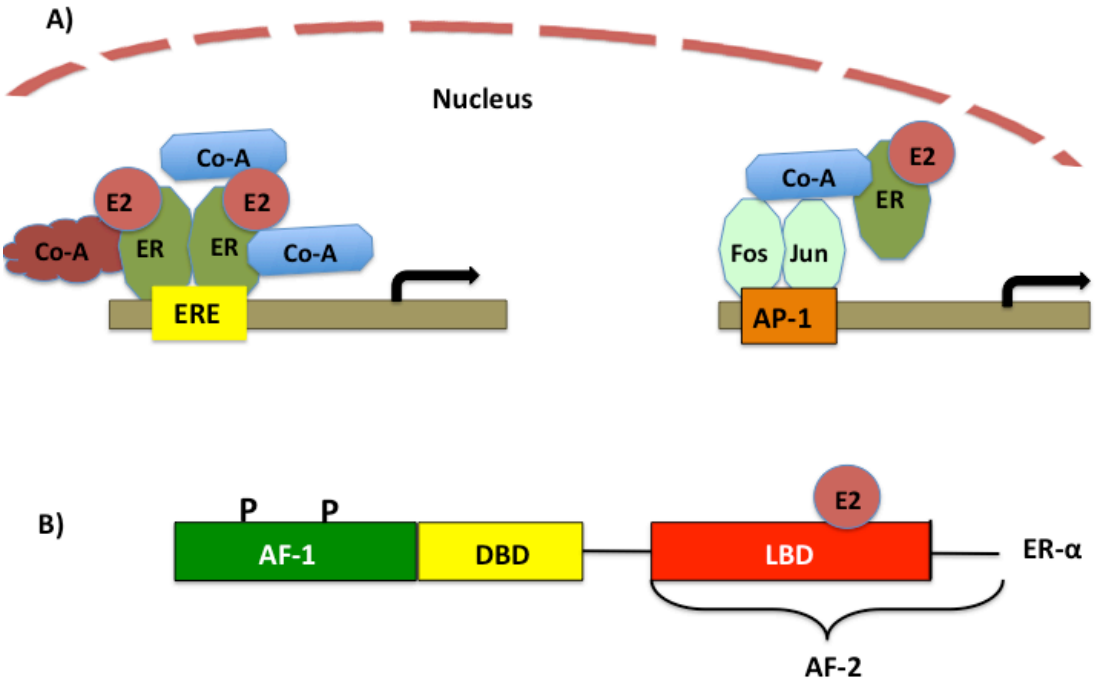

Figure 1.2: The transcriptional activity of the Estrogen receptor

(A) E2 (estrogen) binds to estrogen receptor-α (ERα) and induces a conformational change and translocation to the nucleus. The E2-ER complex binds to the ERE (the estrogen response element) as a dimer and recruit different Co-A proteins (co-activator) to initiate transcriptional machinery that leads to the expression of genes. By binding to Co-A proteins, E2-ER complex can also stimulate the transcription of genes without interacting with DNA and linking to other transcription factors such as c-jun and fos, which bind to AP-1 site. (B) At the N terminal side, ERα has an AF-1 (activating function 1) domain that is estrogen independent and activated by phosphorylation. Next to AF-1 is the DBD (DNA binding domain), which can bind to consensus ERE sequence on the DNA. At the C-terminal side is the third major domain is the AF-2 (activating function 1) that consists of the LBD (ligand binding domain) and thus requires estrogen for activation. The figure was adopted from references [3, 22].

AF-1 is localized close to the N-terminus of the ERα, and it is hormone-independent and is activated by phosphorylation. On the other hand, AF-2 is localized in the ligand-binding domain and is hormone-dependent (Fig 1.2B). In most cells, AF-1 and AF-2 act together, but in some cases the two domains

were found to act independently of each other to turn on transcription [28, 29]. AF-1 and AF-2 act by recruiting co-regulatory proteins which function as either co-activators or co-repressors and these co-regulatory proteins modulate the interaction between estrogen, ERα and the ERE. Some of the co-activators for ERα are AIB1 (amplified in breast cancer) protein, CREB associated protein (CBP) among many others [30, 31]. ERα can also regulate gene expression indirectly by interacting with other transcription factors such as c-Jun and fos [26].

The link between tamoxifen and ERα was established when tamoxifen was shown to bind strongly to ERα after being metabolized to 4-hydroxytamoxifen (4HT) [32, 33]. Hence tamoxifen can compete with estrogen for ERα binding and this leads to a different conformational change compared to the binding of estrogen. 17β-estradiol binds to the hydrophobic pocket of the ligand-binding domain of ERα [34, 35], leading to the sealing of the pocket by the so-called helix-12 (Fig 1.3). Tamoxifen binding in contrast does not lead to the sealing of the hydrophobic pocket by helix-12 [35]. Thus, AF-2 activation is prevented, as the ligand-induced conformational change is a perquisite for AF-2 activation. Moreover, co-activators cannot bind to the conformation induced by tamoxifen [36] and studies have also showed that tamoxifen when bound to the ERα interact more with co-repressors [36].

In this way, tamoxifen blocks the transcriptional upregulation of genes that require AF-2-dependent ERα activation resulting in its anti-proliferative effects. However, transcriptional upregulation that requires only AF-1- dependent

activation of ERα would still remain unaffected, and tamoxifen might even act as an agonist in such situations [36, 37].

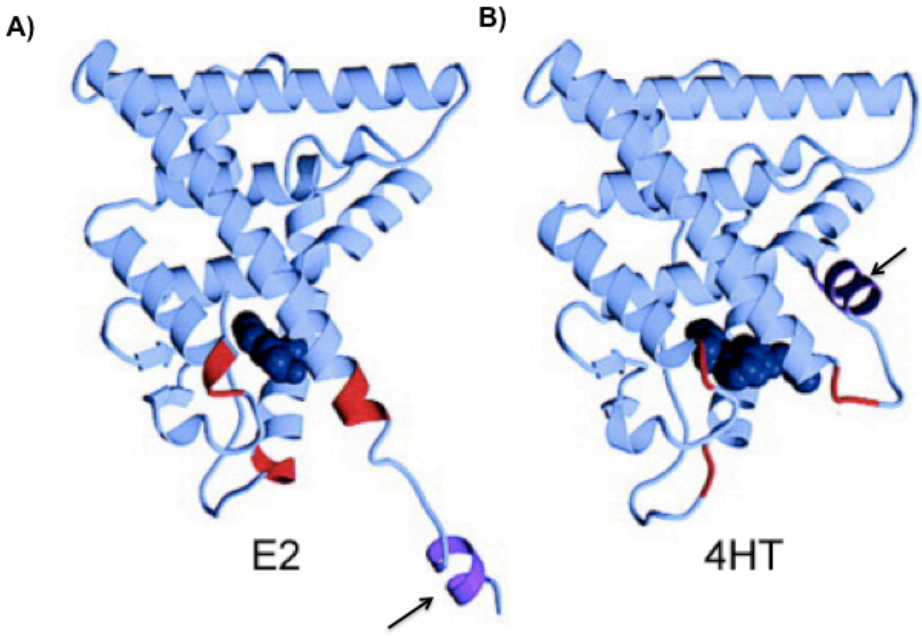

Figure 1.3: The binding of E2 and 4HT induce a different conformation of ERα.

A ribbon representation of the ligand-binding domain of ERα with (A) amino residues 421 to 423 shown in red and binding to E2 and (B) 4HT represented by space filling models with residues 527 to 530 colored in red. Arrows represent helix-12. The figure has been adapted from the reference [35].

In order to ascertain the effect of tamoxifen on cell proliferation and survival, it is important to determine the prevalence of either AF-1 or AF-2 regulated genes, in the tissue of interest. Breast tissue, for instance, has mostly AF-2 regulated genes whereas the uterus has mostly AF-1 regulated genes [3].

1.4.2 Signaling pathways influencing the genomic actions of ERα

ERα interacts with growth factor receptors and key signaling molecules, such as the EGFR, PI3K, matrix metalloproteinases (MMPs), Src family kinases and MAPKs [38, 39].

MAPKs such as ERK1 and ERK2 phosphorylate ERα at the serine-118 position within AF-1 region. Such phosphorylation enhances the sensitivity of ERα to ligand and may also stimulate ligand-independent ERα transcription of genes [40]. Similarly, ERα can also interact with PI3K, more specifically with the p85 regulatory subunit of PI3K [41]. PI3K catalyzes the phosphorylation of phosphoinosidites which can then recruits the phosphoinositide-dependent protein kinase (PDK) and Akt (Protein kinase B, PKB) through their PH domains to the membranes [42]. This results in the phosphorylation and subsequent activation of Akt by PDK. Akt, which is a serine/ threonine kinase, has been implicated in cellular proliferation and cell survival pathways [43]. Once activated, Akt can phosphorylate ERα at Serine-167 position leading to ligand-independent activation [44]. Moreover, signaling from growth factors receptors can indirectly affect ER by stimulating changes in the activity or localization of their co-regulatory proteins [45, 46].

The next sections will discuss the other two estrogen receptors, ERβ and GPR30.

1.4.3 Estrogen receptor-β

ERβ was discovered 30 years after the identification of ERα [47] and is also a ligand-activated transcription factor sharing a 55% sequence homology to the ligand-binding site of ERα and 96% homology to the DBD [48]. Its cDNA was cloned from a cDNA library of rat prostate, but it is also ubiquitously expressed in other tissues including normal and malignant breast tissues [48, 49]. Both ERα and ERβ have similar physiological ligand binding characteristics as well as similar binding affinities to tamoxifen [50]. However, their distinction lies in the relative level of receptor expression in tissues as well as differential transcriptional responses owing to differential affinity towards co-regulatory proteins. These nuances have led to opposite effects on proliferation, apoptosis and migration [49, 51].

After the identification of ERβ, it was found that about 50% of primary breast cancers co-express ERα and ERβ. About 15% of those tumors expressed either ERα or ERβ and tamoxifen as adjuvant treatment led to more favorable outcome in those patients with ERβ expression [52-55].

1.4.4 G-protein coupled estrogen receptor (GPR30)

Both ERα and ERβ are ligand-activated transcription factors, however, several reports have shown that estrogen can exert a rapid non-genomic event on cells such as increase Ca^{+2}, activation of PI3K, MAPK and other key cell signaling proteins in a time frame of second to minutes [56]. These effects are independent of the genomic actions that are normally associated with

estrogens, which requires hours before taking effect. Thus a plethora of cellular effects attributed to estrogens could be explained by the rapid non-genomic signaling in addition to the genomic effects.

Rapid cell signaling effects are normally associated with activation of plasma membrane bound growth factor receptors and could not be fully explained by soluble cytosolic proteins receptors such as ERα and ERβ. Hence, until the identification and the characterization of the G-protein coupled estrogen receptor, known as GPR30, there appeared to be gaps in our understanding of estrogen's action and the activities of its receptors.

GPR30 is a transmembrane protein predominantly localized on the endoplasmic reticulum. It has the same-conserved seven transmembrane domains similar to other G-protein coupled receptors. Hence, the rapid effects of estrogen can partly be explained by the binding of estrogen to GPR30 and subsequent activation of downstream signaling proteins [56-61]. However before the identification of GPR30 these effects of estrogen were attributed to ERα and ERβ through palmitoylation-mediated membrane recruitment followed by binding of ERα and ERβ to signaling proteins such as PI3K, which induced rapid activation [56].

In light of the identification of GPR30, some of the earlier studies need to be reevaluated and this is evident in the study that showed that the estrogen-mediated transactivation of the epidermal growth factor receptor, which was previously attributed to ERα, has been shown to be GPR30-mediated [56, 61].

Hence, more studies need to be done to delineate the specific roles of GPR30, ERα and β in the rapid effects of estrogen.

Interestingly, tamoxifen has been shown to induce the activation of GPR30, to the level similar to the activation observed by the estrogen 17β-estradiol [56, 61, 62], in stark contrast to its role in counteracting the genomic actions of ERα and ERβ.

The next Section, 1.5, will focus on the induction of apoptosis to better understand how the different signaling mediators modulated by tamoxifen could contribute to its role in cytotoxic effect.

1.5 Suicide on cellular scale

Cellular suicide known as apoptosis is a highly regulated series of cellular events that leads to a programmed cell death. Organisms evolved such a suicide program to either remove undesirable cells in the process of development such as for sculpting limbs or to remove unhealthy cells under the context of cellular stressors [63, 64] such as infections or induced cell death as would be produced by tamoxifen. This programmed suicide is initiated by the activations of family of intracellular cysteine-containing proteases called caspases. Caspases are proteases that cleave their substrates after an aspartate residue in a tetrapeptide-sequence specific manner [65]. Caspases are further classified as initiator caspases and executioner caspases. Initiator caspases such as Caspase-2, -8, -9 or -10 are upstream to executioner caspases such as caspase-3 or -7. Once activated by apoptotic stimuli, the initiator caspases then go on to activate the executioner caspases by cleaving

them and such cleavage of executioner caspases is a hallmark of apoptosis [64].

Apoptotic stimuli can be broadly classified as belonging to the extrinsic and intrinsic pathway. The extrinsic route of apoptosis uses external ligands such as Fas Ligand and tumor necrosis factor-α (TNF-α) that bind to their cognate receptors leading to the assembly of the DISC (death inducing signaling complex) [66], which results in the activation of the initiator caspases-8 or-10 [64]. On the other hand the intrinsic route of apoptosis will directly lead to the permeabilization of the outer membrane of mitochondria causing the release of cytochrome c [67] and a protein called SMAC (second mitochondria-derived activator of caspase) to the cytosol [68]. SMAC enhances the activation of caspases by cytochrome C by binding and neutralizing cytosolic inhibitor of apoptosis protein (IAP), which block the activities of executioner caspases [64] (Fig. 1.4)

The decision to induce mitochondria outer membrane permebilization (MOMP) is very finely balanced between the levels of pro-apoptotic and anti-apoptotic proteins. An imbalance towards one will lead to cell death or an inherent resistance to apoptosis, a phenomenon well observed in oncogenesis. Both the pro-apoptotic and anti-apoptotic proteins belong to the BCL-2 (B-cell lymphoma 2) family of proteins containing conserved BH (BCL-2 homology) domains. BCL-2, BCL-XL and BCL-W are among the proteins promoting the blockage of apoptosis and are thus anti-apoptotic. On the other hand, proteins

such as BAX, BAK, BAD, BIM, and BID etc are pro-apoptotic and mediate the permeabilization of mitochondria [69].

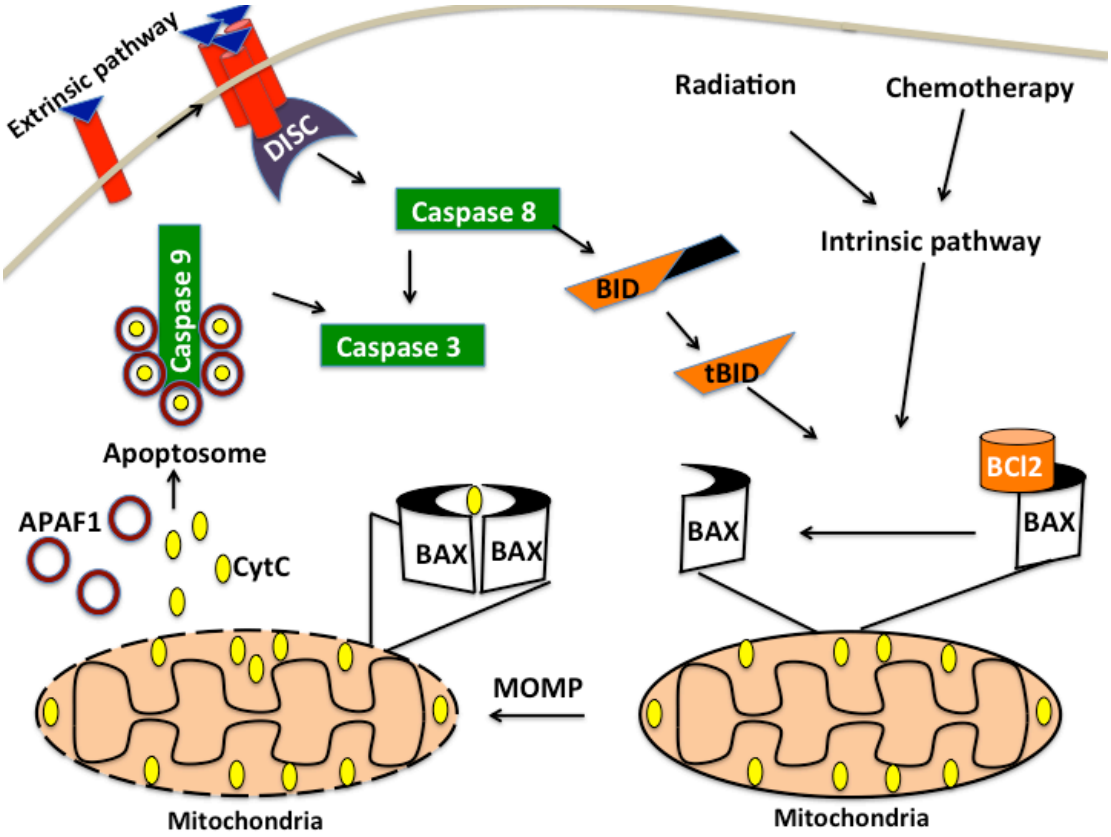

Figure 1.4: Apoptosis initiation through executioner caspases

Extrinsic apoptosis stimuli such as FASL or TNF-α bind to their receptors and cause downstream assembly of DISC (death inducing signaling complex) that activates initiator caspase 8 by cleaving pro-caspase 8. On the other hand intrinsic apoptotic stimuli such as radiation or chemotherapy cause MOMP (mitochondria outer membrane permebilization) leaking Cytc (cytochrome C) to the cytosol. Shown in the diagram MOMP is caused by oligomerization of BAX forming a pore on mitochondria. BAX prior to oligomerization is sequestered by anti-apoptotic protein Bcl2. Cytc in the cytosol will bind to APAF1 (Apoptotic protease activating factor 1) causing the formation of apoptosome complex that cleaves and activates another initiator caspase 9. Both initiator caspases 8 & 9 cleave and activate executioner caspase 3, which initiates apoptosis. The extrinsic apoptosis pathway through initiator caspase 8 can also cleave the pro-apoptotic protein Bid to tBid (truncated-Bid), tBid can then induce MOMP by facilitating BAX oligomerization.

In a very simplified depiction upon apoptotic stimulus as shown in Fig. 1.4 above, the pro-apoptotic proteins which posses only the BH3 domain (such as BAD, BIM and BID) are activated and cause the oligomerization of BAX or BAK causing the formation of a pore on the mitochondria and the subsequent activation of caspases. The anti-apoptotic proteins on the other hand sequester the pro-apoptotic proteins and prevent their activation [64].

The extrinsic pathway of apoptosis does not act independently but “cross-talks” with the intrinsic apoptotic pathway at the level of the mitochondrion. The intersection of these two pathways happens through the activation of the pro-apoptotic protein Bid through cleavage to tBid (truncated bid). tBid then leads to the oligomerization of BAX/BAK and result in the permeability of mitochondria in similar fashion to the intrinsic pathway [70].

One of the mechanisms employed by cancer cells to ensure survival and tumor development is to evade apoptosis induced by intrinsic and extrinsic apoptotic stimuli using several mechanisms that involve up-regulation and down-regulating of pro- and anti-apoptotic proteins respectively. Certainly, those mechanisms are not the only ones used cancer cells [64]. From this perspective, the ultimate objective of intrinsic apoptotic stimuli such as radiation therapy, chemotherapy and oxidative stress is to push the balance scale towards the activation of the pro-apoptotic proteins and force cancer cells to undergo apoptosis.

Cell death can also occur independently of the apoptosis by cellular process known as necrosis, autophagy or the newly described cell death

ferroptosis. For cell death to be classified as apoptosis, features such as nuclear condensation and fragmentation, cleavage of chromosomal DNA into internucleosomal fragments and packaging of the deceased cell into apoptotic bodies without plasma membrane breakdown must be observed [71]. As such, cell death by apoptosis does not activate the immune system since cellular contents, some of which are pro-inflammatory are not released to the outside. Phagocytic cells recognize these apoptotic bodies through the exposition of phosphatidylserine on the outer leaflet of plasma membrane [72] and so are neatly removed without inflammation. Such well-orchestrated apoptosis mechanism requires the use of ATP; on the other hand, cell death by necrosis/autophagy could result from cells running out of ATP [71]. In cell death by necrosis cellular contents are released to the outside environment, which results in inflammation around the dying cell. Such cell death may be preferable in certain circumstances that require immune education of invading pathogens [71]. In addition to apoptosis and necrosis, cells can also die by a process known as autophagy. Autophagy is characterized by vacuolization, which encapsulates whole organelles and cytoplasmic proteins and lipids in what is known as an autophagosome. Such an attempt by cells is aimed at catabolizing cellular constituents for the purpose of energy production during times of nutrient starvation. As such, some research groups have suggested that autophagy is, in fact, a cell survival strategy rather than cell death [71]. Nevertheless, it is easy to envision that autophagy will eventually lead to cell death, especially if the condition that initiated autophagy is not averted. Finally,

cells could also die due to a process known as ferroptosis, which is distinct from cell death by apoptosis, necrosis or autophagy. Morphologically, ferroptosis is characterized by the presence of smaller than normal mitochondria, condensed mitochondrial membrane and the rupture of mitochondrial membranes. Feroptosis is also characterized by the accumulation of lipid peroxidation byproducts and production of reactive oxygen species (ROS) [73]. Lipid peroxidation is the oxidation of lipids containing double bonds by ROS, especially those lipids with polyunsaturated fatty acids [74]. Feroptosis is negatively regulated by glutathione peroxidase 4 (GPX), and nuclear factor erythroid 2-related factor 2 (Nrf2), whereas NADPH oxidase (NOX) and the tumor suppressor p53 are positive regulators. NOX and p53 promote feroptosis through generating ROS and inhibition of cystine/glutamate antiporter (SLC7A11), respectively [73].

1.5.1 Ceramide and apoptosis

Ceramide is a name given to diverse group of sphinglolipids, all of which have a sphingosine backbone that is N-acylated to fatty acids of varying chain-lengths. The attachment of the phosphorylcholine head group to ceramides forms the lipid sphingomyelin, which serves an integral membrane lipid located on the outer leaflet of plasma membrane [75]. Sphingomyelin preferentially associates with cholesterol, which is known to maintain the structural order, fluidity and integrity of plasma membrane [76, 77].

SMases (sphingomyelinases) generate ceramide by degradation of sphingomyelin and based on their pH requirements for optimum activities are

classified into NSMase (neutral SMase) and ASMase (acidic SMase). NSMAse is mostly associated to plasma membranes, whereas ASMase is linked to endosomal membranes [78]. Ceramide can also be synthesized de novo from the precursors serine and palmitate by the enzyme SPT (Serine Palmitoyl Transferase) resulting in 3-ketosphinganine, which is the first step in ceramide synthesis occurring at the endoplasmic reticulum [79]. The newly generated ceramide can later be transported to the Golgi apparatus for processing, such as glycosylation, which is important in drug resistance [80].

Ceramide-mediated pathways are evolutionary conserved and are even present in primitive organism such as yeast, which do not undergo apoptosis. Thus the functions of ceramides appear to be evolutionary older than caspase-mediated death programs [81, 82]. As such, several studies have shown that treatment of various mammalian cells types with different stressors that belong to both the intrinsic and extrinsic apoptosis stimuli such as UV, etoposide and FASL are accompanied by concomitant generation of ceramides [83], indicating their general role in cell death process.

A series of experiments done by Tepper and colleagues elegantly showed that sustained ceramide generation by various apoptotic stimuli are delayed and occur later after the induction of apoptosis [84, 85]. In another study they also showed this generation of ceramide was a direct consequence of phospholipid scrambling event causing the flipping of sphingomyelin from the outer leaflet to the inner leaflet of the plasma membrane. This affords access to SMase, which then acts on the now readily available substrate resulting in

ceramide formation. The flipping of sphingomyelin to the inner leaflet and its subsequent degradation was found to occurs concurrently with the flipping of phosphatidylserine in the opposite direction so that it is being exposed to the outer leaflet of plasma membrane [86]. The exposure of phosphatidylserine is a well-known hallmark of cells undergoing apoptosis [87]. More importantly, the degradation of sphinglomylein leads to loss of cholesterol and subsequent loss plasma membrane integrity contributing to the membrane blebbing [86], an occurrence also routinely observed in cells dying of apoptosis. Hence this delayed and sustained generation of ceramide could be an important and conserved mechanism that necessarily accompanies the execution phase of apoptosis. This would explain the ubiquity of ceramide generation in different cell death processes.

There are other studies, however, arguing for the role of ceramide in directly triggering apoptosis. This role of ceramide to act as a second messenger in cell death pathways is supported by its ability to cooperate with BAX in leading to the formation of MOMP and leaking out of cytochrome c (Fig 1.4) and mitochondrial proteins and thus leading to apoptosis [88, 89]. Furthermore, TNFα-mediated death signaling is accompanied by generation of ceramide through the activation of SMase. It is postulated that the formation of ceramide helps in the coalescing and assembly of the DISC complex necessary for activation of caspase-8 [90]. Despite all of these effects of ceramide, it has been reported that ceramide levels alone were not sufficient to induce MOMP

[88, 89] even though MOMP correlates with the levels of ceramide [91]. Moreover, ceramide formation that is induced by TNFα-mediated signaling was found to be necessary, but not sufficient, for TNFα-induced apoptosis [92]. This would suggest that ceramide might have a cooperative role in pathways that trigger apoptosis.

Ceramides have been shown to directly activate PP2A (protein phosphatase 2A). By virtue of this, ceramide can thus modulate the functioning of a myriad of signaling proteins also regulated by PP2A, such as inactivating Akt [93, 94]. It is well know that the activity of Akt is upregulated in many types of cancer since its activity upsets the balance of pro-apoptotic versus anti-apoptotic proteins favoring cell survival. In addition to PP2A other signaling mediators were also shown to be activated by ceramides such JNK/SAPK, as reviewed [82, 90, 95]. This role of ceramides does not negate the cooperative role of ceramides, nor does it exclude the possibility of ceramide to trigger of apoptosis.

As described in this Section, it is quite obvious that the generation of ceramide is intimately linked to cell death. This could make it necessary for cancer cells to develop strategies to mitigate the up-regulation of ceramides by de novo synthesis through SPT or by hydrolysis of sphingomyelin by SMase, enabling cancer cells to survive and evade apoptosis. As such researchers have reported evidence for such strategies namely the downregulation of SMases in human cell lines of liver and colon cancer cells [96] and also reviewed [90]. Another strategy for decreasing ceramide accumulation would

be glycosylating ceramides and thereby halting their role in collaborating with apoptotic pathways. This is evident in MCF-7 breast cancer cells that develop resistance to doxorubicin after enforced expression of GCS (glucosylceramide synthase) [97], the enzyme that glycosylates ceramides. Additionally, multi-drug resistance cell lines have elevated glucosylceramide levels compared to drug sensitive cell lines [98]. However, glycosylation of ceramides appears to not be involved in the late and sustained generation of ceramide at the plasma membrane [80]. A plausible explanation for this lies in the topological segregation of ceramide glycosylation, which occurs at the Golgi as opposed to plasma membrane. Thus ceramides generated at the cell surface by the virtue of their location, are rendered inaccessible to GCS [80]. This is highlighted by studies that showed that only those ceramide synthesized *de novo* and exogenous ceramide that could be shuttled to Golgi were targeted by GCS for glycosylation. Thus ceramides formed at the plasma membrane by various stimuli at the execution phase of apoptosis are not targeted for glycosylation [80].

The conversion of ceramide to glucosylceramide is just one way in which the effects of ceramides could be modulated and cancer cells do posses several other means of regulating ceramide. One such way would be degrading the ceramide to sphingosine followed by phosphorylation to sphingosine-1-phosphate (S1P) by the enzyme sphingosine kinases (SK) [90]. SK overexpression is observed in many cancers including those cells that have been developed to be resistant to tamoxifen [99]. Moreover, this rheostat of

ceramide–sphingosine–S1P is thought to mediate the fate of cancer cell survival [100].

Overall the overexpression and downregulation of proteins involved in the metabolism ceramide goes to highlight the importance of ceramide as a tumor suppressor lipid. As such, cancer cells must tightly regulate its levels if they are to ensure continued survival or otherwise risk cell death. Additionally, the role of ceramides in cooperating with apoptotic pathways appear to be distinct from the late and sustained induction of ceramide observed in cells committed to die. To prevent the effect of ceramides in collaborating with pathways that trigger apoptosis, cancer cells most likely endeavor to decrease the formation of ceramides early in the apoptosis initiation rather than the ceramide generated at end-stage of the execution phase of apoptosis program, after the cell has committed to die.

1.5.2 JNK/SAPK and apoptosis

Similar to the generation of ceramides, in response to different cellular stressors such as UV, TNFα and oxidative stress, the SAPK (stress-activated protein kinases) or otherwise know as JNK are routinely activated [95, 101-103].

There are three mammalian JNKs encoded by three separate genes and identified as JNK1, JNK2 and JNK3 (restricted to the brain). JNKs along with p38/Hog and the ERK (extracellular regulated kinase) belongs to a member of the MAPK (mitogen-activated protein kinase) family, which are activated by a two tier system of MAP2K (MAPKK), which itself is activated by MAP3K (MAPKKK) [82, 103].

There are about twenty MAP3K and out of those fourteen MAP3K have been identified to activate JNKs through MAP2Ks, MKK4 or MKK7 [103]. The given stimulus dictates the specific MAP3K involved and accordingly specifies the downstream MAPK to be activated. This can either be ERK, JNK, p38 or any different combinations of those kinases. ERK kinases have been largely implicated in cell proliferative and anti-apoptotic role, whereas JNK and p38 have been implicated in both cell survival and cell death pathways [104]. Furthermore, it has been shown that ERK activation can attenuate the apoptotic signaling directed by JNK [104] showing the complexity in delineating the activation of these kinases and tying them down to a specific cellular fate. Nevertheless, it is now widely believed that sustained JNK activation signifies the involvement of JNK in pro-apoptotic pathways, whereas transient activation will lead to pro-survival pathways [103].

Upon activation by upstream kinases, JNK can translocate to the nucleus and phosphorylate and activate c-Jun, which forms the AP-1 (activator protein 1) complex involved in the transcription of genes known to be pro-apoptotic such as TNF-α, Fas-L, and Bak. Additionally, JNKs can also phosphorylate other transcription factors such as Elk, the well-known tumor suppressor p53 and several others influencing their activities [103]. Evidence from studies conducted by several groups has clearly shown the involvement of JNK-c-jun/AP-1 in apoptosis and as such mutants c-jun that cannot be phosphorylated confer resistance to MEFs (mouse embryonic fibroblast) receiving UV radiation. Furthermore, dominant/negative JNK constructs also confer resistance and

protection against neuronal cell death, all highlighting the importance of JNK in the apoptosis machinery [103, 105].

JNK is also involved in the extrinsic apoptosis pathway through ASK-1 (apoptosis signal regulating kinase), which is an upstream MAP3K. ASK-1 is activated by TNF-α along with diverse other signals such oxidative stress, lipopolysaccharide and ER stress. Upon TNF-α stimulation, TRAF-2 (TNF-receptor-associated factor 2) activates ASK1 leading to activation of JNK and signaling for apoptosis [106]. ASK-1 to JNK activation has also been shown in cisplatin-induced apoptosis of ovarian carcinoma cells [107] and so the ASK-1-JNK signaling is not only limited to extrinsic apoptotic stimuli.

JNK can also potentiate apoptosis by phosphorylating pro-apoptotic proteins such as BAD at Ser128 [108]. In addition to modulating the transcription of genes and inducing apoptosis, pro-survival kinases like Akt phosphorylate BAD at Ser-136 [109], which reduces its pro-apoptotic activity. Moreover, BAD is sequestered by 14-3-3 proteins preventing its activity [110] and JNK's specific phosphorylation of BAD at Ser128 inhibits its interaction with 14-3-3 proteins [111]. Additionally, JNK also phosphorylate 14-3-3ζ at Ser184, which further prevents the sequestering of BAD by 14-3-3 and releases BAD allowing it to promote MOMP [103, 111].

Several stressors that signal for JNK activation also lead to SMase mediated generation of ceramides. Moreover, ceramides have been shown to activate JNK in a pro-apoptotic signaling through MKK4 (MAP2K), as dominant/negative MKK4 blocked ceramide induced-death in bovine

endothelial and U937 cells [95]. Additionally, the effect of ceramide-induced JNK activation and apoptosis in Jurkat cells was blocked with dominant/ negative Rac1, suggesting the small G-protein Rac1 mediates the ceramide-induced JNK activation [112], probably through one of the upstream MAP2Ks. It is also interesting to note that cells derived from Niemann-Pick disease deficient in ASMase, lack the ability to active JNK upon UV treatment and this is bypassed by adding synthetic ceramides. This shows the link between stress activated ceramide formation and JNK activation [113]. Furthermore, in the first evidence that linked JNK activation to apoptosis, the authors also observed a delayed but sustained JNK activation to γ-ray treatment [114], similar to delayed and sustained ceramide formation by the actions of SMases. Thus ceramide and JNK relay apoptotic messages to cells in response to several stressors. Oxidative stress is one such stressor known to influence the levels of ceramide and JNK activation and this will be discussed in the following section.

1.6 Oxidative stress

Cellular oxidative stress is a type of stress that arises from imbalance between the generation of ROS (reactive oxygen species) and thier elimination [115]. ROS are primarily derived from oxygen and are broadly classified as any oxygen-containing species with very high reactive properties. These include free radicals species such as superoxides ($O_2^{\cdot -}$), hydroxyl radical ($HO^{\cdot}$) and non-radical molecules such as hydrogen peroxide (H_2O_2) [115, 116].

For example, superoxides can be generated by reactions involving one electron reduction of molecular oxygen, $O_2 + e \rightarrow O_2^{\cdot -}$, where as two electron

reduction of O_2 results in H_2O_2, $O_2 + 2e + 2H^+ \rightarrow H_2O_2$. Hydroxyl radicals on the other hand are the neutral version of OH− (hydroxide) ion generated by Fenton reaction through the oxidation of metals such as Iron (II) to Iron (III), hydrogen peroxide and hydroxyl radical [116-118].

Cellular metabolic activity or external oxidizing agents in the cells environment such as chemotherapy or radiation can induce the generation of ROS. In case of cellular metabolism for instance, about 2% of the oxygen consumed by the mitochondria, which functions in making ATP by coupling the flow of electrons to reduce molecular oxygen, ends up as superoxide [119, 120]. Hence mitochondria serve as the major source of ROS in cells [115, 119, 120]. On the other hand, organelles such as peroxisomes and endoplasmic reticulum also serve as a source for ROS and do so enzymatically using $NADP^+$/NADPH as a cofactor [115]. Peroxisomes are organelles that are known to carry out oxidation reactions, such as β-oxidation of long chain fatty acids not metabolized by mitochondria [121], leading to the production of H_2O_2 [122]. The H_2O_2 produced by such reactions in peroxisomes is decomposed to water by the enzyme, catalase, or can be used to oxidize and breakdown of other organic molecules such as uric acid and amino acids [122]. On the other hand, the endoplasmic reticulum can also generate ROS by the virtue of having a unique oxidative environment distinct from the cytosol, which is paramount for the proper folding of proteins. The oxidative environment allows the generation of a disulfide bridge between adjacent cysteine residues of nascent proteins to help in their folding. This process subsequently generates ROS as a byproduct

[123]. Interestingly while the mitochondria, peroxisome and endoplasmic reticulum generate ROS as a by-product, the membrane bound enzyme NOX (NADPH oxidase), however, directly generates superoxide as its main product [124-126]. Hence, ROS is not simply a harmful byproduct that needs to be destroyed, but it can serve as an important signaling molecule stimulating cell division and inflammation when increases of ROS are well controlled. [126, 127]. These signaling roles of ROS are now gaining more appreciation and are documented by different research groups [128, 129].

ROS generation is thus part and parcel of cellular metabolism and cell signaling. However, unmitigated rises in cellular ROS can induce protein oxidation as well as lipid peroxidation, which affect the normal functioning of cells and result in apoptosis [115, 127].

To alleviate these detrimental effects, cells have developed different strategies to counteract the rise in ROS and do so through enzymatic and non-enzymatic process. The non-enzymatic detoxification of ROS is not so specific but is very important for cellular redox regulation and involves the use of GSH (glutathione), bilirubin, co-enzyme Q and dietary antioxidants such as vitamin E, vitamin C, selenium and β-carotene [115, 127, 130]. Vitamin E for example is a lipid soluble antioxidant that exerts its effect by scavenging ROS and converting them to tocopheryl radicals thereby reducing ROS-induced damage [131]. On the other hand enzymes such as SOD (superoxide dismutase), catalase, peroxiredoxin, thioredoxin reductase, HMOX1 (heme oxygenase 1),

NQO1 (NAD(P)H dehydrogenase, quinone 1) , etc are involved in the more specific enzymatic detoxification of ROS [115, 127, 130].

GSH is the major anti-oxidants utilized by cells and is tri-peptide synthesized from glutamate, cysteine and glycine. The link between the glutamate and cysteine in GSH is a gamma linkage, which is a bond between the side chain γ-carboxy group of glutamate and amino terminus of cysteine (Fig. 1.6C) and so it is not an ordinary peptide linkage involving α-carboxy group [132]. The enzyme GCL (gamma glutamyl ligase also known as gamma glutamyl synthethase) catalyzes this reaction, which is the first step in the synthesis of glutathione. The second step is catalyzed by glutathione synthetase, which links glycine to cysteine in canonical peptide bond [132].

Mammalian cells have abundant GSH levels of concentration up to 1-10 mM that protects them against any potential rise in ROS [132]. The enzyme GPX (glutathione peroxidase) for example detoxifies ROS using GSH as a substrate and oxidizing it to GSSG [115, 127, 132], which are two GSH molecules linked with a disulfide cysteine bridge. Cells maintain a >50:1 ratio of GSH/GSSG in the cytoplasm with exception of the lumen of endoplasmic reticulum, due to oxidative environment necessary for protein folding, which has a ratio of 1:1 to 3:1 [123, 133]. Hence, a change in this tightly regulated ratio of GSH/GSSG is indicative of an imbalance in the redox hemostasis. Additionally, GSH can also be conjugated to xenobiotics by the enzyme GST (glutathione-s-transferase) [134], this conjugation allows xenobiotics to be expelled out of cells

by drug transporters such as ABCC1 or the RALBP1, which will be discussed Section 1.6.2 and 1.7.5 respectively.

During oxidative stress the small protein, thioredoxin (TXN) participates in a thiol disulfide exchange, owing to the presence of two vicinal cysteines that can remove the formation of disulfide bridges from oxidized cellular proteins [135]. Oxidized TXN is reduced back to its active form by the enzyme Thioredoxin-reductase (TXNRD), which uses NADPH as a cofactor. For example, the enzyme peroxiredoxin (PRDX), which catalyzes the conversion of H_2O_2 to water, is oxidized and inactivated in the process and is recharged back to its active reduced form by TXN. TXN also forms a complex with the MAP3K, ASK-1 (Fig. 1.6B), sequestering it in an inactive state. However, upon interacting with ROS species, ASK-1 is released from TXN to its active and oxidized state [115, 135], ASK-1 then subsequently phosphorylates and activates downstream MAPKs such as JNK and p38 in a stress activated response.

To ensure continued survival cells, maintain redox homeostasis, thus ROS that is generated as a byproduct of cellular metabolism, xenobiotic stress or deliberately initiated by enzymes (like the NOX) is, therefore, effectively managed. Nevertheless, the use chemotherapy, radiation, mutations or environmental toxins could disrupt this failsafe mechanism [115] putting an increased selective pressure on cells. Hence, cells have to either adapt to the selective pressure or undergo apoptosis and cell death.

The next section will discuss the protein Nrf2, a master regulator that orchestrates these adaptive process enabling cells to survive under increased oxidative insult.

1.6.1 Nrf2: Adaptive process to oxidative stress

Nrf2 (nuclear factor erythroid 2 related factor 2) belongs to the basic leucine zipper transcription factor family, which contains the so-called leucine zipper motif [136, 137]. The motif is a dimer of two alpha helixes with leucine embedded in the hydrophobic part of the helixes and the dimers interact at the base to form a zipper and hence the name “leucine zipper” (Fig. 1.5).

The Nrf2’s leucine zipper tightly binds to the ARE (anti-oxidant response element), which is a cis–acting regulatory element that mediates the transcription of genes responsible for mitigating oxidative stress [137, 138]. Nrf2 by binding to ARE maintains the steady state ROS levels in cells through regulating the basal expression of the anti-oxidant genes. Thus, expression of proteins such as SOD1, NQO1, HMOX1, MDRT (multi-drug resistance proteins) and GCL (which can boosts GSH synthesis), are all turned on by Nrf2 [115, 137].

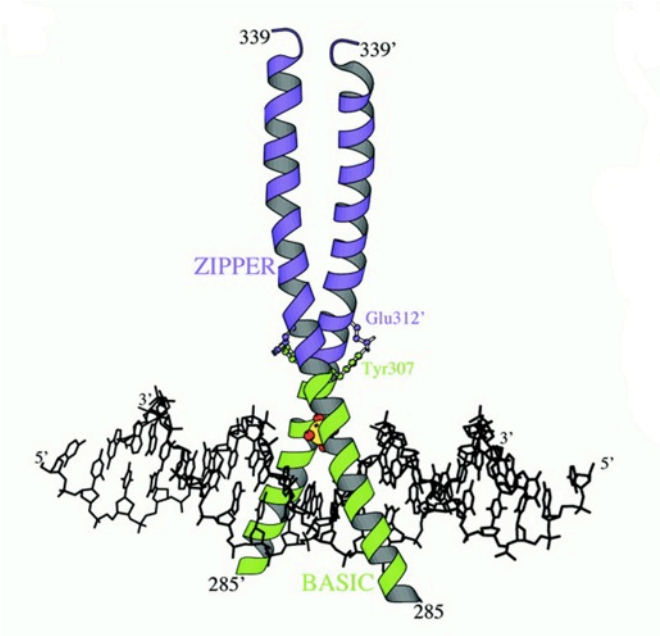

Figure 1.5: An example of the basic leucine zipper (bZip) binding to DNA.

The diagram is a ribbon representation of the bZIP domain of the protein CREB binding DNA. The basic residues of are represented in green and the zipper residues are colored in magenta. A hexahydrated magnesium bound to the bzip is also depicted in the diagram represented by yellow for magnesium and red for oxygen. Structural diagram obtained from the paper on reference [139].

The antioxidant protein, SOD, for instance catalyzes the dismutation reaction which is the simultaneous oxidation and reduction of a superoxide species generating molecular oxygen and H_2O_2 [140]; H_2O_2 can then be handled by either GPX or PRDX. Mitochondria generate lots of superoxides and thus have thier own SOD termed SOD2, where as SOD1 is cytoplasmic [141]. Additionally, mitochondria also have the enzyme NQO1 [142]. NQO1 catalyzes the formation of hydroxyquinone and thereby prevents the one electron reduction of quinone, resulting in the formation of quinone radical and a rise in cellular ROS [143]. In addition NQO1 has roles in directly scavenging superoxides [144], maintenance of lipid soluble antioxidants like vitamin E in their active form [145] and stabilization of tumor suppressor p53 [146]. On the

other hand, HMOX1 serves as antioxidant by catalyzing the breakdown of heme to biliverdin, which is subsequently reduced to bilirubin, an effective antioxidant [147, 148]. Furthermore, the levels of HMOX1 are also induced by factors that are known to generate ROS and cause the depletion of GSH [147], indicating the important role of HMOX1 in redox homeostasis. Hence Nrf2 orchestrates an antioxidant response by mediating the expression of several antioxidant proteins.

The 70kDa-binding partner, Keap-1, which is a scaffold protein that binds two distinct domains of Nrf2 [149], regulates Nrf2 protein by recruiting another scaffold protein, cul3 (cullin 3) (Fig. 1.6A). Cul3 is an E3 ubiquitin ligase that targets Nrf2 for ubiquitination-mediated proteasomal degradation [137, 150, 151]. Due to this targeting Nrf2 has a short lifetime of about 20 min, however the presence of reactive cysteine residues in Keap-1 make it an optimal target for ROS induced covalent modification [137].

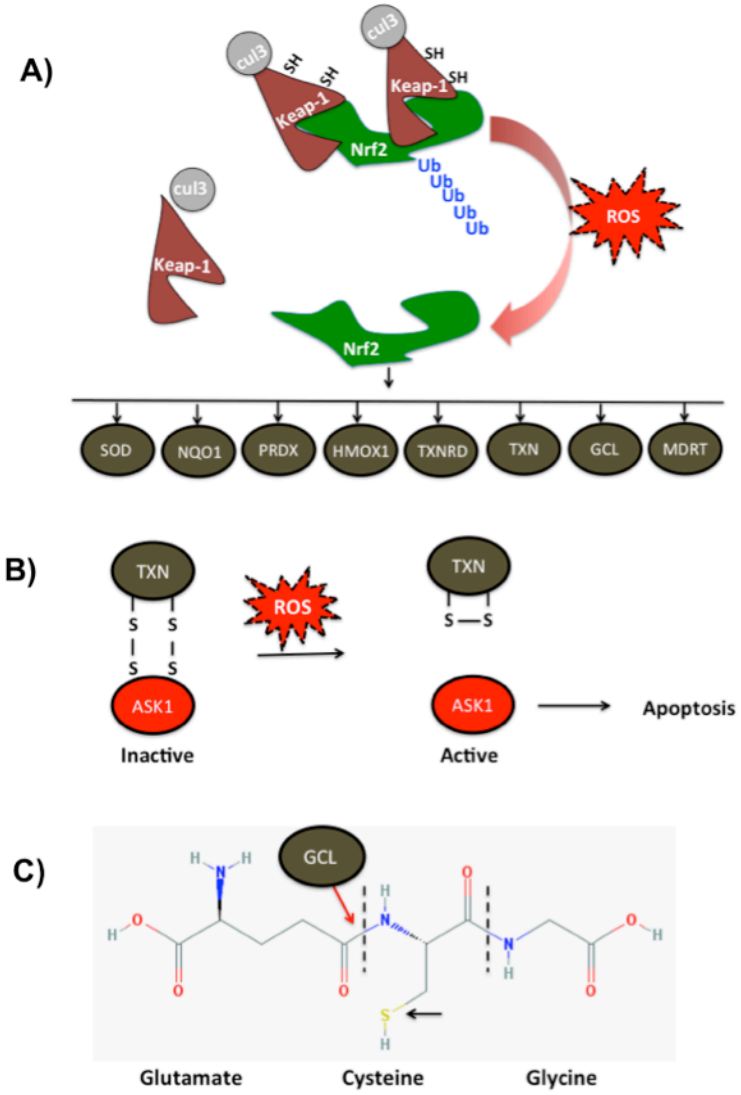

Figure 1.6: Antioxidant defense orchestrated by the master regulator Nrf2.

(A) The protein Keap1 binds to Nrf2 at two distinct sites and recruits cul3 leading to ubiquitination-mediated proteasomal degradation of Nrf2. An increase in ROS will result in the release of Nrf2 from the Keap1 complex and leads to the transcription expression of a several different proteins that help in the antioxidant defense of cells. (B) The protein TXN sequesters ASK1 in its inactive state and if the increase in ROS is not mitigated by the Nrf2 mediated antioxidant defense system, the TXN-ASK1 complex is disrupted and ASK1 will be activated. (C) The structure of glutathione is shown with the red arrow depicting the gamma linkage between glutamate and cysteine catalyzed by the enzyme GCL. The dotted lines show the amide bond and the black arrow shows the sulfhydryl functional group that participates antioxidant defense. The figure was adopted from reference [115, 137]. The glutathione picture was taken from PubChem database at the NCBI website.

An imbalance in redox status can thus disrupt the Nrf2 and Keap-1 complex sparing Nrf2 from proteasome degradation and leading to increased Nrf2 protein, which subsequently result in increased expression of antioxidant proteins during oxidative stress through activation of the ARE.

Cancer cells are generally characterized by an uncontrolled proliferation and to sustain such proliferation, high metabolisms is obligatory requirement. Consequently, cancer cells have a higher basal ROS status compared to normal cells. Incongruously, the hypoxia arising from such increased proliferation also stimulates mitochondrial ROS production further sustaining the high ROS levels and signaling for angiogenesis by the activation of HIF1 (hypoxia-inducible transcription factor 1) [115, 152]. The corollary of this increase in ROS levels is an adaptation towards increased expression of antioxidant proteins that boosts the antioxidant capacity of cancer cells. As such studies have shown cancers cells downregulate the expression of keap1 through methylation-mediated silencing providing an explanation for observed increased expression of Nrf2 in many cancer cells [153]. As Nrf2 is a master regulator mediating the expression of antioxidant proteins, such adaptation enables cancer cells to thrive in increased oxidative environments.

The next subsection will discuss the ABC transporters family. The expressions of certain members of these transporters are under Nrf2 regulation and thus form an integral part of the adaptation to cellular oxidative stress.

1.6.2 ABC transporters

ABC (ATP binding cassettes) transporters are found in all kingdoms of life and are integral membrane proteins that use energy from hydrolysis of ATP to translocate substrates across plasma membrane [154-156]. In eukaryotic organisms ABC transporters function exclusively as exporters whereas in prokaryotic organisms, they can serve as either importers or exporters [156]. The transporters have a characteristic architecture that consist of 4 main domains; two transmembrane domains embedded in the lipid bilayer and a highly conserved two ABC domains located in the cytoplasm [156, 157]. These transporters are normally found on the luminal side of enterocytes, proximal tubules of kidney, brain capillary endothelial cells and also on bile canaliculi [158]. In human beings, ABC transporters are classified into seven different groups from ABCA all the way to ABCG and in total there are about 49 ABC transporters (Table 5, Appendix section) [154]. Members of these seven groups have several roles in cells such as the transporting cholesterol and lipids, exporting chemotherapeutic drug and toxins (Fig. 1.7) and also mediating ATP-dependent regulation of ion channels [156]. The vital roles of the transporters in cells are best illustrated in the manifestation of several diseases that are associated to mutation in ABC transporters gene causing diseases like cystic fibrosis, hypercholesterolaemia and diabetes [156].

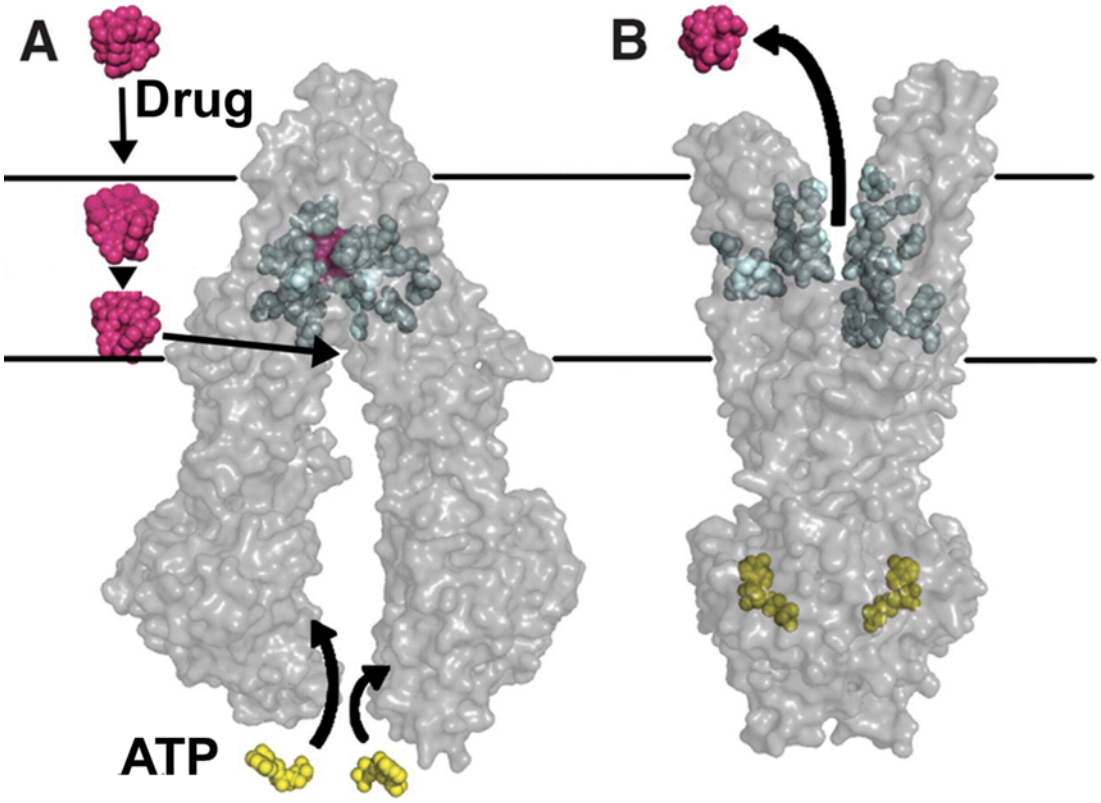

Figure 1.7: A representative model for the efflux of drug by the ABC transporter, ABCB1 (p-glycoprotein)

(A) Drug from the outside partitions in to the lipid bilayer of cells and binds to the drug-binding pocket of ABCB1 through an open portal. The residues of this drug-binding pocket are represented by cyan colored spheres and bind the drug in an inward facing confirmation. (B) ATP shown in yellow binds to the nucleotide-binding domain of ABCB1 and trigger an outward facing conformational change in ABCB1. Such confirmation sterically occludes the entry of the drug to the inner leaflet of the plasma membrane facilitating drug efflux to the outside. Structural model were adopted from reference [159].

A case in point is a mutations arising from single nucleotide deletion that leads to an inactive ABCC7 that impairs the transport of chloride ions, a phenomenon observed in patients with cystic fibrosis. ABCC7 is thus referred to as CFTR transporter (cystic fibrosis transmembrane conductance regulator) [154, 160, 161]. Other ABCC members transport glucurionic and glutathione conjugates of steroid hormones, bile salts and xenobiotics such as doxorubicin

and lipid peroxidation byproducts 4HNE (4-hydroxynonenal) out of cells [154, 162, 163].

Despite the varied substrates exported, there is no clear evidence for the export of tamoxifen by ABC transporters, however glucuronate conjugated to tamoxifen could potentially be a substrate for ABCC transporters, since ABCC are known to transport glucuronide conjugates [162, 163]. UDP-glucuronic transferase (UGT) enzymes primarily UGT1A8, UGT1A10 and the UGT2B7 and UGT2B15 are known to participate in the glucuronidation of tamoxifen using the UDP-glucuronic acid as a susbtrate [158, 164, 165]. Glucuronic acid is similar to a glucose molecule but it has carboxylic acid instead of an aldehyde group and participates glucuronidation, which is important step in xenobiotic metabolism [166].

Metabolism of tamoxifen happens primarily in the liver and follows two different pathways that are either 4-hydoxylation and/or N-demethylation of tamoxifen. The cytochrome p450 family of enzymes primarily CYP2D6, CYP3A4/5 catalyzes these processes. The hydroxylation of tamoxifen to 4HT is catalyzed by CYP2D6 whereas CYP3A4/5 catalyze N-demethylation reaction resulting N-desmethytamoxifen [167, 168] (Fig. 1.8). These different tamoxifen metabolites are glucuronidated or sulfonated by the enzymes UGT and sulfotransferase, respectively, followed by export through the ABCC transporters [158]. It is interesting to note that most of these enzymes involved in tamoxifen metabolism and excretion are polymorphic allowing different individuals to metabolize tamoxifen at different rates and as such the steady

state concentration of tamoxifen in different people are different due to this varied rate excretion [158].

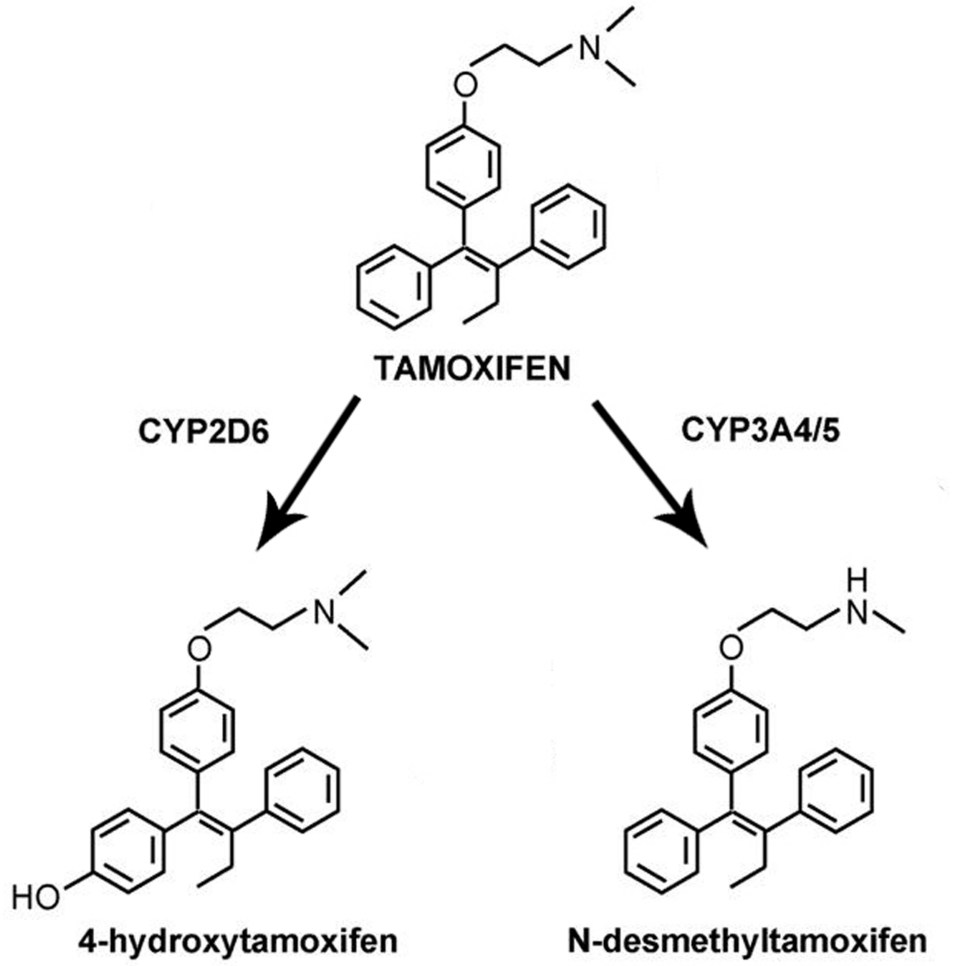

Figure 1.8: Structure of tamoxifen and its metabolites.

Tamoxifen has a characteristic tri-phenyl structure and is metabolized by hydroxylation or demethylation resulting in 4-hydroxytamoxifen and N-desmethyltamoxifen respectively. Picture adapted from reference [169].

The ABC transporters, specifically the ABCC1-3, ABCB1 and ABCG2 are often overexpressed in solid tumors and cancer cell lines and have been linked to chemotherapeutic drug resistance [158, 163]. For this reason, the ABCC family is colloquially called MRP (multidrug resistance associated protein)

whereas the name MDR (multi-drug resistance transporter) or p-glycoproteins (permeability glycoprotein) has been given to ABCB1 protein due to its well-known role in exporting various chemotherapeutic drugs and causing resistance. On the other hand ABCG2 is called BCRP1 (breast cancer resistance protein 1) [154, 158]. These nomenclatures given by different research groups to the ABC transporters highlight their important role in chemotherapeutic resistance and are hence collectively referred to as multi drug resistance transporters (MDRT). Interestingly, under conditions of oxidative stress, Nrf2 has been shown to mediate the expression of ABCC1-3 and ABCG2 in different cells [170-173]. This underlines the central role of Nrf2 along with MDRTs in mediating chemo-resistance.

The next section will discuss the development of chemo-resistance and the different factors that aid and abet such processes like phospholipase D, autotaxin, and RALBP1. The deregulated actions of these proteins can culminate in treatment failure.

1.7 Chemo-resistance of tumors to therapies

Different treatment such as taxanes, antracylines, cyclophosphamides, cisplatin, tamoxifen and aromatase inhibitors are some of the common drugs prescribed for cancer management. These drugs effectively mitigate tumor progression for some time. Sadly however, the once treatable tumor will eventually develop resistance to prescribed drugs leading to a phenomenon known as chemo-resistance [3, 7, 174, 175]. The failed treatment due to this acquired chemo-resistance manifests in metastases and result in death of

patients. Chemo-resistance can be divided in to intrinsic resistance and acquired resistance, the distinction between two lies on the basis of initial response to therapy, with acquired resistance providing a positive initial response as opposed to negative initial response observed in intrinsic resistance [174, 175]. The thesis will focus mostly on acquired chemo-resistance.

Chemo-resistance can be attributed to cellular factors at the level of tumor cells or be caused by pharmacological factors that trigger systemic effect and result in decreased drug bioavailability at the tumor site. Both factors could contribute to chemo-resistance [174]. An example of a pharmacological factor that leads to chemo-resistance is the increased tamoxifen execration caused by elevated activity of the cytochrome p450 family of proteins that metabolize tamoxifen. This results in lower systemic tamoxifen in circulation and subsequent tamoxifen resistance [158]. On the other hand chemo-resistance that arises from tumor cells is recognized as the primary cause for treatment failure [174]. It is caused by various cellular factors through a multitude of pathways such as decreased intracellular drug concentration via expression of MDRTs [172, 174, 176] or changes in tumor cells affecting drug to target interaction [174]. For instance chemo-resistance to drug like fluorouracil and tamoxifen have been attributed to increased expression of thymidilate synthase [177, 178] or decreased expression of estrogen receptor respectively [3]. Alternatively cancer cells could become resistant by changing their cellular response to drugs through the deregulation of proteins. An example would be

deregulating proteins involved in ROS detoxification process, which can lead to elevated capacity to mitigate cellular stress, or deregulating proteins that signal for survival [174, 175]. Such changes in cellular responses are brought about by either overexpression or down-regulation of key cellular proteins. An example of which is methylation-induced down-regulation of Keap1 protein, which results in increased levels of Nrf2 [153], described in the previous section.

It now understood that multifactorial processes lead to chemo-resistance and therapies that aim to target a single mechanism of resistance have been largely unsuccessful. Interestingly tumors that acquire resistance to a particular drug also develop cross-resistance to other structurally and functionally distinct drugs showing the interconnected routes for the progression to a chemo-resistant phenotype [174].

Overall, individual differences arising from polymorphism and the increased adaptability of tumors makes the search for magic bullet that targets all the different mechanism of resistance, a difficult prospect. Therefore, it is most sensible to target the problem of chemo-resistance through targeted therapies that are customized to the particular tumor and also tailored towards the pharmacological characteristics of each individual patient. The success of such endeavors depends largely on the identification and molecular characterization of drugs and their mechanism of actions, which will undoubtedly aids in the customization of treatments. The next subsection will discuss the role of autotaxin and its enzymatic function that make it a key

player in the development of chemo-resistance and an excellent prospect for targeted therapy.

1.7.1 Role of Autotaxin in chemo-resistance

ATX (Autotaxin) was originally isolated in 1992 from media derived from A2058 human melanoma cells. While studying the motility of tumor cells, Stracke et al. discovered that these melanoma cells secreted an autocrine motility factor, which they purified, sequenced and named autotaxin [179]. ATX is a member of a pyrophosphatase/phosphodiesterase family and it is also known as ecto-nucleotide pyrophosphatase/phosphodiesterase family member 2 (ENPP 2). It was so named due to its sequence homology to plasma cell glycoprotein-1 (PC-1) [180], which has nucleotide pyrophosphatase and phosphodiesterase (NPP) activity [181, 182] allowing it to degrade nucleotide phosphates. As ATX is a secreted protein, it was called ENPP2 with PC-1 being named NPP1 [183, 184]. However, later studies on the lysophphospholipase D activity in serum identified the enzyme responsible for such activity was ATX. The lysophphospholipase D of ATX uses LPC (lysophphosphophatidyl choline) as a substrate and catalyzes the removal of choline group resulting in LPA (lysophosphatidate) as a product [185-187]. Later findings showed that ATX has a much lower K_m value for LPC as compared to that of nucleotide phosphates indicating that LPC is a preferred physiological substrate of ATX. In fact, the physiological function of ATX is to produce LPA and not to degrade nucleotide phosphates [185, 186].

Physiologically, ATX and LPA play major roles in forming the embryonic vasculature and stabilizing blood vessels during embryonic development. This is illustrated by the observation that ATX-knockout mice die at embryonic day 9.5 with profound vascular and neural tube defects [188-192]. In wild-type mice, extra-embryonic endothelial cells create a vascular network connecting with the embryo, whereas the ATX-knockout mice become necrotic due to the lack of vasculature and are thus reabsorbed. Consistent with conditions of malformed vasculature and hypoxia, these knockout mice up-regulate the expression of VEGF (vascular endothelial growth factor) [188, 189]. Such a role of ATX highlights its importance in the normal vascularization process. ATX is also important in tissue repair since the local production of LPA promotes re-epithelialization and wound healing. This role of ATX is reinforced by findings of increased ATX activity in blister fluids [193] and also by the fact that its product LPA promotes platelet aggregation, migration of fibroblasts into a wounded area, which stimulates angiogenesis and healing [194, 195].

ATX is expressed in High Endothelial Venules (HEV) of lymph nodes and other secondary lymphoid tissues [184, 196], which are characteristic venules that allow lymphocytes in the blood to directly cross in to the lymph nodes [197]. ATX also modulates lymphocyte trafficking by promoting lymphocyte extravasation [198-200], which is a necessary step in initiation of inflammation. Moreover, in damaged and inflamed tissues, ATX mediates inflammatory cytokine production and recent studies have also found ATX to

be important for myeloid differentiation in human bone marrow further emphasizing the role of ATX in immunological systems [198-201].

Under pathological conditions such as cancer, asthma, rheumatoid arthritis and other inflammatory diseases these normal physiological processes become dysfunctional with increased ATX and LPA signaling contributing to disease progression [184]. In regards to cancer, ATX was found to be among the top 40 most up-regulated genes in metastatic cancers [202]. This is further corroborated by studies that show that mice that overexpress ATX develop spontaneous metastatic mammary tumors [203].

After the initial identification of ATX in stimulating motility in melanomas, the invasive and aggressive natures of several cancers of the breast, ovarian, thyroid, kidney, lung, liver (hepatocellular carcinoma) and of the brain (neuroblastoma and glioblastoma multiforme) have been correlated with the activity of ATX [184, 204, 205] and signaling from its product LPA. Furthermore, pharmacological inhibition of ATX activity delayed breast tumor growth and metastases to lung in 4T1-syngenic mouse model of breast cancer further highlighting its the vital role of ATX in tumor progression [206].

Cancers such as neuroblastomas, melanomas and thyroid carcinomas produce copious amounts of ATX. However, ATX does not necessarily need to be produced by the tumors themselves such as in breast cancers, which produce very little ATX. Instead, ATX is produced by other cells like adjacent adipocytes and other stromal cells to aid in the progression of breast cancer [184, 207-209]. For instance dissemination of primary breast cancer to bone,

liver and lung is a quite common occurrence [210] and recent work showed that such metastasis to bone is made possible by the activity of platelet-derived ATX [211]. The platelet-derived ATX could then interact with $\alpha_V\beta_3$ integrins on breast cancer cells [211], presumably producing local LPA. The formation of local LPA could aid in tumor progression, as it is quite well known that the activation of LPA receptors significantly increases tumor growth, angiogenesis and cell migration which causes metastasis and contributes to chemo-resistance [185, 205, 212-215].

Enzymatic function of ATX and Lysophosphatidate formation

LPA is a simple phospholipid with a phosphate head group and a single fatty acid (either saturated or unsaturated) attached at the sn-1 or sn-2 position of the glycerol backbone (Fig. 1.9). Thus, there are different LPAs depending on the fatty acid and the position of the glycerol backbone to which it is attached. LPA mediates most of the biological effects of ATX through its ability to activate at least six G-protein coupled receptors [216-220]. The action of ATX on extracellular LPC provides the major route for the production of circulating LPA. This is illustrated by experiments where ATX activity is inhibited and this leads to a dramatic fall in circulating LPA [221-223].

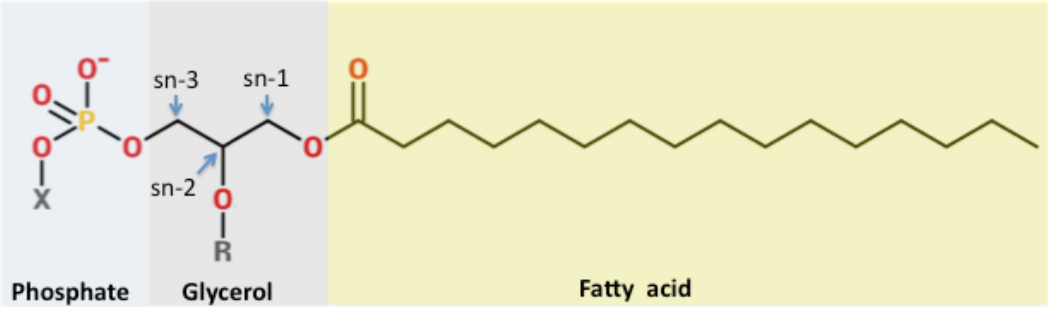

Figure 1.9: General structure of phospholipids

The R group can either be hydrogen or fatty acid and the X group can also be a hydrogen atom or head group such as choline or ethanolamine. If both the R and X group are hydrogen the resulting compound is called lysophosphatidate and if the X group is replaced with choline it is called lysophosphatidylcholine. On the other hand the attachment of fatty acid at the R group will make the compound phosphatidate or phosphatidylcholine, respectively.

Lysophosphatidylcholine (LPC) (Fig. 1.9) is the most abundant phospholipid in blood plasma where it reaches concentrations of >200 μM in human beings [224]. The liver and probably other organs secrete unsaturated LPC [225]. Saturated LPC is produced mainly by lecithin:cholesterol acyltransferase acting on the phosphatidylcholine that is present in high density lipoproteins by transferring the unsaturated fatty acid (mainly linoleate) to cholesterol [226]. These reactions provide a continuous supply of LPC that is readily accessible to most tissues.

It was proposed that the activity of ATX is partially regulated by feedback inhibition from LPA or S1P, the sphingolipid analogue of LPA [227]. However recent study showed that under physiological conditions such feedback inhibition of the ATX activity by LPA is unlikely since the substrate LPC is in high excess compared to the product LPA [228]. Nonetheless, the same study showed that LPA through activating the PI3K decreased the expression of ATX

and as such the feedback regulation by LPA occurs indirectly through mediating ATX expression rather than activity [228]. Under the context of inflammation, high levels of LPA coexist with high ATX levels and this possible since increased levels inflammatory cytokines circumvent the block in the expression of ATX by LPA, which is compatible with the findings of feedback through expression of ATX rather than activity [184, 228].

In addition to ATX, there are other pathways for producing extracellular LPA. The first involves the action of secreted phospholipase A2, which converts phosphatidate (PA), which is present in micro-vesicles released during inflammatory reactions, to LPA [229]. There is also evidence that group VIA phospholipase A_2 (Ca^{2+}-independent phospholipase A2β, iPLA2β) produces extracellular LPA by human epithelial ovarian cancer cells [230, 231]. Tumorigenesis and ascites formation were decreased in iPLA2β$^{(-/-)}$ null mice compared with wild-type mice [231]. LPA and LPC concentrations were decreased in the tumor microenvironment of iPLA2β $^{(-/-)}$ mice to about 80% of that in wild-type mice. LPA, but not LPC, stimulated cell migration and invasion when iPLA2β expression was knocked down *in vitro*. LPA, but not LPC, also enhanced ascites formation *in vivo* by about 5-fold and tumorigenesis in iPLA2β $^{(-/-)}$ mice [231].

1.7.2 Metabolism of extracellular LPA

Plasma LPA concentrations are normally <1 μM, but they can reach >10 μM in patients with cancer, as reviewed in [205], depending partly on LPA production by ATX. The other major component in regulating the concentration of extracellular LPA is its degradation by lipid phosphatase phosphatases (LPP) (Fig. 1.9). These are family of three enzymes (LPP1-3) that are able to dephosphorylate a large variety of bioactive lipid phosphates and pyrophosphates, including LPA [232]. The LPPs are expressed on the surface of cells with the active phosphatase site being exposed to the outer leaflet of the plasma membrane [233]. Increasing the expression of LPP1 on the surface of fibroblasts increase their ability to degrade various extracellular lipid phosphates including LPA, phosphatidate (PA) (Fig. 1.9) and ceramide 1-phosphate [234].

The activity of ecto-LPP on LPA is to quench its active signaling role by converting LPA to monoacylglycerols (MAG) since MAGs with the exception of 2-monoarachidonoylglycerol (an endocannabinoid) are not signaling molecules. The dephosphorylation of LPA by LPP is very rapid such that the half-life of circulating LPA is about 3 min in mice [222, 235]. The LPP isoform, LPP1, plays a major role in circulating LPA degradation based on experiments in LPP1 hypomorph mice (*Ppap2a*$^{tr/tr}$), which have 35-95% decreases in LPP activity in most tissues, except the brain [235]. Plasma LPA concentrations in these LPP1 hypomorph mice are significantly increased compared to control mice, and the half-life of intravenously injected LPA was about 4-fold higher in

the *Ppap2a*$^{tr/tr}$ mice compared to controls ($t_{1/2}$ = 12 min *versus* 3 min). Although other studies have shown that exogenously supplied LPA is rapidly up-taken by the liver with half-life of 30 sec and this is independent of degradation or accumulation [236, 237]. These discrepancies between half-life of LPA is due to variations in measurements in those studies, with the earlier studies measuring LPA remaining in systemic circulation after the majority of the injected LPA has probably been sequestered by the liver. On the other hand the more recent studies measured half-life LPA relative to initially injected LPA levels. Overall, the concentration of LPA in circulation as well as in the tumor microenvironment is mainly determined by the balance between the production of LPA by ATX versus hydrolysis by the LPPs [238].

Also the ecto-activity of LPPs, mainly LPP3 contribute to the degradation of S1P [237]. S1P can activate up to five G-protein coupled receptors and also plays a crucial role in the ceramide-S1P rheostat, which dictates the commitment of cells in to apoptosis or survival pathways, described in Section 1.5.1. Increased S1P production and secretion is associated with increased chemo-resistance and a stimulation of angiogenesis for the growing tumour [238]. Therefore, LPP3 could also function to regulate the effects of S1P on these processes [237].

The functions of LPPs are not just limited to extracellular degradation lipid phosphates, especially since LPPs are expressed in the Golgi apparatus [239] and the endoplasmic reticulum[240] with the active site probably positioned towards the lumen of these organelles[184]. Hence, inside cells

LPPs could affect signaling by degrading lipid phosphates and such role is observed in studies that show that overexpression of LPPs blocks thrombin-induced ERK activation [241]. Thrombin being a protein and not a lipid phosphate supports the intracellular role of LPPs in effecting changes downstream of receptor activation. In addition other studies showed that increased LPP1 expression blocked protease-activated receptor-1 (PAR-1) peptide and wls-31 (LPA $_{1/2}$ receptor agonist) mediated migration along with generation of Ca^{2+}-transients [242, 243]. As wls-31 cannot be dephosphorylated [242] such findings further consolidate the intracellular functions of LPPs.

The expression of LPP1 and LPP3 is very low in several cancer cells and a recent study showed that lentiviral expression of LPP1 in breast cancer cells significantly attenuated mouse in vivo tumor growth and metastasis in mice [243]. Another study showed that LPP3 over-expression decreases growth and colony-formation by ovarian cancer cells by degrading extra-cellular LPA [244]. Therefore, the increased plasma concentrations of LPA that are associated with cancer patients could in part be explained by this repression of LPP in cancer [244-247]. Consequently re-expression of LPP1/3 could be a potential for cancer therapy [244, 248] and this is supported by studies using gonadotropin-releasing hormone that increased ecto-LPP expression resulted in anti-proliferative effects in ovarian cancer [246]. Additionally, tetracycline mediated increase in LPP expression was shown to decrease LPA levels both *in vivo* and *in vitro* [237] and thus has promise in attenuating cancer

progression as well. However, not much is known about the link between LPP2 and cancer with expression study in fibroblast showing LPP2 causes premature entry in to cell-cycle with knockdown having an opposite effect [249]. Moreover, gene microarray identified LPP2 to be overexpressed in transformed cells as well as different cancer cell lines and knockdown of LPP2 blocked anchorage-dependent growth of cancer cells [250, 251].

In general the combination of high ATX and low LPP1/3 exposes cancer cells to a microenvironment with elevated extracellular LPA concentrations. This promotes tumor growth, angiogenesis, metastasis and chemo-resistance[184, 238].

1.7.3 Signaling of lysophosphatidate and its effect in cancer

Extracellular LPA has several roles; one of its physiological roles is in stimulating the proliferation and migration of fibroblasts to facilitate wound healing [194, 195]. On the other hand, LPA is found in high concentrations in ascites fluid and plasma of ovarian cancer patients, where it has been shown to promote ovarian tumor progression [195]. LPA receptors are also overexpressed in many cancers[205] and similar to ATX, overexpression of LPA_{1-3} receptors in mice leads to spontaneous metastatic mammary tumors [203] demonstrating the critical role of LPA signaling in cancer development. This is reinforced by studies that show that LPA led to an increase in VEGF production stimulating angiogenesis [252], which is crucial for tumor progression. LPA also decreases the expression of tumor suppresser, p53 that aids in cancer cell survival[253]. Generally LPA's potent action as survival

factor has been shown in ovarian and breast cancer cells, macrophages, fibroblasts and also neonatal cardiac myocytes [253-256].

The role of LPA in cancer is not only restricted to tumor progression but also extends to chemotherapy and radiotherapy resistance. This aspect is demonstrated by studies that show LPA signaling strongly antagonizes paclitaxel-mediated cell death in breast and melanoma cancer cells[205, 238, 254, 257]. Moreover LPA signaling confers resistance to other chemotherapeutics such as carboplatin [258] and doxorubicin [259] perturbing the cytotoxic action of these drugs along with blocking radiation-induced cell death [205, 260, 261]. Additionally, our laboratory recently showed that signaling from LPA stabilizes Nrf2 leading to increased Nrf2 levels and downstream anti-oxidant genes and MDRTs [259]. This study links LPA to anti-oxidant defense system described in Section 1.6.

The actions of LPA can be explained by the different signaling mechanisms that LPA utilizes to produce its effects and is mediated through at least six G-protein coupled receptors: LPA_1/EDG2, LPA_2/EDG4, LPA_3/EDG7, LPA_4/GPR23/p2y9, LPA_5/GRP92 and LPA_6/p2y5 [217, 218]. The first three LPA receptors belong to Edg (endothelial differentiation gene) family while LPA_{4-6} belong to different family of receptors known as P2Y purinergic family of receptors [262, 263]. The expression of these receptors is cell type specific, allowing different cells to respond differently to a common signaling molecule LPA. The binding of LPA to its cognate receptor then signals through pathways involving the G-proteins G_i, G_s, G_q, and $G_{12/13,}$ all of which having a distinct

downstream effects (Fig. 1.10). The signaling cascade could involve the activation of the ERK pathway, PI3K and Akt pathway, mTOR, Ca^{2+}-transients and the small G-proteins Rac, Rho and Ras through which LPA can mediate cellular activities such as cell division and migration [256, 264, 265].

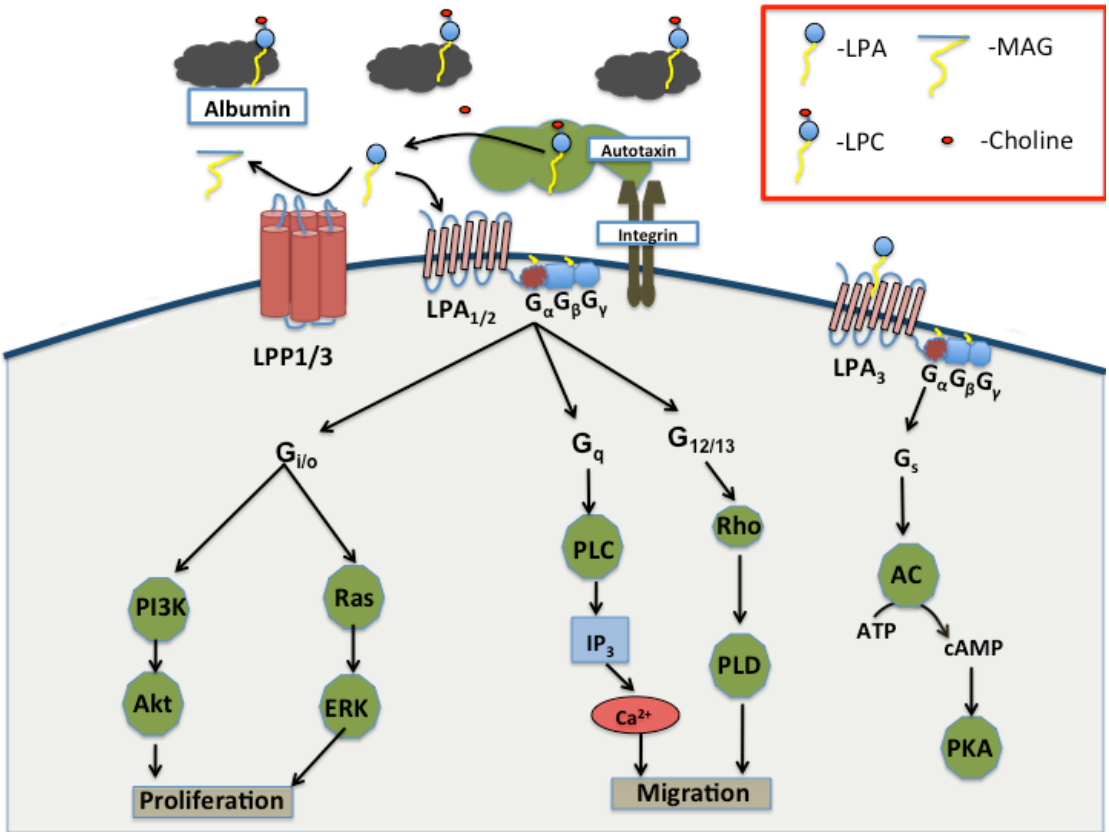

Figure 1.10: Autotaxin–lysophosphatidate-signaling axis.

ATX I converts the abundant LPC to LPA, which binds to its cognate LPA1–6 receptors (LPA1–3 are shown) to activate multiple signaling pathways, leading to proliferation and migration of target cells. LPA3 can couple to Gs; it can also couple to Gi/o and Gq but not G12/13. Moreover, LPA can directly or indirectly activate other signaling pathways not shown in the figure. LPPs on the other hand, regulate the ATX–LPA signaling axis by dephosphorylating LPA to the biologically inactive MG.

AC: Adenylate cyclase; ATX: Autotaxin; IP3: Inositol 3-phosphate; LPA: Lysophosphatidate; LPC: Lysophosphatidylcholine; LPP: Lipid phosphate phosphatase; MG: Monoacylglycerol; PKA: Protein kinase A; PLC: Phospholipase C; PLD: Phospholipase D.

LPA can also increase SK1 mRNA levels and knocking down SK1 blocked LPA-induced migration and invasion of MNK1 gastric cancer cells [266], suggesting that some of LPA's actions are mediated through S1P formation. Like LPA, S1P is a potent stimulator of angiogenesis. S1P is formed during platelet activation and is also secreted by tumor cells [267, 268]. It is known that S1P makes up about 80% of the stimulating activity for endothelial cell migration present in plasma [267], which highlights the important role S1P in neovascularization process. S1P is formed through the action of sphingosine kinase isoenzymes (SK1 and SK2) on sphingosine [100]. S1P signals through five different G-protein coupled receptors that like LPA_{1-3} belong to the Edg family of receptors [262]. S1P thus provides another route for an extracellular lipid to promote tumor development through activation of cell division by stimulating the ERK pathway and also increasing the level of Ca^{2+} transients [267, 269]. Interestingly, the estrogen, 17β-estradiol was shown to stimulate SK1 activity in a non-genomic mechanism in MCF-7 breast cancer cells [270]. The same study also showed that this estrogen activation of SK1 leads to export of S1P through the MDRTs ABCC1 and ABCG2 leading to S1P inside out signaling [268]. Hence MDRTs have an extra axis to initiate tumor progression through secreting S1P in addition to exporting out toxic by products of oxidation and chemotherapeutic drugs and causing chemo-resistance. S1P is also exported out of cells by the transporter Spinster 2 (Spns2) [271].

Overall, the strong association of autotaxin expression with breast cancer cell survival, growth, migration, invasion, and metastasis coupled with

the actions of LPA and S1P in many cancers firmly establish LPA and S1P as important pro-survival signals in cancer biology [100, 212, 213, 215]. The next section will discuss the enzyme phospholipase D activity, which is acutely activated by LPA. Moreover the activity of PLD links the LPA signaling to S1P formation.

1.7.4 Phospholipase D signaling pathways and its role in cancer

Phospholipase D (PLD) is an enzyme that catalyzes the hydrolysis of the phosphodiester bond in phosphatidylcholine (PC) to phosphatidate (PA) and a free head group, choline. PLD can also use other amine containing glycerophospholipids as a substrate such as phosphatidylethanolamine (PE) to generate PA and free head group like ethanolamine [272, 273]. In addition, PLD can catalyze transphosphatidylation reaction, which is the preferential transfer of primary alcohol instead of water to generate phosphatidylalcohol [272]. Thus due to this transphosphatidylation reactions primary alcohols have been widely utilized to block PLD activity. However, phosphatidylalcohols are not overtly inert and can imitate some of the signals given out by PA [273]. In this thesis we have used transphosphatidylation reaction solely to assess PLD activity (detailed in Chapter 2 of methods section) and instead relied on pharmacological inhibitors [274] to block PLD actions.

The PLD substrate PC is one of the most abundant phospholipid on membranes typically making up 30-50% of glycerophospholipids and basal PA levels make up 2-6% of cellular membranes, which is about 10% of the total PC levels [272, 273, 275]. Thus the PA generated by PLD is an important

intracellular signaling lipid and has diverse cellular functions such as vesicle trafficking, exocytosis, cellular metabolism and cellular proliferation and survival [272, 273]. It is thus no wonder that the PLD super family is found in different kingdoms of life such as prokaryotes, fungi, yeast and other eukaryotic species. PLDs even have functions in viruses [276]. However, the PLD superfamily also consists of other enzymes such as endonucleases and cardiolipin (CL) synthase [277, 278].

To be part of the PLD super family proteins must have a characteristic HKD domain, which is a stretch of sequence with the amino acids histidine, lysine, and aspartic acid of the general formula $HxKx_4Dx_6G(G/S)$, with 'x' denoting any amino acid [272, 273]. There are other non-HKD PLDs in addition to classical PLDs that hydrolyze PC to PA. The non-HKD PLDs also generate PA from other non-PC substrate such as glycosylphosphatidylinositol (GPI)-PLD [273, 279]. GPI-PLD release GPI anchored protein from membranes generating PA [279], however in the thesis will focus only on the two mammalian PC hydrolyzing PLDs, PLD1 and PLD2.

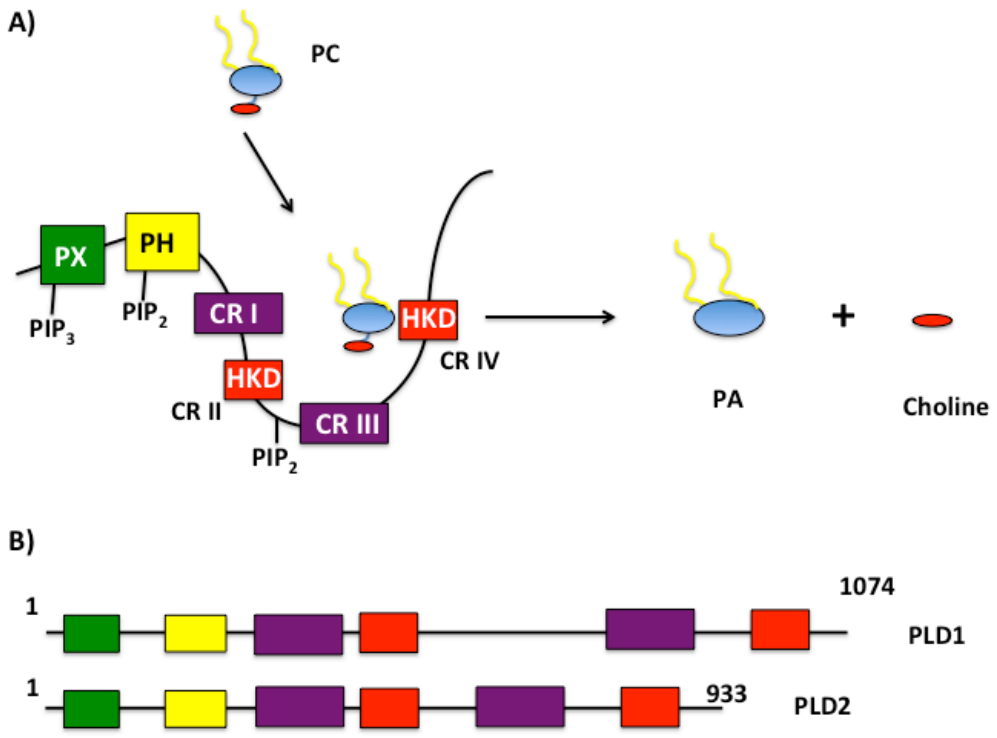

Figure 1.11: The domain structure and activity of Phospholipase D

(A) Phospholipase D is composed of four conserved regions CRI-IV, a PX domain that binds to the phosphoinositide, PIP3, and PH domain that binds to PIP2 such binding to PIP2 and PIP3 affects the membrane localization of PLD. PIP2 can also bind to the polybasic region between CRII and CRIII affecting PLD activity by inducing a conformational change that affects the binding of the substrate PC (phosphatidylcholine) to the catalytic core. PC binds to the catalytic core that is composed of the duplicate HKD domains. The histidine residues in HKD domains facilitate the hydrolysis of PC to PA (phosphatidate) and choline group. (B) Domain structure of PLD1 shown here from residues 1-1074 and PLD2 from 1-933. Both PLDs have similar motifs however PLD2 does not have the loop region found between CRII and CRIII of PLD1. Diagrammatic illustrations were adapted from reference and are not drawn to scale [272, 273].

The activity of PLD was first described in plants and the gene was initially cloned from castor beans [280]. The sequence information obtained from the cloning allowed the identification of the two main mammalian phospholipase D, PLD 1 [281] and PLD2 [282]. As above described above, based on the ability to hydrolyze PC, PLDs have been identified in prokaryotic and eukaryotic species.

Nevertheless, cloning and subsequent sequence analyses from the different organisms revealed little homology between the different PLDs with four very small regions of sequence showing an actual homology [272]. Even mammalian PLD1 and PLD2 are only 51% identical with the most notable homology within the central catalytic core [283]. These homologous sequences within the catalytic core of PLDs are referred to as CRI-IV (conserved regions) with the HKD domain being the most highly conserved of all and are found in both CR-II and CR-IV (Fig. 1.11) [272, 273].

The duplicate HKD domains within PLDs are vital for the reaction mechanism, with the first histidine acting as nucleophile and attacking the substrate PC. On the other hand, the second histidine donates a proton to the choline-leaving group allowing the formation phosphatidylhistidine intermediate with the PLD enzyme. To replace the proton-donated to choline group, the second histidine in the HKD domain will abstract a proton from water resulting in an activated water molecule which can then hydrolyze the phosphatidylhistidine intermediate to the final product PA (Fig.1.10) [272, 273, 284, 285]

Located towards the N-terminal side of the catalytic core, the primary structure of PLD1 and 2 are composed of a tandem regulatory Pleckstrin (PH) and Phox (PX) homology domains (Fig. 1.11), which bind to phosphatidylinositol lipids, anchoring PLDs on membranes and regulating their intracellular localization [286, 287]. This is demonstrated by studies that show mutation of amino acid residue R179 in the PX domain of PLD1 hinders its

binding to the phosphoinositide, PIP_3 [288, 289], which prevents activation and membrane recruitment of PLD1 after stimulation by platelet-derived growth factor (PDGF) [289]. The PX domain of PLD1 preferentially binds to PIP_3 instead of mono or di-phosphorylated phosphoinositide [288]. As such inhibiting PI3K, the enzyme that phosphorylates phosphoinositides at the D3 position of the inositol ring [290], have been shown to also block PLD activated by the insulin receptor [291]. On the other hand mutation of key residues in the PH domain known to mediate phosphoinositide binding [292] resulted in the abolition of PLD2 activity in vivo[293]. Nonetheless, when the same mutant protein was immunoprecipitated and assayed in vitro it displayed similar activity to the wild type protein [293] suggesting that the PH domain regulates PLD activity through protein localization. Moreover other studies with truncation mutants of PH/PX domains showed unaltered in vitro PLD activity *in vitro*, indicating that PH/PX domains are not required for the catalytic activity but required for membrane recruitment [272, 273].

Despite the presence of the tandem PH and PX domain on PLD1 and 2, under basal conditions PLD1 is mostly found on perinuclear and intracellular membranes of secretory vesicles, lysosomes, endosomes, Golgi, and endoplasmic reticulum [294, 295], whereas PLD2 is found primarily on plasma membrane [273, 283, 296]. However in studies that used phorbol-12-myristate-13-acetate (PMA) to stimulate fibroblast and COS-7 cells, PLD1 was recruited to the plasma membrane [295, 297]. Thus indicating that when stimulated PLD1 can move from its basal localization.

As described above phosphoinositides, PIP_2 and PIP_3 mediate the intracellular localization of PLDs through binding the PH and PX domain respectively. In addition to regulating localization PIP_2 also mediates the catalytic activity of PLDs by binding to regions other than the PH/PX region, with studies locating an extra PIP_2 binding site on the polybasic region between CRII and CIII of the catalytic core [298]. The PIP_2 binding induces a conformational change in the catalytic core of PLDs that facilitates PC to bind to the active site [299]. As such for robust activity both PLDs are highly dependent on the PIP_2, phosphatidylinositol 4,5-bisphosphate [272, 273].

The regulation of PLD activity is quite complex and phosphoinositides are not the only modulators of PLD activity with multiple other cellular factors such as small GTP binding proteins (of the Arf, Rho and Ral family), Ca^{+2}, PKC and phosphorylation all known to regulate the activity of PLDs [272, 273]. A list of some of the known activators of PLD is provided in Table 1. In addition extracellular ligands such as LPA, EGF and insulin through binding to receptor tyrosine kinases and G-protein coupled receptors can induce activation of PLD [272, 273]. Also due to different subcellular localization as well as difference in overall sequence homology, the extent PLD1 and PLD2 regulation is also quite different. For instance, the small G-protein Arf (ADP-ribosylation factor) that consists of six members [300], Arf1-6 are all recognized activators of PLD [273] with Arf1 and Arf3 specifically activating PLD1 [301] while Arf4 and Arf6 activate PLD2 [302, 303]. The specific Arf-PLD interaction site has not been conclusively determined but studies have shown that the N-terminal side of

PLD is not required for Arf activation [273]. Moreover, Arf can also regulate PLD activity indirectly through regulating PIP5K (Phosphatidylinositol 4-phosphate 5-kinases) activity [273, 304], which can in turn activate PLD through catalyzing the formation of phosphatidylinositol 4,5-bisphosphate. Similarly, other G-proteins of the Ral and Rho family have been shown to activate PLD1, but as opposed to Arf, the Ral and Rho family had no influence on PLD2 [273, 282]. The Rho family of G-proteins, more specifically RhoA, are a direct activator of PLD1 through binding to the non-conserved C-terminal side of PLD1 and this interaction is thought to enhance substrate binding [305, 306]. On the other hand Ral G-proteins are an indirect activators of PLD1 [273]. Interestingly, the Ral G-proteins, RalA is found constitutively bound to PLD1 [307] and may thus potentiate PLD1 activation through modulating the activation of other small G-proteins such as Arfs [273]. Such perspective for Ral- mediated PLD activation is supported by studies that identified a ternary complex of Arf, RalA and PLD1, with inhibitors of Arf activation also leading to a decrease in RalA-induced PLD1 activation [273, 308].

Proteomics studies have identified that both PLD1 and 2 are phosphorylated at several residues [309, 310] with serine/threonine and tyrosine kinases being implicated. However, the functional significances of a particular phosphorylation event is not very clear with different research groups ascribing phosphorylation as having either a stimulatory or inhibitory role on PLD. Presumably, the effect of the different phosphorylation events is dependent on the cell system and stimulation used for the study [273]. A case

in point is the activation of PLD1 by PKC on fibroblasts by direct protein-protein interaction without requiring catalytic activity [311] and thus without the need for phosphorylating PLD, with the isoforms PKC *α*, *β*1 and *β*2 being implicated in such activation of PLD1 (Table.1). On the other hand in neutrophils, PKCα activates PLD1 through phosphorylation [312] and furthermore the activation of PLD2 by PKC isoforms PKC *α* and PKC*δ* also requires phosphorylation [309, 313].

It is known that covalent modification of proteins by phosphorylation not only mediates activity of the proteins but also serves as a docking site for other proteins. Such docking sites promote the close interactions of different proteins. As such PLD2 is tyrosine phosphorylated at residues Y169/Y179 allowing the binding of the well-known adaptor protein Grb2 via its characteristic SH2 domain [314]. Grb2 also posses an SH3 domain, which can bind to son of sevenless (SOS), a guanine nucleotide exchange factor (GEF) for Ras. Thus the binding of Grb2 to PLD2 links it to SOS and thereby activating the oncogenic small G-protein Ras in the process [315, 316]. The PLD2-Grb2 interaction is localized at the PX domain of PLD2 and thus catalytic inactive mutants of PLD2 can also bind to Grb2 and possibly recruit SOS as well [314]. In addition to residues Y169 on PLD2, studies have found EGF also modulated PLD2 by phosphorylating different tyrosine residues [273].

Overall studies have showed that some tyrosine residues are inhibitory whereas some are stimulatory and the level of PLD activity may be determined by ratio of inhibitory versus stimulatory phosphorylation on these different residues [273, 314].

Table 1: The Role of phosphatidate and the different regulators of PLD activation.

Signaling from PA-induced by PLD		Activators PLD		
Protein Name	**Role of Phosphatidate (PA)**	**Protein Name**	**Isoform**	**Mechanism**
Raf1	Membrane recruitment	PKC α,β1,β2	PLD1	Protein–protein interaction
PKCε	Membrane recruitment	Arf	PLD1/PLD2	Protein–protein interaction
PKCα, ζ, δ	Activation	RhoA family	PLD1	Protein–protein interaction
mTOR	Activation	PKN	PLD1	Protein–protein interaction
PIP5K	Activation	Rheb	PLD1	Protein–protein interaction
Akt	Membrane recruitment	Ras	PLD1	Indirect protein–protein interaction
Lipin1β	Membrane localization	RaIA	PLD1	Indirect protein–protein interaction
Rac-GDI	Inhibition	AMPK	PLD1	Phosphorylation
ArfGAP1/2	Activation	p90 RSK	PLD1	Phosphorylation
SOS	Membrane recruitment	Cdk5	PLD2	Phosphorylation
PLCβ1, γ1, ε, δ3	Activation	Grb2	PLD2	Protein–protein interaction
NADPH oxidase	Activation	PKCδ	PLD2	Phosphorylation
Rac1	Membrane recruitment	PKCα	PLD1/PLD2	Phosphorylation

mTOR: mammalian Target Of Rapamycin; PKN: Protein Kinase N; Rheb: Ras homolog enriched in brain, a small G-protein; AMPK: Adenosine Monophosphate-activated Protein Kinase; RSK: ribosomal S6 kinase; Cdk5: cyclin dependent kinase 5. Table adapted from reference [273], which provides an extensive catalog of proteins that are activated by activity of PLD and also proteins that modulate PLD activity.

The functions of PLD within cells mainly centers on its product phosphatidate being involved in signaling pathways as second messenger [317, 318]. One such study showed that SK1 (Sphingosine Kinase 1) responds

to PA formation by translocating from cytosol to membranes where SK1 interacts with sphingosine to form S1P [318]. This would inevitably link the activity of PLD to survival pathway mediated with the bioactive lipid S1P, with PLD acting as upstream regulator. In addition to SK1, different laboratories have now identified several different PA targets such as Raf-1 [319], which is a MAP3K and SOS [320], which are both recruited to the membrane through binding to PA formed by PLD. Thus the formation of PA by PLDs can also lead to the recruitment of SOS to the membranes, in addition to the Grb2 mediated SOS recruitment by PLD which does not require catalytic activity. More recently Akt has also been identified as a direct binding target for PA formed by PLD2 in glioblastoma cells [321]. A summary of some of proteins modulated by PA is provided in Table 1 above.

Tumor progression is a complex process that requires multiple steps in order to reach a malignancy and eight hallmarks have been recently proposed to contribute to such neoplastic transformation which are 1) sustaining proliferative signaling, 2) evading growth suppression, 3) activating invasion and metastasis, 4) enabling replicative immortality, 5) inducing angiogenesis, 6) resisting cell death, 7) avoiding immune destruction, and 8) deregulating cellular energetics [322]. PA signaling modulates the activity of various signaling mediators and PLD has the multiple motifs, which can act as docking sites enhancing the actions key signaling proteins linked to cancer. Hence, it is no wonder that increased signaling from PLD has been implicated in each of the eight proposed steps for tumor progression[273]. A case in point is the

transformation of cells with viral oncogenes v-src, v-Ras and v-Raf all showed elevated PLD activity compared to control non-transformed cells [323-325]. Similarly rat fibroblast transformed with the proto-oncogene c-src undergo apoptosis upon serum withdrawal unless PLD1 or PLD2 is also co-expressed [326]. Moreover, the identification of elevated levels of PLD1 and/or PLD2 mRNA and protein in cancerous breast tissue compared to the surrounding tissue also underlines the vital roles of PLDs in oncogenesis [327, 328].

The aggressive nature of tumors is determined by their metastatic potential, to migrate and invade surrounding and distant tissues. As such, PA generated by PLD has been implicated in invasiveness of tumors [329]. This aspect is reinforced by studies of fibroblast migration towards LPA [330] as well as endothelial cells migration towards S1P [331] both requiring the activity of PLD2. In addition MDA-MB-231 breast cancer cells also need the activity of PLD2 for migration [274]. The association of PLD to metastatic potential tumor is not surprising since PLDs intimately interact with small G-proteins of the Rho family, which are routinely linked to cytoskeletal rearrangement necessary for migration [332].

The next section will discuss RALBP1, which like PLD also closely interacts with the small G-proteins of the Ral and Rho family.

1.7.5 The role of RALBP1 in chemo-resistance

RALBP1 (Ral binding protein 1) was discovered as a novel protein interacting with the small G-protein RalA and mediating clathrin-coated vesicle-dependent endocytosis of cell surface receptors such as the EFGR, insulin

receptor, TGF-β-R [333-335]. However, studies on erythrocytes using the xenobiotic, 1-chloro-2, 4-dinitrobenzene (DNP) showed that these erythrocytes possessed the ability to expel glutathione-conjugated DNP (DNP-SG) in an ATP-dependent manner suggesting the presence of an active transporter [335-337]. The transporter was purified using affinity chromatography and named DNP-SG ATPase due its intrinsic ability to hydrolyze ATP [338]. Interestingly the transporter was also able to export doxorubicin from cells [339, 340]. A decade later, with the advent of highly specific polyclonal antibodies, the immunoscreening of human bone marrow cDNA library for the transporter was possible and DNP-SG ATPase was confirmed to be RALBP1 [340]. This finding was a significant breakthrough since it unified the signaling of the small G-protein Ral, the endocytosis of cell surface receptors and the export of glutathione conjugates and xenobiotics through the RALBP1 protein.

Studies have identified a protein called cytocentrin, which has a 98.4 % amino acid sequence homology to RALBP1. It migrates at a similar molecular weight to RALBP1 on SDS PAGE gels. Cytocentrin, however, has a much shorter half-life compared to RALBP1 and is thought to regulate centrosomal function during mitosis [341, 342]. It is not clear, however, if cytocentrin is a splice variant of RALBP1 or product from a different gene [335]. Thus, more studies need to be done to decipher the distinct contribution of each of the protein in different cell activities.

Sequence studies and domain analysis on RALBP1 reveled that it has multi-functional motifs such as Rho/Rac GAP domain, Ral binding domain,

binding sites for ATP [343, 344] and other proteins such as Reps-1 (RALBP1-binding EH domain containing protein) [345], POB1 (partner of RalBP1) [346] and HSF-1 (Heat shock factor 1) [347]. The presence of these diverse motifs allows RALBP1 to participate in even more functions within cells. Moreover RALBP1 has PKC and tyrosine phosphorylation sites [335].

The RALBP1 interaction partners Reps1 and POB1, both have a polyproline motif allowing them to bind to other proteins with Src homology domain 3 (SH3) such Src kinase, a non-receptor tyrosine kinase, and the well known adaptor protein, Grb2. Grb2 links tyrosine kinases with other protein substrate resulting in phosphorylation and subsequent activation. The protein Reps1 is also important in the clathrin-mediated endocytosis [335].

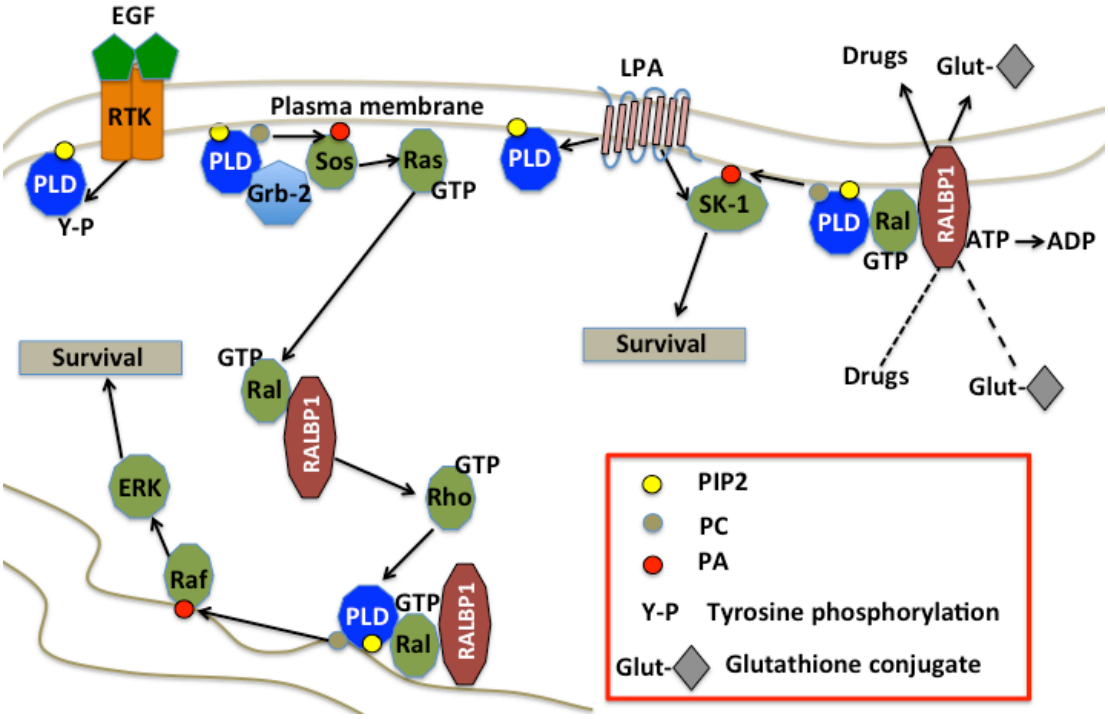

Figure 1.12: Effects of Phospholipase D and RALBP1 in cells.

EGF binds to its receptor and tyrosine phosphorylates PLD regulating its function. PLD localizes to the membrane by binding to phosphoinositides such as PIP2 and at the membrane it can be activated by GPCR stimulated by LPA. The activity of PLD results in the second messenger PA (phosphatidate). PA then binds and recruits key signaling proteins such as SK1, SOS and Raf1 to the membrane. At the membrane SK-1 makes the potent signaling lipid S1P. SOS activates the proto-oncogene Ras and Raf is activated at the membrane, all of which will subsequently elicits survival signals to cells. PLD can also recruit SOS to the membrane and activate RAS by bind to the adaptor protein, Grb2. Ras once activated can in turn activate the small G-protein Ral. Ral indirectly activates PLD through binding RALBP1 that can signal for the increased activity of small proteins Rho. The RALBP1 ATPase domain and use the energy from hydrolysis of ATP to transport drugs like doxorubicin and glutathione-conjugated-xenobiotics (represented by the gray diamond symbol) outside of cells.
EGF: Epidermal growth factor receptor; PLD: Phospholipase D; PC: phosphatidyl choline; PA: Phosphatidate; SK1: Sphingosine kinase 1; SOS: Son of Sevenless; Raf: Rapidly Accelerated Fibrosarcoma; RALBP1: Ral binding protein 1; RTK: receptor tyrosine kinase; LPA: lysophosphatidate; GPCR: G-protein coupled receptor. Diagrammatic illustrations inspired by reference [273].

Once activated, the proto-oncogene Ras will activate Ral GDS (Ral guanine nucleotide dissociation stimulator), which facilitates the dissociation of

GDP bound to Ral and loading with GTP [348-350]. This leads to the activation of Ral and its subsequent binding to RALBP1. This interaction of RALBP1 with the Ras superfamily of G-proteins such as Ral, Rho, and Rac highlights the importance of RALBP1 in cancer biology.

Similar to other G-proteins, Ral transduces downstream signals to its targets either by directly affecting activity, structure, and protein-to-protein interactions or indirectly through activating other G-proteins. However, studies have not yet identified which specific functions of RALBP1 are regulated by its binding to Ral. Presumably Ral may induce a conformational change in RALBP1 leading to change in ATPase activity and/or the nature of interaction to other binding partners, which will ultimately regulate export and endocytosis functions of RALBP1.

The Rho/Rac GAP domain within RALBP1 facilitates the hydrolysis of GTP and cycling Rho/Rac back to the GDP bound state [351]. Rho/Rac G-proteins function by modulating cytoskeletal proteins and as such they regulate cell shape and cell migration [351, 352]. In such a way, RALBP1 provides a link between Ral and Rho/Rac signaling pathways; moreover, signaling through the Rho/Rac also regulates the activity of the stress- activated protein kinase JNK [353]. Thus increased RALBP1 expression could block the sustained activation of JNK through the Rho/Rac pathway [354].

Overall, both PLD and RALBP1 by being Ral downstream effectors feed into the signaling from hyperactive RAS (Fig. 1.12), which is known to initiate neoplastic transformation [355]. Moreover both proteins through their multiple

modular domains interact with a multitude of proteins and thus participate in many cellular functions. Therefore, the deregulations of such versatile proteins either through increased activity or expression will undoubtedly contribute to tumor progression and chemo-resistance.

1.8 Thesis objectives

The purpose of the thesis was to **improve our understanding of how tamoxifen increases the death of cancer cells and how resistance to the therapeutic actions of tamoxifen occurs**. Estrogens, through binding and activating the ERα, promote tumor development. Tamoxifen blocks the proliferative signal given by ERα by acting as a competitive inhibitor for estrogens. Thus, it is well justified that the therapeutic actions of tamoxifen have been largely attributed to its antagonism of ERα. Nevertheless, several research groups have shown that tamoxifen has other effects within cells and modulates the action of several other key signaling proteins, as mentioned in Section 1.3. Moreover, since the link between tamoxifen and ERα was established, other estrogen receptors have been identified. Thus, it is of paramount importance to investigate and update the model for the therapeutic action of tamoxifen, especially since tamoxifen is the most widely used breast cancer treatment in the clinics.

The mechanism/resistance to the action of tamoxifen treatment through the ERα has been studied extensively. Thus, to achieve our objective of understanding the mechanism of tamoxifen action we chose to study the role tamoxifen independently of its effect on ERα. For this purpose, I employed the

use of ERα-positive and ERα-negative breast cancer cell lines to study the common effects of tamoxifen in both types of cells. I also studied the anti-proliferative effect of tamoxifen at cytotoxic, but clinically relevant concentration of tamoxifen. Such cytotoxic concentrations are much higher than what is necessary to act as a competitive inhibitor of the ERα. In addition, I also employed the use starvation medium devoid of estrogens and other growth factors to study the role of tamoxifen. All such strategies were designed to achieve the objective to understand the action of tamoxifen on breast tumors without invoking its well-known actions on ERα. However, my main objective in this thesis was not to show the utility of tamoxifen treatment in ERα negative tumors, which make up only one third of the breast cancer population. I used ERα negative tumors solely as a model system to investigate the action of tamoxifen independently of its effects on ERα.

As part of my thesis objective, I also aimed to extend my cell culture studies and investigate its significance in an animal model. To achieve this I made use of a syngeneic mouse breast cancer model using 4T1 mouse mammary cancer cells which closely mimics tumor progression in human and is an established non-surgical animal model for stage IV human breast cancer. Moreover, 4T1 cancer cells have an added advantage of being ERα-negative allowing the investigation of tamoxifen action independently of ERα.

My second objective was to understand the role of lysophosphatidate (LPA) in mediating resistance to tamoxifen. LPA is known to cause resistance to several other chemotherapeutics, however its effect on tamoxifen treatment has

not been investigated. Moreover, LPA by activating different downstream survival signals could perturb the extra-ERα-action of tamoxifen. Thus I aimed to identify any such signaling pathways that would provide a novel insight into the development of tamoxifen resistance. Furthermore, to achieve my objective of finding a new mechanism of resistance, I also made use of tamoxifen resistant cell-lines. The use of such resistant cell lines helps to identify signaling mechanisms that are dysregulated in the resistant cells by comparing them to their respective syngeneic control.

The final objective of my thesis was to help in the treatment of breast cancer patients by improving prognostic outcomes through the application of my research findings in the cell culture and animal model and applying them into the Clinics. It is thus my hope that the studies presented in this thesis would be translated from ‘bench to bed-side’ and improve the efficacy of tamoxifen treatment by paving the way for the development of novel strategies to overcome chemo-resistance in general and tamoxifen resistance in particular.

2 CHAPTER: Methodology and Materials

2.1 Reagents

Ceramide standards, oleoyl-lysophosphatidate (LPA), 1,2-dioleoly-sn-glycero-3-phosphobutanol (PB, standard) and inhibitors for PLD1 (VU0359595, PLD1i) and PLD2 (VU0285655-1, PLD2i) were purchased from Avanti Polar Lipids (Alabaster, AL, USA). MTT reagent, crystal violet, 4-hydroxytamoxifen (4HT), N-desmethyltamoxifen (NDMT), vitamin E (α-Tocopherol), TBHQ (tert-Butylhydroquinone), PMC (2,2,5,7,8-Pentamethyl-6-chromanol), DMSO, protease inhibitors cocktail, sodium orthovanadate and formic acid were from Sigma (Oakville, ON, Canada). ONO-8430506 was from Ono Pharmaceuticals Ltd. (Osaka, Japan). Acetic acid, acetonitrile, 2-propanol and methanol were purchased from Fisher Scientific (Ottawa, Ontario, Canada). Inhibitor for JNK (JNKi, SP 600125) and ASK1 (ASKi, TC ASK 10) were from Tocris Bioscience (Ellisville, MO, USA). [^{3}H]-palmitate was from Perkin-Elmer Life Sci (Waltham, Massachusetts, USA). Tamoxifen (TAM) and Microcystin-LR were from Cayman chemical (Ann Arbor, MI, USA), Matrigel was from BD Biosciences (Mississauga, ON, Canada), TLC silica gel plates were from Millipore (Etobicoke, ON, Canada) and peanut oil was from Sobeys (Edmonton, AB, Canada). Primary antibodies were obtained as follows: Anti- ER-alpha, Anti-PARP, Anti-Cleaved, Anti-Caspase-3, Anti-PARP and Anti-P-SAPK/JNK were from Cell Signaling (Danvers, MA, USA), Anti-PLD1 (PLD1, 44-322) was from Invitrogen (Carlsbad, CA, USA), Anti-4HNE and Anti β-actin was from Abcam (Toronto, ON, Canada), Anti-PLD2 was a kind gift from Dr. Sylvain Bourgoin, Anti-GAPDH and Anti-α-Tubulin was from (Sigma), Anti-Nrf2 (H-300) and Anti-NQO1 (A180) were from Santa Cruz (Santa Cruz, CA, USA), Anti-Calnexin and

Anti-ABCC1 (MRP1-m6) was from Enzo Life Sciences (Farmingdale, NY, USA) and Anti-GPR30 was from Genscript (Piscataway, NJ, USA). Rabbit Anti-IgG and mouse Anti-IgG secondary antibodies conjugated to infrared fluorescent dyes (IRDye) were purchased from LI-COR Biosciences (Lincoln, NE, USA) and used at 1:10000 concentrations. All cell lines were purchased from ATCC (Manassas, VA, USA).

2.2 Cell culture

Cell lines: Human breast cancer cells, MCF-7 (HTB-22) and MDA-MB 231 (HTB-26), Balb/c mouse derived 4T1 cancer cells (CRL-2539TM) and human embryonic kidney cells HEK293T (CRL-11268) were all purchased from the American Type Culture Collection (ATCC) (Manassas, VA, USA). Cell were cultured on cell culture plates from Corning (Corning, NY, USA) in an incubator that was maintained at 37°C, 5% CO_2 and 95% humidity. All cells were grown in either DMEM media or RPMI-1640 medium with 10% FBS and 1% of Antibiotic-Antimycotic purchased from Gibco/Life Technologies (Burlington, ON). To maintain optimal pH in a 5% CO_2 incubator the level of sodium bicarbonate was adjusted to 2 g/L. All experiments were conducted with cells that were cultured and maintained at a low passage number. All experimental treatment that included tamoxifen was delivered in phenol red free medium.

MCF-7 cells used in luciferase assay, stably expressed an inducible antioxidant response element upstream to a luciferase reporter gene [356] and were a kind gift from Prof. Roland Wolf, from Cancer Research UK, University of Dundee, Scotland, United Kingdom. MCF-7 derived tamoxifen resistant cells

(MCF-7- TAMR) and their corresponding control syngeneic wild type cells (MCF-7 WT) were obtained from our collaborator Dr. Pu Xia from University of Sydney, Sydney Australia. MCF-7-TAMR and MCF-7 WT cells were always cultured in the phenol red free DMEM media with 10% FBS and 1% Antibiotic-Antimycotic in the presence of 1μM 4-hydroxytamoxifen or vehicle respectively.

2.3 Microscopy

All phase contrast microscopy images were taken at either 10X or 40X magnification and images were acquired from 3 different fields for each sample from three independent experiments performed. The analysis of images was done by Image J software.

For immunocytochemistry cells were seeded on to a coverslips precoated with fibronectin (10 μg/ml) and allowed to grow overnight. The following day the cells were treated accordingly and fixed with 4% paraformaldehyde for 30 min followed by permeabilization with 0.25-10% Triton X-100. Afterwards, the fixed cells were blocked for an hour to prevent non-specific binding of antibodies using with 1% BSA, 22.52 mg/ml glycine in PBST (PBS+ 0.1% Tween 20). The primary antibody, were prepared at 1:100 concentrations in 1% BSA in PBST and the cells were then stained at 4^0C overnight. The primary antibody was removed and followed by staining with rabbit Anti-IgG conjugated to Alexa Fluor 488 secondary antibody (Invitrogen) and counterstained with DAPI (Hoechst dye 33342) for nuclei staining (Life Technologies). The secondary antibody was prepared in 1% BSA at 1:500 concentration. After each step of the above procedure coverslip was washed three times for 5 min with PBS. Finally the

coverslip was mounted on to a microscope slide with Prolong Gold Antifade (Invitrogen, Carlsbad, CA, USA). Coverslips were then viewed with fluorescent microscope (Leica Microsystems, Concord ON, Canada) with 40X magnification.

2.3.1 Translocation of Nrf2 to nucleus

To study the translocation of Nrf2 by tamoxifen, HEK293T cells were utilized and the cells were grown on coverslips as done for immunocytochemistry experiment described above. However, before proceeding to tamoxifen treatment, transfection procedure was performed in starvation media. The transfection of the cells was done with EGFP-NRF-2 expression plasmid (21549) on a pCDNA3 vector purchased from Addgene (Cambridge,MA,USA). Escherichia Coli strain DH5α (Life Technologies) were then transformed using the plasmids and plated in LB Agar (1.5% w/v agar in LB medium) containing 100 µg/ml Ampicillin and incubated at 37^0C for obtaining E. Coli colonies.The plasmid DNA was isolated using the QIAprep kits (Qiagen, Toronto, ON) and quantified using a nanodrop spectrophotometer ND-1000 (Thermo Scientific, Rockford, IL, USA). Each coverslips was transfected using Polyjet transfection reagent (Signagen,Gaithersburg, MD, USA) according to the manufacturer's instructions and the cells were left to grow for 24 h. After which the cells were treated with tamoxifen accordingly and immunocytochemistry was performed as described above and followed by confocal microscopy using Leica SP5 confocal microscope (Concord,ON,Canada) for acquiring representative images.

The translocation experiments were done with the assistance of Dr. Ganesh Venkatraman.

2.3.2 Superoxide measurement.

Cells were grown in a 12-well plate to 50 % confluence after which the media was removed and the cells were washed with HBSS (Hank's Balanced Salt Solution) followed by a 1 h pretreatment with 25 μM dihydroethidium (DHE), from Life Technologies. Cells were then treated as described for 24 h in DMEM starvation medium. Oxidized DHE has fluorescence excitation/Emission wavelength of 518/605(nm). This signal intensity, which is a measure of superoxide formation, was analyzed after taking images with a live cell fluorescent microscope (Leica Microsystems, Concord ON, Canada) with 40X magnification. Images were acquired using Openlab 4.0.2 software. Signal intensity was quantified using Image J software from 3 independent experiments with images taken from 3 different fields for each treatment condition.

2.4 MTT assay for cell viability

10,000 cells were seeded in to each well of a 96 well plate in the presence of 100 μl medium. The cells were allowed to adhere to the well overnight after which the wells were washed with HBS (HEPES-buffered saline) and treated accordingly. At the end of the treatment the media were removed and replaced with 1mg/ml MTT (prepared in the same medium) and incubated for 2 h. Finally the MTT containing medium was removed and the purple formazan formed inside cells was extracted with DMSO and its absorbance was measured at 570 nm using an Easy Reader EAR 340 AT (SLT-Labinstruments, Austria).

2.5 Nrf2 knockdown experiment

For RNAi silencing of Nrf2, 200,000 4T1 cells were seeded in 6-well plates and grown for 24 h. Then DsiRNAs (5'-dicer-substrate siRNA) were added in a fresh antibiotic-free medium at a final concentration of 40 nM in each well. The DsiRNA transfections were done using Lipofectamine RNAiMAX transfection reagent (Life technologies) in Opti-MEM reduced serum medium (life technologies) according to the manufacturer's protocol.

The DsiRNA duplexes were designed using Predesigned DsiRNA selection tool from Integrated DNA Technologies Inc. (Coralville, IA, USA). A non-targeting siRNA duplex that does not target any sequence in human, mouse and rat transcriptomes was used as a control. Five targeting sequences were designed and used for experiments. The DsiRNA sequences are shown below:

Table 2: Nrf2 DsiRNA sequences

No	Sequences
Dsi-1	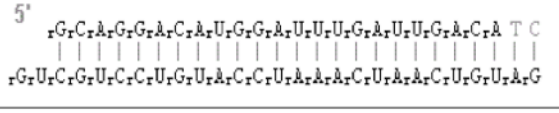
Dsi-2	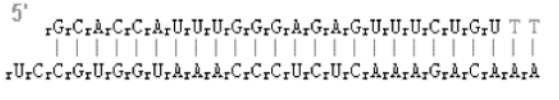
Dsi-3	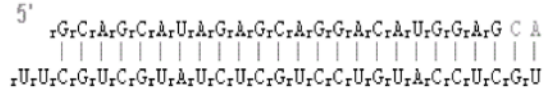
Dsi-4	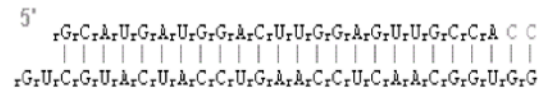
Dsi-5	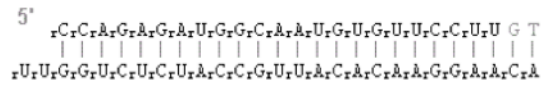

2.6 Cell proliferation assay

Cells were grown over night in a 6 well plate followed by the appropriate treatment for up to 3 days. At the end of the treatment the cells were collected by trypsinization and counted using Countess® Automated Cell Counter (Life Technologies) according to the manufacturer's instruction to assess the proliferation of cells. Another method for measuring cell proliferation is Crystal violet staining described in the section below.

2.6.1 Crystal violet staining

Cells were seeded overnight in 24 well plates and treated accordingly for 24 h. The cells were then fixed with paraformaldehyde for 30 min and stained for 10 min with 0.5 mg/ml crystal violet prepared in equal volumes of methanol

and water. Excess crystal violet was removed by washing three times with PBS. The crystal violet bound to cells was then extracted in 10% acetic acid and its absorbance was measured at 600nm using an Easy Reader EAR 340 AT (SLT-Labinstruments, Austria).

2.7 Western blotting

Cells were seeded in either a 6-well plate or a 35 mm dish and grown for 24 h prior to treatment. After treatment, cell lysates were collected by scraping with rubber spatula in 150-300 µl of RIPA buffer (150 mM NaCl, 1.0% NP-40, 0.5% sodium deoxycholate, 0.1% SDS (sodium dodecyl sulphate) and 50 mM Tris-HCl at pH 8.0, protease Inhibitors cocktail, Microcystin-LR and sodium orthovanadate). In order to process equal amount of protein on an SDS-PAGE (polyacrylamide gel electrophoresis) gel, the protein yield from each sample was determined using a BSA standard curve.

Protein Assay: A standard curve was set up using 20, 10, 5, 2.5 and 1.25 µg of BSA (Bovine serum albumin) protein each dissolved in 10µl RIPA buffer and loaded on to 96 well-plates in duplicates.

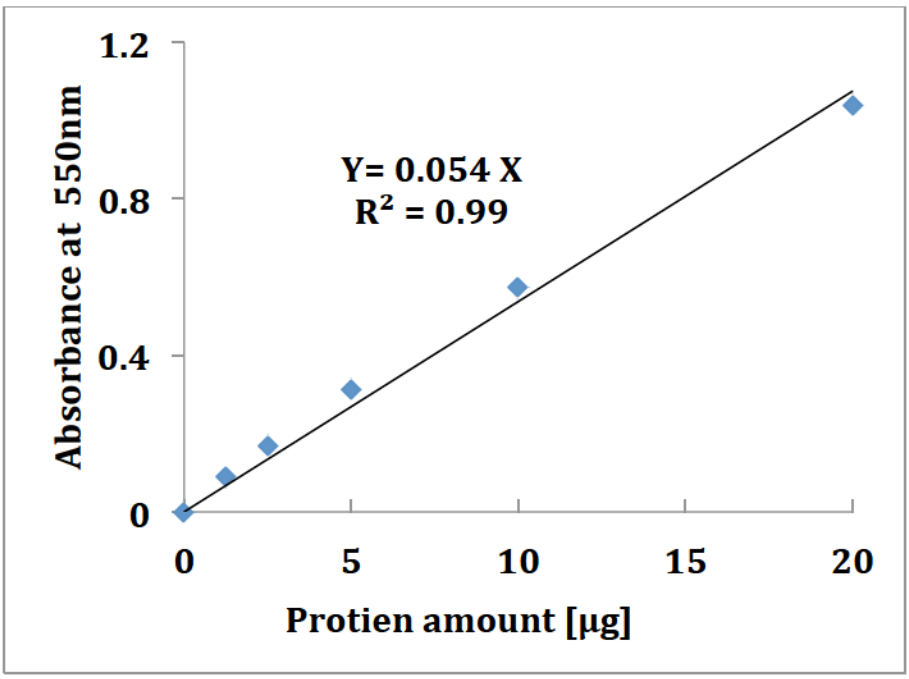

Figure 2.1: Example of standard curve with Bovine Serum Albumin (BSA) protein.

A plot of BSA standard cure with protein amount on the X-axis and the absorbance on the Y-axis with best fit line trend line and the calculated relation ship between absorbance and protein amount and R^2 displayed.

Cell lysates were diluted in RIPA buffer in 1:10 ratio and were then loaded in to the 96-well plate. Then 200 µl mixture of reagent A and reagent B from BCA™ kit reagents (Fisher Scientific) mixed in 50:1 ratio respectively was added to each standard and sample well. The absorbance was then measured using an Easy Reader EAR 340 AT (SLT-Labinstruments, Austria) at 550nm. The protein content from each experimental sample was then calculated using the formula determined from the relationship between the absorbance and protein amount (Fig. 2.1).

Gel preparation and running samples on PAGE: Gels for PAGE consisted of staking gel (which comprised of 125 mM Tris-HCl pH 6.8, 0.1% SDS, 3.9% acrylamide and 0.1% bisacrylamide) and a separating gel (375 mM Tris-HCl pH

8.8, 0.1% SDS, 10% acrylamide and 0.28% bisacrylamide) polymerized using 10% APS (ammonium persulfate) and TEMED (N,N,N′,N′-Tetramethylethane-1,2-diamine). For sample loading, the stacking gel was made to have either 10 or 15-well pocket by using well comb (biorad). The gel was then placed in Mini-Protean II protein electrophoresis apparatus (Bio-Rad), which was filled with Laemmli electrophoresis buffer (25 mM Tris base pH 8.3, 192 mM glycine, 0.1 % SDS). Each gel well was loaded with equal amounts of up to a 40 µg protein in 1x sample loading buffer that was prepared by diluting in to in 6x sample loading buffer (375 mM Tris-HCl pH 6.8, 6% SDS, 45% glycerol, 0.005% bromphenol blue) and 10% 2-mercaptoethanol that was also freshly added before each PAGE. At least one well in each gel was designated for loading 10 µL of Precision Plus® All-Blue Protein Standards (Bio-Rad) consisting of 250, 150, 100, 75, 50, 37, 25, 20, 15 and 10 kDa protein standards as a marker for identifying the molecular weight of blotted proteins. The proteins in the sample were separated based on size by applying 150 V for about 2 h.

Protein transfer and developing western-blot membrane: The gel was placed in a Biorad transfer apparatus and transferred on to a 0.45 µM Nitrocellulose membrane (Biorad, Mississauga, ON, Canada) using a current of 400 milliampere at 4°C in Tris- glycine buffer (25 mM Tris base, 192 mM glycine) containing 20% methanol and 0.05% SDS for 4 h. After the transfer the membrane was blocked for 1 h at room temperature. For blots developed by infrared image scanner, a buffer made up of equal volumes of Odyssey blocking buffer (LI-COR biosciences) and PBS was used. For blots developed

by chemiluminecsence a buffer made up 5% milk powder in TBS (20 mM Tris base, 137 mM NaCl at pH 7.6) was used. After blocking, the membrane was incubated overnight at 4°C with primary antibodies (concentration of 1:1000 was used for all antibodies with the exception of Anti-Nrf2, Anti-NQO1 and Anti-PLD2 used at 1:500 and Anti-ABCC1 used at 1:100 concentration) that was prepared in 1:1 ratio of Odyssey blocking buffer and PBST (PBS with 0.1% Tween-20). The blots were washed three times each with PBST for 5 min and then incubated for 1 h at room temperature with secondary antibodies which was prepared in the same composition of blocking buffer used to block the membrane plus an additional 0.01% SDS for blots prepared for infrared imaging or with an additional 0.1% Tween-20 for chemiluminecsence imaging, which was done to remove non-specific antibody binding. At the end of incubation with secondary antibodies, blots were washed 3 times for 5 min each with PBST and scanned with Odyssey infrared image scanner for blots stained with IRDYE secondary antibodies. Blots for Nrf2, ABCC1, ERα were developed by using horseradish peroxidase (HRP)–conjugated goat anti-rabbit/mouse immunoglobulin G (IgG) secondary antibodies at 1:2000 dilution (Santa Cruz Biotechnology Inc, Santa Cruz, CA, USA) and exposing the chemiluminecsence generated by application of the ImmunstarWesternCkit (Bio-Rad, Hercules, CA, USA) on to autoradiography film (Kodak, Rochester, NY, USA). For infrared imaging the IRDye secondary antibodies were at 1:10,000 concentration. The densitometric analysis for the blotted protein was

done using loading control proteins GAPDH, actin or tubulin and performed using ImageJ software (NIH, Bethesda, MD, USA).

Western blots for NQO1 and Nrf2 were done with the assistance of Dr. Ganesh Venkatraman.

2.8 Quantitative real-time PCR (qRT-PCR)

Cell or tumor tissue lysates were collected and homogenized in 500µl lysis binding buffer (Qiagen). The lysates were then passed through a sterile 25-gauge-syringe 3-4 times to break up the lysate. To the each lysates a 500µl of 64% ethanol was added and mixed by inverting. The lysate/ethanol mixture was placed on a filter cartridge (Qiagen) fitted on to a collection tube supplied from a Qiagen kit and spun for 1 min at 13000 RPM in a micro-centrifuge. The mRNA bound on to the filter cartridge and the flow-through collected in the collection tube was discarded. The filter cartridge was washed sequentially with wash solution 1 and 2/3 from RNA aqueous kit (Qiagen) and then filter cartridge was spun for 1 min at 13000 RPM to remove the wash solution. The mRNA was then eluted in to a fresh tube by applying 105 µl of elution solution on to filter cartridge.

Any remaining genomic DNA that was eluted with the mRNA was digested using rDNSAE digestion step using DNA-Free Kit (Qiagen). The mRNA was then reverse transcribed in to cDNA (complementary DNA) by running a PCR protocol of STEP 1: 25°C for 10 min; STEP 2: 42°C for 60 min and STEP 3: 95°C for 5 min and cooled down to 4°C till running qRT-PCR

using 4µl qscript cDNA super mix (Quanta BioSciences Gaithersburg, MD, USA) and 16 µl of eluted mRNA.

The qRT-PCR procedure was preformed by combining the cDNA, 10 µM of sense (forward) and antisense (reverse) primer set, RT^2 SYBR green qPCR mastermix (Qiagen) in to a PCR plate. The plate was placed on to an Applied Biosystems 7500 real-time RT-PCR thermocycler (Life Technologies) and a PCR program: STEP 1: 50^0C for 2 min; STEP 2: 95^0C for 10 min; STEP 3: 40 x 95^0C for 15 s and 60^0C for 1 min was run. Followed by another PCR program that consisted of STEP 1: 95^0C for 15s; STEP 2: 60^0C for 1 min; STEP 3: 95^0C for 15s for 40 cycles was performed to analyze the melting point of the PCR product formed from the previous PCR reaction. A cDNA dilution curve was set up and run alongside with the samples.

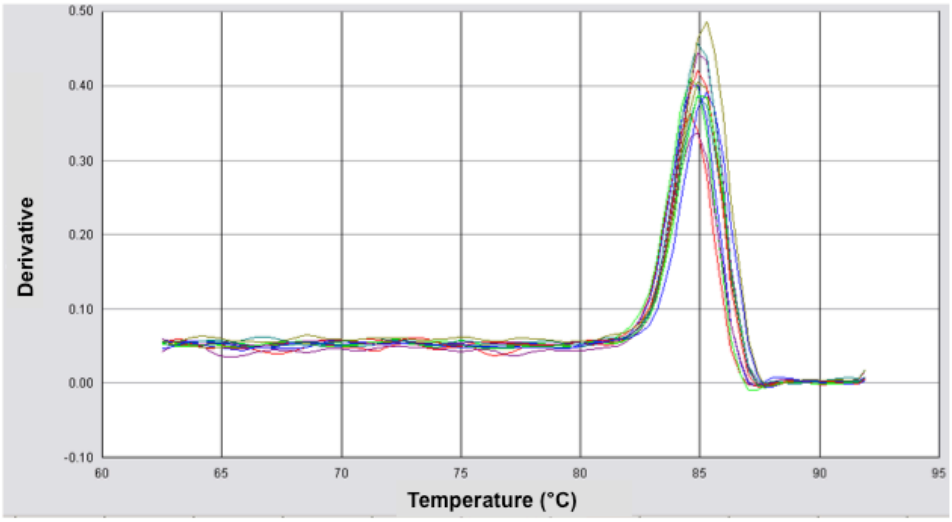

Figure 2.2: Dissociation plot for Estrogen receptor-α primer

The different colored lines represent different samples and the maximum point of peak is the melting temperature (Tm), which is around 85°C for ER-α primer set. Tm is defined as the temperature at which 50% of the product has melted. The derivative shown on the Y-axis is the is the negative of the rate of change in fluorescence as a fraction of temperature

The SYBR green in the master mix will bind to cDNA at each of the PCR cycle and emit a fluorescent signal. The change in SYBR green dye fluorescence will be recorded by a specific-filter inside the machine and the ROX-dye in the master mix will be was used as a passive reference dye. The recorded signal intensity is proportional to the amount of cDNA in each well. The number of cycles need to reach a particular fluorescent intensity threshold level termed as C_T value for each sample will then be used to asses the amount of cDNA in the different wells by comparing it to the cDNA standard curve which plots log of C_T value to dilution curve ratio.

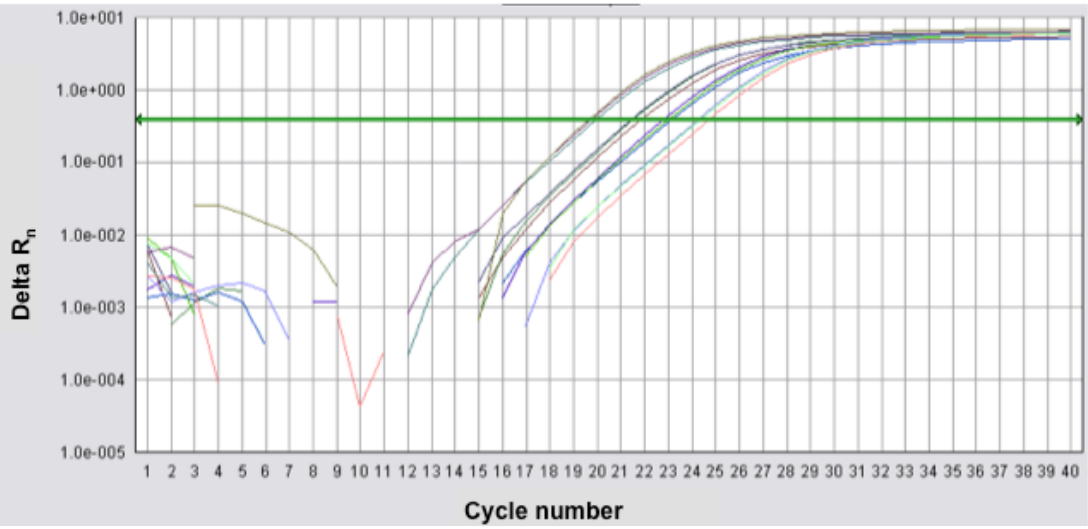

Figure 2.3: Graphical representation of an amplification plot for Estrogen receptor-α gene expression.

The different colored lines represent an amplification plot for specific sample and show the variation of log (Delta R_n) with PCR cycle. The plot shown here is of delta R_n, which is the fluorescence signal of the reporter dye divided by the fluorescence signal of a passive reference dye (ROX™) and plotted against PCR cycle number. Delta R_n indicates a baseline background subtraction.

The fluorescent intensity threshold, which is the C_T value is the same for all samples and is on the earlier portion of the amplification curve. The C_T value is inversely proportional to the expression level of the gene of interest.

The mRNA level of the gene of interest were expressed relative control treatments after normalizing to housekeeping gene, cyclophilin A (CypA). Equivalent results were also obtained using hypoxanthine phosphoribosyltransferase (HPRT). Results that compare the relative expression of genes between mouse and humans cells were expressed relative to GAPDH (glyceraldehyde 3-phosphate dehydrogenase). The Primers used for qRT-PCR were designed with Primer-BLAST software algorithm from NCBI website. The designed primers used for RTPCR were then ordered from Integrated DNA Technologies (Coralville, Iowa, USA). The primer sequences are listed in Table 3.

qRT-PCR for anti-oxidant genes and MDRTs were done with the assistance of Dr. Ganesh Venkatraman.

Table 3: Primer sequences

Species	Gene	Primer Sequence
Human & Mouse	ERα	Sense: 5'-CCTGGACAAGATCACAG-3' Antisense: 5'-AGCAGGTCATAGAGGGG-3'
Human & Mouse	GPR30	Sense: 5'-CCTGTACTTCATCAACCTG-3' Antisense: 5' TCATCCAGGTGAGGAAG-3'
Human & Mouse	GAPDH	Sense: 5'-ACTTTGTCAAGCTCATTTCC-3' Antisense: 5'-TCTTACTCCTTGGAGGCCAT-3',
Mouse	Nrf2	Sense: 5'CAAGACTTGGGCCACTTAAAAGAC-3' Antisense: 5'-AGTAAGGCTTTCCATCCTCATCAC-3',
Mouse	NQO1	Sense: 5'-AGCTGGAAGCTGCAGACCTG-3' Antisense: 5'-CCTTTCAGAATGGCTGGCA-3',
Mouse	HMOX1	Sense: 5'-GCTAGCCTGGTGCAAGATACTG-3' Antisense: 5'-CACATTGGACAGAGTTCACAGC-3'
Mouse	ABCC1	Sense: 5'-GCGCTGTCTATCGTAAGGCT-3' Antisense: 5'-AGAGGGGCTGACCAGATCAT-3'
Mouse	ABCG2	Sense: 5'-TGGACTCAAGCACAGCGAAT-3' Antisense: 5'-ATCCGCAGGGTTGTTGTAGG-3'
Mouse	ABCC3	Sense 5'-GGGCTCCAAGTTCTGGGAC-3' Antisense 5'-CCGTCTTGAGCCTGGATAAC-3'
Mouse:	CypA	Sense 5'-CACCGTGTTCTTCGACATCAC -3' Antisense 5'-CCAGTGCTCAGAGCTCGA AAG -3'
Mouse	SOD1	Sense 5 '-CCA GTG CAG GAC CTC ATT TT -3' Antisense 5'-CAC CTT TGC CCA AGT CAT CT-3',
Mouse	HPRT	Sense: 5'-GCTGGTGAAAAGGACCTCT -3' Antisense: 5'-CACAGGACTAGAACACCTGC -3'
Human	PLD1	Sense: 5'- TGC CCC TGC TCA TCT GGT CCT -3' Antisense: 5'- TGT TGT CAG TGC CTT TGG GAG CA-3'
Human	PLD2	Sense: 5'-AAA GGA GCA CGG AGG CAC GG -3' Antisense: 5'-GGG GCG TAG CTG TCA TGC CG -3'
Mouse	RALBP1	Sense: 5'- CTG GCC ACT CTT GTT TGT GC -3' Antisense: 5'- AAG AGG CCT TTG CTG ATC CC -3'

2.9 Measurement of ceramide concentration

Lipids were extracted from treated cells using a modified Bligh and Dyer extraction method using 1 ml of methanol, 1 ml of chloroform and 0.9 ml aqueous solution (2M KCl/ 10 mM HCl solution). For the analysis 800 µl of the chloroform phase was then aspirated, dried under N_2 and then redissolved in 100µl methanol. C17:0 ceramide was used as the internal standard at a concentration of 0.1 pmol/µl in all standard and sample solutions.

The ceramide level in each sample was assessed by tandem liquid chromatography mass spectrometric (LC-MS/MS) analysis using standards of C16:0-, C22:0-, C24:1- and C24:0- ceramides plus C16:0- and C24:0-dihydroceramides that were diluted with methanol to prepare calibration solution mixtures with concentrations of 2, 1, 0.5, 0.2, 0.1, 0.05, 0.02 and 0.01 pmol/µl of each component. These were stored at -20℃ prior to use. LC conditions: Separation of ceramide species was performed on an Agilent 1200 series HPLC system (Agilent Technologies, Palo Alto, CA) using an Ascentis C18 column (5 cm × 2.1 mm I.D., 3 µm particle size, Supelco, Bellefonte, PA). The mobile phase consisted of (A) 0.1% formic acid in water and (B) 0.1% formic acid in a mixture of acetonitrile and 2-propanol (40:60, v/v). The flow rate of mobile phase was 0.3 ml/min and the injection volume was 5 µl. Chromatographic analysis was performed using the following gradient: 0-1 min, 50% B; 1-4 min, 50% to 100 % B; 4-12 min 100% B. The column was then re-equilibrated at the initial conditions (50% B) for 5 min prior to the next analysis.

Table 4:MRM transition ions and optimized operation parameters

Analyte	Q1 mass (amu)	Q3 mass (amu)	Scan time (s)	DP (V)	EP (V)	CEP (V)	CE (V)	CXP (V)
C14 Cer	510.4	492.3	0.8	50	6	25	20	6
	510.4	264.5	0.8	50	6	25	25	3
C16 Cer	538.3	520.4	0.8	50	4	20	15	4
	538.3	264.5	0.8	50	4	25	35	3
dHC16 Cer	540.7	522.8	0.8	50	6	20	25	4
	540.7	284.3	0.8	50	6	20	35	3
C17 Cer (IS)	552.6	534.6	0.8	50	4	20	20	6
	552.6	264.2	0.8	55	3.5	20	35	3
C18 Cer	566.5	548.7	0.8	36	4.5	18	15	5
	566.5	264.1	0.8	40	4	18	35	3
C20 Cer	594.5	576.2	0.8	50	4.5	20	20	6
	594.5	264.3	0.8	50	5	20	35	3
C22 Cer	622.7	604.8	0.8	50	6	25	20	6
	622.7	264.5	0.8	45	4.5	20	40	3
dHC22 Cer	624.5	606.3	0.8	50	6	23	32	6
	624.5	284.2	0.8	50	6	23	40	3
C24:1 Cer	648.3	630.8	0.8	40	4.5	18	20	6
	648.3	264.2	0.8	50	4	25	40	3
C24 Cer	650.5	632.4	0.8	50	6	25	25	6
	650.5	264.1	0.8	45	4.5	20	40	3
dHC24 Cer	652.8	634.6	0.8	57	6	20	32	5
	652.8	284.1	0.8	45	6	20	40	3
C26:1 Cer	676.6	658.3	0.8	50	5	25	30	6
	676.6	264.3	0.8	50	5	25	42	3

DP, EP, CEP, CE and CXP are declustering potential, entrance potential, collision cell entrance potential, collision energy and collision cell exit potential.

MS/MS conditions: MS analysis was performed on a 3200 QTRAP mass spectrometer (AB SCIEX, Concord, ON, Canada) using Analyst 1.4.2 software. The mass spectrometer was operated using positive ion electrospray ionization (ESI) in the multiple reaction-monitoring (MRM) mode. Nitrogen was used as curtain gas (CUR), nebulizer gas and drying gas. The instrumental parameters were set as follows: CUR, 10 psi; collision gas (CAD), 5; ionspray voltage (IS), 5200V; temperature (TEM), 400℃; Gas 1, 50 psi; Gas 2, 60 psi. The ceramide levels were normalized to total lipid phosphorous levels determined by a phosphate assay (Section 2.9.1) and expressed relative to control treatment.

Si Mi, in Dr. Jonathan M. Curtis laboratory, (Department of Agricultural, Food and Nutritional Science in University of Alberta) performed the LC-MS/MS portion of experiment.

2.9.1 Phosphate assay

Lipids were extracted into the organic phase by chloroform as mentioned in Section 2.9. Phosphate assay was then performed to determine the total phospholipid phosphorous levels in each sample. For this purpose, a standard curve was set up in a glass tubes using 1-100 nmol of glycerol-3-phosphate prepared in water, which was then evaporated along with the samples. A volume of 50 µl of perchloric acid was added to the glass tubes and heated to 180°C for 30 min allowing the digestion and the subsequent conversion of the organic phosphate in the samples into an inorganic phosphate. The glass tubes were cooled to room temperature and a mixture of 278 µl of water followed by 55 µl of 2.5% ammoniummolybdate and 55 µl of fresh 10% ascorbic acid was added. The samples were then placed in 90°C water bath for 15 min. A volume of 180 µl of this mixture was transferred in duplicate to a 96-well plate and absorbance was measured at 700 nm using an Easy Reader EAR 340 AT (SLT-Labinstruments, Austria). Phosphate assay was performed with the assistance of Jay Dewald.

2.10 Luciferase Assay

MCF-7 cells stably expressing the ARE sequence upstream of the reporter gene were used for the luciferase assay experiments. 500,000 cells were seeded in 6 well plates and grown overnight before adding treatments. The cells were left in the treatment medium for 24 h after which they were washed twice and collected for the luciferase assay, which was performed according manufacturer's instructions with a kit from Promega Corporation (Madison, WI, USA) using a Perkin Elmer Wallac Microbeta Trilux 1450 (Massachusetts, USA).

2.11 Phospholipase D assay

Cells were seeded at 50% confluence on a 35 mm cell culture plates with 2 ml DMEM-media containing 10% FBS. The cells adhered to the bottom of the plate and were left to grow overnight in 37^0C incubator. The following day the FBS containing DMEM-media was aspirated and the cells were washed with HBS and left for 1 hour in 1 ml of DMEM with 0.1% BSA (starvation media). After the incubation period the starvation media was replaced with 1ml of labeling media containing 4µCi of [^{3}H] palmitate that was prepared in starvation media. The cells were radiolabeled for 2 hour, which resulted in the incorporation of [^{3}H] palmitate in to phospholipids such as phosphatidylcholine and also in to other lipids. The labeling media was aspirated and the cells were transferred back into 1 ml of starvation media and incubated for another hour.

The activity of PLD was assessed by transphosphatidylation reaction that involves the hydrolysis phosphatidylcholine to phosphatidylalchohol. Hence

prior to assessing PLD activity the cells were treated with 30 mM butan-1-ol for 15 min. After which the cells were treated with agonist of choice for 6-120 min.

After stimulation the cells were washed 3 times with 1ml ice-cold HBS. The HBS was removed and the cells were scraped off the plate with two rounds of 0.5 ml ice-cold methanol, which makes up a total volume 1 ml of methanol that was pipetted into glass tubes and placed on ice. In to the glass tube 1ml of chloroform followed by 0.9 ml of 2M KCl with10 mM HCl solution was added. The mixture was then centrifuged for 15 min at 2500 RPM allowing the separation of lipids in to the chloroform bottom-phase. The aqueous top phase was aspirated and 800μl of the bottom organic phase was pipetted in to a fresh glass tubes and was dried under a stream of N_2. After which 100 μl of chloroform: methanol (9:1 by volume) was added before loading the sample on to silica gel plates for thin layer chromatography (TLC).

Lipid standards consisting of 2.8 mM PA, 13 mM PC, 13 mM PE and 16 mM PB were used. The lipid standards allowed the identification of area of the plate where each lipid migrated after TLC procedure. In addition, PB standard was also loaded as an internal standard along with the samples.

PB standard does not interfere with assaying the lipid levels coming from cells, as cellular lipids will be radioactive due to the labeling procedure described above.

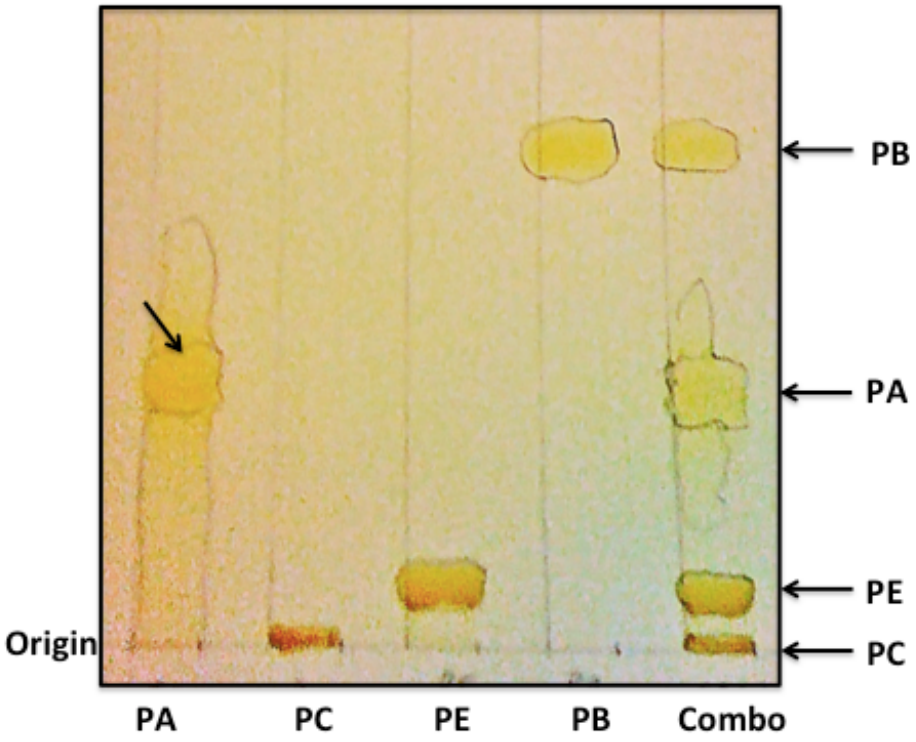

Figure 2.4: An example of TLC-plate run with lipid standards.

A TLC plate run with standards shown from left to right PA, PC, PE, PB and all standard combined abbreviated as Combo. The arrows indicate where each of the standards run up-to on the TLC plate depicting different Rf (retention factor) values of the standards. Rf is defined as the distance traveled by the samples divided by distance traveled by the solvent front. In the mobile phase used the lipid PB has the highest Rf value.

After the preparation of the TLC plate, 50µl of sample was loaded and developed using a mobile phase. The TLC mobile phase was a top-phase of mixture of 130ml ethyl acetate, 20 ml iso-octane, 30 ml acetic acid and 100 ml of water. The mobile phase was run up to 1 cm from top of the TLC plate, after which it was removed from in TLC tank and left to dry. The TLC plate was stained with Iodine (I_2) giving each of the standards bright yellow color for identification (Fig. 2.4). Hence, the PA, PC, PE and PB bands on the plates of each sample were identified by comparison with standards. As I_2 will evaporate quickly, each of lipid bands were marked by circling the I_2 stained area-using

pencil. Each of the marked bands on the TLC plate will be scraped off and placed into scintillation vials. The bands corresponding to PB will be separated from the remaining lipid bands consisting of mainly PE and PC. To each vial 200 μl water and 2 ml scintillation liquid were added and the radioactivity of each vial was measured using Beckman Coulter LS 3801 Scintillation Counter (ON, Canada).

The relative PLD activity is calculated as the percentage of radioactivity coming from PB bands relative to the total lipids.

2.12 Mouse model of Breast cancer

Tamoxifen was prepared in 100% peanut oil at stock concentration of 50mg/ml and was delivered orally to mice. Tamoxifen has a long half–life of 7 days [357] and thus to achieve a therapeutic level we treated the mice with a loading dose of 400mg/kg for two days, followed up with a maintenance dose of 200mg/kg for next 4 days and finally at 100mg/kg for the remaining 4days before tumor excision. Control mice were gavaged with just peanut oil.

2.12.1 Establishment of orthotropic tumors in mouse

Female Balb/c mice were bought from Charles River (Kingston, ON Canada). Mice were maintained in the animal facility at 21°C, 55% humidity and access to standard laboratory diet and water. At 10-week of age they were orthotopically injected in the mammary fat pad with 20,000 syngenic mouse 4T1 breast cancer cells, as previously established [206]. The 4T1 cells were prepared in phenol red-free and serum-free DMEM at a concentration of

400,000 cells/ml and then mixed 1:1 with Matrigel (BD Biosciences, Mississauga, ON). Each mouse was anesthetized with isoflurane and then injected with 100µl of cells plus matrigel suspension using a 27-gauge needle.

Figure 2.5: Balb/c mouse developing mammary tumor mass

Images show a Balb/c mouse that had developed a tumor in the lower mammary nipple as shown by the red arrow.

The following day treatment was commenced and continued till the end of the experiment. At day 11 the mice were euthanized and the primary tumors were excised and weighed. Orthotopic tumor injection procedure, drug gavage and tumor resection was done with the assistance of Dr. Xiaoyun Tang and Jay Dewald.

All animal experiments were as approved by the University of Alberta Animal Welfare Committee (Animal User Protocol 226).

2.13 Immunohistochemistry

Tumor tissues were fixed in formalin and were processed in paraffin wax and were later sectioned from paraffin block on to a microscopy slides for immunohistochemistry (IHC). Paraffin processing, embedding and sectioning was performed at HistoCore in University of Alberta. To remove wax from each section the first step is to de-wax the IHC slides with Xylene followed by sequential hydration of the tissue section in 100%, 80% and 50% ethanol, after which the slides will be ready with for antigen retrieval and primary antibody staining. After the last hydration step with 50% ethanol, the IHC slides were washed with dripping tap water for 6 min.

The Antigen retrieval is done using the pressure cooker system, whereby the slides will be boiled for 20 min in citric acid at pH of 6.0 (adjusted with NaOH) inside a microwave. The slides are then cooled off in cold water for about 20 min and washed by dripping water for 6 min. After the antigen retrieval step endogenous peroxidase activity was blocked by submerging slides in a mixture of methanol and 30% hydrogen peroxide in a 9:1 ratio respectively, for 10 min. Tumor tissue sections were then outlined with a wax pen (Dako, Burlington, ON) and blocked in a humidified chamber for 30 min at room temperature with background reducing reagents (Dako). The solution was then shaken off the slides and anti-RALBP1 primary antibodies raised in rabbit was added at concentration of 1:100 and the slides were incubated at 4°C overnight.

The slides were washed on the second day with two changes of PBST for 5 min. Samples were then covered with Dako EnvisionTM+ anti-Rabbit IgG

secondary antibody conjugated to horseradish peroxdiase (Dako) at room temperature for 30 min followed by a wash step in PBST.

The IHC Samples were then developed with Liquid DAB+ (diaminobenzidine) Substrate Chromogen System (Dako) for 0.5-5 min. The reaction was quenched in PBS, and the slides were washed in running distilled water for 5 min. The slides were next soaked in a 1% copper sulphate aqueous solution for 3 min and then rinsed again in water. The slides were counterstained with Hematoxylin stain (Fisher Scientific) for 3 min, and then washed under warm tap water. Next, the slides were dehydrated with increasing ethanol concentrations (50%, 80% and 100%) and three changes xylene, and glass coverslips were mounted with xylene-based mounting medium (Fisher Scientific). Images were acquired from at least 3 random fields per specimen at either 5X (for TMA IHC slides described in Section 2.14) or 40X using a Zeiss Axioskop 2 imaging system (Carl Zeiss Canada, Ltd., Toronto, ON).

Dr. Matthew Benesch performed the IHC staining. The tumor samples from ONO-8430506 and vehicle treated mice were obtained from the previously published study by Benesch, M. G. et.al, treatment protocol is also described in the paper [206].

2.14 Patient samples

Breast tumors from 176 primary, treatment-naive breast cancer patients and 10 normal breast tissue samples (from breast reduction surgery) were obtained through the Canadian Breast Cancer Foundation Tumor Bank

(Edmonton, AB, Canada) with approval from the Health Research Ethics Board of Alberta: Cancer Committee (ID 26195).

2.14.1 Patient tumor Gene microarray

Gene expression microarray analysis was performed on tumors from Total RNA was isolated from frozen human breast tumor biopsies using TRIZOL reagent (Sigma-Aldrich, Oakville, Canada) and further purified using QIAGEN RNeasy columns (Mississauga, Canada) according to the manufacturer's recommended protocol. The RNA was then quantified using a NanoDrop 1000 spectrophotometer (NanoDrop Technologies, Wilmington, DE) and its integrity evaluated using a Bioanalyzer 2100 (Agilent Technologies, Santa Clara, CA) according to the manufacturer's protocol. RNA samples with RNA Integrity Numbers (RIN) greater than 7.0 were used in this study.

The RNA samples were linearly-amplified, labelled with Cy3 and hybridized to Agilent Whole Human Genome Arrays using Agilent kits (One Color Low RNA input Linear Amplification Kit Plus, One Color RNA Spike-In Kit and Gene Expression Hybridization Kit) according to manufacturer's directions. The arrays were scanned using an Agilent Scanner. The data were extracted and quality-evaluated using Feature Extraction Software 9.5, and normalized and analyzed using GeneSpring GX 7.3 (Agilent Technologies).

mRNA levels of each gene were determined based on normalized gene microarray signal intensity.

Receiver Operating Characteristic (ROC) curve analysis was used to determine the cut-off point for each gene to categorize the values into "high" or

“low” levels. ROC analysis determines the cut-off point by considering gene expression results from patients with cancers and those from normal patients. These two patient groups have overlapping gene expression values, which can then be used to determine the cut-off point using the MedCalc software.

Dr. Rong-Zong Liu in Dr. Roseline Godbout laboratory at University of Alberta performed the patient gene microarray analysis. The prognostic significance for genes of interest was also done with the assistance of Dr. Rong-Zong Liu.

2.14.2 Patient tumor Tissue Microarray staining and quantification

A Tissue microarrays (TMA) was setup by dotting each patient tumor in triplicates on to an IHC slides. The IHC slides were obtained from our collaborator Dr. John Mackey. Tissue microarray slides were immune-stained using anti-RALBP1 primary antibody at 1:50 concentration, counterstained and developed as described in detail in Section 2.13. Tissue staining intensity was quantified for 142 breast cancer samples and 6 normal breast tissue samples using ImageJ software.

2.15 Statistical analysis

All results are reported as means ± SEM from n ≥ 3. P values were determined by t-test or ANOVA for multiple comparisons. Values of $p < 0.05$ was considered statistically significant and depicted with * for $p<0.05$, ** for $p<0.01$ and *** for $p<0.001$. Prism software was used to calculate statistics and plot the graphs. Statistics for analyzing human patient survival data was done using logrank test on Kaplan-Meier survival curves using MedCalc software version 15.4 (Ostend, Belgium).

3 CHAPTER: RESULTS

Anti-oxidant response mitigates tamoxifen efficacy

3.1 Introduction

Tamoxifen has been credited with much of the decrease in breast cancer mortality over the last decade. Nevertheless, clinical resistance to tamoxifen, as demonstrated by recurrence or progression on therapy, is frequent, as nearly one-third of patients receiving adjuvant tamoxifen eventually experience disease relapse and almost all patients with metastatic tumors treated with tamoxifen will have progression and die from their disease [3, 7]. To improve breast cancer treatment it is vital to understand the mechanisms that result in tamoxifen resistance. The work presented in this Chapter was thus designed to improve our understanding of how tamoxifen increases the death of cancer cells and how resistance to its therapeutic actions can occur. It is clinically relevant to study resistance to tamoxifen, as it is the most widely used therapy for patients with estrogen receptor-α (ERα)-positive breast cancer, which make up about three fourth of all breast cancer.

The overarching hypothesis of Chapters 3 and 4 is that: **Tamoxifen induces oxidative stress independently of the ERα, this leads to the killing of cancer cells, and the adaptive mechanism employed by cancer cells to mitigate this oxidative stress causes resistance to tamoxifen.**

Following up on the above hypothesis the study presented in this Chapter shows that concentrations of tamoxifen and its metabolites, which accumulate in tumors of patients, killed both ERα-positive and ERα−negative breast cancer cells. This depended on oxidative damage and anti-oxidants rescued the cancer cells from apoptosis. Breast cancer cells responded to

tamoxifen-induced oxidation by increasing Nrf2 expression and subsequent activation of the anti-oxidant response element (ARE). This increased the transcription of anti-oxidant genes and multidrug resistance transporters. This adaptive response enabled cancer cells to destroy or export toxic oxidation products, thus increasing survival from tamoxifen-induced oxidative damage. These responses in cancer cells also occur in breast tumors of tamoxifen-treated mice. Additionally, high levels of expression of Nrf2, ABCC1, ABCC3 and NAD(P)H dehydrogenase quinone-1 in breast tumors of patients at the time of diagnosis are prognostic of poor survival. We conclude that overcoming the tamoxifen-induced activation of the ARE could increase the efficacy of tamoxifen in treating breast cancer.

3.2 Tamoxifen decreases the proliferation of ERα-positive and ERα-negative breast cancer cells.

As introduced in Chapter 1, tamoxifen has been ascribed to have several other therapeutic effects in addition to blocking ERα signaling. To study these latter effects, human MCF-7 breast cancer cells that expressed ERα and GPR30 as demonstrated by qRT-PCR and Western blotting (Fig. 3.1A and B) were used. In addition human MDA-MB-231 and mouse 4T1 breast cancer cells that expressed relatively little ERα and GPR30 were also used (Fig. 3.1A).

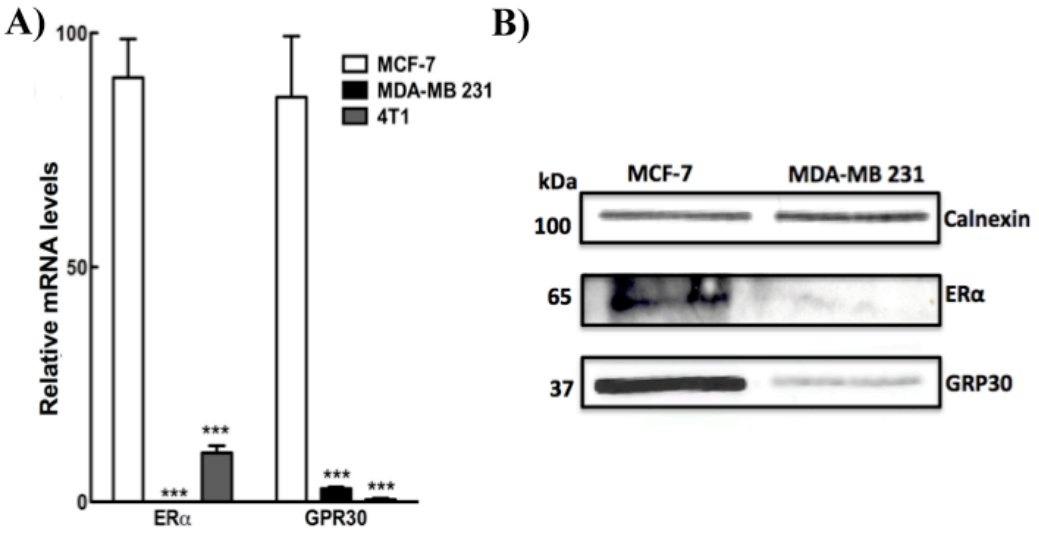

Figure 3.1: Relative Expression level of ERα and GPR30 in different breast cancer cells.

(A) mRNA expression levels for ERα and GPR30 in MCF-7, MDA-MB 231 and 4T1 cells. (B) Protein expression for ERα and GPR30 was confirmed by Western blot for human breast cancer lines MCF-7 and MDA-MB 231 cells. Results are means ± SEM for n=3. Significant differences were indicated with ***= $p<0.001$.

Early stage breast cancer patients typically receive a 20 mg tamoxifen tablet daily for over 5 years [358]. Due to the prolonged half-life of tamoxifen and its metabolites 4-hydroxytamoxifen (4HT), N-desmethyltamoxifen (NDMT) [357, 359], the accumulation of tamoxifen and its metabolites in tumor tissue can easily build up to >5 μM [357, 358]. Thus, to measure the proliferation of ERα-positive and ERα-negative cancer cells, concentrations from 0.3-10 μM 4HT were used. The proliferation was then measured over three days in the presence of 10% fetal bovine serum (Fig. 3.2A-D). ERα-positive MCF-7 cells exhibited growth-retardation at <5μM 4HT (Fig. 3.2A). However, to significantly inhibit the proliferation of ERα-negative, MDA-MB-231 and 4T1 cells, a higher 4HT concentration were required (Fig. 3.2B-D). Nevertheless, 5-10 μM 4HT

significantly blocked the proliferation of all of the cancer cells, regardless of ERα status.

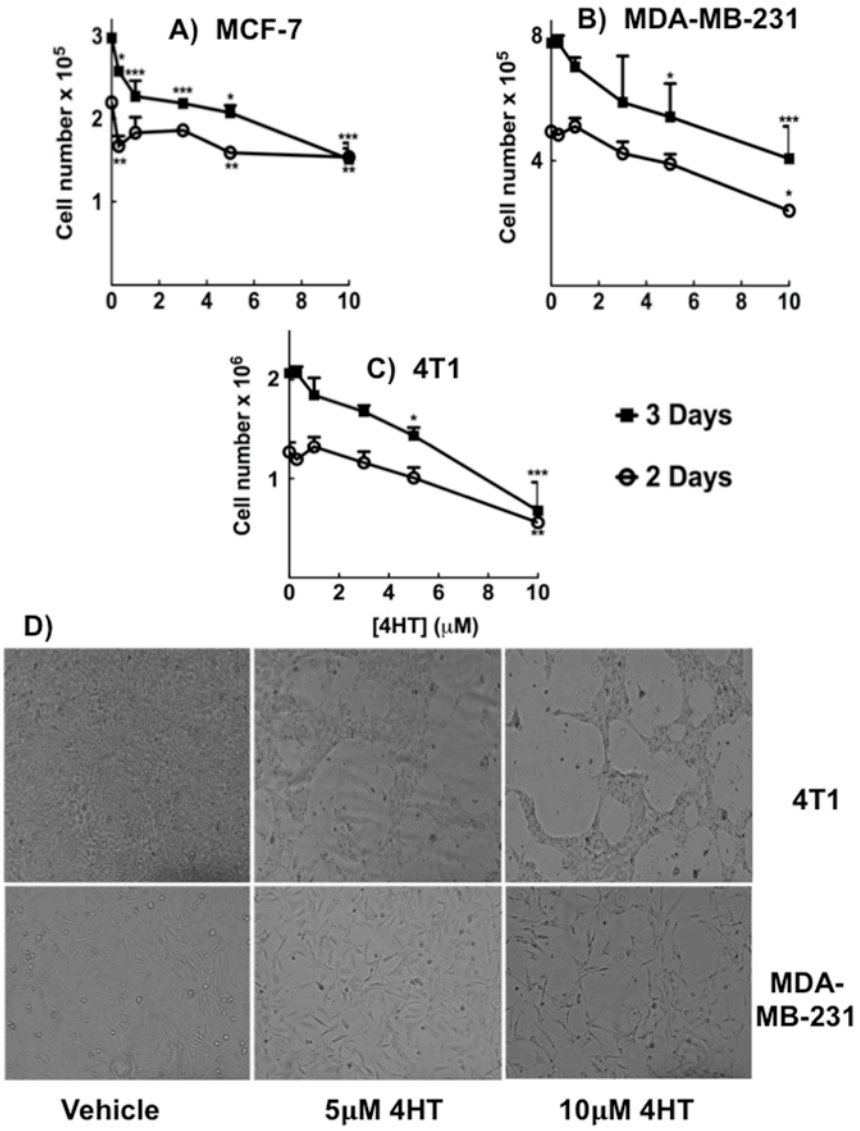

Figure 3.2: Tamoxifen slows the proliferation of breast cancer cells independently of the ERα.

(A) MCF-7, (B) MDA-MB 231 and (C) 4T1 cells were treated with 4HT and the proliferation of the cells were monitored 2 and 3 days post treatment using an automated Cell Counter. (D) Representative microscopy images of 4T1 (top) and MDA-MB 231 cells (bottom) grown for 3 days in the presence of vehicle, 5 μM or 10-μM of 4HT. Results are means ± SEM from for n=3 experiments. Significant differences were indicated with *= $p<0.05$, **= $p<0.01$ and ***= $p<0.001$.

To study this phenomenon further, serum-free medium, which was devoid of growth factors including estrogen, was used. Hence, the effects tamoxifen and its metabolites could be studied independently of their competitive inhibitory role against estrogens and effects of other growth factors. Different cancer cell lines were treated with 10 μM 4HT for 48 h, which resulted in cell death for both ERα-negative and ERα-positive cells (Fig. 3.3A-C).

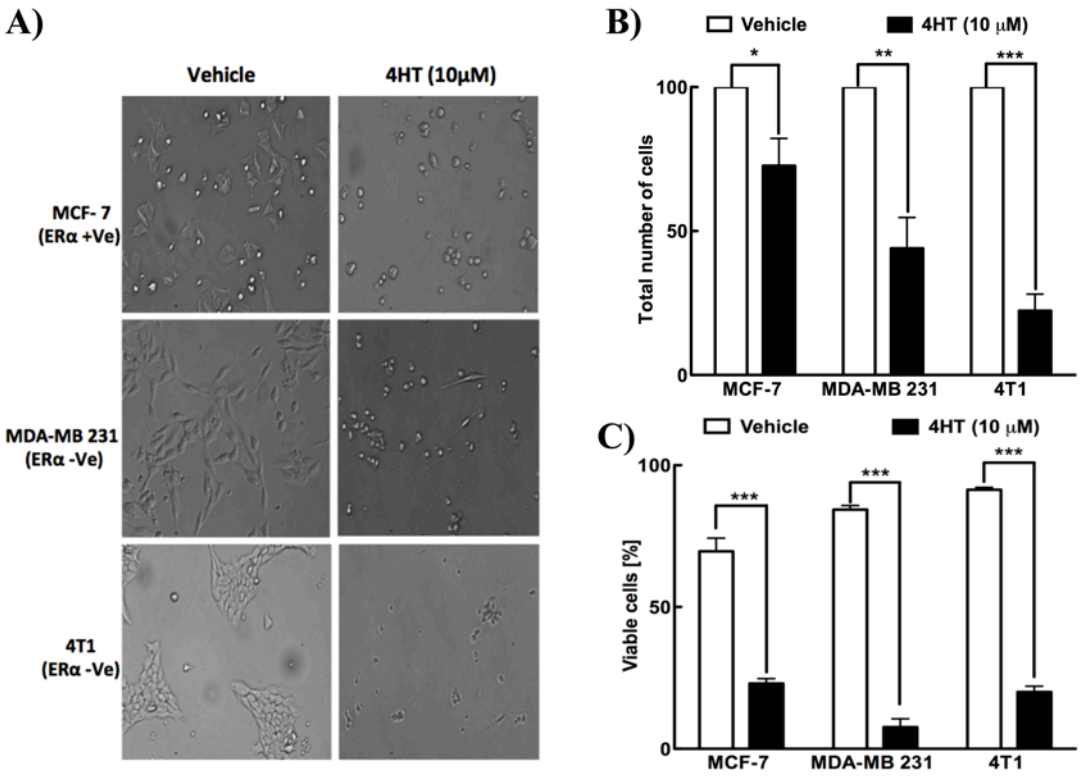

Figure 3.3: Tamoxifen kills both ERα positive and negative breast cancer cells.

(A) Microscopy images of different breast cancer cells treated with or with out 10 μM 4HT for 48 h in starvation media. (B) Total number of cells and (C) percent of viable cells quantified from microscopy images. Results are means ± SEM from for n=3 experiments. Significant differences were indicated with *= $p<0.05$, **= $p<0.01$ and ***= $p<0.001$.

The relative viability of the cells was also quantified by counting the number of cells that were judged to exhibit abnormal cell morphology such as cell shrinkage and blebbing (Fig. 3.3C).

To investigate the killing effects of the different metabolites of tamoxifen, 4T1 cells were treated with 10 μM TAM, NDMT or 4HT. As shown by the microscopy images (Fig. 3.4A) and crystal violet staining (Fig. 3.4B), tamoxifen and its metabolites significantly induced killing of 4T1 cells. This work demonstrates that killing induced by tamoxifen is not restricted to just one metabolite.

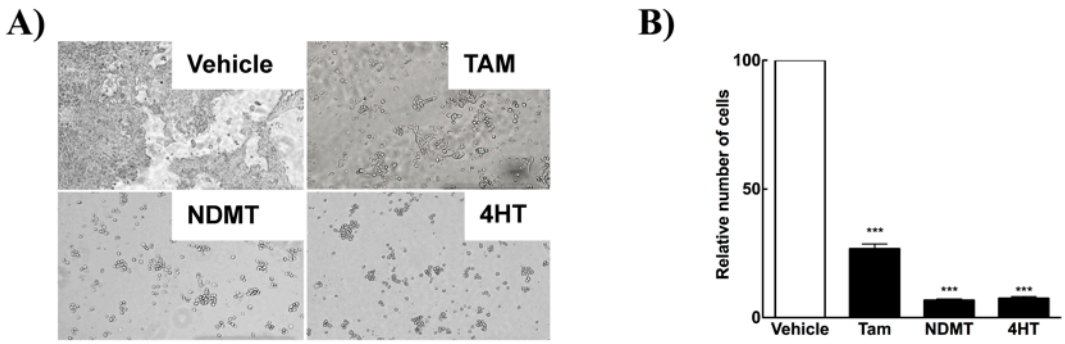

Figure 3.4: Tamoxifen and metabolites exert killing in ERα negative 4T1 cells.

(A) Representative microscopy image showing killing of 4T1 cells. (B) Relative number of cells as determined by crystal violet staining after treatment of cells with tamoxifen and metabolites. Results are means ± SEM from for n=3 experiments. Significant differences were indicated with ***= p<0.001.

As shown in Fig 3.2, the killing efficacy of tamoxifen in ERα-positive cells was different from the ERα-negative cells. This depended on the concentration of tamoxifen, with lower tamoxifen concentration only effective in the ERα-positive MCF-7 cells. These effects of tamoxifen were also tested in serum-free medium. For this purpose, different breast cancer cells were treated with

0.3-10 μM 4HT (Fig. 3.5) and the effects of tamoxifen were assessed by measuring the relative cell number, using crystal violet staining (Fig. 3.5A) and the relative viability, using MTT assay that measured the metabolic activity of the cells (Fig. 3.5B).

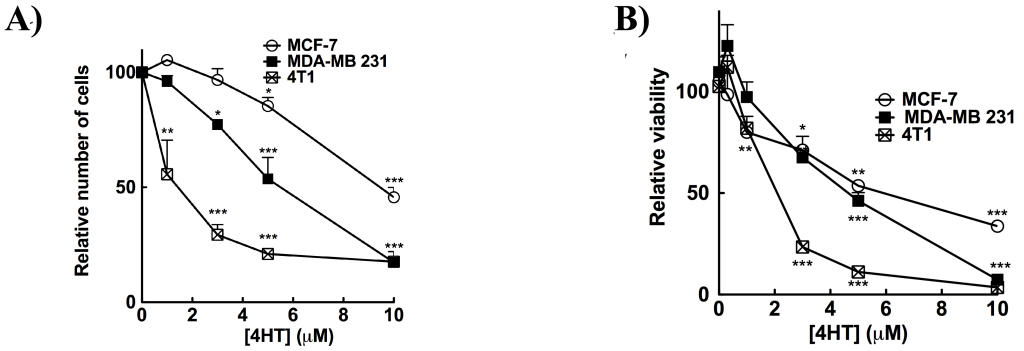

Figure 3.5: Concentration dependent killing effects of tamoxifen in ERα positive and negative breast cancer cells.

(A) Cell number as measured by crystal violet staining. (B) Cell viability as measured by MTT assay after 24h treatment with 4HT. Results are means ± SEM from for n=3 experiments. Significant differences were indicated with *= $p<0.05$, **= $p<0.01$ and ***= $p<0.001$.

In the absence of serum, the effect of tamoxifen was more pronounced in the ERα negative cells as the 4T1 cells were killed by 1 μM 4HT, where as MDA-MB-231 and MCF-7 cells responded from 3 μM onwards (Fig. 3.5A and B). This shows that MDA-MB-231 and 4T1 cells are more dependent on signals from serum growth factors for their overall proliferation and metabolic activity.

Overall, the results from Fig. 3.2-5 show that tamoxifen exerts killing effects in both ERα-positive and ERα-negative cells at clinically relevant concentrations. These effects of tamoxifen appear to be independent of ERα signaling. Hence, the next objective was to determine the mechanisms behind these actions of tamoxifen and its metabolites.

3.3 Tamoxifen treatment induces oxidative stress

Tamoxifen is hydrophobic and it rapidly accumulates in phospholipid bilayers of membranes where it is postulated to induce oxidative stress [16]. To investigate this, 4T1 cancers cells were pretreated with the superoxide indicator, dihydroethidium (DHE), which is oxidized to produce a bright fluorescent red color when it interacts with superoxide. After DHE pretreatment, the cells were treated with 10 μM tamoxifen for 24 h. The results show that tamoxifen significantly increased the intensity of red staining in 4T1 cells, indicating greater superoxide generation (Fig. 3A and B).

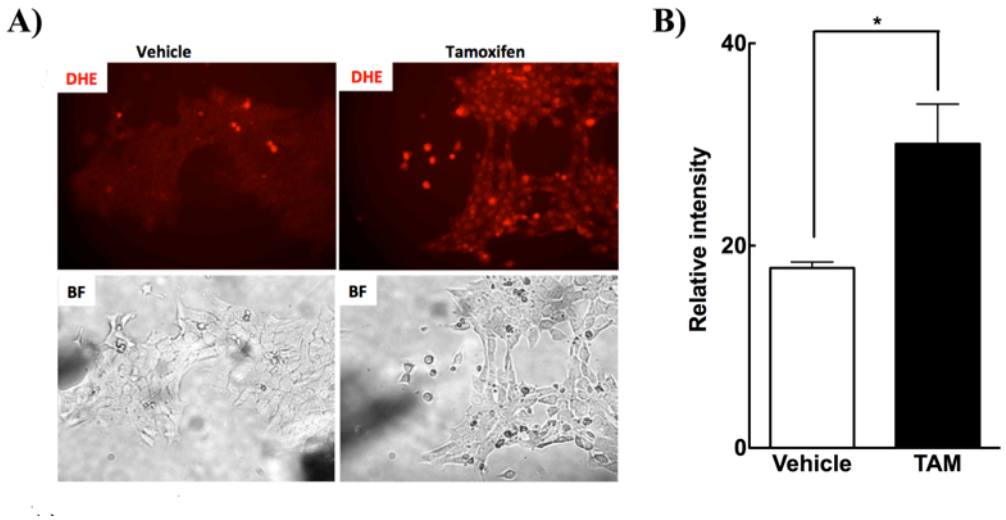

Figure 3.6: Tamoxifen generates superoxides.

(A) Representative fluorescence microscopy images from DHE stained 4T1 cells followed by either vehicle or 10μM tamoxifen treatment. (B) Quantification of relative superoxide formation as measured by DHE staining intensity. Results are means ± SEM from for n=3 experiments. Significant differences were indicated with *= $p<0.05$.

Generation of reactive oxygen species such as superoxides could lead to lipid peroxidation. Hence, the production of 4-hydroxynonenal (4HNE), which is a very reactive byproduct that results from the oxidation of membrane lipids, was measured in response to tamoxifen. The reactive 4HNE conjugates with cell proteins and this can be visualized by Western blotting with an anti-4HNE antibody [360].

Treatment of 4T1 cells with 10 μM 4HT for 24 h significantly increased the conjugation of proteins at 65 kDa with 4HNE and this effect was partially blocked with the antioxidants, vitamin E and/or PMC (2,2,5,7,8-pentamethyl-6-chromanol, a vitamin E moiety without a lipid tail) (Fig. 3.7 A and B). Increased conjugation of cellular proteins with 4HNE was also observed in MCF-7 cells treated with tamoxifen (Fig. 3.7 C-E). Hence, treatment of breast cancer cells with 4HT increases oxidative stress leading to the oxidation of membrane lipids and the production of 4HNE (Fig. 3.7).

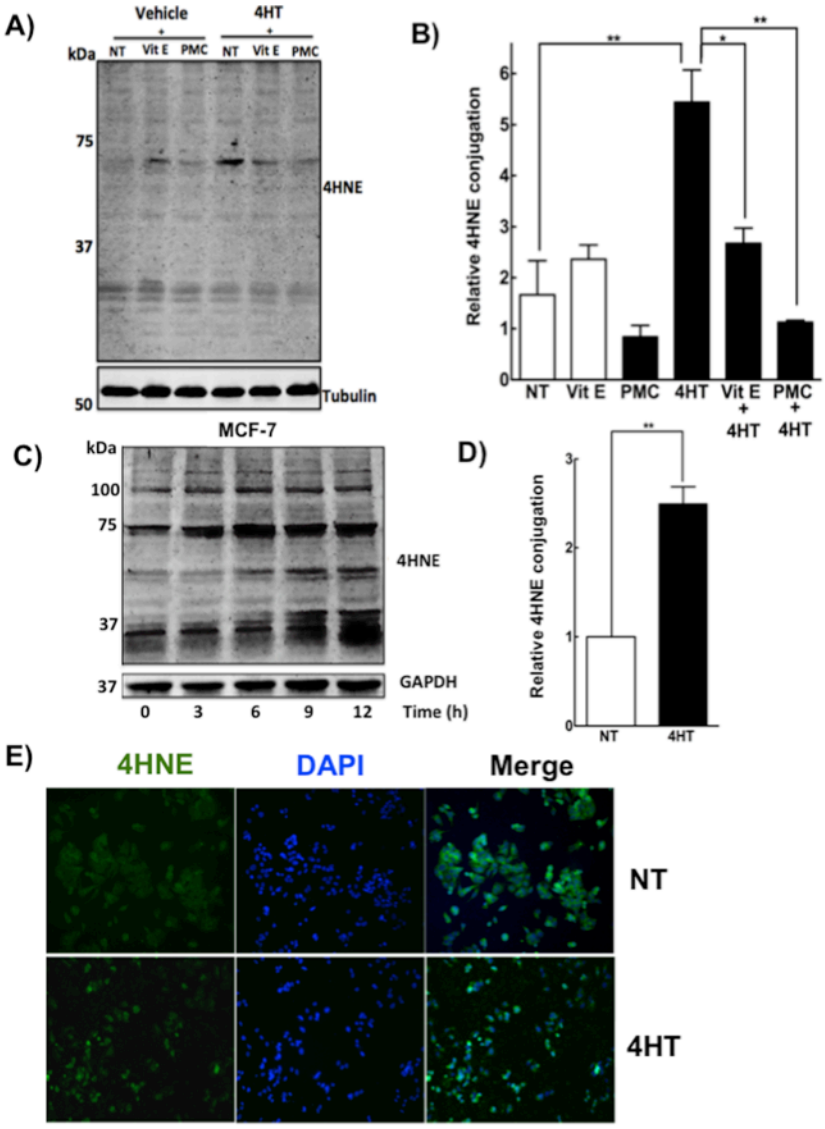

Figure 3.7: Tamoxifen treatment induces lipid peroxidation in ERα positive and negative cells.

(A) 4T1 cells were pretreated with the antioxidants vitamin E (100 μM) or PMC (100 μM) for 3 h followed by 24 h treatment with 10 μM 4HT. The extent lipid peroxidation was detected by western blot using anti-4HNE antibody. (B) Results of the relative 4HNE conjugations were quantified from Western blots at 65 kDa. (C) Time-dependent conjugation of cellular proteins with 4HNE in MCF-7 cells after treatment with 20 μM 4HT and (D) the corresponding quantification of this 4HNE conjugation at the 12 h time point. (E) Representative immunofluorescence images of MCF-7 cells treated with either vehicle or with 5 μM 4HT for 24 h and cells were stained with anti-4HNE antibody and then counterstained with DAPI for nuclei staining. Results are means ± SEM from for n=3 experiments. Significant differences were indicated with *= $p<0.05$, **= $p<0.01$ and ***= $p<0.001$.

3.4 Tamoxifen induces apoptosis.

Caspase-3 is a protease, which is known to cleave poly (ADP-ribose) polymerase (PARP) and other proteins leading to apoptosis. Caspase-3 activation occurs through proteolytic cleavage resulting in an increase in a 17-kDa fragment, which is indicative of apoptosis-initiation [361]. To determine the effects of tamoxifen on caspase-3 activation, 4T1 cells were treated for 24 h with 10 μM 4HT. The results show that 4T1 cells had an increased caspase-3 cleavage indicating tamoxifen-induced apoptosis. Furthermore, this increase in apoptosis by tamoxifen was partially blocked by the anti-oxidants, vitamin E or PMC (Fig. 3.8).

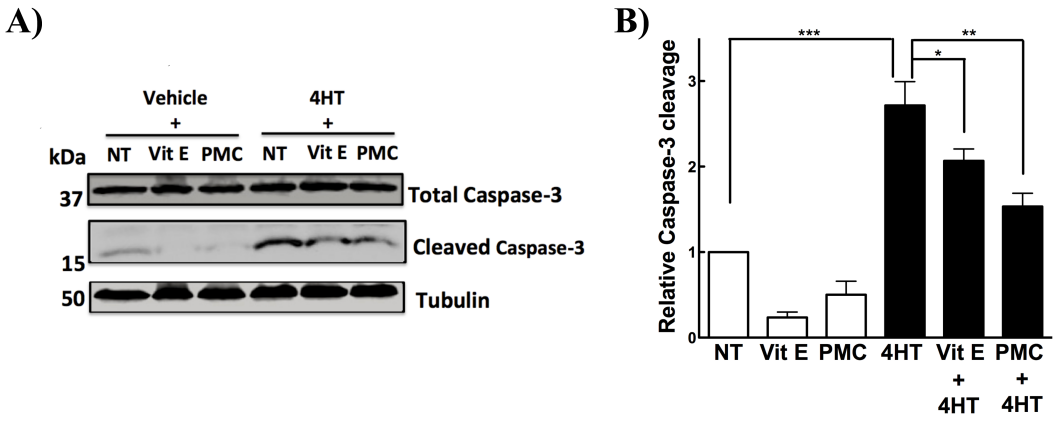

Figure 3.8 : Tamoxifen induces apoptosis as measured by cleaved caspase-3.

(A) Treatment of 4T1 cells with 10 μM 4HT leads to cleavage of caspase-3 and this is partially rescued with vitamin E (100 μM) or its analog PMC (100 μM). (B) The respective quantification of the western blots. Results are means ± SEM from for n=3 experiments. Significant differences were indicated with *= $p<0.05$, **= $p<0.01$ and ***= $p<0.001$.

As activation of caspase-3 leads to cleavage of PARP; measurement of PARP cleavage can also serve as a surrogate for caspase activation and subsequent initiation of apoptosis. Therefore, MCF-7, MDA-MB-231 and 4T1 cells were treated with 4HT and PARP cleavage was measured by Western blotting. As shown in Fig. 3.9, all the cells treated with tamoxifen showed PARP cleavage. However, as opposed to caspase-3 cleavage (Fig 3.8), the antioxidants vitamin E and PMC were not able to rescue cells from 4HT-induced PARP cleavage (Fig. 3.9C). As anti-oxidant were able to partially block caspase-3 activation, this results indicate a caspase-3-independent cleavage of PARP by tamoxifen.

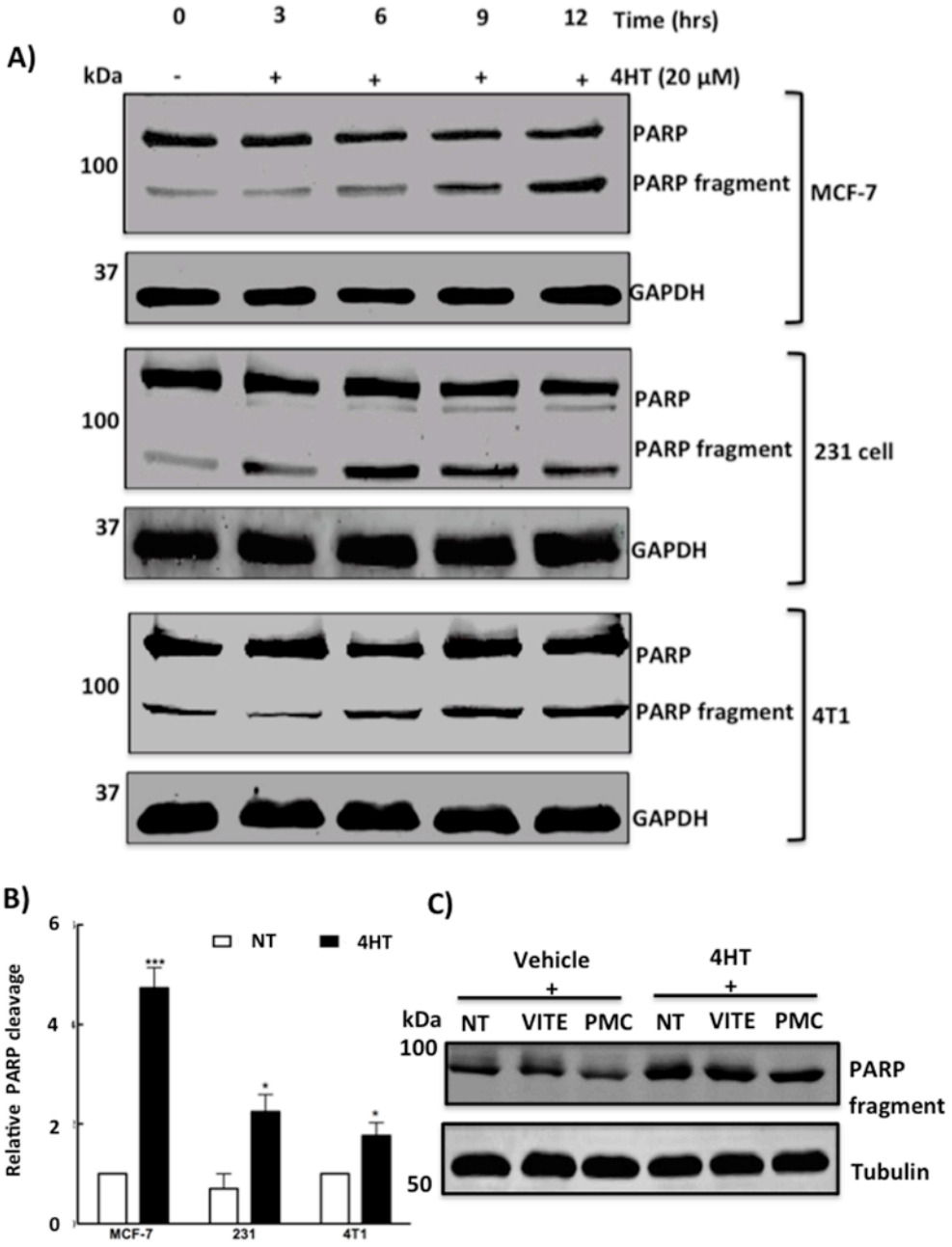

Figure 3.9: Tamoxifen increases PARP cleavage, which is not blocked by vitamin E or PMC.

(A) MCF-7 cells (top), MDA-MB-231 cells (middle) and 4T1 cells (bottom) were treated with 20 μM 4HT after which PARP cleavage was assessed by western blotting (B) Western blot quantification of the relative cleaved PARP levels was estimated at the 12 h time point. (C) Treatment of 4T1 cells with 10 μM 4HT for 24 h increased PARP cleavage but this increase is not blocked by either 100 μM vitamin E or 100 μM PMC. Results are means ± SEM from for n=3 experiments. Significant differences were indicated with *= $p<0.05$ and ***= $p<0.001$.

3.5 Tamoxifen leads to an increase in ceramide accumulation.

Cell death following radiotherapy and/or chemotherapeutic agents is often accompanied by the accumulation of ceramides. Ceramides are lipid-signaling mediators, which are highly responsive to stress and relay apoptotic messages leading to activation of caspases [362-364].

To investigate if tamoxifen-induced oxidative stress was accompanied by increased ceramide accumulation, different breast cancer cells were treated with tamoxifen followed by measurement of ceramide levels. As shown in Fig. 3.10, 4HT treatment significantly increased the accumulation of different ceramide species.

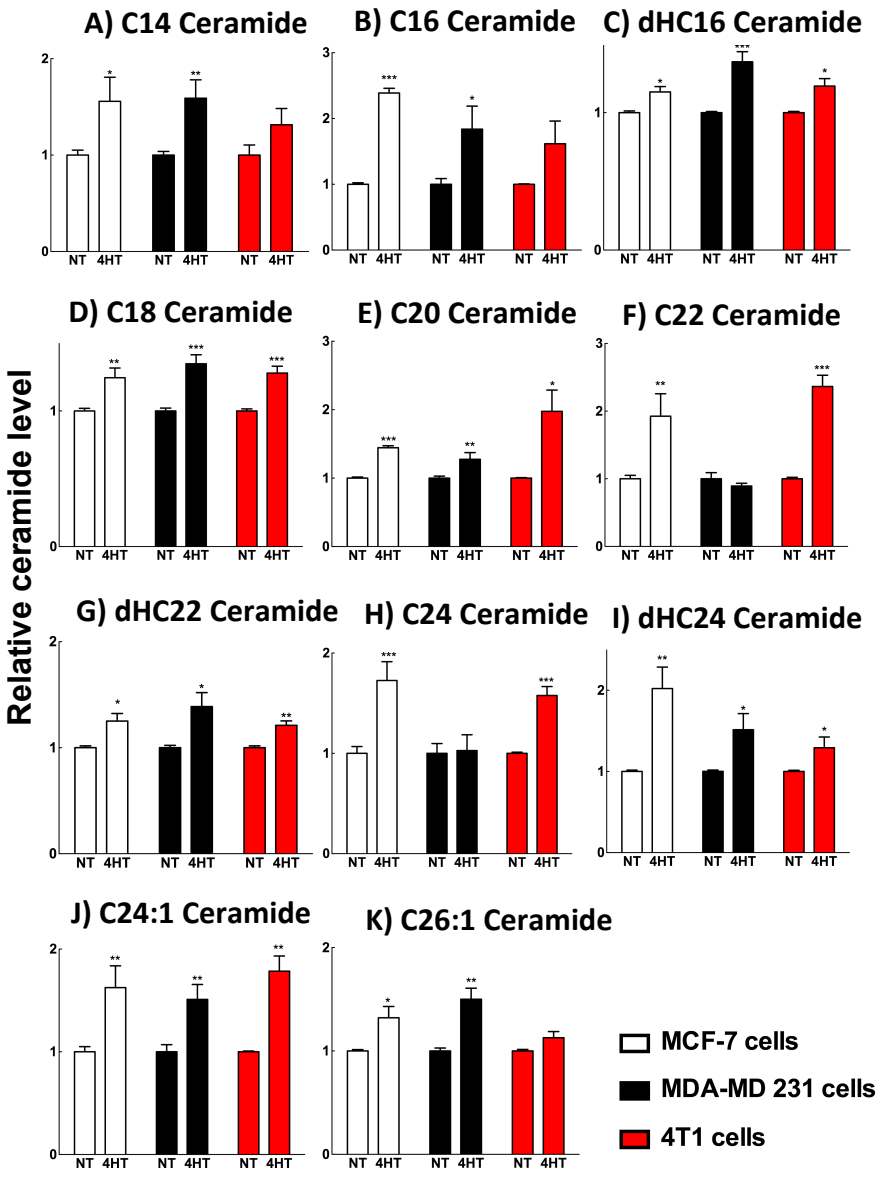

Figure 3.10: Tamoxifen increases the accumulation of different ceramide species.

(A- K) Cells were treated for 12 h with 20 μM 4HT in MCF-7 cells indicated by white bar, MDA-MB-231 indicated by black bar and 4T1 indicated by red bar. Then the relative ceramide levels were assessed by mass spectroscopy. The prefix dH stands for dihydro-ceramide species. Results are means ± SEM from for n=4 experiments. Significant differences were indicated with *= p<0.05, **= p<0.01 and ***= p<0.001.

The antioxidant, vitamin E, was able to block caspase-3 activation induced by tamoxifen (Fig. 3.8). Hence, to investigate if the accumulation

ceramide could also be blocked by vitamin E, 4T1 cells were treated with 10-μM 4HT for 24 hours in the presence or absence of vitamin E. The levels different ceramide species were then assayed.

Treatment of 4T1 cells with 4HT significantly increased the accumulation of C16-, dHC16-, C18-, C20-, dHC20-, dHC22-ceramides ($p<0.05$). However, similar to the PARP cleavage, vitamin E was not able to block the accumulation of ceramide (Fig. 3.11). These results show that tamoxifen initiates the cleavage of PARP and the accumulation ceramide independently from the activation of caspase-3.

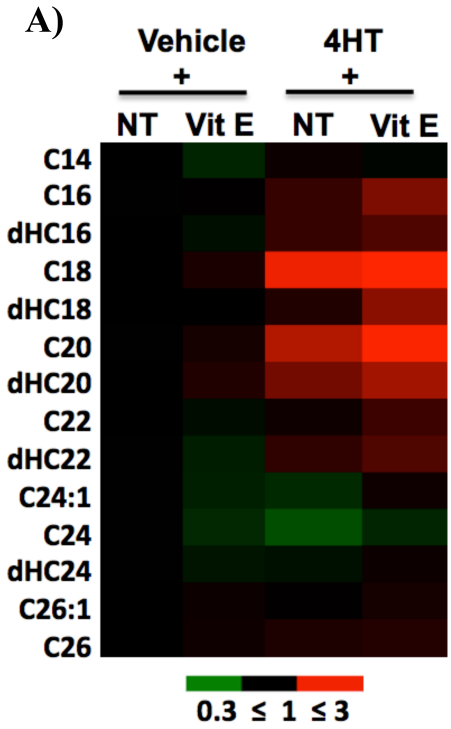

Figure 3.11: Tamoxifen-induced ceramide accumulation is not reversed by vitamin E.

A heat map with black representing no change, green showing a decrease and red showing a significant increase in ceramide levels was set up from the relative average levels of the different ceramide species. Results are from n=4 experiments in 4T1 cells that were treated with vehicle, 100 μM vitamin E, 10 μM 4HT or the combined vitamin E and 4HT. The prefix dH stands for dihydro-ceramide species. .

3.6 Tamoxifen increases JNK phosphorylation levels.

The protein JNK belongs to a family of stress-activated protein kinases and the two isoforms, JNK-p54 and JNK-p46 are activated through phosphorylation of Thr183/Tyr185 residues. This activation of JNK is stimulated by different stressors, such as oxidative stress and moreover, its activation is also linked to increased ceramide levels [82].

Studies have previously shown that treatment of cells with exogenous C2-ceramide leads to endogenous ceramide production [365]. Hence, 4T1 cells were treated with C2-ceramide and the levels of JNK phosphorylation was measured by Western blotting. Bioactive C2-ceramide was able to increase the levels of JNK phosphorylation compared to the inactive dihydro-C2-ceramide (Fig. 3.12A). It is thus logical to postulate that JNK phosphorylation levels would also be increased upon tamoxifen treatment. To test this postulate, 4T1 and MCF-7 cells were treated with 4HT and as shown (Fig. 3.12B-E), 4HT-induced a significant increase in JNK phosphorylation levels.

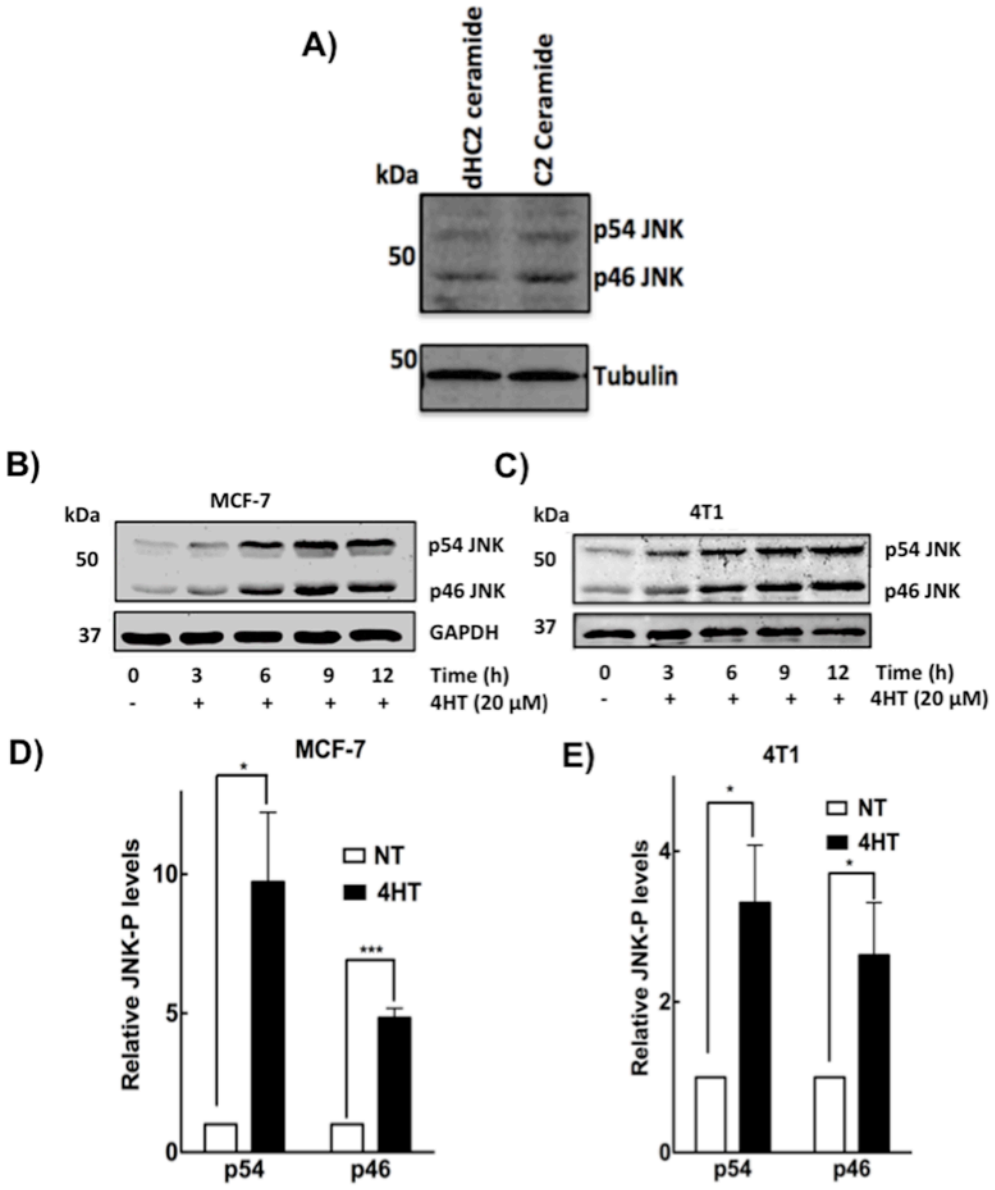

Figure 3.12: Tamoxifen and ceramide stimulate an increase in JNK phosphorylation levels.

(A) 4T1 cells were treated with 100 µM of bioactive C2-ceramide or with the inactive control dihydro-C2-ceramide (dHC2 Ceramide) followed by Western-blot for phosphorylated p54 JNK and p46 JNK. (B to E) Western blot for phosphorylated JNK after 3, 6, 9 and 12 h of 4HT treatment in (D) MCF-7 cells (C) 4T1 cells. The corresponding quantification for the phosphorylated p54 JNK and p46 JNK at 12-h mark in (D) MCF-7 and (E) 4T1 cells. Results are means ± SEM from for n=3 experiments. Significant differences were indicated with *= $p<0.05$ and ***= $p<0.001$.

Vitamin E was not able to block ceramide accumulation. Therefore, if ceramide activation were responsible for increased JNK activation, then the likelihood would be that treatment with vitamin E would similarly not affect the levels of phosphorylated JNK. As expected, treatment of MCF-7 with 4HT was able to activate JNK but the addition of vitamin E did not block JNK activation by tamoxifen (Fig 3.13A).

Another mechanism for activation of JNK would be through the enzyme, Apoptosis Signal regulating Kinase-1 (ASK1), which has been shown by other studies to increase the activation of JNKs [366]. Hence, to test if blocking ASK1 would inhibit the activation of JNK by tamoxifen, MCF-7 cells were treated with ASK1 specific inhibitor (TC ASK 10).

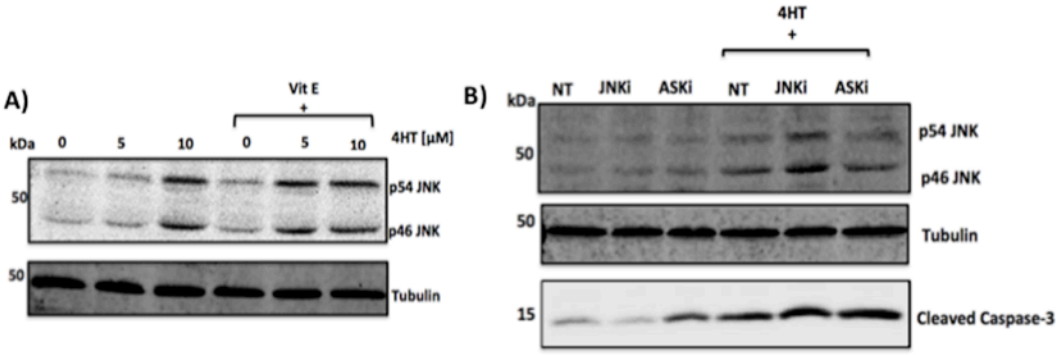

Figure 3.13: The effects of vitamin E and inhibition of AKS1 and JNK on the effects of tamoxifen.

(A) MCF-7 Cells were treated with 4HT as indicated in the presence or absence of 100 μM vitamin E and the levels of p54 JNK and p46 JNK were assessed with western blotting. (B) 4T1 cells were treated with vehicle, inhibitor for JNK (JNKi, SP 600125), and ASK1 (ASKi, TC ASK 10) in the presence or absence of 10 μM 4HT followed by western blot for JNK phosphorylation and cleaved caspase-3. Representative Western blots from n=3 experiments are shown.

Additionally, the effect of JNK and ASK1 on tamoxifen-induced activation of caspase-3 was assessed using the specific inhibitors for JNK (SP 600125) and ASK1 (TC ASK 10). The results show that inhibiting ASK1

was not able to reverse the activation JNKs by tamoxifen. In addition both inhibitors for JNK and ASK1 did not reverse the activation of caspase-3 by tamoxifen (Fig 3.13B).

These results provide further credence to the proposal that tamoxifen-induced increase in ceramide levels and the subsequent JNK activation (Fig 3.12-13) is occurring separately from the tamoxifen-induced caspase-3 activation.

3.7 Tamoxifen increases the level of Nrf2 and activates the anti-oxidant response element.

The results so far show that oxidative stress is a major consequence of tamoxifen treatment. Cancer cells often respond to oxidative damage by increasing the expression of the transcription factor, Nrf2, which activates the ARE in a protective response to limit the oxidative damage [136, 367, 368]. To examine if tamoxifen treatment would also elicit a similar increase in the accumulation of Nrf2, MCF-7 cells were treated with 1 to 30 μM 4HT. The results showed that tamoxifen treatment increased Nrf2 levels along with NQO1 (NAD(P)H dehydrogenase quinone-1), a downstream anti-oxidant gene regulated by Nrf2 (Fig. 3.14A).

To further corroborate the role of Nrf2 in response to tamoxifen, we employed MCF-7 cells stably expressing the ARE sequence upstream to a luciferase reporter gene.

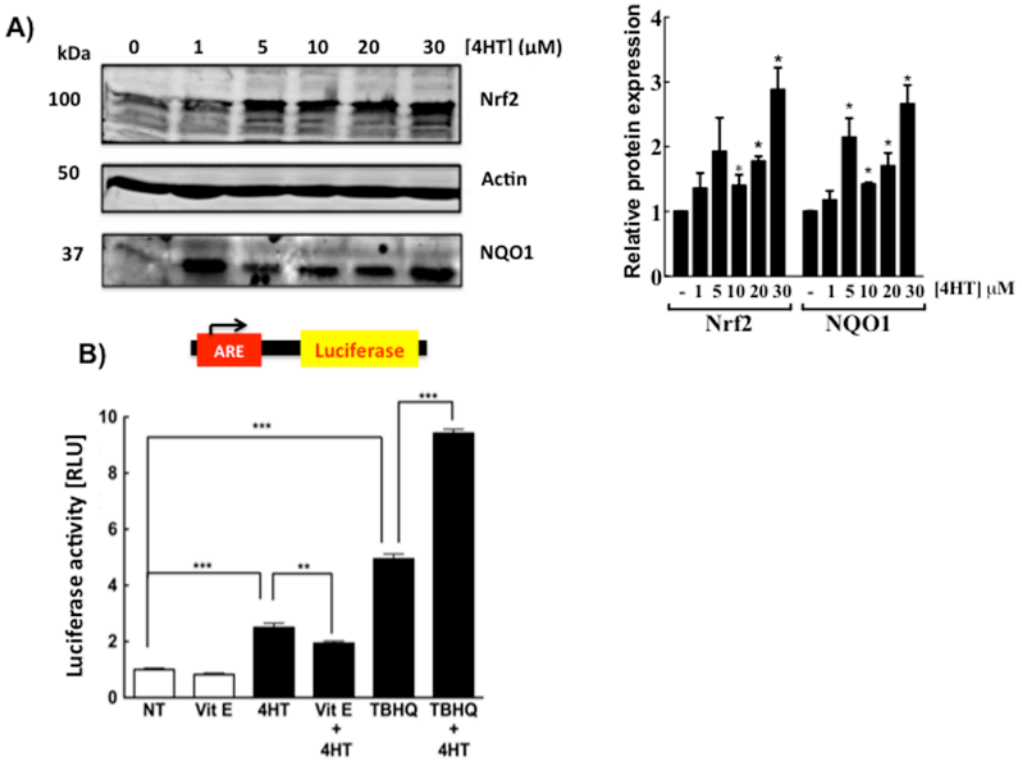

Figure 3.14: Tamoxifen increases Nrf2 levels and thereby activates the ARE.

(A) 4HT stimulates a dose-dependent increase in Nrf2 levels and the anti-oxidant gene NQO1 in MCF-7 cells. Western blot for Nrf2 and NQO1 (left) with the corresponding quantification (right). (B) Luciferase activity assay after treatment with vehicle, 100 μM vitamin E and 10 μM TBHQ alone or in combination with 10 μM 4HT in MCF-7 cells expressing a luciferase reporter gene. Results are means ± SEM from for n=4 experiments. Significant differences were indicated with **= $p<0.01$ and ***= $p<0.001$.

As shown in Fig. 3.14B, tamoxifen by itself increased luciferase expression and this increase was partially blocked by vitamin E. Moreover, the addition of 4HT with TBHQ (tert-butylhydroquinone), a known activator of ARE and Nrf2, caused a further increase in luciferase expression.

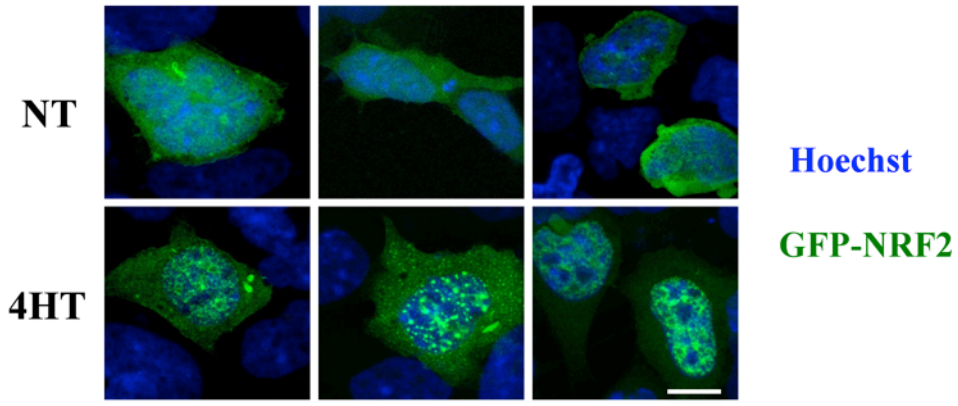

Figure 3.15: Tamoxifen treatment induces the translocation Nrf2 to nucleus.

Confocal microscopy images of HEK 293 cells transfected with GFP-Nrf2 and treated with either vehicle (top three images) or with 4HT (bottom three images). Hoechst was used to stain for nuclei. Representative images are shown.

The effect of tamoxifen treatment on the localization of Nrf2 was also tested. For this purpose, GFP-tagged NRF2 was overexpressed in HEK-293, which are very receptive to transfection by plasmids. Following this transfection, the cells were treated with 4HT and confocal microscopy was used to study the localization of Nrf2. The result shows that tamoxifen treatment increased both the levels and also the nuclear localization of GFP-tagged Nrf2 (Fig 3.15).

Previous work in our laboratory showed that lysophosphatidate (LPA), a lipid growth factor that acts through six G-protein coupled receptors, promotes chemo-resistance to Taxol [254] and doxorubicin [259]. The induction of chemo-resistance by LPA depends partly on its ability to increase Nrf2 levels and lead to the activation of the ARE and the consequent

transcription of anti-oxidant genes and multidrug resistance transporters [259].

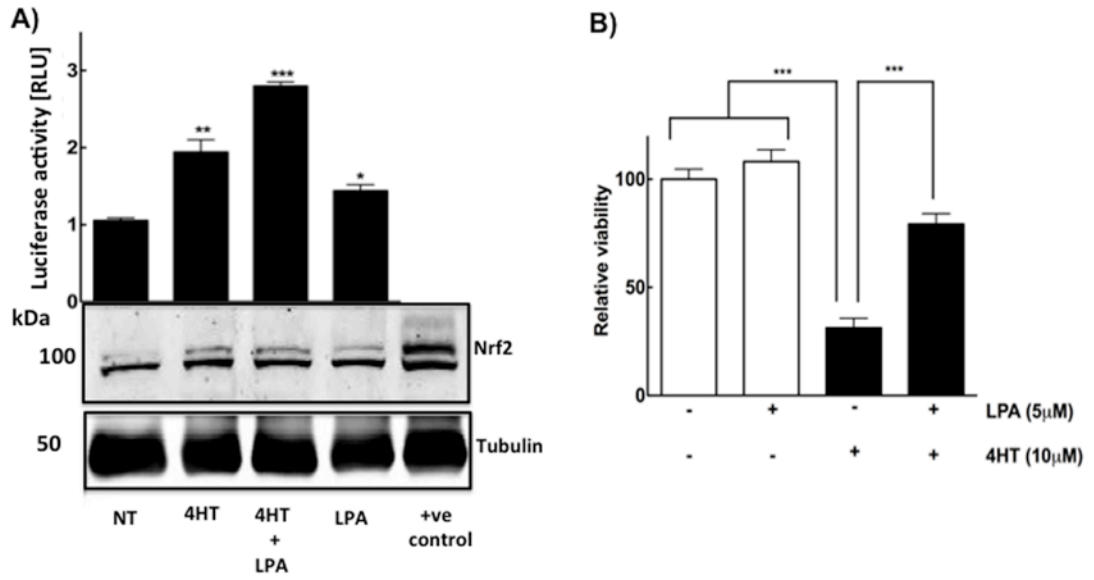

Figure 3.16: Lysophosphatidate amplifies the response of cancer cells and protects them from tamoxifen-induced killing.

(A) Luciferase activity (top) and Western blot for Nrf2 (bottom) after treating cells with vehicle and LPA alone or in conjunction with 10 μM 4HT. (B) Treatment of MCF-7 cells with 5 μM LPA rescued cells from tamoxifen-induced cell killing. Results are means ± SEM from for n≥3 experiments. Significant differences were indicated with *= $p<0.05$, **= $p<0.01$ and ***= $p<0.001$.

Due to LPA's role in stimulating an increase in Nrf2 levels, a logical postulate would be that LPA could also amplify the ARE response of the breast cancer cells to tamoxifen and thereby lead to a decrease in tamoxifen-induced killing. As predicted, treatment of MCF-7 cells with 4HT in the presence of LPA further increased ARE-dependent luciferase expression (Fig. 3.16A) and also blocked the killing effects of tamoxifen (Fig 3.16B).

3.8 Effects of tamoxifen on tumor growth in mouse model of breast cancer

The next objective was to test whether the effects of tamoxifen observed in cell culture could be recapitulated *in vivo*. Hence, an orthotopic syngeneic mouse model was established by injecting 4T1 breast cancer cells, which do not express ERα, into the mammary fat pad of female Balb/c mice, as previously published [206].

This syngeneic model produced a substantial tumor burden within 10 days and tamoxifen treatment decreased breast tumor weight significantly by about 35% compared to the control group (Fig. 3.17A). Furthermore, tamoxifen treated animals had significantly increased Nrf2 and NQO1 expression levels in their breast tumors (Fig 3.17B and C).

Additionally, tamoxifen also increased mRNA expression of NAD(P)H dehydrogenase quinone 1 (NQO1), heme oxygenase 1 (HMOX1), superoxide dismutase 1 (SOD1) and the ATP-binding cassette (ABC) transporters, ABCC1, ABCG2 and ABCC3 (Fig. 3.17D). These results indicate that tamoxifen inhibited tumor growth of tumor *in vivo* but at the same time an anti-oxidant response is activated with the levels of Nrf2 and the genes regulated by Nrf2 subsequently increased.

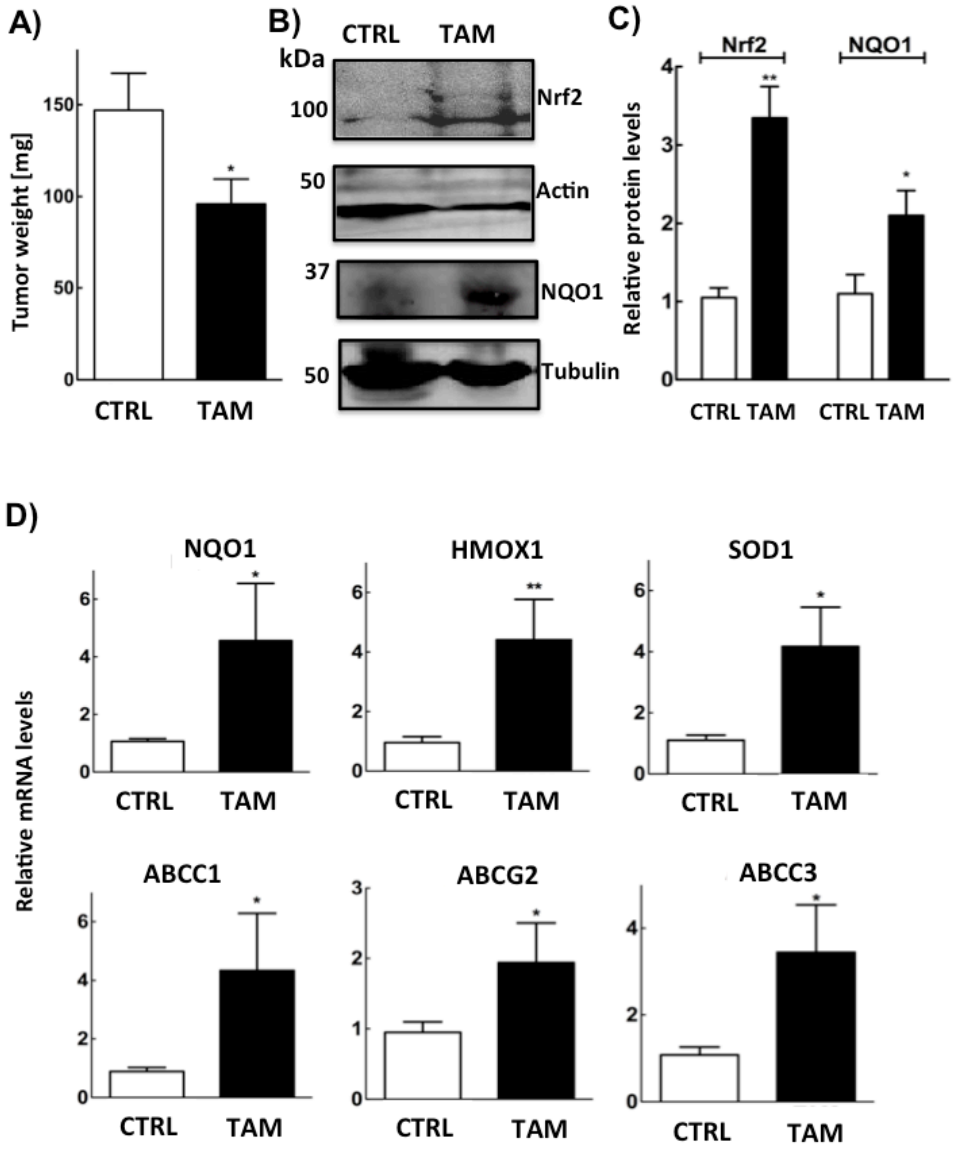

Figure 3.17: Tamoxifen decreases the tumor burden in mice and increases Nrf2 dependent genes in an orthotropic mouse model of breast cancer.

(A) Primary tumors were excised and weighed (results from n=6 mice per group). (B) Western blots showing images for the expressions of Nrf2 and NQO1 in tumors from control and tamoxifen-treated mice with (C) the corresponding quantification for Nrf2 relative to actin and NQO1 relative to tubulin. (D) The relative mRNA levels for NQO1, HMOX1, SOD1, ABCC1, ABCG2 and ABCC3 in control versus tamoxifen treated mice. Significant differences were indicated with * = $p<0.05$ and **= $p<0.01$.

The tamoxifen treatment regimen is described in the Methods section of Chapter 2. This regimen was well tolerated by the animals as depicted by the body weight measurement below (Fig 3.18).

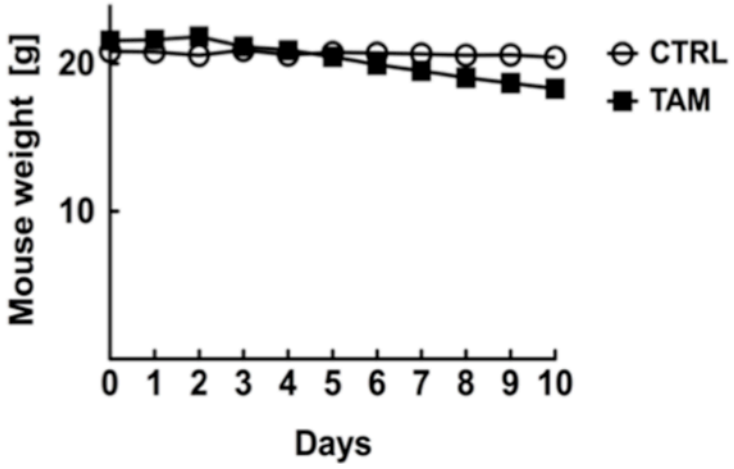

Figure 3.18:Tamoxifen treatment regimen is well tolerated in mice.

To gauge the health status of mice body weight was measured every day before treatment gavage. Results were from n=6 mice in each of the control and tamoxifen treatment group.

3.9 Prognostic values of Nrf2, ABCC1, and NQO1 in human cancer patients treated with tamoxifen.

To determine the validity of the findings from the cell culture and the syngeneic mouse model to responses in human patients, a collection of human breast tumors included in the Breast Cancer Relapsing Early Determinants study was used [369]. This collection included 176 patients diagnosed with primary breast cancer who had their tumors resected before treatment. Of these patients, 64% had ERα-positive tumors and ~84% of these patients were treated with tamoxifen. The ERα-positive patients who were not treated with tamoxifen were mainly postmenopausal and they received aromatase inhibitors. Other treatments included trastuzumab for those with Human Epidermal growth factor Receptor 2 (HER2) positive tumors, or anthracycline for high-risk node-negative disease and adjuvant cytotoxic chemotherapy for those with high-risk features. Additional information about the clinical and pathological features of the breast cancer cases used in this study is provided in Table 4 (Appendix section).

Dr. Rong-Zong Liu determined the gene expression profiles of the patient's resected tumors. Employing this gene expression data, a prognostic analysis for the survival probability of tamoxifen-treated patients and those that did not receive tamoxifen was performed. Patients with tumors that had high expression of Nrf2 had a significantly lower survival probability of $p=0.002$ and a hazard ratio (HR) value of 4.0 for the tamoxifen-treated cohort.

This indicated a 4-fold decrease in overall survival probability as compared with the low Nrf2 expressing group (Fig. 3.19A).

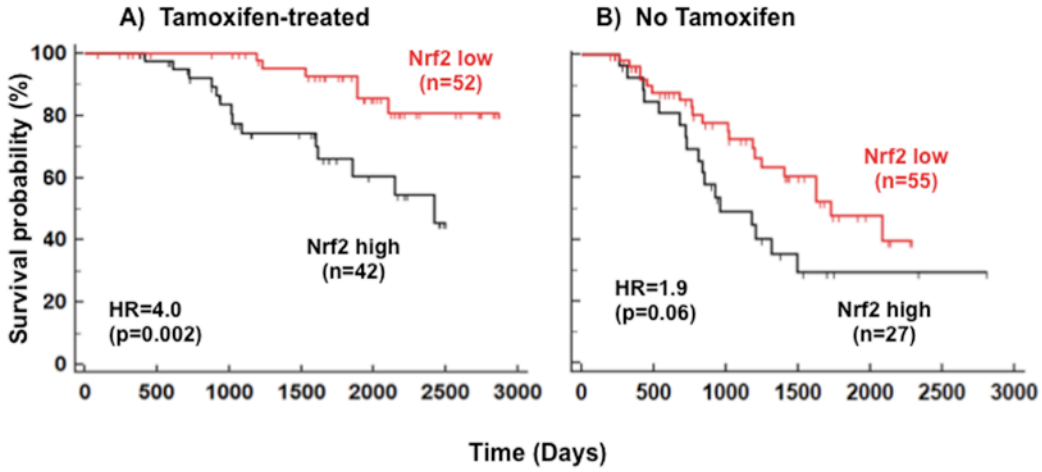

Figure 3.19: The prognostic significance of Nrf2's gene expression levels.

Patients stratified as high and low expressers of Nrf2, (A) Tamoxifen treated and (B) non-tamoxifen treated patients. The red lines show the survival probability of patients with low expression while the black lines show high expression for Nrf2 gene.

In patients that did not receive tamoxifen, the difference in survival probability was not statistically significant (p=0.06) but there was a trend towards better survival in the low Nrf2 expresser group with HR value of 1.9 (Fig. 3.19B).

For ABCC1 and ABCC3 the overall survival probability within the tamoxifen-treated group showed a better survival probability for the low ABCC1 expressers (p=0.04) and HR value of 4.0 (Fig. 3.20A), and p=0.01 and an HR value of 4.2 for ABCC3 (Fig. 3.20C). Nevertheless in the patients who did not receive tamoxifen treatment, the results were not statistically significant and did not show a trend for ABCC1 (p=0.94 and HR value of 1.0)

(Fig. 3.20B). However, there was a trend towards better survival in the low ABCC3 expresser group with HR value of 1.7 (Fig. 3.20D).

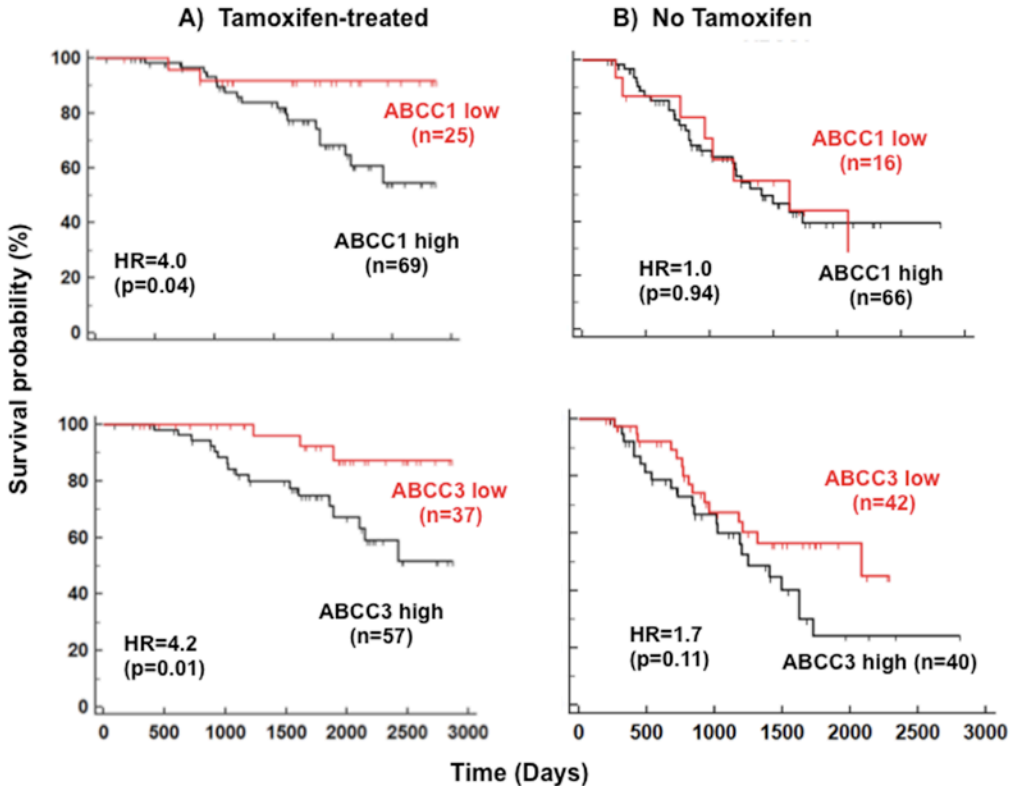

Figure 3.20: The prognostic significance of ABCC1 and ABCC3 gene expression level.

Patients stratified as high and low expressers for (A) ABCC1 gene in tamoxifen treatment cohort, (B) ABCC1 gene in non-tamoxifen treated patients cohort, (C) ABCC3 gene in tamoxifen treatment cohort and (D) ABCC3 gene in non-tamoxifen treated patients cohort. Red-lines show the survival probability of patients with low expression while the black lines show high expression for ABCC1 and ABCC3 genes.

For NQO1 within the tamoxifen-treated patients there was only a trend towards increased survival (HR=2) in the low NQO1 expressers (Fig. 3.21A) and patients that were not treated with tamoxifen did not show any prognostic value (Fig. 3.21B).

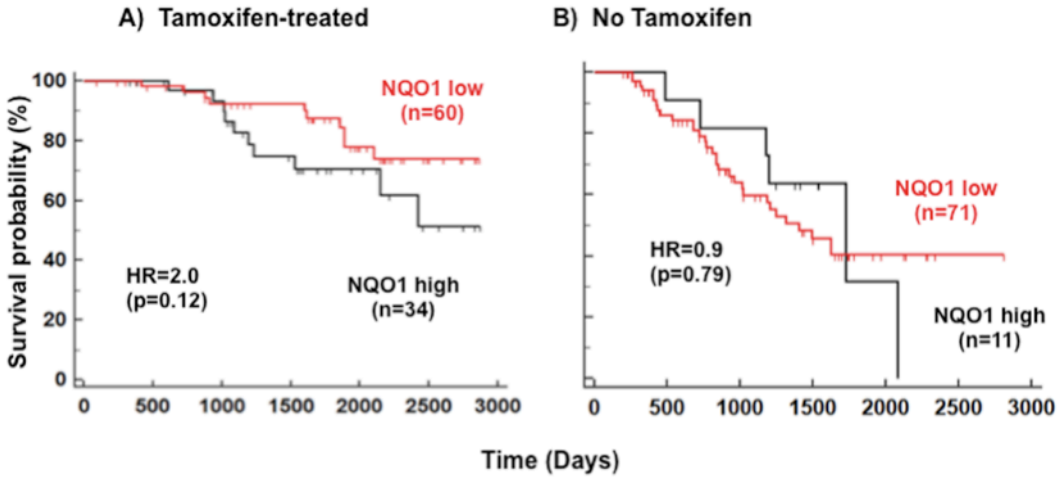

Figure 3.21: The prognostic significance of NQO1 gene expression levels.

Patients stratified as high and low expressers for NQO1, (A) Tamoxifen treated and (B) non-tamoxifen treated patients. The red lines show the survival probability of patients with low expression while the black lines show high expression for NQO1 gene.

A statistically significant ($p<0.0001$) correlation between the expressions of NQO1 and ABCC3 was identified (Fig. 3.22A). This prompted an analysis of the survival probability by grouping patients into double high expressers for NQO1 and ABCC3 and comparing them to double low expressers. As shown in Fig. 3.22B, the double high expressers had a significantly lower survival with $p=0.02$ and an even higher HR value of 5.1 with in the tamoxifen-treated group.

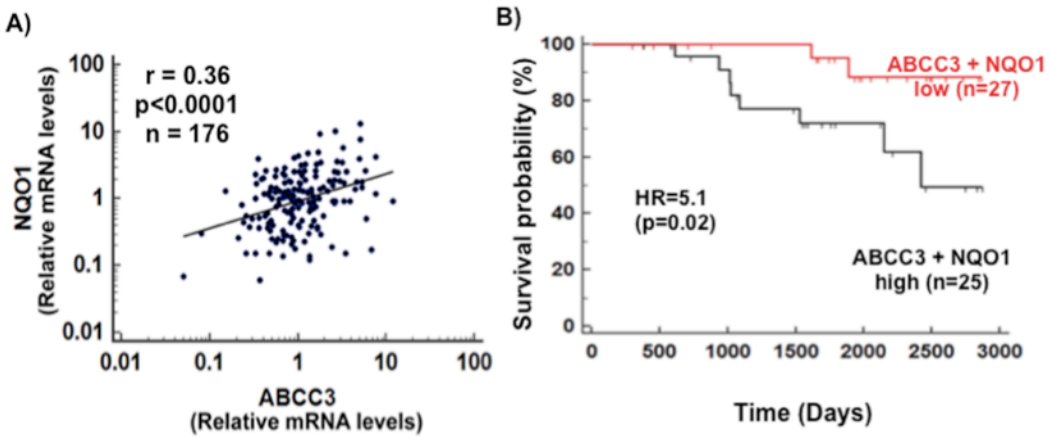

Figure 3.22: NQO1 moderately correlates with expression profile of ABCC3 and improves prognostic significance

(A) Correlation between the expression levels of ABCC3 and NQO1 in breast cancer biopsies at original diagnosis. The correlation analysis was performed on breast tumors derived 176 patient samples. (B) Patients stratified as high and low expressers for both NQO1 and ABCC3. The red lines show the survival probability of patients with low expression while the black lines show high expression for both NQO1 and ABCC3 gene.

3.10 Conclusion

In summary the study presented in this Chapter emphasizes the importance of the oxidative response of cancer cells to tamoxifen treatment. On the one hand, this oxidative damage to cancer cells has a positive therapeutic effect of killing the cancer cells, but on the other hand it amplifies the anti-oxidant response leading to increased expression of MDRT and anti-oxidant genes. This latter effect protects cancer cells from further oxidative damage and thereby produces resistance to the continued therapeutic effects of tamoxifen (Fig 3.23). Thus, evaluating breast tumors of patients for the expression of Nrf2, ABCC1, ABCC3 and NQO1 warrants formal assessment as predictive markers for tamoxifen response. Furthermore, blocking the

activation of the ARE during tamoxifen therapy could improve its efficacy and alleviate acquired resistance.

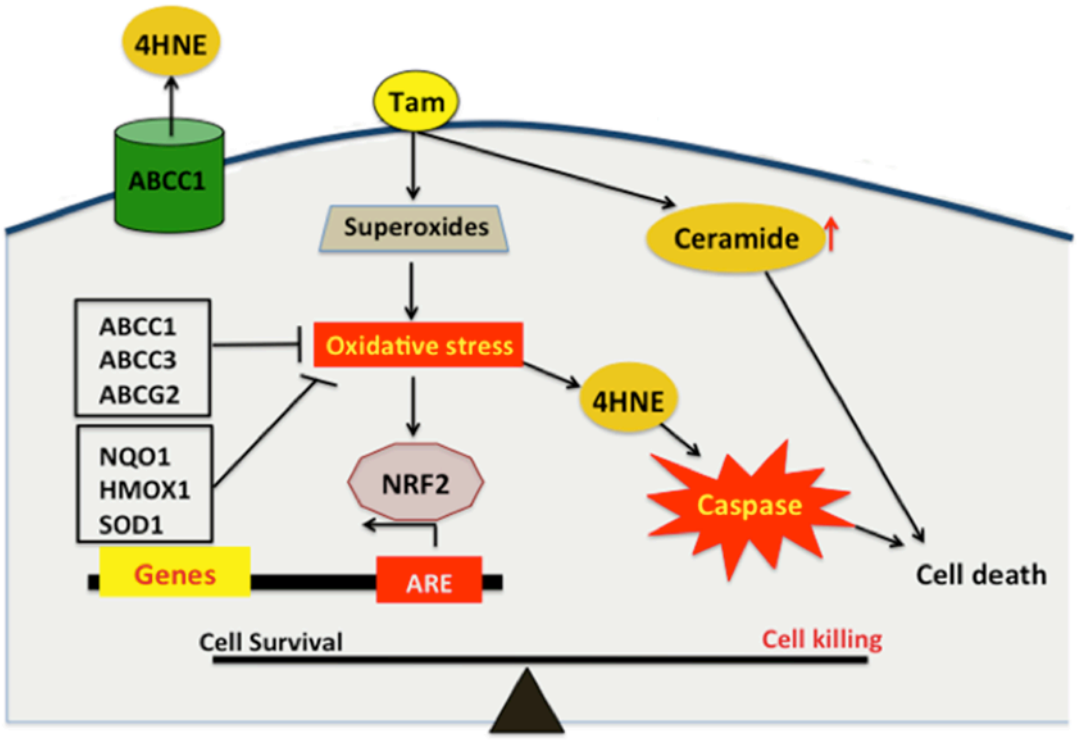

Figure 3.23: Proposed signaling scheme for the effects of tamoxifen in breast cancer and the development of resistance.

Tamoxifen embeds itself in the lipid bilayer and generates superoxide, which causes a lipid peroxidation and subsequent 4HNE formation. 4HNE activates the caspase-3 and leads to cell killing. In addition, tamoxifen also increases ceramide levels in cells. Breast cancer cells respond to the oxidative stress environment by increasing Nrf2 levels and thereby activating ARE leading to the expression of antioxidant genes (NQO1, HMOX1, SOD1) and the multidrug resistant transporters (ABCC1, ABCG2, ABCC3), which mitigate the effects of tamoxifen induced oxidative stress and thus contributing to resistance.

4 CHAPTER: RESULTS

RALBP1 and Phospholipase D regulated by oxidative stress induced by tamoxifen

4.1 Introduction

In Chapter 3, it was shown that the efficacy of tamoxifen therapy is jeopardized as consequence of an adaptive response to the induction of oxidative stress. This is caused by an upregulation of genes downstream Nrf2 that mitigate oxidative stress causing resistance to tamoxifen. Chapter 4 continues further on this avenue of investigation leading to identification of two other targets that are regulated by tamoxifen-induced oxidative stress, phospholipase D and RALBP1. Interestingly, both proteins are downstream Ral effector proteins [307].

Phospholipase D catalyzes the formation of phosphatidic acid (PA) from phosphatidylcholine, which is the most abundant lipid on the membranes of cells [272]. PA can then bind to signaling proteins as a second messenger recruiting them membranes leading to their activation [317, 318]. As such, activation of PLD1/2 resulting in PA formation is important in various cellular events as described in Chapter 1. Moreover, the PLD1 isoform is a Ral downstream effector and the N-terminus of the small G-protein Ral is found constitutively bound to PLD1 [307]. Additionally, oxidizing agents such as H_2O_2, which lead to induction of oxidative stress, activate PLD in different cells such as vascular smooth muscle cells [370] and also in endothelial cells [371]. In both studies, oxidants-induced increases in PLD activity were attributed to tyrosine phosphorylation of PLD.

Oxidants have been postulated to block the activity of protein tyrosine phosphatases (PTP) due to the presence of a thiol group in their catalytic

sites and so PTPs are quite sensitive to oxidative stress [372]. Hence, upon redox imbalance, the thiol residue on PTPs is oxidized leading to inhibition of the protein tyrosine phosphatases. This has the net effect of increasing tyrosine phosphorylation [373-375], providing a mechanistic explanation for the activation of PLD by oxidative stress. Hence, this would mean that tamoxifen-induced oxidative stress could also contribute to the activation of PLD. Moreover, the reactive lipid peroxidation by product, 4HNE, activates PLD and tyrosine phosphorylation [376-378] and as shown in Chapter 3 tamoxifen induces an increase in 4HNE levels.

PLD causes resistance to rapamycin [379] and taxotere (docetaxel) [380]. Moreover, increased PLD activity has been implicated in aggressive and metastatic breast cancers [381]. Its activity is also elevated in melanoma [382], colorectal [383], gastric [380] and renal [384] cancers and also in tumors with activating Ras mutations [385]. Thus it is important to study the potential of PLD activation by tamoxifen and its role in the development of resistance to tamoxifen therapy.

RALBP1 is the other target identified to be modulated by oxidative stress induced by tamoxifen. Similar to PLD, RALBP1 has been ascribed to have multifaceted roles within cells; owing to its multiple motifs such as the Ral G-protein binding domain, the Rho/Rac GAP domain, ATP binding sites, ATPase domain among others, as reviewed in Chapter 1. However, as opposed to PLD the link between RALBP1 and oxidative stress is more direct, since full-length RALBP1 has intrinsic transport activity allowing it to expel

glutathione conjugates such as the lipid peroxidation by product, 4HNE [354]. Hence, RALBP1 has a potential to mitigate oxidative stress in cells and this is evident from studies using RALBP1 knockout mice, which have increased levels of oxidative stress markers [335]. Moreover, RALBP1 can also expel amphiphilic chemotherapeutic agents such as anthracyclines [340] and vinca-alkaloids [386] and thereby contribute to resistance to these therapies by decreasing their intracellular concentration.

As previously established, tamoxifen results in the formation of the lipid peroxidation byproduct, 4HNE, and leads to the initiation of apoptosis. Thus, it is well warranted to study the role of RALBP1 in the context of tamoxifen treatment. As such, this study was conducted with a postulate that cells will respond to lipid peroxidation induced by tamoxifen by upregulating RALBP1. The corollary to this proposition could be that the transcription factor Nrf2 also regulates the expression of RALBP1 in similar fashion to the antioxidant proteins and multidrug resistance transporters.

In the study presented in Chapter 4, tamoxifen activated PLD and this is dependent on oxidative stress induced by tamoxifen since antioxidants abrogated this increase in PLD activity. Furthermore, tamoxifen-resistant cells had a significant increase in both basal and stimulated PLD activity, showing the importance of PLD in resistance. Inhibitors against PLD1 and PLD2 were also used and PLD2 inhibition abrogated LPA's rescue of cells from tamoxifen-induced cell death. LPA is a potent activator of PLD and it also leads to upregulation of Nrf2. In regards to the other Ral effector protein,

RALBP1, oxidative stress induced by tamoxifen was identified to upregulate the expression of RALBP1 and its levels are also significantly upregulated in tamoxifen-resistant cells.

In the setting of breast cancer patients, cancerous breast tissues had a significantly higher expression of RALBP1 compared to normal breast tissue. Furthermore, combination chemotherapy (such as taxanes and anthracycline) was only efficacious in low RALBP1 expression patients. However, in patient-cohort with high RALBP1 expression, therapy of patients with combination chemotherapy offered no significant advantage as compared to those patients receiving mono-or non-cytotoxic chemotherapies.

The study in this Chapter is made even more pertinent as RALBP1 transports anthracycline and within our patient cohort high levels of both PLD1 and RALBP1 were prognostic for poor survival after anthracycline therapy. The increased PLD activity could contribute to the aggressiveness and metastatic potential for otherwise tamoxifen responsive neoplasms. This is evident from our patient cohort with high PLD1 expression having a lower survival probability in all treatments conditions.

Overall the effect of tamoxifen on RALBP1 and PLD1/2, which results in resistance to tamoxifen and cross-resistance to other therapies, offers new paradigm to tamoxifen therapy. Thus, results presented in this Chapter could have implication on the delivery of tamoxifen to patients.

4.2 Chronic tamoxifen treatment results in tamoxifen-resistant cells

A model for studying tamoxifen resistance would be using tamoxifen resistant cells that have acquired resistance to tamoxifen by continual growth of these breast cancer cells in the presence of 1 μM 4HT for a period of about 6 months or longer [99]. These tamoxifen resistant cells (MCF-7 TAMR) along with their syngeneic control cells (MCF-7 WT) were obtained from our collaborator Dr. Pu Xia.

To confirm the resistance of MCF-7 TAMR cells, the cells were treated with 1μM 4HT, which was the concentration used to develop the MCF-7 TAMR cells. The MCF-7 TAMR cells were also treated with 5 μM 4HT as another concentration control. The results show that there was only a slight decrease in viability in both cells after 24 h treatment with 1μM 4HT. However, at 5 μM 4HT there was a considerable loss in cell viability in both wild type and resistant cells with the resistant cells having a significantly higher viability compared to the wild type cells (Fig. 4.1A). Interestingly, this increased resistance, as seen from increased viability, was also observed after 24 h treatment with 5 μM 4HT, even though these cells were developed to resist only 1 μM 4HT. However, at 48 h of treatment the MCF-7 TAMR cells were only resistant at 1 μM 4HT and they did not lose any viability as compared to vehicle treatment (Fig 4.1A).

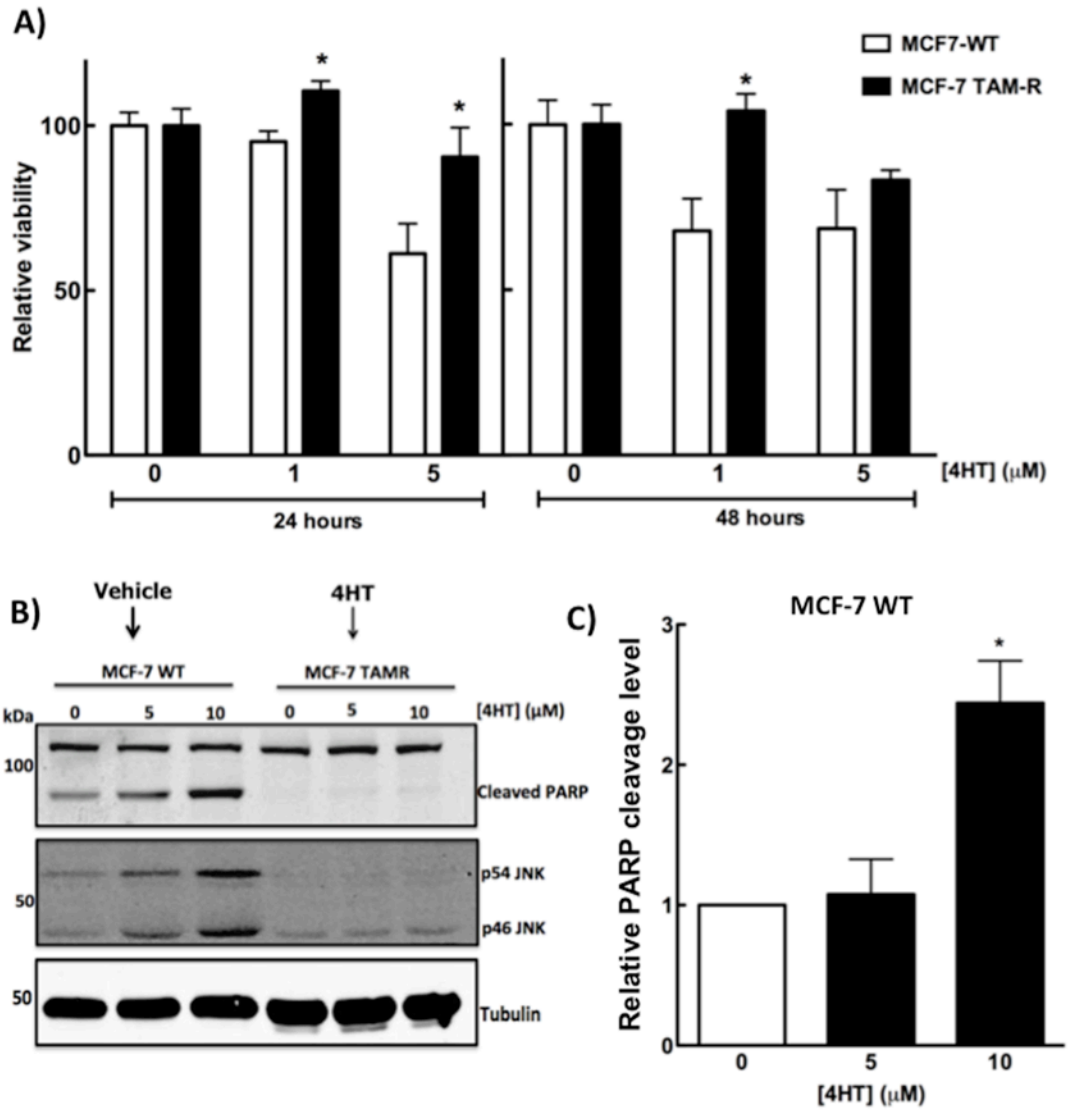

Figure 4.1: Differential effects of tamoxifen in wild type versus resistant cells.

(A) Viability of MCF-7 WT and MCF-7 TAMR cells treated with different 4HT concentration after 24 and 48 h respectively. (B) Cleavage of PARP and the activation of p54 and p46 JNK in the presence of tamoxifen. (C) Quantification for PARP cleavage. Results are means ± SEM from for n=3 experiments. Significant differences were indicated with *= $p<0.05$.

The cleavage of PARP was also measured as an indication of apoptosis and it was identified that MCF-7 WT cells were able to cleave PARP as opposed to the resistant MCF-7 TAMR cells (Fig. 4.1B and C). Moreover, treating the resistant MCF-7 TAMR cells with tamoxifen did not

activate JNK phosphorylation, indicating a better adaptation to dealing with tamoxifen-induced stress induction (Fig. 4.1B).

4.2.1 Total Tyrosine phosphorylation of proteins in tamoxifen-resistant cells.

PTPs dephosphorylate receptor tyrosine kinases and other substrates returning them to their basal state. The activities of PTPs are affected by oxidative stress due to the presence of reactive cysteine residues in the catalytic sites. Thus their reduced activity could result in increased tyrosine-phosphorylation of protein residues.

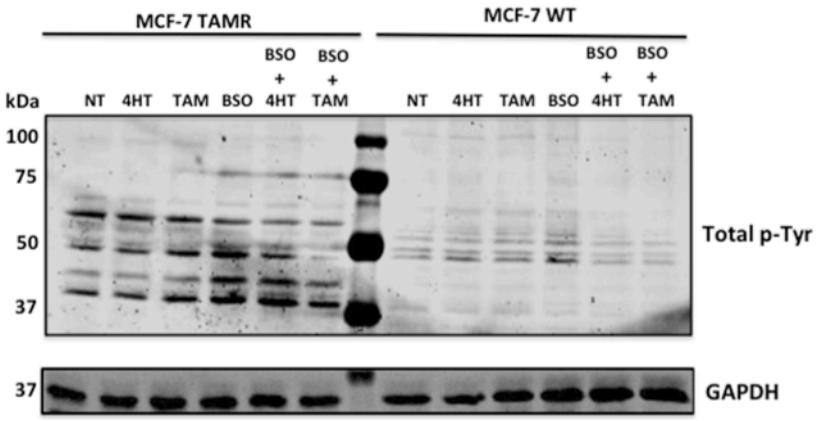

Figure 4.2: Tamoxifen resistant cells have increased basl tyrosine phosphorylation levels

A Western blot for the total tyrosine phosphorylation (p-Tyr) of proteins in MCF-7 TAMR (left) and MCF-7 WT (right) cells. The cells were treated for 24 h with either 10 μM 4HT, 10 μM TAM, 100 μM of L-Buthionine sulphoximine (BSO) alone or in combination. Results are from n=2 experiments.

As tamoxifen induce oxidative stress, the development of tamoxifen resistant cells by chronic treatment of MCF-7 cells may result in reduced activity of PTPs. Thus, the total tyrosine phosphorylation in the protein lysates from wild type and resistant MCF-7 cells was measured. In addition, the cells

were treated with tamoxifen and its metabolite, 4HT, along with L-buthionine sulphoximine (BSO) alone or in combination with tamoxifen. BSO inhibits the gamma glutamyl cysteine synthetase and leads to the depletion of glutathione [387]. Nevertheless, none of the added treatments lead to a significant increase in total tyrosine phosphorylation over the 24 h period. Interestingly however, the resistant cells had an increased level of tyrosine phosphorylation (Fig. 4.2). Thus, chronic tamoxifen treatment might be required for the oxidative stress to result in an increase in total tyrosine phosphorylation of proteins.

4.3 The effect of tamoxifen on Phospholipase D.

The enzymes PLD1/2 are gaining prominence as a key mediator in development of resistance in breast cancer. Furthermore, studies have linked increased oxidative stress to the activation of PLD. Hence, the role of tamoxifen-induced oxidative stress in the activation PLD was investigated. In addition, to gauge the importance of PLD in tamoxifen resistance, the expression levels and activation of PLD in wild type cells and tamoxifen resistant cells was measured.

4.3.1 Activation of PLD in wild-type versus tamoxifen-resistant cells

To study the activation of PLD by tamoxifen, wild type MCF-7 and tamoxifen resistant MCF-7 TAMR cells were treated with 4HT or vehicle as a control and the activation of PLD was then measured.

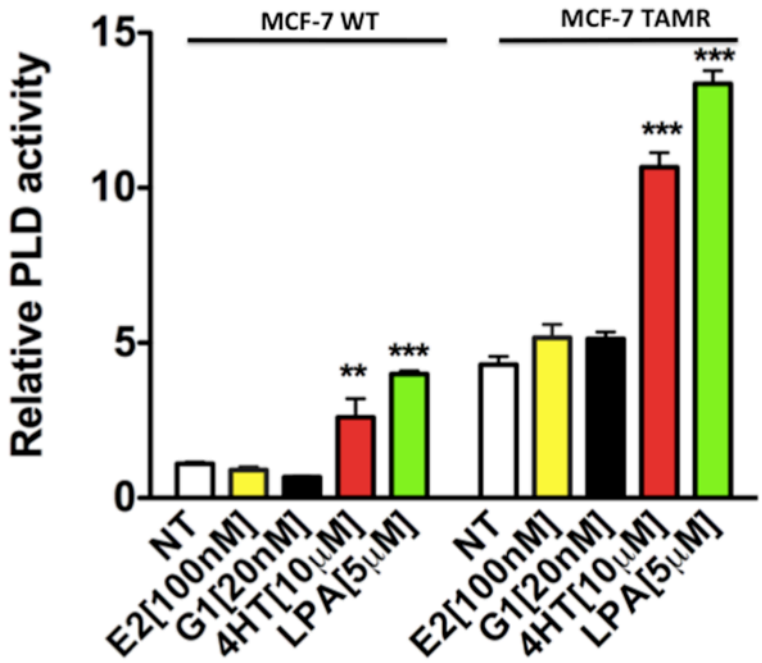

Figure 4.3: Tamoxifen activates PLD independently of the estrogen receptors.

MCF-7 WT and MCF-7 TAMR cells were treated with 100 nM E2, 20 nM G1, 10 μM 4HT and 5 μM LPA for 1 h and compared to vehicle controls. After the specified treatment, PLD activity was estimated by measuring the formation of phosphatidylbutanol. Results are means ± SEM from for n=3 experiments. Significant differences were indicated with **= $p<0.01$ and ***= $p<0.001$.

MCF-7 cells express both ERα and GPR30 (Fig. 3.1A and B) and so tamoxifen could possibly activate PLD through non-genomic rapid signaling event by binding to either of these estrogen receptors, in addition to oxidative

stress. Hence, to delineate the pathway responsible for PLD activation by tamoxifen, a specific agonist for ERα, 17β-estradiol (E2) and a specific GPR30 agonist, G1, were utilized. LPA, a known activator of PLD through its cognate G-protein coupled receptors, was also used a positive control.

The results from Fig. 4.3 show 10 μM 4HT was able to active PLD over a period of 1 h in both the wild type and resistant MCF-7 cells. Interestingly, the basal PLD activation in the resistant cells was as high as maximal activated PLD levels. Thus, these results indicate that chronic treatment of tamoxifen results in a phenotype of high basal PLD activity. Furthermore, when stimulated by 4HT or the natural PLD activator, LPA, the resistant cells were able to activate PLD at a much higher levels compared to wild-type cells. However, the specific agonist for ERα and GPR30, 100 nM E2 and 20 nM G1 respectively, were not able to stimulate PLD activity in both the resistant and wild type cells.

4.3.2 The antioxidant N-acetyl cysteine blocks 4HT-induced PLD activation.

The specific agonists for estrogen receptors were not able to activate PLD. Hence, tamoxifen binding to either GPR30 or ERα should also not result in PLD activation. As such, oxidative stress induction could provide an alternate route for the activation of PLD by 4HT.

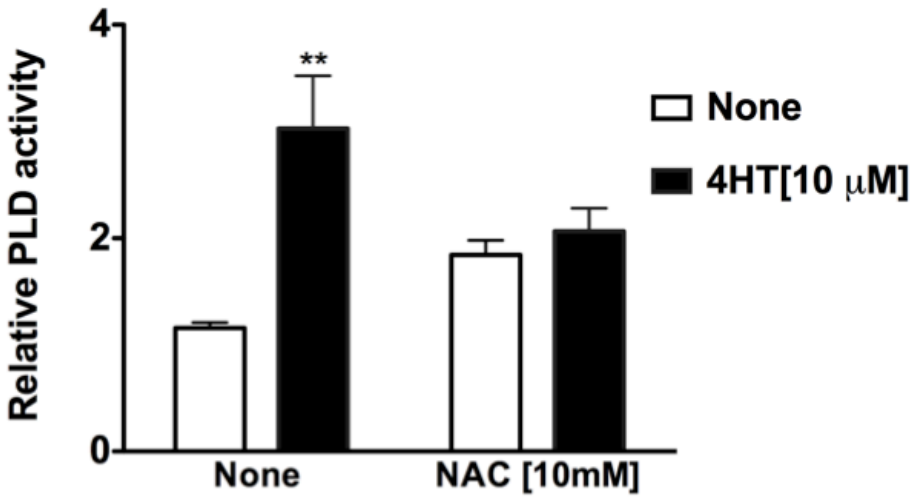

Figure 4.4: Oxidative stress mediates the activation of PLD by tamoxifen.

The relative PLD activity as measured in MCF-7 TAMR cells after 1 h treatment with vehicle or 10 μM 4HT in the presence or absence of 10mM NAC. Results are means ± SEM from for n=3 experiments. Significant differences were indicated with **= $p<0.01$.

To test the role of oxidative stress in activation of PLD by tamoxifen, MCF-7 TAMR cells were treated with 10 μM 4HT for 1 h and PLD activation was measured in the presence or absence of the antioxidant N-acetyl cysteine (NAC). The results (Fig. 4.4) showed that tamoxifen activated PLD and these increases in PLD activity were abrogated in the presence of NAC. Surprisingly, the result also showed that NAC by itself was able to induce PLD activity; nonetheless among the NAC treatment group, tamoxifen was neither able to increase PLD activity, nor was it able to activate PLD to the level increased by tamoxifen alone treatment.

4.3.3 Expression of PLDs in MCF-7 WT versus MCF-7 TAM-R cells.

Since the basal activation of PLD was much higher in the resistant cells compared to wild type cells (Fig 4.3), the expression levels of PLD1/2 in wild type versus resistant cells was measured.

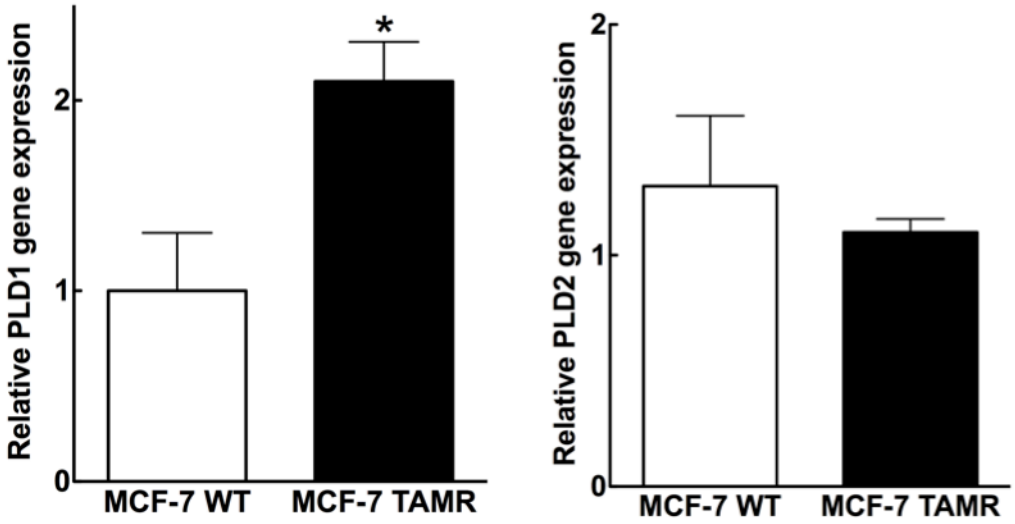

Figure 4.5: Relative PLD expression in wild type and resistant cells.

Relative mRNA expression levels for (A) PLD1 and (B) PLD2 in MCF-7 WT versus MCF-7 TAMR cells. Results are means ± SEM from for n=3 experiments. Significant differences were indicated with *= $p<0.05$.

As shown from qRT-PCR result above (Fig 4.5), the MCF-7 TAMR cells have a significantly higher PLD1 mRNA levels compared to MCF-7 WT cells but there was no detectable change in PLD2 expression levels. Western blot for PLD2 also showed no change in protein expression levels in these cells (Fig. 7.1, Appendix). However, using antibody for PLD1 (PLD1, 44-322, Invitrogen), endogenous PLD1 protein could not be detected in these cells. Thus, the increased basal PLD activity observed in Fig 4.3 could be attributed to increase in PLD1 expression levels.

4.3.4 Tamoxifen, 4-Hydroxytamoxifen and N-desmethyltamoxifen activate PLD.

As shown from the result in Chapter 3, the oxidative stress effect of tamoxifen was not attributed to just one metabolite of tamoxifen but was observed across all the tested metabolites. The next objective was then to test if all the metabolites of tamoxifen will also lead to the activation of PLD.

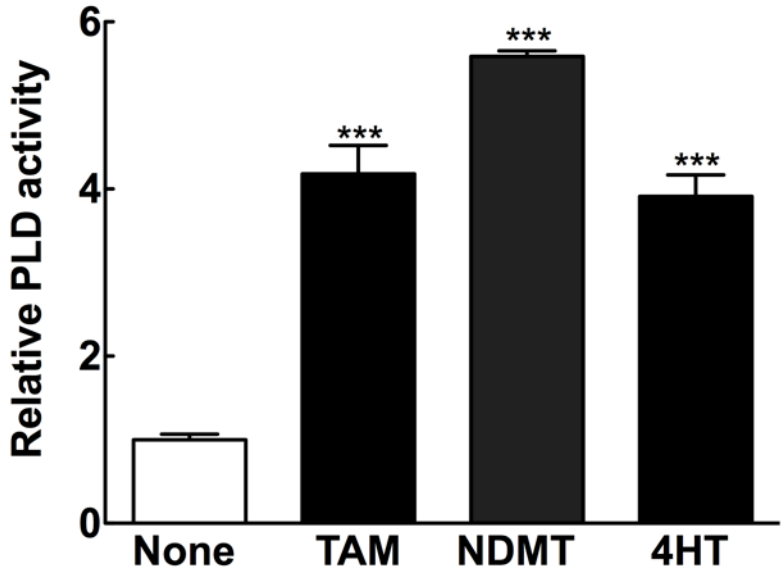

Figure 4.6: Tamoxifen and metabolites activate PLD.

PLD activity was measured in MCF-7 TAMR cells after treatment of cells with 10 μM of tamoxifen and metabolites for 1 h. Results are means ± SEM from for n=3 experiments. Significant differences were indicated with ***= p<0.001.

Hence, cells were treated 10 μM tamoxifen (TAM), 4HT or N-desmethyltamoxifen (NTAM) for 1 h. As shown (Fig. 4.6), the different metabolites of tamoxifen were also able to significantly activate PLD. Thus, demonstrating that PLD activation was not restricted to a single metabolite of tamoxifen since oxidative stress could also be induced by all the metabolites of tamoxifen.

4.3.5 Time course and concentration needed for tamoxifen to activate PLD.

The next objective was to determine concentration and time dependent effect of tamoxifen treatment on PLD activity. To determine the concentration dependent effect of tamoxifen, 5 and 10 μM 4HT were chosen, since these concentrations produced estrogen receptor-independent killing as well as increases in oxidative stress.

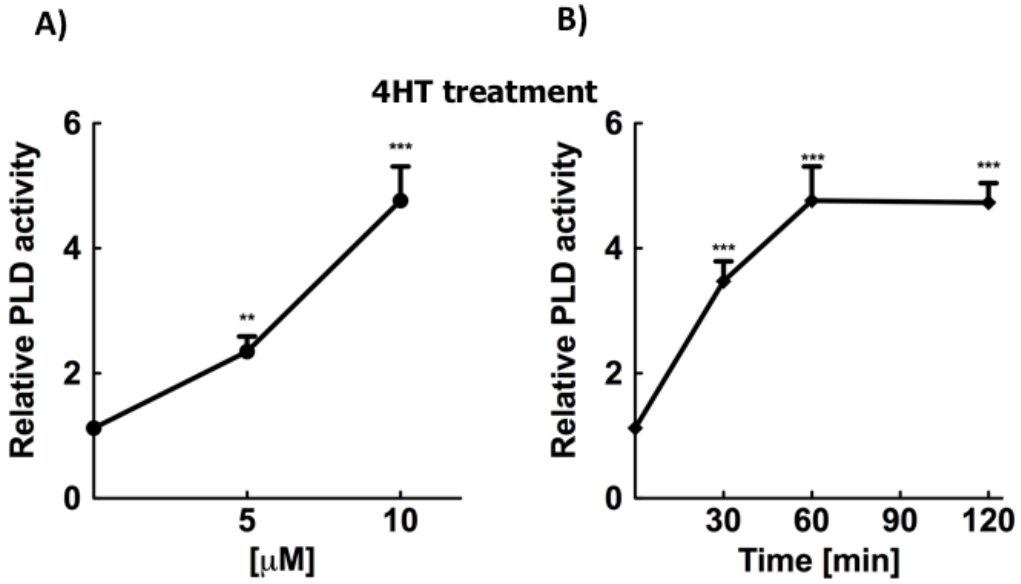

Figure 4.7: Activation of PLD at different concentration and time points.

(A) Effect of 5 and 10 μ M 4HT treatment on PLD activity after 1 h of treatment. (B) Time course for the activation of PLD by 10 μM 4HT in MCF-7 TAMR cells. Results are means ± SEM from for n=3 experiments. Significant differences were indicated with **= p<0.01 and ***= p<0.001.

The results from Fig. 4.7 show that effect of 4HT depended on the concentration of tamoxifen as increasing tamoxifen concentration from 5 to 10 μM led to an increased PLD activation. Additionally tamoxifen activated PLD within 30 min and maximal activation was obtained after 1 h of treatment. A

time course for the activation of PLD by all the different metabolites is shown in the Appendix section (Fig. 7.2).

4.4 Blocking Phospholipase D2 blocks Lysophosphatidate mediated rescue of cells from tamoxifen.

The previous Sections showed that tamoxifen activated PLD and this activation is further amplified in tamoxifen resistant cells. This could reflect the importance of PLD in resistance. Hence, pharmacological inhibitors against PLD activation in the presence and absence of 4HT were used and the viabilities of the cells were then measured. Treating MCF-7 cells with inhibitors against PLD1 or PLD2 alone did not affect the viability of cells (Fig. 4.8A). Since LPA is a potent activator of PLD (Fig. 4.3) and also protects against tamoxifen-induced killing (Fig. 3.16B), the effect blocking PLD activation in the presence of LPA was tested to determine if blocking PLD could abrogate this rescue. Inhibitor for PLD2 (PLD2i) blocked the rescue of cells by LPA from tamoxifen-induced killing, whereas PLD1 inhibitor (PLD1i) did not have a similar effect (Fig. 4.8B). Hence, the activity of PLD2 is vital to the effect of LPA in instigating a rescue from tamoxifen-induced killing.

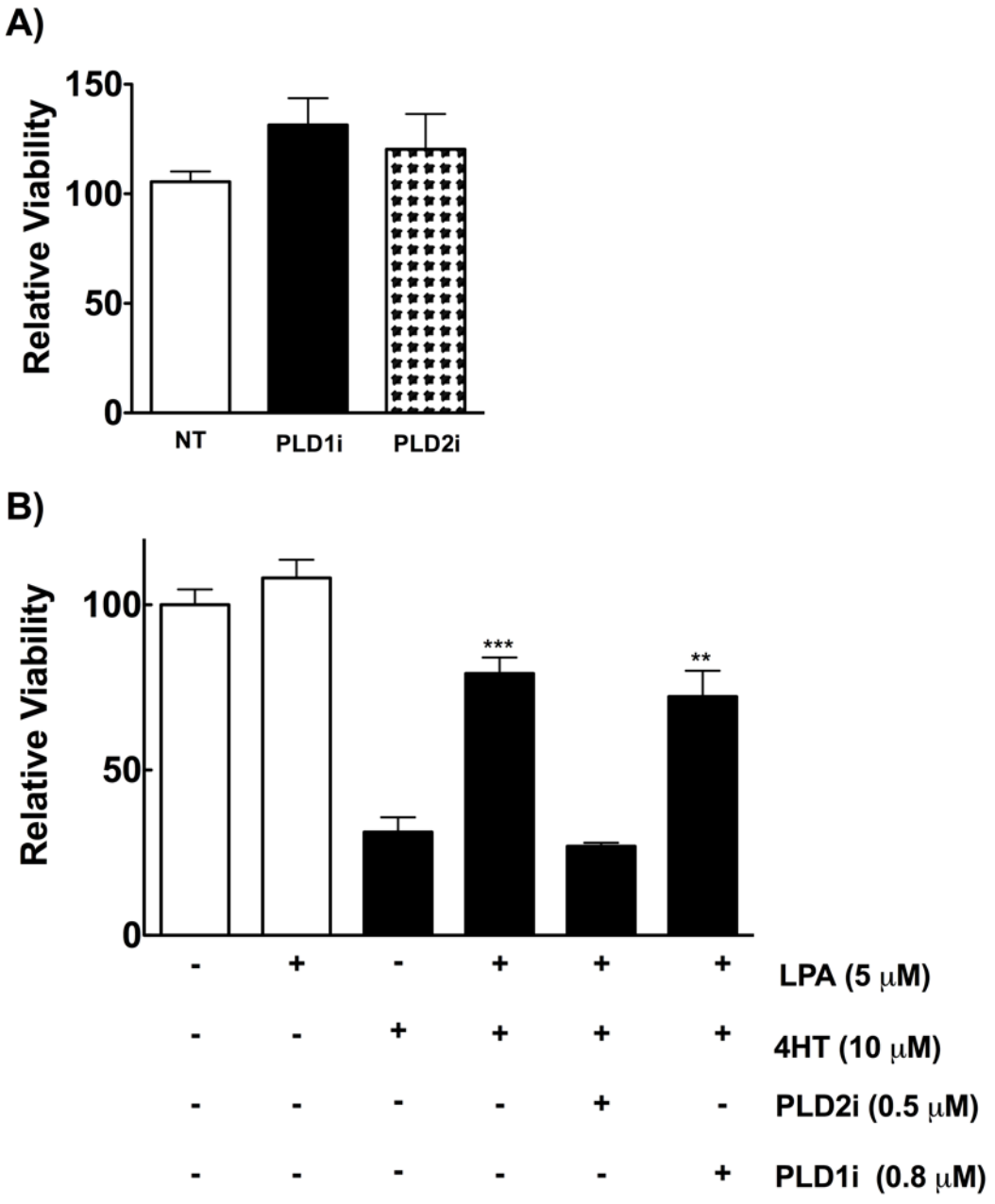

Figure 4.8: PLD2 inhibitor abrogates LPA induced rescue of cells from tamoxifen.

MCF-7 cells treated for 24 h with either vehicle, LPA at 5 μM, PLD1 inhibitor at 0.8 μM (VU0359595, PLD1i) and PLD2 inhibitor at 0.5 μM (VU0285655-1, PLD2i) in the presence or absence of 4HT (10 μM) followed by cell viability measurement. Results are means ± SEM from for n≥3 experiments. Significant differences were indicated with **= $p<0.01$ and ***= $p<0.001$.

4.5 Prognostic values of the expression of PLD1/2 in human patients.

Prognostic analysis for the expression level of PLD1/2 was done in the same way as described in Section 3.9 of Chapter 3. The analysis was performed for all treatment conditions as well as confined to particular treatments. This was done to examine the specific effects of the high and low expression for the PLD1/2 gene in a particular treatment setting. The high and low PLD1/2 expression in the patient tumors were determined at the time of initial diagnosis, possibly caused due to individual differences, and are thus independent of prescribed treatments. As shown in Fig. 4.9B, D, F and H, PLD2 gene expression was not prognostic for any of the analysis that was performed. On the other hand, PLD1 expression provided a significant prognostic value for patients. As such, patients with tumors that had high expression for PLD1 had a significantly lower survival probability of p=0.01 and a HR value of 2.0, in all treatment conditions (Fig. 4.9A). Nevertheless, when the analysis was confined to the patients that were treated with tamoxifen by excluding non-tamoxifen treated patients, PLD1 expression was not prognostic (p=0.6 and a HR=1.2). However, it is interesting to note that within tamoxifen treated patient cohort only ~14 % of the patients were high for PLD1 expression (n=13) with the rest having a low PLD1 expression (n=81) (Fig. 4.9C). In addition, when considering combination chemotherapy treated patients PLD1 expression was significantly prognostic with p=0.01 and a HR value of 2.3 (Fig. 4.9E). Furthermore, for PLD1 gene expression, the best prognostic significance was seen in the patient cohort treated with

anthracyclines with p=0.002 and a HR value of 2.9 (Fig. 4.9E). Indicating that patients high in PLD1 expression have a three times lower survival probability after anthracyclines treatment than those with lower PLD1 expression.

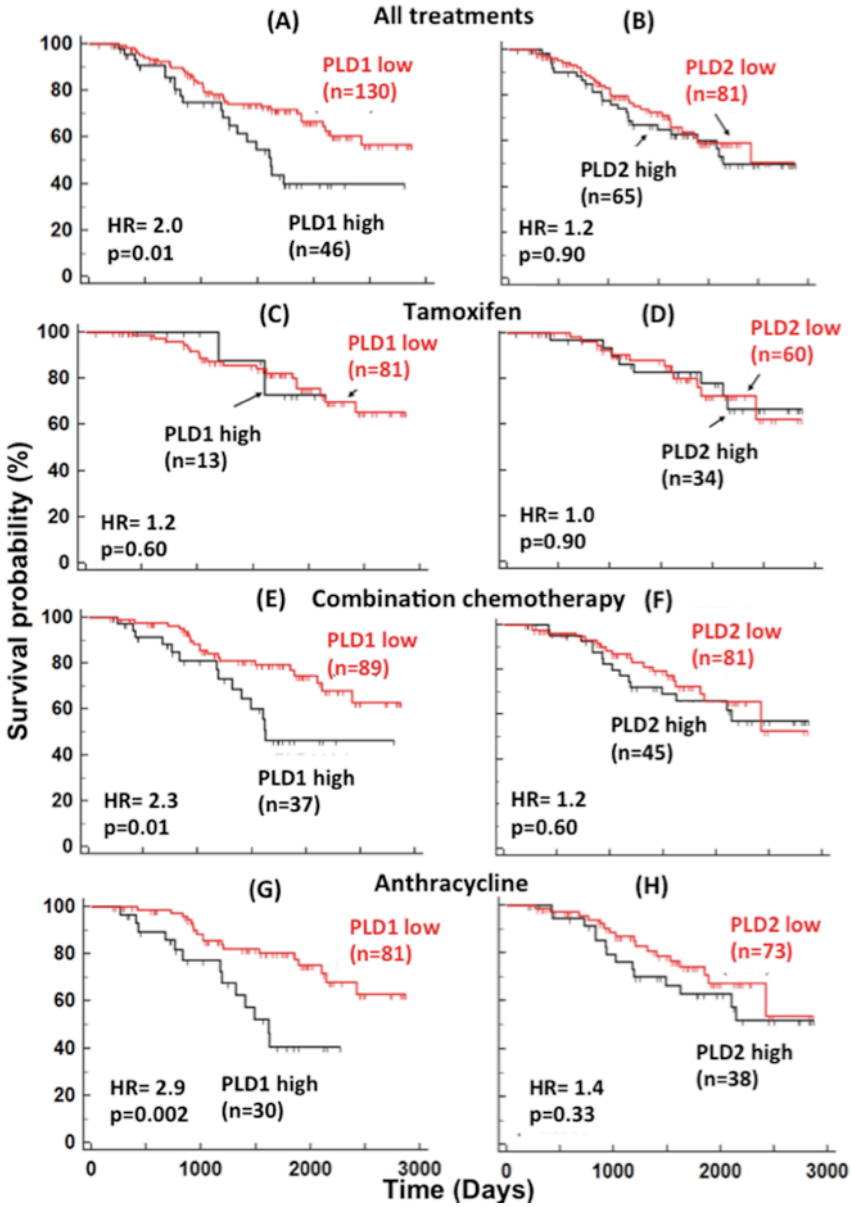

Figure 4.9: PLD1 expression levels provides a good prognostic value

Patients stratified as high and low expressers for PLD1 (A, C, E and G) and PLD2 (B, D, F and H). Prognostic value for all treatments (A and B), tamoxifen (C and D), combination chemotherapy (E and F) and anthracycline (G and H) treated patients. The red lines show the survival probability of patients with low expression while the black lines show high expression for PLD1/2 gene.

4.6 The effect of tamoxifen on RALBP1.

RalBP1 is the major exporter of the lipid peroxidation byproduct, 4HNE [354, 388]. As shown in Chapter 3 (Fig 3.7), tamoxifen-induced oxidative stress causes lipid peroxidation and this leads to the formation of 4HNE. Hence, breast cancer cells could respond to this oxidative insult that results in 4HNE formation by upregulating the expression of RALBP1 transporter protein. To test this tamoxifen resistant and wild type cells were used to gauge the expression level of RALBP1 and its role in tamoxifen resistance.

4.6.1 RALBP1 is upregulated in tamoxifen-resistant cells and also increased by tamoxifen treatment.

Endogenous expression of wild-type cells (MCF-7 WT) was compared to tamoxifen resistant cells (MCF-7 TAMR). As shown in Fig. 4.10, MCF-7 TAMR cells expressed a lot more RALBP1 compared to MCF-7 WT cells. Moreover, both wild-type and resistant cells were treated with 5 and 10 μM 4HT. In addition to an increased expression of RALBP1 in the resistant cells, 4HT treatment in the wild-type cells led to a significant increase in expression of RALBP1. However, in the resistant, MCF-7 TAMR cells, 4HT did not activate any further increases in expression of RALBP1, indicating that those cells are probably at maximal protein expression levels for RALBP1.

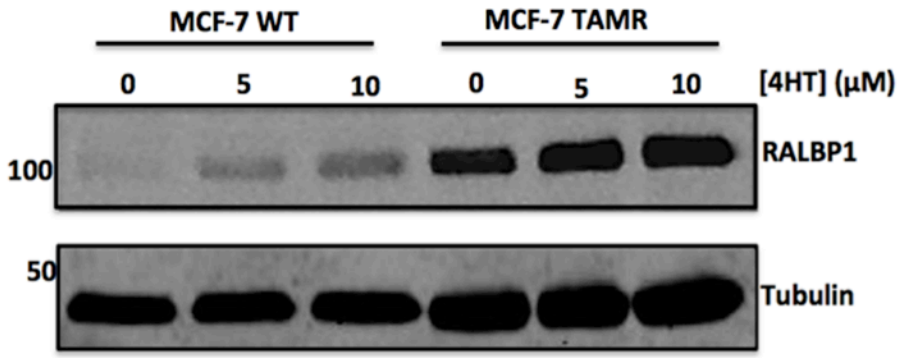

Figure 4.10: Tamoxifen stimulates expression of RALBP1.

(A) Western blot showing expression of RALBP1 in MCF-7 WT versus MCF-7 TAMR cells after treatment with 0, 5 and 10 μM 4HT. Representative western blot from n=3 experiments is shown.

4.6.2 Tamoxifen induced increase in RALBP1 is dependent on oxidative stress

To link the increased expression of RALBP1 to oxidative stress, MCF-7 WT cells were treated with 5 or 10 μM 4HT for 24 h in the presence or absence of vitamin E. Treatment with 10 μM 4HT potently activated the expression of RALBP1 and furthermore treating the cells in the presence of vitamin E blocked this effect on RALBP1 (Fig. 4.11).

As with our other findings the increased expression of RALBP1 is also following a similar pattern of being modulated by oxidative stress induction by 4HT, as its expression is also blocked by the anti-oxidant vitamin E. This goes to shows the role of lipid peroxidation in mediating the effect of tamoxifen on RALBP1.

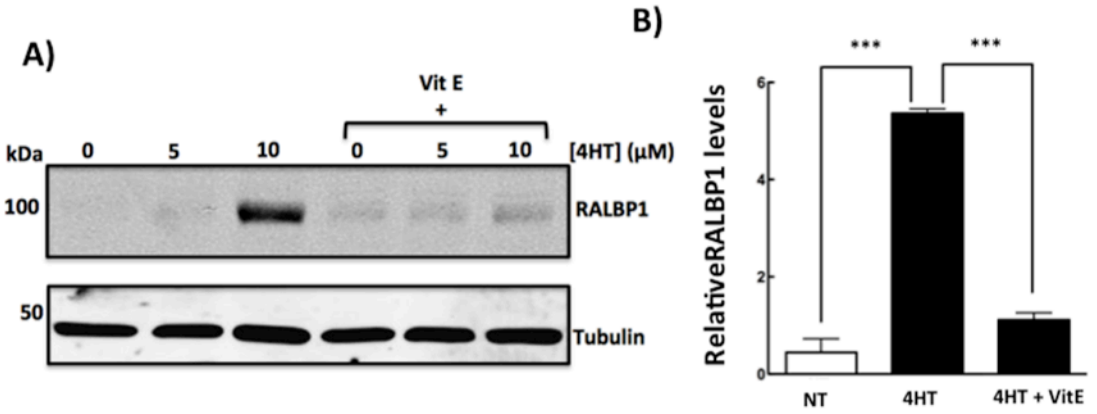

Figure 4.11: Oxidative stress mediates increase in expression of RALBP1 by tamoxifen

(A) Representative Western blot showing MCF-7 WT cells treated 5 and 10 μM 4HT for 24 hours in the presence or absence of 100 μM vitamin E. (B) Corresponding quantification of western blot for 10 μM 4HT. Results are means ± SEM from for n=3 experiments. Significant differences were indicated with ***= p<0.001.

4.7 Nrf2 regulates the expression of anti-oxidant genes and multi-drug resistance transporters but not RALBP1.

Nrf2 is key protein that coordinates an adaptive response of cancer cells to an oxidative insult. Hence, it would be logical to postulate that expression of RALBP1, which is mediated by the oxidative stress induction of tamoxifen, is under the control of Nrf2. To test this hypothesis, RNA interference (RNAi) was utilized and the expression levels of Nrf2 was knockdown using 5 different DsiRNAs (dicer-substrate siRNA) sequences (Fig. 4.12).

The Nrf2 knockdown was confirmed by qRT-PCR and Western blotting (Fig. 4.12A and B). Then using qRT-PCR the expression levels of RALBP1 was measured and compared between cells treated in the presence of non-targeting DsiRNA (NT-Dsi) or those that were treated Nrf2-targeted DsiRNAs (Dsi-Nrf2 1-5). In addition, as a positive control, the expression levels of downstream target genes, which are regulated by Nrf2, were also measured.

Knocking down Nrf2 decreased the expression of the known downstream targets genes such NQO1, SOD1 and ABCC1 (Fig. 4.12 C-E). However, the expression of RALBP1 was not affected (Fig. 4.12F). Hence, Nrf2 does not regulate the expression of RALBP1 as it does with the expression of anti-oxidant genes and multidrug resistance transporters. This establishes that tamoxifen induction of RALBP1 is probably going through Nrf2-independent mechanisms.

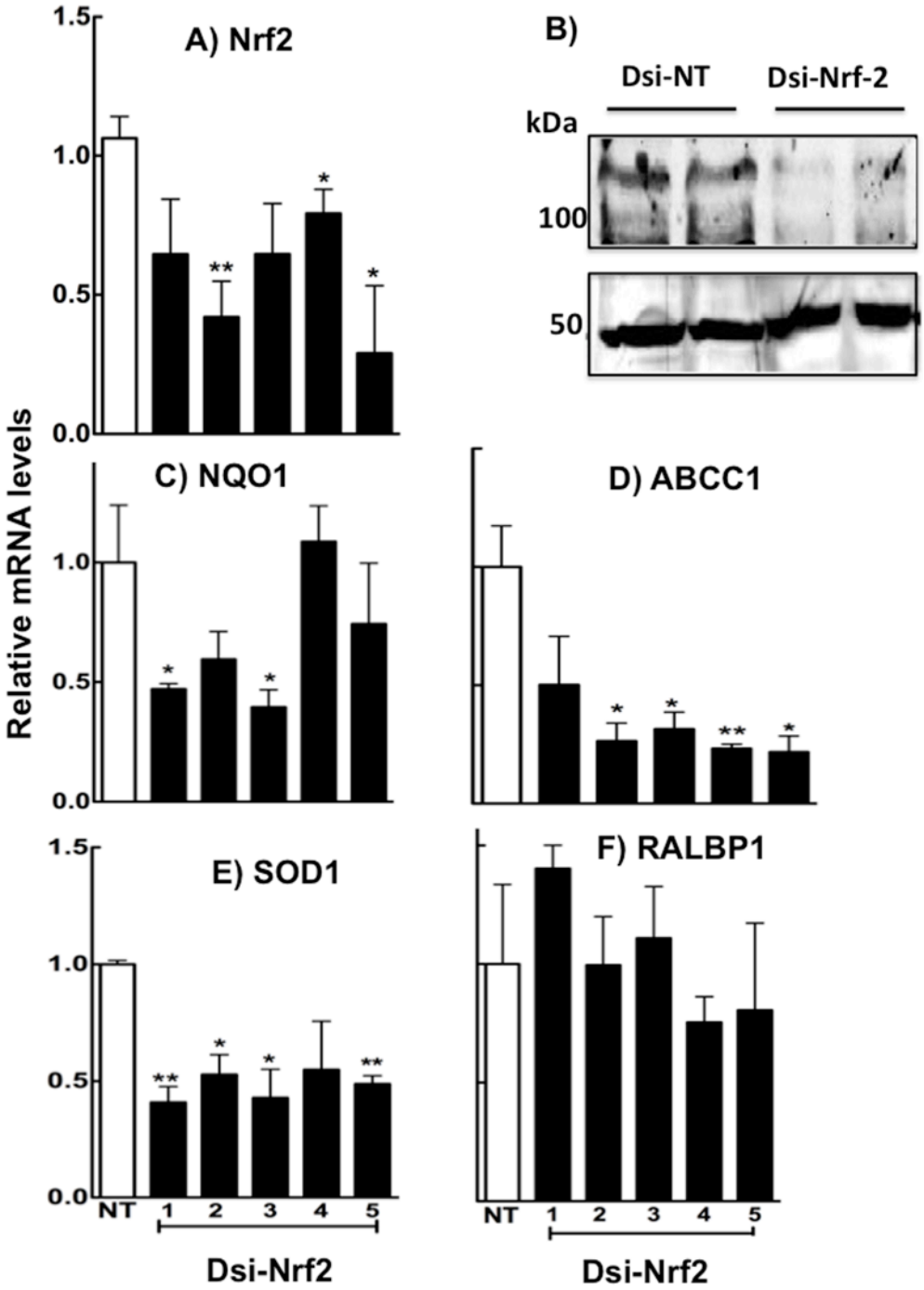

Figure 4.12: RALBP1 is not a downstream target of the transcription factor Nrf2

(A) Western blot (B) mRNA expression levels for Nrf2 in 4T1 cells treated with control NT DsiRNA and Nrf2 targeted DsiRNA sequences 1-5. After knockdown of Nrf2 the mRNA expression of (C) NQQ1 (D) SOD1 (E) (ABCC1 (F) RALBP1 were measured. Results are means ± SEM from for n=3 experiments. Significant differences were indicated with *= $p<0.05$ and **= $p<0.01$.

4.8 Tamoxifen resistant cells also up regulate the expression of ABCC1.

Even though RALBP1 is the major exporter of the toxic oxidation byproduct, 4HNE, ABCC1 has also been shown to exports 4HNE from cancer cells [389]. Thus, the expression levels of ABCC1 were measured in the wild type cells and compared to resistant cells. ABCC1 expression, like RALBP1, is also upregulated in resistant cells (Fig. 4.13). Hence, the resistant cells could possibly utilize the increased expression of both RALBP1 and ABBC1 to mitigate the effect of lipid peroxidation byproduct 4HNE.

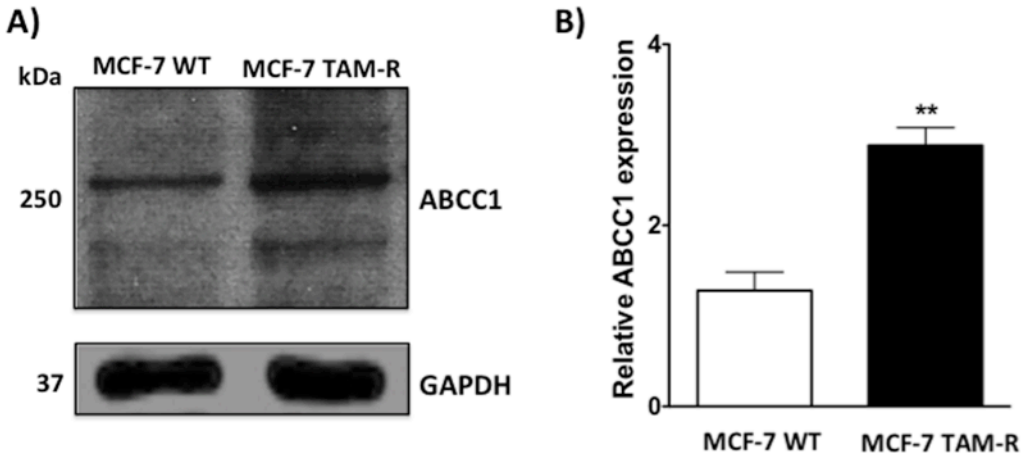

Figure 4.13: ABCC1 is overexpressed in tamoxifen-resistant cells.

Western blot (A) and the corresponding quantification (B) showing the expression of ABCC1 in wild type versus resistant MCF-7 cells. Results are means ± SEM from for n=3 experiments. Significant differences were indicated with **= p<0.01.

4.9 The autotaxin inhibitor, ONO-8430506, decreases RALBP1 levels.

Autotaxin is an extracellular enzyme that helps to maintain the steady state concentrations of plasma LPA. Our laboratory recently published work showing that the autotaxin inhibitor, ONO-8430506, potently knocks-down

circulating LPA levels and this leads to a significant decrease in tumor progression and metastasis [206] along with decreased plasma levels of TNF-α and G-CSF (granulocyte-colony stimulating factor) [390].

Recent studies showed that TNF-α regulates the expression of RALBP1 [391]. Hence, the ONO-induced decrease in TNF-α could also affect the expression of RALBP1. To investigate this postulate, immunohistochemistry slides and tumor tissue lysates of control versus ONO-8430506 treated mice sacrificed after 10 days of treatment were probed for RALBP1 expression. The results indicate that ONO-8430506 treated mice had significantly decreased RALBP1 levels in their breast tumors, as shown by immunohistochemistry (Fig. 4.14A) and western blot of tumor tissues (Fig. 4.17B). The corresponding quantifications are shown in Fig. 4.14C and D, respectively.

As ONO-8430506 potently decreases LPA levels, we investigated if treatment of cells with LPA will induce the expression of RALBP1. Our preliminary result (Fig. 7.3, Appendix section) shows that LPA does not induce RALBP1 expression as compared to positive controls of tamoxifen and metabolites. However, this experiment is preliminary and needs more optimization for more conclusive interpretation.

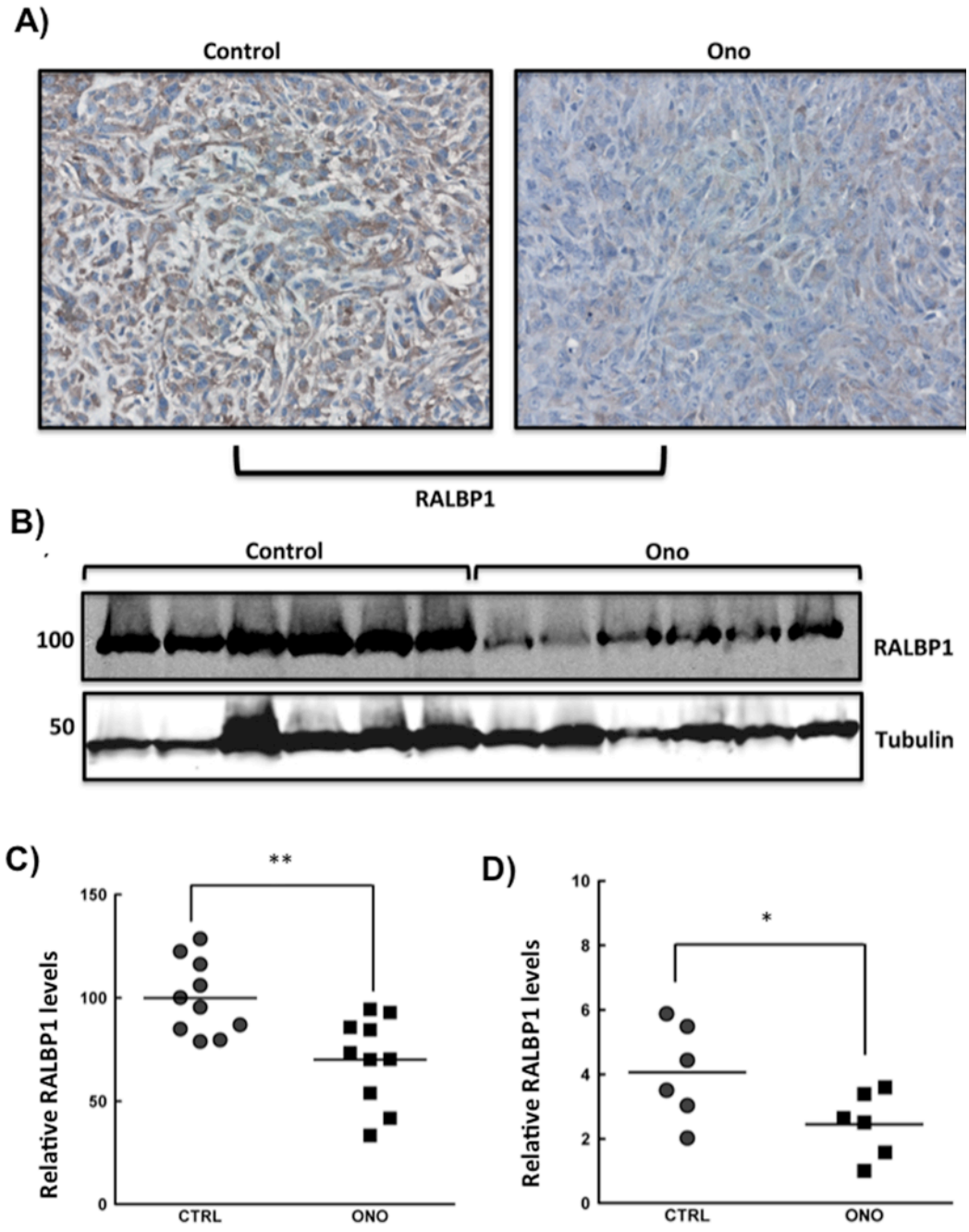

Figure 4.14: Mouse tumors treated with the autotaxin inhibitor ONO-8430506 have lower RALBP1 expression levels.

Mice were injected with 4T1 cancer cells at day zero and were then treated with either vehile or autotaxin inhibtor (ONO-8430506) for the next 10 days. The tumor was then excised and the expression of RALBP1 was measured by (A) IHC staining for n=10 per each group. (B) Western blotting for the tumor tissue lysates for n=6 per each group. The coresponding quantification are shown for (C) IHC and (D) Western blot. Results are means ± SEM. Significant differences were indicated with *= $p<0.05$ and **= $p<0.01$.

4.10 Cancerous breast tissue from human patients expressed high levels of RALBP1

To further extend our studies into human patients, we again employed the tumor tissue arrays from the Breast Cancer Relapsing Early determinants (BREAD) study.

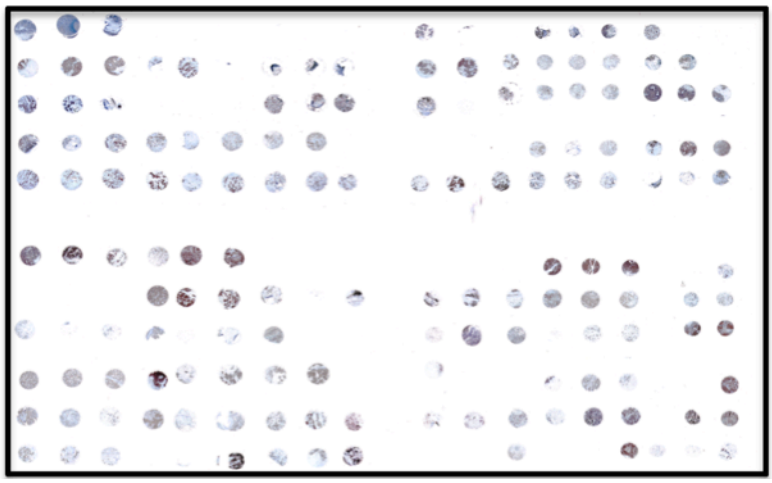

Figure 4.15: An example of tumor tissue array stained with RALBP1 antibody.

Each dot represents a tumor specimen stained with RALBP1 antibody and specimen coming from each patient was dotted in triplicates running across from left to right.

Tumor tissue from each of these patients was dotted in triplicate on an immunohistochemistry (IHC) slide. In addition, these tumor arrays contained normal breast tissue obtained from breast reduction surgery and also tissues from other human organs. These tumor tissues were stained with RALBP1 antibody (Fig. 4.15).

Comparing the normal breast tissue with the cancerous breast tissue, we identified that breast cancer patients had elevated RALBP1 levels (Fig. 4.16A).

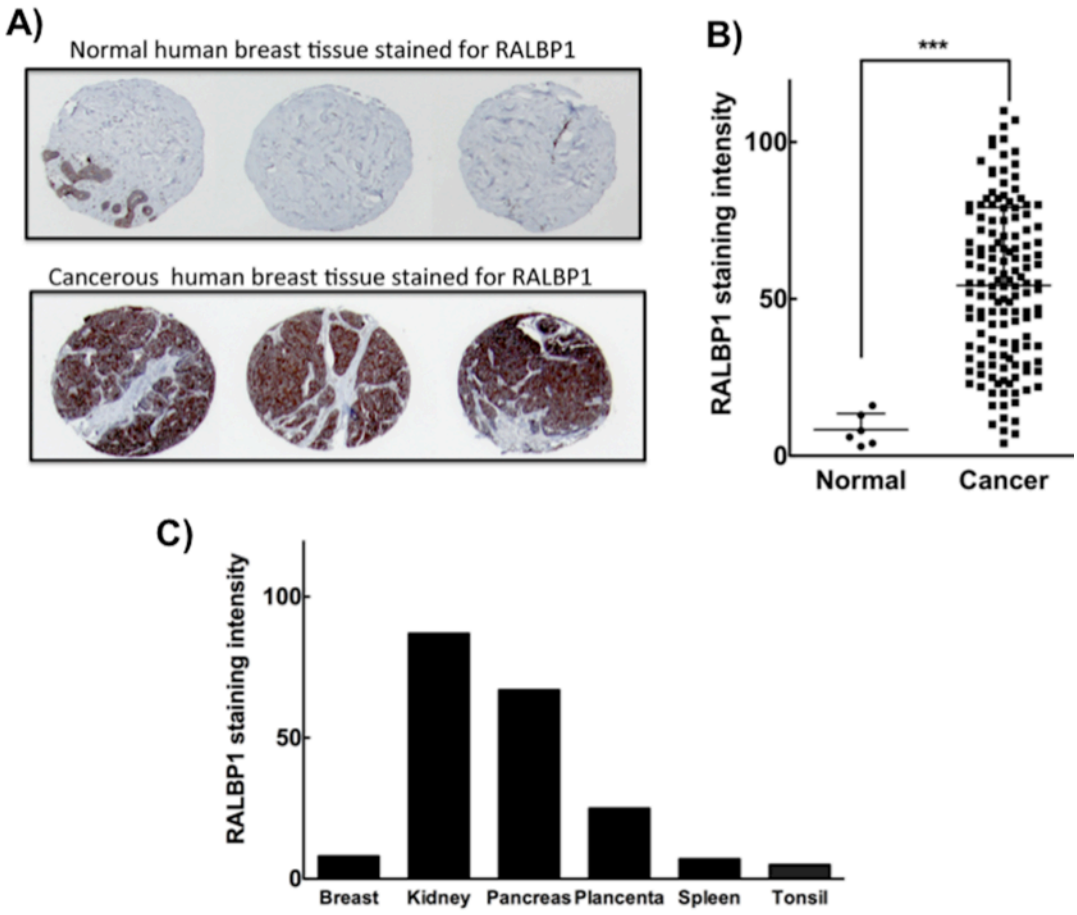

Figure 4.16: RALBP1 expression levels from different normal tissues and Breast tumors.

(A) Representative IHC images. (B) Quantified and averaged staining intensity for normal (n=6) and cancerous breast tissue (n=142) stained with RALBP1 antibody (C) expression of RALBP1 in different normal tissues. Results are means ± SEM. Significant differences were indicated with ***= p<0.001.

The RALBP1 intensity was then quantified from all the tumor tissues cores and the result shows that an overwhelming majority of these patients expressed significantly higher RALBP1 levels compared to normal breast tissue (Fig. 4.16B). The expression levels of RALBP1 in different noncancerous human tissues were also measured. The results show that organs such as kidney, pancreas and placenta had the highest expression of RALBP1 and this was considerably higher than normal breast tissue. It is thus

remarkable that cancerous breast tissue overexpressed RALBP1 to levels of expression close to kidney and placenta.

4.10.1 Prognostic values of the expression of RALBP1 in human patients.

As done with the expressions of PLD1/2 gene (Section 4.5), the prognostic value of RALBP1 gene expression was evaluated in human patients by grouping patients in to high and low expressers and analyzing the survival probability in all treatments and also in particular treatment conditions.

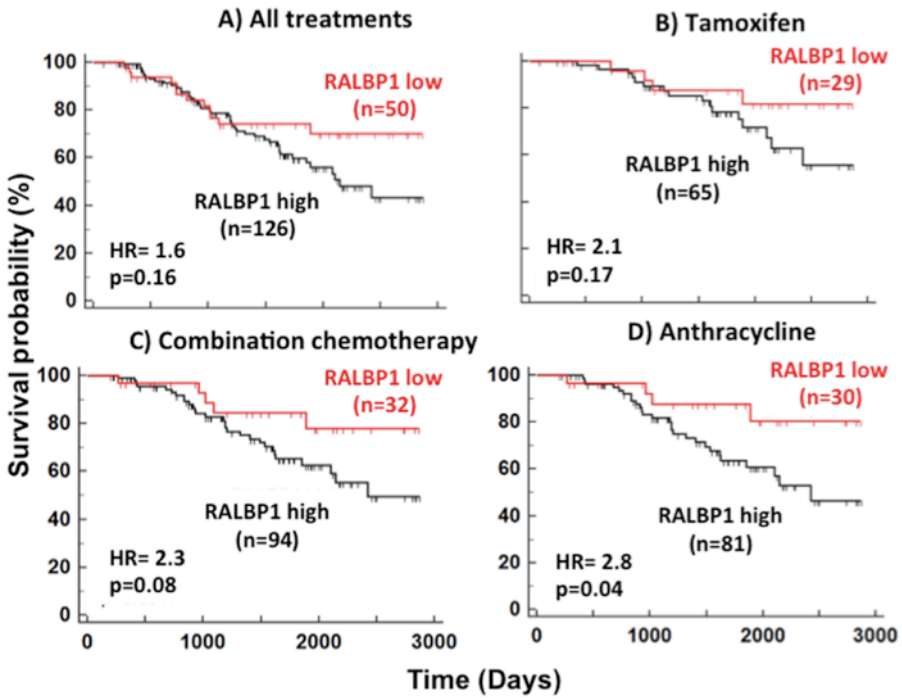

Figure 4.17: The prognostic significance of RALBP1 gene expression levels.

Patients stratified as high and low expressers for RALBP1 and prognostic value for (A) all treatments, (B) tamoxifen, (C) combination chemotherapy, and (D) anthracycline treated patients. The red lines show the survival probability of patients with low expression while the black lines show high expression for RALBP1 gene.

RALBP1 gene expression levels did not show a significant prognostic value for all treatments p=0.16 and HR value of 1.6 (Fig. 4.17A). Similarly, there were no significant prognostic values for tamoxifen treated (p=0.17) and for combination chemotherapy (p=0.08) treated patients but there was a trend of better survival for low RALBP1 expressers for both treatment groups with HR value of 2.1 (Fig. 4.17B) and 2.3 (Fig. 4.17C) respectively. Nevertheless, RALBP1 was significantly prognostic for patient cohorts treated with anthracyclines with p=0.004 and a HR value of 2.8 (Fig. 4.17D). Interestingly, in the anthracycline treated patient cohort, the prognostic value of RALBP1 (HR= 2.8) and PLD1 (HR= 2.9) (Fig. 4.9E) were very similar, which may suggest an intimate link between the two proteins.

4.10.2 Patients with high RALBP1 levels do not respond to combination chemotherapy

An overwhelming majority of the breast cancer patients had elevated RALBP1 levels (Fig. 4.16). Moreover, the prognostic significance of RALBP1 expression level was only restricted to anthracycline-treated patients (Fig. 4.17). Hence, the effect of this overexpression on the prognostic outcome was investigated in combination chemotherapy treatment by making use of the available IHC quantification data (Fig. 4.16B) as a means to stratify patients as high and low expressers for RALBP1.

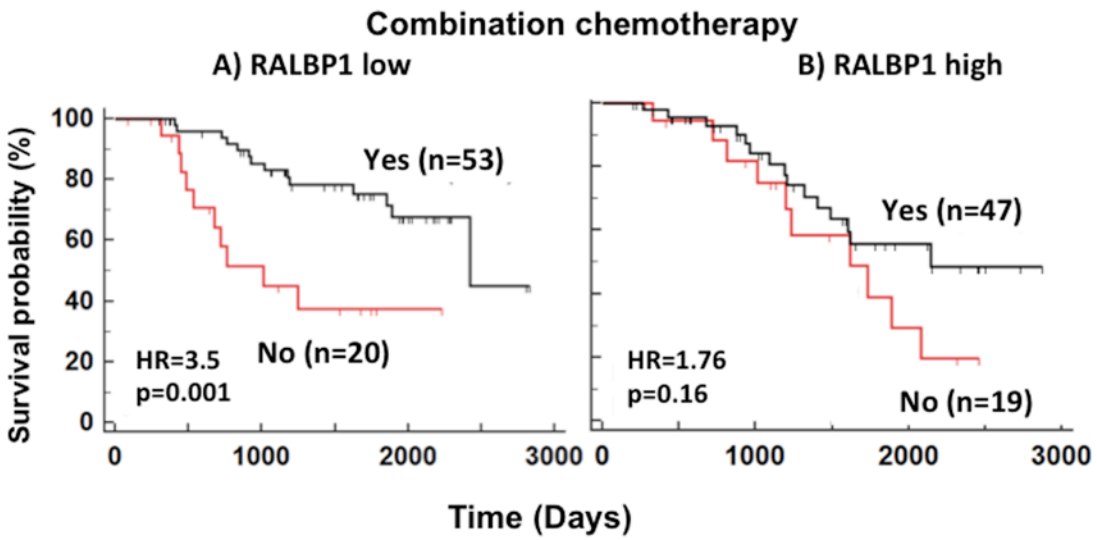

Figure 4.18: Increased RALBP1 protein expression status associated with decreased response of combination chemotherapy.

Patient stratified as 'yes' for receiving combination chemotherapy and 'No' for those patients that did not and grouped in to (A) RALBP1 low expresser and (B) RALBP1 high expresser. The red lines show the survival probability of patients with not treated with combination chemotherapy while the black lines show combination chemotherapy treated patients

The patients were stratified as being treated with combination chemotherapy or not and then this is split further into separate graphs by grouping the high RALBP1 expressing patients in one graph and in another the patient that were low RALBP1 expressers.

As is expected, patients receiving combination chemotherapy had a better prognosis than those that did not receive such treatment (Fig 4.18A). However, the analysis also shows that those patients that had high RALBP1 expression levels in their tumors did not benefit from the combination chemotherapy (Fig 4.18B) as much as those patients that expressed low RALBP1.

4.11 Conclusion

Overall the results from Chapter 4 show that the production of oxidative stress by tamoxifen could have far-reaching consequences by imparting its effect on key-signaling mediators. This could modify diverse cellular functions such as RALBP1 expression and PLD activation and expression, which would inevitably abrogate the efficacy of tamoxifen by contributing to the development of resistance in breast cancer cells.

Furthermore, our results also show long–term tamoxifen treatment induces a significant RALBP1 expression. Since RALBP1 exports other chemotherapeutic drugs and oxidation byproducts, this could have implication of making breast tumors resistant to other drugs.

5 CHAPTER: DISCUSSION AND FUTURE DIRECTIONS

5.1 Discussion on tamoxifen-killing and the anti-oxidant defense

The work presented in Chapter 3 expands our understanding of how tamoxifen kills breast cancer cells and it elucidates the adaptive mechanisms that decrease the efficacy of tamoxifen treatment. We showed that concentrations of tamoxifen and its metabolites (≥5 μM), which occur in breast tumors of patients [357, 358], kill breast cancer cells independently of ERα expression. A major part of this effect was through oxidative stress caused by tamoxifen accumulation since the cancer cells were partially protected from apoptosis by the anti-oxidants, vitamin E and PMC.

Tamoxifen partitions into lipid membranes resulting in increased oxidative damage [16]. We demonstrated this since tamoxifen treatment increased the formation of superoxides and the lipid peroxidation product 4HNE in breast cancer cells. Other studies showed that adding tamoxifen to calf thymus DNA in the presence of microsomal preparations increased 8-hydroxy-2'–deoxyguanosine levels (a marker for oxidative stress) on the DNA. This oxidative damage on DNA was diminished by adding SOD1 [392]. Tamoxifen also inactivates protein kinase C through oxidative stress and this effect was reversed in the presence of SOD1 or vitamin E [16]. Also, studies using MCF-7-derived xenografts tumors in athymic mice showed that tamoxifen treatment increased SOD1 levels and long-term treatment of these tumors with tamoxifen led to tamoxifen-resistance [393]. We showed that blocking this oxidative stress partially rescued breast cancer cells from lipid peroxidation and subsequent apoptosis. This tamoxifen-induced generation of reactive oxygen species (ROS) could be mediated by the membrane bound

enzyme, NADPH oxidase, since its inhibition blocked tamoxifen induced ROS production and apoptosis in human hepatoblastoma cells [394]. Hence, oxidative stress contributes to killing cancer cells during tamoxifen therapy, but this action also has the consequence of increasing tamoxifen-resistance.

We substantiated this conclusion by showing that treatment of cancer cells with 4HT increased Nrf2 stability and gene transcription through the ARE. This effect was also observed in our mouse model of breast cancer, using ERα-negative 4T1 cells. Tamoxifen treatment decreased tumor size and this was accompanied by increased Nrf2 expression in the breast tumors. The latter result explained the tamoxifen-induced increases in the expressions of NQO1, HMOX1, SOD1, ABCC1, ABCG2 and ABCC3, which are transcribed downstream of the ARE. These results are also compatible with the characteristics of MCF-7 breast cancer cells, which were selected for tamoxifen-resistance. Resistant cells had increased expression of Nrf2 and knocking down Nrf2 expression decreased the high expression of anti-oxidant genes in the tamoxifen resistant cells [395]. Knockdown of Nrf2, in the same study, also increased tamoxifen-induced cell death and the increased expression of the anti-oxidant genes did not depend on ERα signaling. We conclude that the oxidative damage caused by tamoxifen elicits an anti-oxidant response, which attempts to protect the cells from cell death.

Our studies showed that <5 μM tamoxifen retarded the growth of ERα–positive MCF-7 cells, but these concentrations had little effect in ERα–negative MDA-MB-231 and 4T1 cells. Higher tamoxifen concentrations

(>5 μM) killed breast cancer cells independently of ERα expression. This ERα independent killing was also observed in studies with ERα–negative BT-20 breast cancer cells [396], ovarian A2780 cancer cells, T-leukemic Jurkat cells [397] and hepatoblastoma cells [394]. This concentration-dependent action of tamoxifen is especially significant since tamoxifen and its metabolites can accumulate preferentially to >5 μM in breast tumors compared to normal breast tissue [357, 358]. At these concentrations, tamoxifen has a therapeutic action through oxidative damage that is independent of ERα. However, cancer cells then mount an anti-oxidant response that decreases the efficacy of the oxidative component of tamoxifen therapy. This cytotoxic accumulation of tamoxifen could be aided by Antiestrogen Binding Site (AEBS) to which tamoxifen has high affinity as opposed to estrogen. AEBS are found in various tissues including estrogen receptor-negative breast cancer cells. [398]

We also found that tamoxifen stimulated the accumulation of several ceramide species, increased PARP cleavage and JNK activation. However, these effects were not blocked by vitamin E. This indicates that tamoxifen also initiates mechanisms of cell death that are independent of oxidative stress. Nevertheless, previous studies have linked oxidative stress to the formation of ceramide and subsequent JNK activation [362]. We were also able to activate JNK using C2-ceramide. Moreover, tamoxifen-induced JNK activation was not reversed by inhibiting ASK1 (Apoptosis signal regulating kinase), which was linked in other studies to JNK activation [366]. Also, JNK inhibition did not block caspase-3 activation. Interestingly, several studies

showed that cytokines and stress stimuli such as TNF-α, interleukins, FAS ligand, heat shock, UV irradiation and also stressors that deplete glutathione such as ROS and 4HNE can activate sphingomyelinase, which leads to increased ceramide production [399-401]. Moreover, ceramide formation activates caspase-8-dependent, but caspase-3-independent, necrosis in lymphoid cells treated with FAS ligand [363]. If ceramide formation induces caspase-3-independent cell killing, it would explain why vitamin E could block caspase-3 activity, but not block ceramide accumulation and PARP cleavage. Other studies also showed caspase-3-independent PARP cleavage [402] and this is also evident from our work on PARP cleavage in MCF-7 cells, which are caspase-3 deficient [403].

Our work with the syngeneic mouse model of breast cancer using 4T1 cells demonstrates that tamoxifen decreased tumor growth in an ERα-negative breast cancer. This was accompanied by increased expression of Nrf2, antioxidant genes (NQO1, HMOX1, SOD1) and the multidrug resistant transporters (ABCC1, ABCG2, ABCC3). These results confirm that tamoxifen induces oxidative damage in breast tumors *in vivo* and supports our hypothesis that ARE activation could contribute to the development of tamoxifen resistance. Other studies also showed that tamoxifen attenuates tumor growth in a xenograft model with ERα-negative MDA-MB-468 human breast cancer cells. The authors attributed this to the degradation of cancerous inhibitor of protein phosphatase-2A (PP2A) (CIP2A) by tamoxifen [21]. CIP2A inhibits PP2A, whereas 4HNE activates PP2A [404]. This raises

the possibility that tamoxifen-induced degradation of CIP2A occurs through increased 4HNE formation leading to PP2A activation. PP2A activation leads to subsequent inactivation of survival proteins such as Akt, thus contributing to apoptosis [21].

The proposal that oxidative stress could play a role in the therapeutic effects of tamoxifen is further supported by our analysis of the survival of breast cancer patients treated with tamoxifen. Those patients, who had ERα-positive breast tumors with low expression of Nrf2, ABCC1, ABCC3 and NQO1 at the time diagnosis, had a better prognosis after tamoxifen treatment than those patients that were high expressers, with an HR value as high as 4.2. This HR value further increased to 5.2 when considering patients that were high expressers for both NQO1 and ABCC3. High Nrf2 and ABCC3 expression was also associated with poor prognosis for other treatments including trastuzumab, anthracycline and taxanes. For Nrf2, this was expected since Nrf2-induced activation of the ARE is commonly associated with chemo-resistance [405-407]. By contrast in our work, high ABCC1 expression was only prognostic of a poor outcome within the tamoxifen-treated group. These associations are not predicted from the classical action of tamoxifen through blocking ERα signaling. They support our conclusion that tamoxifen-induced killing of cancer cells through oxidative damage is an important component of tamoxifen action.

This conclusion is compatible with the observation that ABCC1 exports the toxic oxidation product, 4HNE, from cancer cells [389]. Additionally,

ABCC2 is also overexpressed in tamoxifen-resistant cells [408]. Genotyping studies looking at single nucleotide polymorphisms (SNPs) have also revealed that specific variants of the ABCC2 gene were prognostic of tumor recurrence during tamoxifen mono-therapy [409]. SNPs could alter the steady state transcript level of the transporter [410], possibly increasing ABCC levels in some patients. Other reports showed that ABCC1, ABCC11 and ABCG2 are highly over-expressed in subtypes of aggressive breast cancer and that increased expressions of ABCC1 and ABCC11 were significantly associated with shorter disease-free survival [176]. This survival study was analyzed over a short median follow up of 40 months and interpretation could be further complicated because of patients receiving neo-adjuvant therapy. Nevertheless, such studies coupled with our analysis show the importance of the ABCC family of transporters in influencing the outcome of tamoxifen therapy. Despite this, there is no clear evidence that tamoxifen is exported by ABCC1 or ABCC3 [158]. Instead, glucuronide conjugates of tamoxifen could be exported through ABCC transporters [162, 163]. On the other hand, tamoxifen is known to bind to the transporter ABCB1, but ABCB1 does not transport tamoxifen. Instead, tamoxifen binding to ABCB1 blocks its ability to transport other xenobiotics [411].

Despite such effects of tamoxifen, there is not much clinical data showing the benefit of tamoxifen in truly negative breast tumors. The Early Breast Cancer Trialists' Collaborative Group (EBCTCG) performed meta-analysis of 55 randomized clinical trials, which demonstrated a substantial

survival advantage after tamoxifen treatment in ERα positive breast cancer patients [2]. Thus most of the subsequent studies focused on elucidating the action of tamoxifen only in the context of ERα. Nevertheless, EBCTCG reported that tamoxifen had some activity in the patients with very low, or no ERα. A later study by Dowsett et al. [14] showed that ERα-negative breast cancer patients also showed a strong trend to benefit from tamoxifen. Glioblastoma patients also benefit from high dose tamoxifen treatment, which was thought to be due to the effect of tamoxifen on PKC. Additionally, the activity of tamoxifen in advanced melanomas [412] indicates the utility of tamoxifen in cases where ERs are not thought to be important. Nonetheless, it is often difficult to rule out the involvement of ERα and ERβ since other tissues such as gliomas also express the receptors [413].

Previous studies showed that the binding of antiestrogens to ERα and particularly to ERβ could induce the expression of the antioxidant NQO1 [414]. Binding of low μM concentrations of antiestrogen to the ERs caused the receptors to complex with the ARE leading to the expression NQO1 [414]. The authors of that study suggested two pathways for ARE activation and induction of NQO1, one that depended on ERs and the other that was independent of ERs [414]. Since Nrf2 is a master regulator controlling the expressing of antioxidant genes the major component bound to the ARE is most probably Nrf2 and the ERs could thus function in a cooperative role in this system. Our result with cytotoxic concentrations of tamoxifen (>5 μM) could thus activate both pathways to elicit an antioxidant response. ERs can

also regulate gene expression without directly interacting with DNA by influencing other transcription factors through their binding to co-regulatory proteins, as in the case with AP-1 complex [26]. Similarly, ERs could potentially be involved in the anti-oxidant gene expression involving Nrf2 through recruiting co-regulatory proteins.

Our studies indicate that it could be beneficial to decrease the expression of Nrf2, ABCC1, ABCC3 and NQO1 as an adjuvant to improve tamoxifen therapy. One possibility is by blocking the activation of cancer cells by LPA. This growth factor produces resistance to the effects of paclitaxel [254], cisplatins [415], doxorubicin [259] and also tamoxifen, as we showed in this work. Significantly, an important mechanism for this resistance is the role of LPA in increasing Nrf2 stability and activation of the ARE. These effects of LPA on breast tumors can be attenuated by blocking LPA production through inhibition of autotaxin [206], or by using an inhibitory antibody against LPA [416]. Proof of principle for this approach was obtained in a mouse model of breast cancer where autotaxin inhibition decreased ARE activation and the consequent expression of anti-oxidant proteins and MDRT [259]. Other strategies would involve using inhibitor that target Nrf2 such as, the quassinoid brusatol [417], the alkaloid trigonelline [418] and the flavonoid luteolin [419], all of which showed efficacy in inhibiting Nrf2 activity and prevented chemo-resistance. Employing such inhibitors, as an adjuvant to tamoxifen could be beneficial, especially since knockdown of Nrf2 increased tamoxifen-induced cell death in tamoxifen resistant cells [395].

Overall, the anti-oxidant defense system elicited in response to tamoxifen treatment contributes to the development of resistance and hampers the long-term benefits of tamoxifen therapy.

5.2 Discussion on tamoxifen and its effect on RALBP1 and PLD

Long-term tamoxifen treatment leads to tamoxifen resistance, a phenomenon that is also observed in the clinic, as patients who previously responded to a cancer therapy later on developed acquired resistance [420]. A proof of this principle was established by chronic tamoxifen treatment of cells and this resulted in cells becoming resistant to the killing by tamoxifen as demonstrated by decreased PARP cleavage, which is indicative of decreased apoptosis and also an undeterred viability upon tamoxifen exposure (Fig. 4.1).

Employing the tamoxifen-resistant breast cancer cell line model, we identified that tamoxifen and its metabolites were able to activate PLD in a concentration- and time-dependent manner and this activation is exaggerated in tamoxifen resistant cells. This PLD activation was dependent on oxidative stress since the antioxidants, NAC, blocked tamoxifen-induced activation of PLD. Moreover, 17β-estradiol and the GPR30 agonist, G1, were not able to elicit similar PLD activation, indicating that tamoxifen-induced PLD activation was not mediated by the estrogen receptors. This finding is compatible with earlier studies showing that PLD is activated in CCD986SK human mammary fibroblasts by tamoxifen and similarly, the estrogen, 17β-estradiol, also lacked the ability to activate PLD [421]. Another group also showed an activation of PLD by tamoxifen in NIH 3T3 mouse fibroblast cells [422]. In a study with the

human mammary fibroblasts, PLD activation was attributed to the enzyme PKCε since phorboldibutyrate, which downregulated PKC levels, blocked tamoxifen-induced activation of PLD [421]. PKC has structural features that make it a prime target for oxidative modification due to the presence of a cysteine rich motif for zinc binding [423, 424]. Hence, modulation of PKC by oxidative stress provides the necessary link to PLD activation by tamoxifen. In addition, total tyrosine phosphorylation in tamoxifen resistant cells was also markedly elevated compared to wild type cells, indicating the inactivation of PTPs. PTPs are also regulated by oxidative stress [373-375] providing yet another means of sustained PLD activation by tamoxifen since in some cases tyrosine phosphorylation of PLD has been linked to increased PLD activity [378].

Inhibiting the activity of PLD by pharmacological inhibition alone did not have an influence on the viability of the cells. However, inhibition of PLD, specifically the enzyme PLD2 in the presence of LPA, blocked the rescue from tamoxifen-induced killing initiated by LPA. However, Inhibition of PLD1 did not affect the rescue of cells by LPA. Nevertheless, our result also showed that PLD1 gene expression levels are elevated in tamoxifen resistant cells as opposed to PLD2 gene expression. These results are compatible with studies from other research groups that also showed overexpressed PLD1 levels in their tamoxifen resistant cell lines [425]. Additionally, PLD1 was found to be overexpressed in human breast cancer tissues [328].

The differential role of PLD1 and PLD2 could be linked to their cellular localization. PLD2 is predominantly localized at the plasma membrane regulating the functions of proteins downstream of receptor activation. Thus PLD2 inhibition may affect signaling from growth factor such as LPA. On the other hand PLD1 is localized at peri-nuclear space, endosomes and vesicles etc. [283]. Accordingly, inhibitors against PLD2 activity could be more important in signaling events at the plasma membrane and the rescue from tamoxifen-induced killing initiated by plasma membrane bound LPA receptors. Whilst, the localization of PLD in different cellular compartments allows it more flexibility in exerting diverse activities and as such, its overexpression may offer cancer cells better protection against different chemotherapies.

The contrast in the role of PLD1 and PLD2 are also observed in the analysis of the breast tumors from our patient samples, which showed prognostic significance only in patients that were expressing high/low PLD1 levels. However, the expression of PLD2 levels did not show any prognostic value across all the investigated treatment conditions. Surprisingly, PLD1 expression levels did not provide a prognostic value for tamoxifen treated patient cohort, despite our cell-culture results showing increased PLD1 expression levels and total PLD activity in the tamoxifen resistant cells. A plausible explanation could lie in the very low number of patients that had high PLD1 expression within the tamoxifen- treated patient cohort. As tamoxifen treatment was not given to about 86% of the high PLD1 expressing

patients. Hence, it is not achievable to makes any prognostic determination for PLD1 in tamoxifen treated patient cohort. Nevertheless, PLD1 expression was significantly prognostic when considering all treatment conditions and also patients treated with anthracycline or combination chemotherapy. Therefore, the increased expression of PLD1 gene observed in our tamoxifen resistant cells could lead to resistance to other chemotherapies.

Increased PLD activity could be attributed to increased expression levels of RALBP1, as studies have shown RALBP1 can modulate the activity of the ADP Ribosylation Factors (ARFs) [426], which are small G-proteins intimately linked in the activation of PLD as established by different studies [272, 427, 428]. Our results show that tamoxifen-resistant cells have a very high expression of RALBP1. Therefore, the high basal PLD activity measured in tamoxifen resistant cells could be the result of high RALBP1 expression in addition to the activity of PKC and increased tyrosine phosphorylation. It is also interesting to note that both RALBP1 and PLD are activated by small G-protein Ral, have tyrosine kinase and PKC phosphorylation sites and are involved in endocytosis and cell migration events, suggesting a crosstalk between the two proteins (reviewed in Chapter 1).

Our results show tamoxifen resistant cells have an increased RALBP1 expression. These finding support the postulate that lipid peroxidation induced by tamoxifen leads to an adaptive response to mitigate oxidative stress by up-regulating RALBP1. Additionally, treating wild-type breast cancer cells with tamoxifen resulted in an induction of RALBP1 expression, which

was dependent on oxidative stress since the antioxidant, vitamin E, blocked the increase in RALBP1. Thus, further corroborating the adaptive response phenomenon.

The finding of increased expression of RALBP1 by tamoxifen-induced oxidative stress fits with a study that showed K562 and other lung cancer cells lines upregulated RALBP1 expression when challenged with either heat shock or H_2O_2 [354]. Moreover, when these cells were preconditioned with such stressors, they showed increased capacity to export the lipid peroxidation byproduct 4HNE and they were also resistant to apoptosis induced by either 4HNE or H_2O_2. The authors attributed this resistance to the suppression of sustained JNK and caspase-3 activation. Similarly, results presented in Chapter 4 show that tamoxifen-resistant cells were unable to cleave PARP and activate JNK upon tamoxifen exposure, which indicates an adaptation to the killing induced by tamoxifen.

Like RALBP1, the ABCC1 transporter also exports 4HNE [389] and its levels were also overexpressed in the tamoxifen-resistant cells providing tamoxifen-resistant cells with another route for 4HNE export.

As mentioned, a study from our laboratory showed that the autotaxin inhibitor, ONO-8430506, decreased circulating LPA levels and also significantly decreased tumor growth and metastasis in mouse [206]. In addition to decreasing circulating LPA levels, ONO-8430506 also blocked tumor-induced inflammation of adipose tissue by decreasing 20 inflammatory mediators. Blocking the tumor-induced inflammation also resulted in

decreased plasma levels of TNF-α and G-CSF cytokines [390]. As shown in Chapter 4, ONO-8430506 also significantly decreased the expression of RALBP1 in the excised breast tumors. A recent study on human endothelial, ECV304, cells showed for the first time that TNF-α induces the expression RALBP1, but does not mediate the expression of ABCC1 [391]. Additionally, using comparative sequence analysis on mouse, human and rat RALBP1 gene, the authors found a conserved NF-κB transcription factor-binding site. As TNF-α is known to regulate downstream signals through NF-κB [429, 430] and so, RALBP1 expression could be mediated in similar fashion. Likewise, our study with ONO-8430506 treatment decreased both RALBP1 and TNF-α expressions providing a plausible explanation for the observed effect of ONO-8430506 on RALBP1. Moreover, TNF-α induced the expression of RALBP1, but not ABCC1 [391], showing that these two proteins despite sharing a function of exporting lipid peroxidation byproducts, such as 4HNE, are expressed by different signaling pathways. This conclusion is also supported from our studies of knocking down of Nrf-2 transcription factor, which did not block the expression of RALBP1 but resulted in the depletion of other adaptive responses described in Chapter 3 such as ABCC1. Thereby suggesting a separate adaptive response leading to RALBP1 expression, probably involving another transcription factor. Congruently, CHIP studies on the gene promoter region of RALBP1 showed that the binding of the transcriptional co-activator p300/CBP (cAMP-responsive element-binding protein) and the transcription factor cMYB [431] instead of Nrf2. Furthermore,

LPA signaling stabilizes Nrf2 leading to increased Nrf2 levels and downstream anti-oxidant genes and MDRTs [259]. Thus, our preliminary result showing that LPA does not induce RALBP1 expression as compared to positive controls of tamoxifen and metabolites also support the conclusion that Nrf2 does not mediate RALBP1 levels. However, LPA could indirectly increase RALBP1 through up regulating TNF-α levels and more studies are needed to establish this potential link.

In patient setting our results showed that RALBP1 protein was significantly overexpressed in cancerous breast tissue as opposed to normal breast tissue indicating its role in the basis of malignancy. Although other studies have shown the increased expression of RALBP1 in different cancer cell lines, our finding would represent the first study to show such dramatic increase in expression of RALBP1 in patient-derived breast tumors. The increased levels of RALBP1 in the patient's tumors were as high as tissues normally involved in transport and excretion, such as placenta and kidney. Thus, the level RALBP1 expression could serve as useful general biomarker in breast cancer. The corollary form that would be strategies that block the actions or expression of RALBP1 could offer a significant advantage in countering breast tumor progression. This proposition is supported by the study, which showed coating live cells with anti-RALBP1 IgG antibody caused accumulation of 4HNE and doxorubicin in all both SCLC (small cell like lung cancer) and NSLC (non- small cell like lung cancer) [354]. Moreover, targeting RALBP1 using RNA interference and IgG antibody in an xenograft

mouse model caused regression of lung tumor derived from NSCLC, H358 and H520 cells, colon tumor derived from SW480 cells [432], prostate tumor derived from PC3 cell line [433] and kidney tumor derived from Caki2 cells [434].

Despite the overexpression of RALBP1 in cancerous breast tissue, analysis of high/low RALBP1 expression levels in patient tumors did not provide a significant prognostic value in all treatment conditions and it was only trending when the analysis was confined to patients treated with tamoxifen and combination chemotherapy. The reason for the lack of prognostic significances may be attributed to the high overexpression of RALBP1 in cancerous tissue as opposed to normal tissue. Since the 50 patients expressing low RALBP1 may still have higher RALBP1 as compared to normal tissues. Thus, the low RALBP1 expressing patients may have enough RALBP1 expression and any additional increases may not provide an additional survival advantage, especially when considering the redundant role of ABCC1 and RALBP1 for exporting 4HNE out of cells. Nevertheless, when our analysis was confined to patients treated with anthracycline, the expression of RALBP1 provided a significant prognostic value.

As shown by our studies, RALBP1 is generally overexpressed in breast cancer patients and since anthracyclines are direct target for export by RALBP1, the true value of stratifying patients based on high and low RALBP1 expression could be restricted to those patients receiving anthracycline treatments. Similarly, IHC quantification data on RALBP1 expression levels

also indicated that patients with high for RALBP1 do not respond to combination chemotherapy treatment. The failure of combination chemotherapy could thus be attributed to RALBP1 exporting out anthracyclines and rendering the combination chemotherapy futile.

In summary, the findings presented in this thesis could have a great clinical application in helping guide physicians tailor treatments to particular patients depending on their protein and gene expression profiles. As such stratifying patients based on anti-oxidant genes and multi-drug resistant expression levels for administrating tamoxifen could provide utility in improving its efficacy. Also, for administering anthracycline or combination chemotherapy treatment, patients could be stratified based on PLD1 and RALBP1 expression profiles. Tamoxifen treatment leads to the upregulation of PLD1 and RALBP1, therefore, in addition to the standard approved therapies, patients with high RALBP1 and PLD1 expression and also patients given long-term tamoxifen treatments could benefit from adjuvant treatments that target the activities and expression of PLD1 and RALBP1.

5.3 Future directions

We have demonstrated that tamoxifen activates total PLD activity and also increased the expression of PLD1. Tamoxifen also stimulates the expression of RALBP1. In addition, both proteins provide good prognostic significance for patients treated with anthracycline. Hence, It will be interesting to study the role of PLD1 on the transport activity of RALBP1. We will test this by knocking-down the expression of PLD1 in cancer cells and

then measuring the transport activity of RALBP1, which can be done by challenging cancer cells with radioactive 4HNE or doxorubicin. ABCC1 could also be involved in transport, therefore, to distinguish between the two transporters, we will use anti-RALBP1 antibody since studies have demonstrated that coating cells with anti-RALBP1 antibody leads to accumulation of 4HNE [354]. The antibody will thus block the action of RALBP1 in the PLD1 knockout cells and allow us to specifically measure RALBP1-dependent 4HNE or doxorubicin export.

The ADP Ribosylation Factors (ARFs) can stimulate PLD activity, as mentioned in Section 1.7.4 of Chapter 1. Moreover, studies have showed that RALBP1 can stimulate the activity of ARFs. Hence, one possibility of high basal PLD activity in tamoxifen resistant cells could be increased RALBP1 level, acting as an upstream regulator of PLD activity. To investigate this prospect, we will use RNA interference to deplete RALBP1 in the tamoxifen resistant cells and measure both basal and stimulated PLD activity and compare them to control cells.

The autotaxin inhibitor, ONO-8430506, blocked circulating LPA levels and also significantly decreased TNF-α and G-CSF cytokines levels [206, 390]. To investigate if the decreased TNF-α by ONO-8430506 was responsible for decrease in RALBP1, we will stimulate cancer cells with or without LPA and use the conditioned media from the LPA treatment to subsequently treat other batch of cancer cells and then estimate the level of RALBP1 expression levels in those cells.

6 Bibliography

1. Jemal A, Siegel R, Ward E *et al.*: Cancer statistics, 2006. *CA Cancer J Clin* 56, 106-130 (2006).
2. Tamoxifen for early breast cancer: an overview of the randomised trials. Early Breast Cancer Trialists' Collaborative Group. *Lancet* 351, 1451-1467 (1998).
3. Ring A, Dowsett M: Mechanisms of tamoxifen resistance. *Endocr Relat Cancer* 11, 643-658 (2004).
4. Harrell JC, Dye WW, Harvell DM *et al.*: Estrogen insensitivity in a model of estrogen receptor positive breast cancer lymph node metastasis. *Cancer Res* 67, 10582-10591 (2007).
5. Jordan VC: Tamoxifen: a most unlikely pioneering medicine. *Nature reviews. Drug discovery* 2, 205-213 (2003).
6. Jaiyesimi IA, Buzdar AU, Decker DA, Hortobagyi GN: Use of tamoxifen for breast cancer: twenty-eight years later. *J Clin Oncol* 13, 513-529 (1995).
7. Jones A: Combining trastuzumab (Herceptin) with hormonal therapy in breast cancer: what can be expected and why? *Ann Oncol* 14, 1697-1704 (2003).
8. Haddow A, Watkinson JM, Paterson E, Koller PC: Influence of Synthetic Oestrogens on Advanced Malignant Disease. *British medical journal* 2, 393-398 (1944).
9. Jordan VC, Patel R, Lewis-Wambi JS, Swaby RF: By looking back we can see the way forward: enhancing the gains achieved with antihormone therapy. *Breast Cancer Res* 10 Suppl 4, S16 (2008).
10. Jordan VC: Tamoxifen: catalyst for the change to targeted therapy. *Eur J Cancer* 44, 30-38 (2008).
11. Gupta S: Profile of V. Craig Jordan. *Proc Natl Acad Sci U S A* 108, 18876-18878 (2011).
12. Jordan VC: Effect of tamoxifen (ICI 46,474) on initiation and growth of DMBA-induced rat mammary carcinomata. *Eur J Cancer* 12, 419-424 (1976).
13. EBCTCG -CTSU. http://www.ctsu.ox.ac.uk/research/meta-trials/ebctcg/index_html, (2015).
14. Dowsett M, Houghton J, Iden C *et al.*: Benefit from adjuvant tamoxifen therapy in primary breast cancer patients according oestrogen receptor, progesterone receptor, EGF receptor and HER2 status. *Ann Oncol* 17, 818-826 (2006).
15. O'Brian CA, Ioannides CG, Ward NE, Liskamp RM: Inhibition of protein kinase C and calmodulin by the geometric isomers cis- and trans-tamoxifen. *Biopolymers* 29, 97-104 (1990).
16. Gundimeda U, Chen ZH, Gopalakrishna R: Tamoxifen modulates protein kinase C via oxidative stress in estrogen receptor-negative breast cancer cells. *J Biol Chem* 271, 13504-13514 (1996).
17. Horgan K, Cooke E, Hallett MB, Mansel RE: Inhibition of Protein-Kinase-C Mediated Signal Transduction by Tamoxifen - Importance for Antitumor-Activity. *Biochemical Pharmacology* 35, 4463-4465 (1986).

18. Gulino A, Barrera G, Vacca A *et al.*: Calmodulin antagonism and growth-inhibiting activity of triphenylethylene antiestrogens in MCF-7 human breast cancer cells. *Cancer Res* 46, 6274-6278 (1986).
19. Kang Y, Cortina R, Perry RR: Role of c-myc in tamoxifen-induced apoptosis in estrogen-independent breast cancer cells. *Journal of the National Cancer Institute* 88, 279-284 (1996).
20. Perry RR, Kang Y, Greaves BR: Relationship between tamoxifen-induced transforming growth factor beta 1 expression, cytostasis and apoptosis in human breast cancer cells. *Br J Cancer* 72, 1441-1446 (1995).
21. Liu CY, Hung MH, Wang DS *et al.*: Tamoxifen induces apoptosis through cancerous inhibitor of protein phosphatase 2A-dependent phospho-Akt inactivation in estrogen receptor-negative human breast cancer cells. *Breast Cancer Res* 16, 431 (2014).
22. Liang J, Shang Y: Estrogen and cancer. *Annual review of physiology* 75, 225-240 (2013).
23. IUPAC-IUB Joint Commission on Biochemical Nomenclature (JCBN). The nomenclature of steroids. Recommendations 1989. *Eur J Biochem* 186, 429-458 (1989).
24. Prentice RL, Anderson GL: The women's health initiative: lessons learned. *Annual review of public health* 29, 131-150 (2008).
25. Frasor J, Danes JM, Komm B, Chang KC, Lyttle CR, Katzenellenbogen BS: Profiling of estrogen up- and down-regulated gene expression in human breast cancer cells: insights into gene networks and pathways underlying estrogenic control of proliferation and cell phenotype. *Endocrinology* 144, 4562-4574 (2003).
26. Kushner PJ, Agard DA, Greene GL *et al.*: Estrogen receptor pathways to AP-1. *J Steroid Biochem Mol Biol* 74, 311-317 (2000).
27. Schiff R, Massarweh S, Shou J, Osborne CK: Breast cancer endocrine resistance: how growth factor signaling and estrogen receptor coregulators modulate response. *Clin Cancer Res* 9, 447S-454S (2003).
28. Gronemeyer H: Transcription activation by estrogen and progesterone receptors. *Annu Rev Genet* 25, 89-123 (1991).
29. Osborne CK, Schiff R, Fuqua SA, Shou J: Estrogen receptor: current understanding of its activation and modulation. *Clin Cancer Res* 7, 4338s-4342s; discussion 4411s-4412s (2001).
30. Leo C, Chen JD: The SRC family of nuclear receptor coactivators. *Gene* 245, 1-11 (2000).
31. McKenna NJ, Lanz RB, O'Malley BW: Nuclear receptor coregulators: cellular and molecular biology. *Endocr Rev* 20, 321-344 (1999).
32. Jordan VC, Collins MM, Rowsby L, Prestwich G: A monohydroxylated metabolite of tamoxifen with potent antioestrogenic activity. *J Endocrinol* 75, 305-316 (1977).
33. Allen KE, Clark ER, Jordan VC: Evidence for the metabolic activation of non-steroidal antioestrogens: a study of structure-activity relationships. *Br J Pharmacol* 71, 83-91 (1980).

34. Brzozowski AM, Pike ACW, Dauter Z *et al.*: Molecular basis of agonism and antagonism in the oestrogen receptor. *Nature* 389, 753-758 (1997).
35. Shiau AK, Barstad D, Loria PM *et al.*: The structural basis of estrogen receptor/coactivator recognition and the antagonism of this interaction by tamoxifen. *Cell* 95, 927-937 (1998).
36. Lavinsky RM, Jepsen K, Heinzel T *et al.*: Diverse signaling pathways modulate nuclear receptor recruitment of N-CoR and SMRT complexes. *Proc Natl Acad Sci U S A* 95, 2920-2925 (1998).
37. McDonnell DP, Clemm DL, Hermann T, Goldman ME, Pike JW: Analysis of estrogen receptor function in vitro reveals three distinct classes of antiestrogens. *Mol Endocrinol* 9, 659-669 (1995).
38. Migliaccio A, Castoria G, Di Domenico M *et al.*: Sex steroid hormones act as growth factors. *J Steroid Biochem Mol Biol* 83, 31-35 (2002).
39. Kato S, Endoh H, Masuhiro Y *et al.*: Activation of the estrogen receptor through phosphorylation by mitogen-activated protein kinase. *Science* 270, 1491-1494 (1995).
40. Bunone G, Briand PA, Miksicek RJ, Picard D: Activation of the unliganded estrogen receptor by EGF involves the MAP kinase pathway and direct phosphorylation. *EMBO J* 15, 2174-2183 (1996).
41. Simoncini T, Hafezi-Moghadam A, Brazil DP, Ley K, Chin WW, Liao JK: Interaction of oestrogen receptor with the regulatory subunit of phosphatidylinositol-3-OH kinase. *Nature* 407, 538-541 (2000).
42. Franke TF, Kaplan DR, Cantley LC, Toker A: Direct regulation of the Akt proto-oncogene product by phosphatidylinositol-3,4-bisphosphate. *Science* 275, 665-668 (1997).
43. Vanhaesebroeck B, Alessi DR: The PI3K-PDK1 connection: more than just a road to PKB. *Biochem J* 346 Pt 3, 561-576 (2000).
44. Campbell RA, Bhat-Nakshatri P, Patel NM, Constantinidou D, Ali S, Nakshatri H: Phosphatidylinositol 3-kinase/AKT-mediated activation of estrogen receptor alpha: a new model for anti-estrogen resistance. *J Biol Chem* 276, 9817-9824 (2001).
45. Hong SH, Privalsky ML: The SMRT corepressor is regulated by a MEK-1 kinase pathway: inhibition of corepressor function is associated with SMRT phosphorylation and nuclear export. *Mol Cell Biol* 20, 6612-6625 (2000).
46. Wu RC, Qin J, Hashimoto Y *et al.*: Regulation of SRC-3 (pCIP/ACTR/AIB-1/RAC-3/TRAM-1) Coactivator activity by I kappa B kinase. *Mol Cell Biol* 22, 3549-3561 (2002).
47. Toft D, Gorski J: A receptor molecule for estrogens: isolation from the rat uterus and preliminary characterization. *Proc Natl Acad Sci U S A* 55, 1574-1581 (1966).
48. Kuiper GGJM, Enmark E, PeltoHuikko M, Nilsson S, Gustafsson JA: Cloning of a novel estrogen receptor expressed in rat prostate and ovary. *P Natl Acad Sci USA* 93, 5925-5930 (1996).

49. Koehler KF, Helguero LA, Haldosen LA, Warner M, Gustafsson JA: Reflections on the discovery and significance of estrogen receptor beta. *Endocrine Reviews* 26, 465-478 (2005).
50. Kuiper GGJM, Carlsson B, Grandien K *et al.*: Comparison of the ligand binding specificity and transcript tissue distribution of estrogen receptors alpha and beta. *Endocrinology* 138, 863-870 (1997).
51. Thomas C, Gustafsson JA: The different roles of ER subtypes in cancer biology and therapy. *Nature Reviews Cancer* 11, 597-608 (2011).
52. Skliris GP, Munot K, Bell SM *et al.*: Reduced expression of oestrogen receptor beta in invasive breast cancer and its re-expression using DNA methyl transferase inhibitors in a cell line model. *Journal of Pathology* 201, 213-220 (2003).
53. Fuqua SAW, Schiff R, Parra I *et al.*: Estrogen receptor beta protein in human breast cancer: Correlation with clinical tumor parameters. *Cancer Research* 63, 2434-2439 (2003).
54. Mann S, Laucirica R, Carlson N *et al.*: Estrogen receptor beta expression in invasive breast cancer. *Hum Pathol* 32, 113-118 (2001).
55. Saji S, Hirose M, Toi M: Clinical significance of estrogen receptor beta in breast cancer. *Cancer Chemoth Pharm* 56, S21-S26 (2005).
56. Prossnitz ER, Arterburn JB, Sklar LA: GPR30: A G protein-coupled receptor for estrogen. *Mol Cell Endocrinol* 265-266, 138-142 (2007).
57. Carmeci C, Thompson DA, Ring HJZ, Francke U, Weigel RJ: Identification of a gene (GPR30) with homology to the G-protein-coupled receptor superfamily associated with estrogen receptor expression in breast cancer. *Genomics* 45, 607-617 (1997).
58. Takada Y, Kato C, Kondo S, Korenaga R, Ando J: Cloning of cDNAs encoding G protein-coupled receptor expressed in human endothelial cells exposed to fluid shear stress. *Biochem Bioph Res Co* 240, 737-741 (1997).
59. Owman C, Blay P, Nilsson C, Lolait SJ: Cloning of human cDNA encoding a novel heptahelix receptor expressed in Burkitt's lymphoma and widely distributed in brain and peripheral tissues. *Biochem Bioph Res Co* 228, 285-292 (1996).
60. O'dowd BF, Nguyen T, Marchese A *et al.*: Discovery of three novel G-protein-coupled receptor genes. *Genomics* 47, 310-313 (1998).
61. Filardo EJ, Quinn JA, Bland KI, Frackelton AR, Jr.: Estrogen-induced activation of Erk-1 and Erk-2 requires the G protein-coupled receptor homolog, GPR30, and occurs via trans-activation of the epidermal growth factor receptor through release of HB-EGF. *Mol Endocrinol* 14, 1649-1660 (2000).
62. Thomas P, Pang Y, Filardo EJ, Dong J: Identity of an estrogen membrane receptor coupled to a G protein in human breast cancer cells. *Endocrinology* 146, 624-632 (2005).
63. SF. G: Developmental Biology. Chapter 16: Cell Death and the Formation of Digits and Joints. . (6th). Sinauer Associates, Sunderland (MA). (2000).

64. Fernald K, Kurokawa M: Evading apoptosis in cancer. *Trends Cell Biol* 23, 620-633 (2013).
65. Lazebnik YA, Kaufmann SH, Desnoyers S, Poirier GG, Earnshaw WC: Cleavage of poly(ADP-ribose) polymerase by a proteinase with properties like ICE. *Nature* 371, 346-347 (1994).
66. Kischkel FC, Hellbardt S, Behrmann I *et al.*: Cytotoxicity-dependent APO-1 (Fas/CD95)-associated proteins form a death-inducing signaling complex (DISC) with the receptor. *EMBO J* 14, 5579-5588 (1995).
67. Li P, Nijhawan D, Budihardjo I *et al.*: Cytochrome c and dATP-dependent formation of Apaf-1/caspase-9 complex initiates an apoptotic protease cascade. *Cell* 91, 479-489 (1997).
68. Du C, Fang M, Li Y, Li L, Wang X: Smac, a mitochondrial protein that promotes cytochrome c-dependent caspase activation by eliminating IAP inhibition. *Cell* 102, 33-42 (2000).
69. Youle RJ, Strasser A: The BCL-2 protein family: opposing activities that mediate cell death. *Nat Rev Mol Cell Biol* 9, 47-59 (2008).
70. Wei MC, Lindsten T, Mootha VK *et al.*: tBID, a membrane-targeted death ligand, oligomerizes BAK to release cytochrome c. *Genes & development* 14, 2060-2071 (2000).
71. Edinger AL, Thompson CB: Death by design: apoptosis, necrosis and autophagy. *Current opinion in cell biology* 16, 663-669 (2004).
72. Cocco RE, Ucker DS: Distinct modes of macrophage recognition for apoptotic and necrotic cells are not specified exclusively by phosphatidylserine exposure. *Mol Biol Cell* 12, 919-930 (2001).
73. Xie Y, Hou W, Song X *et al.*: Ferroptosis: process and function. *Cell Death Differ* 23, 369-379 (2016).
74. Ayala A, Munoz MF, Arguelles S: Lipid peroxidation: production, metabolism, and signaling mechanisms of malondialdehyde and 4-hydroxy-2-nonenal. *Oxidative medicine and cellular longevity* 2014, 360438 (2014).
75. Koval M, Pagano RE: Intracellular transport and metabolism of sphingomyelin. *Biochim Biophys Acta* 1082, 113-125 (1991).
76. van Blitterswijk WJ, van der Meer BW, Hilkmann H: Quantitative contributions of cholesterol and the individual classes of phospholipids and their degree of fatty acyl (un)saturation to membrane fluidity measured by fluorescence polarization. *Biochemistry* 26, 1746-1756 (1987).
77. Slotte JP, Bierman EL: Depletion of plasma-membrane sphingomyelin rapidly alters the distribution of cholesterol between plasma membranes and intracellular cholesterol pools in cultured fibroblasts. *Biochem J* 250, 653-658 (1988).
78. Wiegmann K, Schutze S, Machleidt T, Witte D, Kronke M: Functional dichotomy of neutral and acidic sphingomyelinases in tumor necrosis factor signaling. *Cell* 78, 1005-1015 (1994).
79. Mandon EC, Ehses I, Rother J, van Echten G, Sandhoff K: Subcellular localization and membrane topology of serine palmitoyltransferase, 3-

dehydrosphinganine reductase, and sphinganine N-acyltransferase in mouse liver. *J Biol Chem* 267, 11144-11148 (1992).
80. Tepper AD, Diks SH, van Blitterswijk WJ, Borst J: Glucosylceramide synthase does not attenuate the ceramide pool accumulating during apoptosis induced by CD95 or anti-cancer regimens. *J Biol Chem* 275, 34810-34817 (2000).
81. Dickson RC: Sphingolipid functions in Saccharomyces cerevisiae: comparison to mammals. *Annu Rev Biochem* 67, 27-48 (1998).
82. Basu S, Kolesnick R: Stress signals for apoptosis: ceramide and c-Jun kinase. *Oncogene* 17, 3277-3285 (1998).
83. Hannun Y: Functions of ceramide in coordinating cellular responses to stress. *Science* 274, 1855-1859 (1996).
84. Tepper AD, Cock JG, de Vries E, Borst J, van Blitterswijk WJ: CD95/Fas-induced ceramide formation proceeds with slow kinetics and is not blocked by caspase-3/CPP32 inhibition. *J Biol Chem* 272, 24308-24312 (1997).
85. Tepper AD, de Vries E, van Blitterswijk WJ, Borst J: Ordering of ceramide formation, caspase activation, and mitochondrial changes during CD95- and DNA damage-induced apoptosis. *J Clin Invest* 103, 971-978 (1999).
86. Tepper AD, Ruurs P, Wiedmer T, Sims PJ, Borst J, van Blitterswijk WJ: Sphingomyelin hydrolysis to ceramide during the execution phase of apoptosis results from phospholipid scrambling and alters cell-surface morphology. *J Cell Biol* 150, 155-164 (2000).
87. Martin SJ, Reutelingsperger CP, McGahon AJ *et al.*: Early redistribution of plasma membrane phosphatidylserine is a general feature of apoptosis regardless of the initiating stimulus: inhibition by overexpression of Bcl-2 and Abl. *The Journal of experimental medicine* 182, 1545-1556 (1995).
88. Ganesan V, Perera MN, Colombini D, Datskovskiy D, Chadha K, Colombini M: Ceramide and activated Bax act synergistically to permeabilize the mitochondrial outer membrane. *Apoptosis* 15, 553-562 (2010).
89. von Haefen C, Wieder T, Gillissen B *et al.*: Ceramide induces mitochondrial activation and apoptosis via a Bax-dependent pathway in human carcinoma cells. *Oncogene* 21, 4009-4019 (2002).
90. Morad SA, Cabot MC: Ceramide-orchestrated signalling in cancer cells. *Nat Rev Cancer* 13, 51-65 (2013).
91. Siskind LJ, Kolesnick RN, Colombini M: Ceramide forms channels in mitochondrial outer membranes at physiologically relevant concentrations. *Mitochondrion* 6, 118-125 (2006).
92. Higuchi M, Singh S, Jaffrezou JP, Aggarwal BB: Acidic sphingomyelinase-generated ceramide is needed but not sufficient for TNF-induced apoptosis and nuclear factor-kappa B activation. *J Immunol* 157, 297-304 (1996).
93. Zhang QJ, Holland WL, Wilson L *et al.*: Ceramide mediates vascular dysfunction in diet-induced obesity by PP2A-mediated dephosphorylation of the eNOS-Akt complex. *Diabetes* 61, 1848-1859 (2012).

94. Mukhopadhyay A, Saddoughi SA, Song P *et al.*: Direct interaction between the inhibitor 2 and ceramide via sphingolipid-protein binding is involved in the regulation of protein phosphatase 2A activity and signaling. *FASEB J* 23, 751-763 (2009).
95. Verheij M, Bose R, Lin XH *et al.*: Requirement for ceramide-initiated SAPK/JNK signalling in stress-induced apoptosis. *Nature* 380, 75-79 (1996).
96. Cheng Y, Wu J, Hertervig E *et al.*: Identification of aberrant forms of alkaline sphingomyelinase (NPP7) associated with human liver tumorigenesis. *Br J Cancer* 97, 1441-1448 (2007).
97. Liu YY, Han TY, Giuliano AE, Cabot MC: Expression of glucosylceramide synthase, converting ceramide to glucosylceramide, confers adriamycin resistance in human breast cancer cells. *J Biol Chem* 274, 1140-1146 (1999).
98. Lucci A, Cho WI, Han TY, Giuliano AE, Morton DL, Cabot MC: Glucosylceramide: a marker for multiple-drug resistant cancers. *Anticancer Res* 18, 475-480 (1998).
99. Sukocheva O, Wang L, Verrier E, Vadas MA, Xia P: Restoring endocrine response in breast cancer cells by inhibition of the sphingosine kinase-1 signaling pathway. *Endocrinology* 150, 4484-4492 (2009).
100. Pyne NJ, Pyne S: Sphingosine 1-phosphate and cancer. *Nat Rev Cancer* 10, 489-503 (2010).
101. Zanke BW, Boudreau K, Rubie E *et al.*: The stress-activated protein kinase pathway mediates cell death following injury induced by cis-platinum, UV irradiation or heat. *Curr Biol* 6, 606-613 (1996).
102. Wilson DJ, Fortner KA, Lynch DH *et al.*: JNK, but not MAPK, activation is associated with Fas-mediated apoptosis in human T cells. *Eur J Immunol* 26, 989-994 (1996).
103. Dhanasekaran DN, Reddy EP: JNK signaling in apoptosis. *Oncogene* 27, 6245-6251 (2008).
104. Xia Z, Dickens M, Raingeaud J, Davis RJ, Greenberg ME: Opposing effects of ERK and JNK-p38 MAP kinases on apoptosis. *Science* 270, 1326-1331 (1995).
105. Tournier C, Hess P, Yang DD *et al.*: Requirement of JNK for stress-induced activation of the cytochrome c-mediated death pathway. *Science* 288, 870-874 (2000).
106. Nagai H, Noguchi T, Takeda K, Ichijo H: Pathophysiological roles of ASK1-MAP kinase signaling pathways. *Journal of biochemistry and molecular biology* 40, 1-6 (2007).
107. Chen Z, Seimiya H, Naito M *et al.*: ASK1 mediates apoptotic cell death induced by genotoxic stress. *Oncogene* 18, 173-180 (1999).
108. Donovan N, Becker EB, Konishi Y, Bonni A: JNK phosphorylation and activation of BAD couples the stress-activated signaling pathway to the cell death machinery. *J Biol Chem* 277, 40944-40949 (2002).

109. Datta SR, Dudek H, Tao X *et al.*: Akt phosphorylation of BAD couples survival signals to the cell-intrinsic death machinery. *Cell* 91, 231-241 (1997).
110. Datta SR, Katsov A, Hu L *et al.*: 14-3-3 proteins and survival kinases cooperate to inactivate BAD by BH3 domain phosphorylation. *Molecular cell* 6, 41-51 (2000).
111. Tsuruta F, Sunayama J, Mori Y *et al.*: JNK promotes Bax translocation to mitochondria through phosphorylation of 14-3-3 proteins. *EMBO J* 23, 1889-1899 (2004).
112. Brenner B, Koppenhoefer U, Weinstock C, Linderkamp O, Lang F, Gulbins E: Fas- or ceramide-induced apoptosis is mediated by a Rac1-regulated activation of Jun N-terminal kinase/p38 kinases and GADD153. *J Biol Chem* 272, 22173-22181 (1997).
113. Huang C, Ma W, Ding M, Bowden GT, Dong Z: Direct evidence for an important role of sphingomyelinase in ultraviolet-induced activation of c-Jun N-terminal kinase. *J Biol Chem* 272, 27753-27757 (1997).
114. Chen YR, Meyer CF, Tan TH: Persistent activation of c-Jun N-terminal kinase 1 (JNK1) in gamma radiation-induced apoptosis. *J Biol Chem* 271, 631-634 (1996).
115. Gorrini C, Harris IS, Mak TW: Modulation of oxidative stress as an anticancer strategy. *Nature reviews. Drug discovery* 12, 931-947 (2013).
116. Birben E, Sahiner UM, Sackesen C, Erzurum S, Kalayci O: Oxidative stress and antioxidant defense. *The World Allergy Organization journal* 5, 9-19 (2012).
117. Kuciel R, Mazurkiewicz A: Formation and detoxification of reactive oxygen species. *Biochemistry and molecular biology education : a bimonthly publication of the International Union of Biochemistry and Molecular Biology* 32, 183-186 (2004).
118. Burkitt MJ, Mason RP: Direct evidence for in vivo hydroxyl-radical generation in experimental iron overload: an ESR spin-trapping investigation. *Proc Natl Acad Sci U S A* 88, 8440-8444 (1991).
119. Finkel T: Signal transduction by mitochondrial oxidants. *J Biol Chem* 287, 4434-4440 (2012).
120. Handy DE, Loscalzo J: Redox regulation of mitochondrial function. *Antioxidants & redox signaling* 16, 1323-1367 (2012).
121. Singh I: Biochemistry of peroxisomes in health and disease. *Mol Cell Biochem* 167, 1-29 (1997).
122. GM. C: The Cell: A Molecular Approach. . (2nd edition.). Sinauer Associates, Sunderland (MA). (2000).
123. Malhotra JD, Kaufman RJ: Endoplasmic reticulum stress and oxidative stress: a vicious cycle or a double-edged sword? *Antioxidants & redox signaling* 9, 2277-2293 (2007).
124. Paletta-Silva R, Rocco-Machado N, Meyer-Fernandes JR: NADPH oxidase biology and the regulation of tyrosine kinase receptor signaling and cancer drug cytotoxicity. *Int J Mol Sci* 14, 3683-3704 (2013).

125. Graham KA, Kulawiec M, Owens KM *et al.*: NADPH oxidase 4 is an oncoprotein localized to mitochondria. *Cancer Biol Ther* 10, 223-231 (2010).
126. Lambeth JD: NOX enzymes and the biology of reactive oxygen. *Nature reviews. Immunology* 4, 181-189 (2004).
127. Ray PD, Huang BW, Tsuji Y: Reactive oxygen species (ROS) homeostasis and redox regulation in cellular signaling. *Cell Signal* 24, 981-990 (2012).
128. Lee SR, Yang KS, Kwon J, Lee C, Jeong W, Rhee SG: Reversible inactivation of the tumor suppressor PTEN by H2O2. *J Biol Chem* 277, 20336-20342 (2002).
129. Ishikawa K, Takenaga K, Akimoto M *et al.*: ROS-generating mitochondrial DNA mutations can regulate tumor cell metastasis. *Science* 320, 661-664 (2008).
130. Bouayed J, Bohn T: Exogenous antioxidants - Double-edged swords in cellular redox state: Health beneficial effects at physiologic doses versus deleterious effects at high doses. *Oxidative medicine and cellular longevity* 3, 228-237 (2010).
131. Brigelius-Flohe R, Traber MG: Vitamin E: function and metabolism. *FASEB J* 13, 1145-1155 (1999).
132. Lu SC: Glutathione synthesis. *Biochim Biophys Acta* 1830, 3143-3153 (2013).
133. Hwang C, Sinskey AJ, Lodish HF: Oxidized redox state of glutathione in the endoplasmic reticulum. *Science* 257, 1496-1502 (1992).
134. Townsend DM, Tew KD: The role of glutathione-S-transferase in anti-cancer drug resistance. *Oncogene* 22, 7369-7375 (2003).
135. Saitoh M, Nishitoh H, Fujii M *et al.*: Mammalian thioredoxin is a direct inhibitor of apoptosis signal-regulating kinase (ASK) 1. *EMBO J* 17, 2596-2606 (1998).
136. Moi P, Chan K, Asunis I, Cao A, Kan YW: Isolation of NF-E2-related factor 2 (Nrf2), a NF-E2-like basic leucine zipper transcriptional activator that binds to the tandem NF-E2/AP1 repeat of the beta-globin locus control region. *Proc Natl Acad Sci U S A* 91, 9926-9930 (1994).
137. Ma Q: Role of nrf2 in oxidative stress and toxicity. *Annual review of pharmacology and toxicology* 53, 401-426 (2013).
138. Itoh K, Chiba T, Takahashi S *et al.*: An Nrf2/small Maf heterodimer mediates the induction of phase II detoxifying enzyme genes through antioxidant response elements. *Biochem Biophys Res Commun* 236, 313-322 (1997).
139. Schumacher MA, Goodman RH, Brennan RG: The structure of a CREB bZIP.somatostatin CRE complex reveals the basis for selective dimerization and divalent cation-enhanced DNA binding. *J Biol Chem* 275, 35242-35247 (2000).
140. McCord JM, Fridovich I: Superoxide dismutase. An enzymic function for erythrocuprein (hemocuprein). *J Biol Chem* 244, 6049-6055 (1969).
141. Zelko IN, Mariani TJ, Folz RJ: Superoxide dismutase multigene family: a comparison of the CuZn-SOD (SOD1), Mn-SOD (SOD2), and EC-SOD

(SOD3) gene structures, evolution, and expression. *Free Radic Biol Med* 33, 337-349 (2002).
142. Edlund C, Elhammer A, Dallner G: Distribution of newly synthesized DT-diaphorase in rat liver. *Bioscience reports* 2, 861-865 (1982).
143. Nebert DW, Roe AL, Vandale SE, Bingham E, Oakley GG: NAD(P)H:quinone oxidoreductase (NQO1) polymorphism, exposure to benzene, and predisposition to disease: a HuGE review. *Genet Med* 4, 62-70 (2002).
144. Siegel D, Gustafson DL, Dehn DL *et al.*: NAD(P)H:quinone oxidoreductase 1: role as a superoxide scavenger. *Mol Pharmacol* 65, 1238-1247 (2004).
145. Siegel D, Bolton EM, Burr JA, Liebler DC, Ross D: The reduction of alpha-tocopherolquinone by human NAD(P)H: quinone oxidoreductase: the role of alpha-tocopherolhydroquinone as a cellular antioxidant. *Mol Pharmacol* 52, 300-305 (1997).
146. Asher G, Lotem J, Kama R, Sachs L, Shaul Y: NQO1 stabilizes p53 through a distinct pathway. *Proc Natl Acad Sci U S A* 99, 3099-3104 (2002).
147. auf dem Keller U, Kumin A, Braun S, Werner S: Reactive oxygen species and their detoxification in healing skin wounds. *The journal of investigative dermatology. Symposium proceedings / the Society for Investigative Dermatology, Inc. [and] European Society for Dermatological Research* 11, 106-111 (2006).
148. Jansen T, Daiber A: Direct Antioxidant Properties of Bilirubin and Biliverdin. Is there a Role for Biliverdin Reductase? *Front Pharmacol* 3, 30 (2012).
149. Tong KI, Katoh Y, Kusunoki H, Itoh K, Tanaka T, Yamamoto M: Keap1 recruits Neh2 through binding to ETGE and DLG motifs: characterization of the two-site molecular recognition model. *Mol Cell Biol* 26, 2887-2900 (2006).
150. Kobayashi A, Kang MI, Okawa H *et al.*: Oxidative stress sensor Keap1 functions as an adaptor for Cul3-based E3 ligase to regulate proteasomal degradation of Nrf2. *Mol Cell Biol* 24, 7130-7139 (2004).
151. Zhang DD, Lo SC, Cross JV, Templeton DJ, Hannink M: Keap1 is a redox-regulated substrate adaptor protein for a Cul3-dependent ubiquitin ligase complex. *Mol Cell Biol* 24, 10941-10953 (2004).
152. Chandel NS, Maltepe E, Goldwasser E, Mathieu CE, Simon MC, Schumacker PT: Mitochondrial reactive oxygen species trigger hypoxia-induced transcription. *Proc Natl Acad Sci U S A* 95, 11715-11720 (1998).
153. Wang R, An J, Ji F, Jiao H, Sun H, Zhou D: Hypermethylation of the Keap1 gene in human lung cancer cell lines and lung cancer tissues. *Biochem Biophys Res Commun* 373, 151-154 (2008).
154. Dean M, Annilo T: Evolution of the ATP-binding cassette (ABC) transporter superfamily in vertebrates. *Annual review of genomics and human genetics* 6, 123-142 (2005).
155. Higgins CF: ABC transporters: from microorganisms to man. *Annual review of cell biology* 8, 67-113 (1992).
156. Rees DC, Johnson E, Lewinson O: ABC transporters: the power to change. *Nat Rev Mol Cell Biol* 10, 218-227 (2009).

157. Biemans-Oldehinkel E, Doeven MK, Poolman B: ABC transporter architecture and regulatory roles of accessory domains. *FEBS Lett* 580, 1023-1035 (2006).
158. Cronin-Fenton DP, Damkier P, Lash TL: Metabolism and transport of tamoxifen in relation to its effectiveness: new perspectives on an ongoing controversy. *Future Oncol* 10, 107-122 (2014).
159. Aller SG, Yu J, Ward A *et al.*: Structure of P-glycoprotein reveals a molecular basis for poly-specific drug binding. *Science* 323, 1718-1722 (2009).
160. Kerem BS, Zielenski J, Markiewicz D *et al.*: Identification of mutations in regions corresponding to the two putative nucleotide (ATP)-binding folds of the cystic fibrosis gene. *Proc Natl Acad Sci U S A* 87, 8447-8451 (1990).
161. Riordan JR, Rommens JM, Kerem B *et al.*: Identification of the cystic fibrosis gene: cloning and characterization of complementary DNA. *Science* 245, 1066-1073 (1989).
162. Paulusma CC, Bosma PJ, Zaman GJ *et al.*: Congenital jaundice in rats with a mutation in a multidrug resistance-associated protein gene. *Science* 271, 1126-1128 (1996).
163. Leslie EM, Deeley RG, Cole SP: Multidrug resistance proteins: role of P-glycoprotein, MRP1, MRP2, and BCRP (ABCG2) in tissue defense. *Toxicol Appl Pharmacol* 204, 216-237 (2005).
164. Ahern TP, Christensen M, Cronin-Fenton DP *et al.*: Functional polymorphisms in UDP-glucuronosyl transferases and recurrence in tamoxifen-treated breast cancer survivors. *Cancer Epidemiol Biomarkers Prev* 20, 1937-1943 (2011).
165. Lazarus P, Blevins-Primeau AS, Zheng Y, Sun D: Potential role of UGT pharmacogenetics in cancer treatment and prevention: focus on tamoxifen. *Ann N Y Acad Sci* 1155, 99-111 (2009).
166. King CD, Rios GR, Green MD, Tephly TR: UDP-glucuronosyltransferases. *Curr Drug Metab* 1, 143-161 (2000).
167. Stearns V, Johnson MD, Rae JM *et al.*: Active tamoxifen metabolite plasma concentrations after coadministration of tamoxifen and the selective serotonin reuptake inhibitor paroxetine. *J Natl Cancer Inst* 95, 1758-1764 (2003).
168. Desta Z, Ward BA, Soukhova NV, Flockhart DA: Comprehensive evaluation of tamoxifen sequential biotransformation by the human cytochrome P450 system in vitro: prominent roles for CYP3A and CYP2D6. *J Pharmacol Exp Ther* 310, 1062-1075 (2004).
169. Jordan VC: New insights into the metabolism of tamoxifen and its role in the treatment and prevention of breast cancer. *Steroids* 72, 829-842 (2007).
170. Adachi T, Nakagawa H, Chung I *et al.*: Nrf2-dependent and -independent induction of ABC transporters ABCC1, ABCC2, and ABCG2 in HepG2 cells under oxidative stress. *J Exp Ther Oncol* 6, 335-348 (2007).
171. Hagiya Y, Adachi T, Ogura S *et al.*: Nrf2-dependent induction of human ABC transporter ABCG2 and heme oxygenase-1 in HepG2 cells by

photoactivation of porphyrins: biochemical implications for cancer cell response to photodynamic therapy. *J Exp Ther Oncol* 7, 153-167 (2008).
172. Singh A, Wu H, Zhang P, Happel C, Ma J, Biswal S: Expression of ABCG2 (BCRP) is regulated by Nrf2 in cancer cells that confers side population and chemoresistance phenotype. *Mol Cancer Ther* 9, 2365-2376 (2010).
173. Canet MJ, Merrell MD, Harder BG *et al.*: Identification of a functional antioxidant response element within the eighth intron of the human ABCC3 gene. *Drug Metab Dispos* 43, 93-99 (2015).
174. Gatti L, Zunino F: Overview of tumor cell chemoresistance mechanisms. *Methods in molecular medicine* 111, 127-148 (2005).
175. Wilson TR, Longley DB, Johnston PG: Chemoresistance in solid tumours. *Ann Oncol* 17 Suppl 10, x315-324 (2006).
176. Yamada A, Ishikawa T, Ota I *et al.*: High expression of ATP-binding cassette transporter ABCC11 in breast tumors is associated with aggressive subtypes and low disease-free survival. *Breast Cancer Res Treat* 137, 773-782 (2013).
177. Longley DB, Harkin DP, Johnston PG: 5-fluorouracil: mechanisms of action and clinical strategies. *Nat Rev Cancer* 3, 330-338 (2003).
178. Banerjee D, Mayer-Kuckuk P, Capiaux G, Budak-Alpdogan T, Gorlick R, Bertino JR: Novel aspects of resistance to drugs targeted to dihydrofolate reductase and thymidylate synthase. *Biochim Biophys Acta* 1587, 164-173 (2002).
179. Stracke ML, Krutzsch HC, Unsworth EJ *et al.*: Identification, purification, and partial sequence analysis of autotaxin, a novel motility-stimulating protein. *J Biol Chem* 267, 2524-2529 (1992).
180. Murata J, Lee HY, Clair T *et al.*: cDNA cloning of the human tumor motility-stimulating protein, autotaxin, reveals a homology with phosphodiesterases. *J. Biol. Chem.* 269, 30479-30484 (1994).
181. Buckley MF, Loveland KA, McKinstry WJ, Garson OM, Goding JW: Plasma cell membrane glycoprotein PC-1. cDNA cloning of the human molecule, amino acid sequence, and chromosomal location. *J. Biol. Chem.* 265, 17506-17511 (1990).
182. Funakoshi I, Kato H, Horie K *et al.*: Molecular cloning of cDNAs for human fibroblast nucleotide pyrophosphatase. *Arch. Biochem. Biophys.* 295, 180-187 (1992).
183. Nakanaga K, Hama K, Aoki J: Autotaxin--an LPA producing enzyme with diverse functions. *J Biochem* 148, 13-24 (2010).
184. Benesch MG, Tang X, Venkatraman G, Bekele RT, Brindley DN: Recent advances in targeting the autotaxin-lysophosphatidate-lipid phosphate phosphatase axis in vivo. *J Biomed Res* 30, (2015).
185. Umezu-Goto M, Kishi Y, Taira A *et al.*: Autotaxin has lysophospholipase D activity leading to tumor cell growth and motility by lysophosphatidic acid production. *J. Cell Biol.* 158, 227-233 (2002).
186. Tokumura A, Majima E, Kariya Y *et al.*: Identification of human plasma lysophospholipase D, a lysophosphatidic acid-producing enzyme, as

autotaxin, a multifunctional phosphodiesterase. *J Biol Chem* 277, 39436-39442 (2002).
187. Moolenaar WH: Lysophospholipids in the limelight: autotaxin takes center stage. *J Cell Biol* 158, 197-199 (2002).
188. Tanaka M, Okudaira S, Kishi Y *et al.*: Autotaxin stabilizes blood vessels and is required for embryonic vasculature by producing lysophosphatidic acid. *J Biol Chem* 281, 25822-25830 (2006).
189. van Meeteren LA, Ruurs P, Stortelers C *et al.*: Autotaxin, a secreted lysophospholipase D, is essential for blood vessel formation during development. *Mol Cell Biol* 26, 5015-5022 (2006).
190. Koike S, Keino-Masu K, Masu M: Deficiency of autotaxin/lysophospholipase D results in head cavity formation in mouse embryos through the LPA receptor-Rho-ROCK pathway. *Biochem. Biophys. Res. Commun.* 400, 66-71 (2010).
191. Koike S, Keino-Masu K, Ohto T, Sugiyama F, Takahashi S, Masu M: Autotaxin/lysophospholipase D-mediated lysophosphatidic acid signaling is required to form distinctive large lysosomes in the visceral endoderm cells of the mouse yolk sac. *J. Biol. Chem.* 284, 33561-33570 (2009).
192. Koike S, Yutoh Y, Keino-Masu K, Noji S, Masu M, Ohuchi H: Autotaxin is required for the cranial neural tube closure and establishment of the midbrain-hindbrain boundary during mouse development. *Dev. Dyn.* 240, 413-421 (2011).
193. Mazereeuw-Hautier J, Gres S, Fanguin M *et al.*: Production of lysophosphatidic acid in blister fluid: involvement of a lysophospholipase D activity. *J Invest Dermatol* 125, 421-427 (2005).
194. Brindley DN: Lipid phosphate phosphatases and related proteins: signaling functions in development, cell division, and cancer. *J Cell Biochem* 92, 900-912 (2004).
195. Chappell J, Leitner JW, Solomon S, Golovchenko I, Goalstone ML, Draznin B: Effect of insulin on cell cycle progression in MCF-7 breast cancer cells. Direct and potentiating influence. *J Biol Chem* 276, 38023-38028 (2001).
196. Umemoto E, Hayasaka H, Bai Z *et al.*: Novel regulators of lymphocyte trafficking across high endothelial venules. *Crit. Rev. Immunol.* 31, 147-169 (2011).
197. Miyasaka M, Tanaka T: Lymphocyte trafficking across high endothelial venules: dogmas and enigmas. *Nature reviews. Immunology* 4, 360-370 (2004).
198. Nakasaki T, Tanaka T, Okudaira S *et al.*: Involvement of the lysophosphatidic acid-generating enzyme autotaxin in lymphocyte-endothelial cell interactions. *Am. J. Pathol.* 173, 1566-1576 (2008).
199. van Meeteren LA, Moolenaar WH: Regulation and biological activities of the autotaxin-LPA axis. *Prog Lipid Res* 46, 145-160 (2007).
200. Budd DC, Qian Y: Development of lysophosphatidic acid pathway modulators as therapies for fibrosis. *Future Med Chem* 5, 1935-1952 (2013).

201. Evseenko D, Latour B, Richardson W *et al.*: Lysophosphatidic acid mediates myeloid differentiation within the human bone marrow microenvironment. *PLoS One* 8, e63718 (2013).
202. Euer N, Schwirzke M, Evtimova V *et al.*: Identification of genes associated with metastasis of mammary carcinoma in metastatic versus non-metastatic cell lines. *Anticancer Res* 22, 733-740 (2002).
203. Liu S, Umezu-Goto M, Murph M *et al.*: Expression of autotaxin and lysophosphatidic acid receptors increases mammary tumorigenesis, invasion, and metastases. *Cancer Cell* 15, 539-550 (2009).
204. St-Coeur PD, Ferguson D, Morin P, Jr., Touaibia M: PF-8380 and closely related analogs: synthesis and structure-activity relationship towards autotaxin inhibition and glioma cell viability. *Arch Pharm* 346, 91-97 (2013).
205. Samadi N, Bekele R, Capatos D, Venkatraman G, Sariahmetoglu M, Brindley DN: Regulation of lysophosphatidate signaling by autotaxin and lipid phosphate phosphatases with respect to tumor progression, angiogenesis, metastasis and chemo-resistance. *Biochimie* 93, 61-70 (2011).
206. Benesch MG, Tang X, Maeda T *et al.*: Inhibition of autotaxin delays breast tumor growth and lung metastasis in mice. *FASEB J* 28, 2655-2666 (2014).
207. Benesch MGK, Ko YM, McMullen TPW, Brindley DN: Autotaxin in the crosshairs: Taking aim at cancer and other inflammatory conditions. *FEBS Lett.* 588, 2712-2727 (2014).
208. Brindley DN, Benesch MGK, Murph MM: *Autotaxin – An Enzymatic Augmenter of Malignant Progression Linked to Inflammation*. In: *Melanoma - Current Clinical Management and Future Therapeutics*, (Ed.^(Eds). InTech Open, (2015).
209. Barbayianni E, Kaffe E, Aidinis V, Kokotos G: Autotaxin, a secreted lysophospholipase D, as a promising therapeutic target in chronic inflammation and cancer. *Prog. Lipid Res.* 58, 76-96 (2015).
210. Weigelt B, Peterse JL, van 't Veer LJ: Breast cancer metastasis: markers and models. *Nat Rev Cancer* 5, 591-602 (2005).
211. Leblanc R, Lee SC, David M *et al.*: Interaction of platelet-derived autotaxin with tumor integrin alphaVbeta3 controls metastasis of breast cancer cells to bone. *Blood* 124, 3141-3150 (2014).
212. Yang SY, Lee J, Park CG *et al.*: Expression of autotaxin (NPP-2) is closely linked to invasiveness of breast cancer cells. *Clin Exp Metastasis* 19, 603-608 (2002).
213. Nam SW, Clair T, Campo CK, Lee HY, Liotta LA, Stracke ML: Autotaxin (ATX), a potent tumor motogen, augments invasive and metastatic potential of ras-transformed cells. *Oncogene* 19, 241-247 (2000).
214. Nam SW, Clair T, Kim YS *et al.*: Autotaxin (NPP-2), a metastasis-enhancing motogen, is an angiogenic factor. *Cancer Res* 61, 6938-6944 (2001).

215. Hama K, Aoki J, Fukaya M *et al.*: Lysophosphatidic acid and autotaxin stimulate cell motility of neoplastic and non-neoplastic cells through LPA1. *J Biol Chem* 279, 17634-17639 (2004).
216. An S, Dickens MA, Bleu T, Hallmark OG, Goetzl EJ: Molecular cloning of the human Edg2 protein and its identification as a functional cellular receptor for lysophosphatidic acid. *Biochem Biophys Res Commun* 231, 619-622 (1997).
217. Lee CW, Rivera R, Dubin AE, Chun J: LPA(4)/GPR23 is a lysophosphatidic acid (LPA) receptor utilizing G(s)-, G(q)/G(i)-mediated calcium signaling and G(12/13)-mediated Rho activation. *J Biol Chem* 282, 4310-4317 (2007).
218. Pasternack SM, von Kugelgen I, Aboud KA *et al.*: G protein-coupled receptor P2Y5 and its ligand LPA are involved in maintenance of human hair growth. *Nat Genet* 40, 329-334 (2008).
219. Williams JR, Khandoga AL, Goyal P *et al.*: Unique ligand selectivity of the GPR92/LPA5 lysophosphatidate receptor indicates role in human platelet activation. *J Biol Chem* 284, 17304-17319 (2009).
220. Yanagida K, Ishii S: Non-Edg family LPA receptors: the cutting edge of LPA research. *J Biochem* 150, 223-232 (2011).
221. Ferry G, Moulharat N, Pradere JP *et al.*: S32826, a nanomolar inhibitor of autotaxin: discovery, synthesis and applications as a pharmacological tool. *J Pharmacol Exp Ther* 327, 809-819 (2008).
222. Albers HM, Dong A, van Meeteren LA *et al.*: Boronic acid-based inhibitor of autotaxin reveals rapid turnover of LPA in the circulation. *Proc Natl Acad Sci U S A* 107, 7257-7262 (2010).
223. Gierse J, Thorarensen A, Beltey K *et al.*: A novel autotaxin inhibitor reduces lysophosphatidic acid levels in plasma and the site of inflammation. *J Pharmacol Exp Ther* 334, 310-317 (2010).
224. Moolenaar WH, van Meeteren LA, Giepmans BN: The ins and outs of lysophosphatidic acid signaling. *Bioessays* 26, 870-881 (2004).
225. Brindley DN: Hepatic secretion of lysphosphatidylcholine: a novel transport system for polyunsaturated fatty acids and choline. *J. Nutr. Biochem.* 4, 442-449 (1993).
226. Aoki J, Taira A, Takanezawa Y *et al.*: Serum lysophosphatidic acid is produced through diverse phospholipase pathways. *J Biol Chem* 277, 48737-48744 (2002).
227. Parrill AL, Baker DL: Autotaxin inhibition: challenges and progress toward novel anti-cancer agents. *Anticancer Agents Med Chem* 8, 917-923 (2008).
228. Benesch MG, Zhao YY, Curtis JM, McMullen TP, Brindley DN: Regulation of autotaxin expression and secretion by lysophosphatidate and sphingosine 1-phosphate. *J Lipid Res* 56, 1134-1144 (2015).
229. Fourcade O, Simon MF, Viode C *et al.*: Secretory phospholipase A2 generates the novel lipid mediator lysophosphatidic acid in membrane microvesicles shed from activated cells. *Cell* 80, 919-927 (1995).

230. Zhao X, Wang D, Zhao Z *et al.*: Caspase-3-dependent activation of calcium-independent phospholipase A2 enhances cell migration in non-apoptotic ovarian cancer cells. *J Biol Chem* 281, 29357-29368 (2006).
231. Li H, Zhao Z, Wei G *et al.*: Group VIA phospholipase A2 in both host and tumor cells is involved in ovarian cancer development. *FASEB J*, (2010).
232. Venkatraman G, Brindley DN: Lipid phosphate phosphatases: their role in lysolipid degradation and cell signaling. . John Wiley and Sons Inc, , NY, USA. . (In press).
233. Zhang QX, Pilquil CS, Dewald J, Berthiaume LG, Brindley DN: Identification of structurally important domains of lipid phosphate phosphatase-1: implications for its sites of action. *Biochem J* 345 Pt 2, 181-184 (2000).
234. Jasinska R, Zhang QX, Pilquil C *et al.*: Lipid phosphate phosphohydrolase-1 degrades exogenous glycerolipid and sphingolipid phosphate esters. *Biochem J* 340, 677-686 (1999).
235. Tomsig JL, Snyder AH, Berdyshev EV *et al.*: Lipid phosphate phosphohydrolase type 1 (LPP1) degrades extracellular lysophosphatidic acid in vivo. *Biochem J* 419, 611-618 (2009).
236. Salous AK, Panchatcharam M, Sunkara M *et al.*: Mechanism of rapid elimination of lysophosphatidic acid and related lipids from the circulation of mice. *J Lipid Res* 54, 2775-2784 (2013).
237. Xiaoyun Tang YYZ, Jay Dewald, Jonathan M. Curtis and David N. Brindley: Doxycycline increases expression of lipid phosphate phosphatases and plasma lysophosphatidate turnover. *submitted to JLR*, (2015).
238. Bekele RT, Brindley DN: Role of autotaxin and lysophosphatidate in cancer progression and resistance to chemotherapy and radiotherapy. *Clinical Lipidology* 7, 313-328 (2012).
239. Kai M, Wada I, Imai S, Sakane F, Kanoh H: Cloning and characterization of two human isozymes of Mg2+-independent phosphatidic acid phosphatase. *J Biol Chem* 272, 24572-24578 (1997).
240. Barila D, Plateroti M, Nobili F *et al.*: The Dri 42 gene, whose expression is up-regulated during epithelial differentiation, encodes a novel endoplasmic reticulum resident transmembrane protein. *J Biol Chem* 271, 29928-29936 (1996).
241. Pyne S, Kong KC, Darroch PI: Lysophosphatidic acid and sphingosine 1-phosphate biology: the role of lipid phosphate phosphatases. *Semin. Cell Dev. Biol.* 15, 491-501 (2004).
242. Pilquil C, Dewald J, Cherney A *et al.*: Lipid phosphate phosphatase-1 regulates lysophosphatidate-induced fibroblast migration by controlling phospholipase D2-dependent phosphatidate generation. *J. Biol. Chem.* 281, 38418-38429 (2006).
243. Tang X, Benesch MG, Dewald J *et al.*: Lipid phosphate phosphatase-1 expression in cancer cells attenuates tumor growth and metastasis in mice. *J. Lipid Res.* 55, 2389-2400 (2014).
244. Tanyi JL, Morris AJ, Wolf JK *et al.*: The human lipid phosphate phosphatase-3 decreases the growth, survival, and tumorigenesis of ovarian cancer cells: validation of the lysophosphatidic acid signaling

cascade as a target for therapy in ovarian cancer. *Cancer Res* 63, 1073-1082 (2003).
245. Martin A, Gomez-Munoz A, Waggoner DW, Stone JC, Brindley DN: Decreased activities of phosphatidate phosphohydrolase and phospholipase D in Ras and tyrosine kinase (fps) transformed fibroblasts. *J. Biol. Chem.* 268, 23924-23932 (1993).
246. Imai A, Furui T, Tamaya T, Mills GB: A gonadotropin-releasing hormone-responsive phosphatase hydrolyses lysophosphatidic acid within the plasma membrane of ovarian cancer cells. *J Clin Endocrinol Metab* 85, 3370-3375 (2000).
247. Tanyi JL, Hasegawa Y, Lapushin R *et al.*: Role of decreased levels of lipid phosphate phosphatase-1 in accumulation of lysophosphatidic acid in ovarian cancer. *Clin Cancer Res* 9, 3534-3545 (2003).
248. Boucharaba A, Serre CM, Guglielmi J, Bordet JC, Clezardin P, Peyruchaud O: The type 1 lysophosphatidic acid receptor is a target for therapy in bone metastases. *Proc Natl Acad Sci U S A* 103, 9643-9648 (2006).
249. Morris KE, Schang LM, Brindley DN: Lipid phosphate phosphatase-2 activity regulates S-phase entry of the cell cycle in Rat2 fibroblasts. *J. Biol. Chem.* 281, 9297-9306 (2006).
250. Flanagan JM, Funes JM, Henderson S, Wild L, Carey N, Boshoff C: Genomics screen in transformed stem cells reveals RNASEH2A, PPAP2C, and ADARB1 as putative anticancer drug targets. *Mol Cancer Ther* 8, 249-260 (2009).
251. Brindley DN, Lin FT, Tigyi GJ: Role of the autotaxin-lysophosphatidate axis in cancer resistance to chemotherapy and radiotherapy. *Biochim Biophys Acta* 1831, 74-85 (2013).
252. So J, Wang FQ, Navari J, Schreher J, Fishman DA: LPA-induced epithelial ovarian cancer (EOC) in vitro invasion and migration are mediated by VEGF receptor-2 (VEGF-R2). *Gynecol. Oncol.* 97, 870-878 (2005).
253. Murph MM, Hurst-Kennedy J, Newton V, Brindley DN, Radhakrishna H: Lysophosphatidic acid decreases the nuclear localization and cellular abundance of the p53 tumor suppressor in A549 lung carcinoma cells. *Mol Cancer Res* 5, 1201-1211 (2007).
254. Samadi N, Gaetano C, Goping IS, Brindley DN: Autotaxin protects MCF-7 breast cancer and MDA-MB-435 melanoma cells against Taxol-induced apoptosis. *Oncogene* 28, 1028-1039 (2009).
255. Fang X, Schummer M, Mao M *et al.*: Lysophosphatidic acid is a bioactive mediator in ovarian cancer. *Biochim Biophys Acta* 1582, 257-264 (2002).
256. Ye X, Ishii I, Kingsbury MA, Chun J: Lysophosphatidic acid as a novel cell survival/apoptotic factor. *Biochim Biophys Acta* 1585, 108-113 (2002).
257. Samadi N, Bekele RT, Goping IS, Schang LM, Brindley DN: Lysophosphatidate induces chemo-resistance by releasing breast cancer cells from taxol-induced mitotic arrest. *PLoS One* 6, e20608 (2011).
258. Vidot S, Witham J, Agarwal R *et al.*: Autotaxin delays apoptosis induced by carboplatin in ovarian cancer cells. *Cell. Signal.* 22, 926-935 (2010).

259. Venkatraman G, Benesch MG, Tang X, Dewald J, McMullen TP, Brindley DN: Lysophosphatidate signaling stabilizes Nrf2 and increases the expression of genes involved in drug resistance and oxidative stress responses: implications for cancer treatment. *FASEB J* 29, 772-785 (2015).
260. Bekele R, Brindley DN: Role of autotaxin and lysophosphatidate in cancer progression and resistance to chemotherapy and radiotherapy. *Clin Lipidol* 7, 313-328 (2012).
261. Deng W, Shuyu E, Tsukahara R *et al.*: The lysophosphatidic acid type 2 receptor is required for protection against radiation-induced intestinal injury. *Gastroenterology* 132, 1834-1851 (2007).
262. Chun J, Hla T, Lynch KR, Spiegel S, Moolenaar WH: International Union of Basic and Clinical Pharmacology. LXXVIII. Lysophospholipid receptor nomenclature. *Pharmacol. Rev.* 62, 579-587 (2010).
263. Yung YC, Stoddard NC, Chun J: LPA receptor signaling: pharmacology, physiology, and pathophysiology. *J. Lipid Res.* 55, 1192-1214 (2014).
264. Tigyi G, Parrill AL: Molecular mechanisms of lysophosphatidic acid action. *Prog Lipid Res* 42, 498-526 (2003).
265. Radeff-Huang J, Seasholtz TM, Matteo RG, Brown JH: G protein mediated signaling pathways in lysophospholipid induced cell proliferation and survival. *J Cell Biochem* 92, 949-966 (2004).
266. Shida D, Fang X, Kordula T *et al.*: Cross-talk between LPA1 and epidermal growth factor receptors mediates up-regulation of sphingosine kinase 1 to promote gastric cancer cell motility and invasion. *Cancer Res* 68, 6569-6577 (2008).
267. English D, Garcia JG, Brindley DN: Platelet-released phospholipids link haemostasis and angiogenesis. *Cardiovasc Res* 49, 588-599 (2001).
268. Takabe K, Kim RH, Allegood JC *et al.*: Estradiol induces export of sphingosine 1-phosphate from breast cancer cells via ABCC1 and ABCG2. *J Biol Chem* 285, 10477-10486 (2010).
269. Brindley DN, Pilquil C: Lipid phosphate phosphatases and signaling. *J Lipid Res* 50 Suppl, S225-230 (2009).
270. Sukocheva OA, Wang L, Albanese N, Pitson SM, Vadas MA, Xia P: Sphingosine kinase transmits estrogen signaling in human breast cancer cells. *Mol Endocrinol* 17, 2002-2012 (2003).
271. Donoviel MS, Hait NC, Ramachandran S *et al.*: Spinster 2, a sphingosine-1-phosphate transporter, plays a critical role in inflammatory and autoimmune diseases. *FASEB J* 29, 5018-5028 (2015).
272. McDermott M, Wakelam MJ, Morris AJ: Phospholipase D. *Biochem Cell Biol* 82, 225-253 (2004).
273. Bruntz RC, Lindsley CW, Brown HA: Phospholipase D signaling pathways and phosphatidic acid as therapeutic targets in cancer. *Pharmacological reviews* 66, 1033-1079 (2014).
274. Scott SA, Selvy PE, Buck JR *et al.*: Design of isoform-selective phospholipase D inhibitors that modulate cancer cell invasiveness. *Nat Chem Biol* 5, 108-117 (2009).

275. Andreyev AY, Fahy E, Guan Z *et al.*: Subcellular organelle lipidomics in TLR-4-activated macrophages. *J Lipid Res* 51, 2785-2797 (2010).
276. Selvy PE, Lavieri RR, Lindsley CW, Brown HA: Phospholipase D: enzymology, functionality, and chemical modulation. *Chem Rev* 111, 6064-6119 (2011).
277. Ivanisevic R, Milic M, Ajdic D, Rakonjac J, Savic DJ: Nucleotide sequence, mutational analysis, transcriptional start site, and product analysis of nov, the gene which affects Escherichia coli K-12 resistance to the gyrase inhibitor novobiocin. *Journal of bacteriology* 177, 1766-1771 (1995).
278. Pohlman RF, Liu F, Wang L, More MI, Winans SC: Genetic and biochemical analysis of an endonuclease encoded by the IncN plasmid pKM101. *Nucleic acids research* 21, 4867-4872 (1993).
279. Schofield JN, Rademacher TW: Structure and expression of the human glycosylphosphatidylinositol phospholipase D1 (GPLD1) gene. *Biochim Biophys Acta* 1494, 189-194 (2000).
280. Wang X, Xu L, Zheng L: Cloning and expression of phosphatidylcholine-hydrolyzing phospholipase D from Ricinus communis L. *J Biol Chem* 269, 20312-20317 (1994).
281. Hammond SM, Altshuller YM, Sung TC *et al.*: Human ADP-ribosylation factor-activated phosphatidylcholine-specific phospholipase D defines a new and highly conserved gene family. *J Biol Chem* 270, 29640-29643 (1995).
282. Lopez I, Arnold RS, Lambeth JD: Cloning and initial characterization of a human phospholipase D2 (hPLD2). ADP-ribosylation factor regulates hPLD2. *J Biol Chem* 273, 12846-12852 (1998).
283. Colley WC, Sung TC, Roll R *et al.*: Phospholipase D2, a distinct phospholipase D isoform with novel regulatory properties that provokes cytoskeletal reorganization. *Curr Biol* 7, 191-201 (1997).
284. Rudolph AE, Stuckey JA, Zhao Y *et al.*: Expression, characterization, and mutagenesis of the Yersinia pestis murine toxin, a phospholipase D superfamily member. *J Biol Chem* 274, 11824-11831 (1999).
285. Stuckey JA, Dixon JE: Crystal structure of a phospholipase D family member. *Nature structural biology* 6, 278-284 (1999).
286. Steed PM, Clark KL, Boyar WC, Lasala DJ: Characterization of human PLD2 and the analysis of PLD isoform splice variants. *FASEB J* 12, 1309-1317 (1998).
287. Sung TC, Zhang Y, Morris AJ, Frohman MA: Structural analysis of human phospholipase D1. *J Biol Chem* 274, 3659-3666 (1999).
288. Stahelin RV, Ananthanarayanan B, Blatner NR *et al.*: Mechanism of membrane binding of the phospholipase D1 PX domain. *J Biol Chem* 279, 54918-54926 (2004).
289. Lee JS, Kim JH, Jang IH *et al.*: Phosphatidylinositol (3,4,5)-trisphosphate specifically interacts with the phox homology domain of phospholipase D1 and stimulates its activity. *J Cell Sci* 118, 4405-4413 (2005).
290. Cantley LC: The phosphoinositide 3-kinase pathway. *Science* 296, 1655-1657 (2002).

291. Standaert ML, Avignon A, Yamada K, Bandyopadhyay G, Farese RV: The phosphatidylinositol 3-kinase inhibitor, wortmannin, inhibits insulin-induced activation of phosphatidylcholine hydrolysis and associated protein kinase C translocation in rat adipocytes. *Biochem J* 313 (Pt 3), 1039-1046 (1996).
292. Lemmon MA: Membrane recognition by phospholipid-binding domains. *Nat Rev Mol Cell Biol* 9, 99-111 (2008).
293. Sciorra VA, Rudge SA, Wang J, McLaughlin S, Engebrecht J, Morris AJ: Dual role for phosphoinositides in regulation of yeast and mammalian phospholipase D enzymes. *J Cell Biol* 159, 1039-1049 (2002).
294. Freyberg Z, Sweeney D, Siddhanta A, Bourgoin S, Frohman M, Shields D: Intracellular localization of phospholipase D1 in mammalian cells. *Mol Biol Cell* 12, 943-955 (2001).
295. Du G, Altshuller YM, Vitale N *et al.*: Regulation of phospholipase D1 subcellular cycling through coordination of multiple membrane association motifs. *J Cell Biol* 162, 305-315 (2003).
296. Du G, Huang P, Liang BT, Frohman MA: Phospholipase D2 localizes to the plasma membrane and regulates angiotensin II receptor endocytosis. *Mol Biol Cell* 15, 1024-1030 (2004).
297. Kim Y, Kim JE, Lee SD *et al.*: Phospholipase D1 is located and activated by protein kinase C alpha in the plasma membrane in 3Y1 fibroblast cell. *Biochim Biophys Acta* 1436, 319-330 (1999).
298. Sciorra VA, Rudge SA, Prestwich GD, Frohman MA, Engebrecht J, Morris AJ: Identification of a phosphoinositide binding motif that mediates activation of mammalian and yeast phospholipase D isoenzymes. *EMBO J* 18, 5911-5921 (1999).
299. Zheng L, Shan J, Krishnamoorthi R, Wang X: Activation of plant phospholipase Dbeta by phosphatidylinositol 4,5-bisphosphate: characterization of binding site and mode of action. *Biochemistry* 41, 4546-4553 (2002).
300. Moss J, Vaughan M: ADP-ribosylation factors, 20,000 M(r) guanine nucleotide-binding protein activators of cholera toxin and components of intracellular vesicular transport systems. *Cell Signal* 5, 367-379 (1993).
301. Hammond SM, Jenco JM, Nakashima S *et al.*: Characterization of two alternately spliced forms of phospholipase D1. Activation of the purified enzymes by phosphatidylinositol 4,5-bisphosphate, ADP-ribosylation factor, and Rho family monomeric GTP-binding proteins and protein kinase C-alpha. *J Biol Chem* 272, 3860-3868 (1997).
302. Caumont AS, Galas MC, Vitale N, Aunis D, Bader MF: Regulated exocytosis in chromaffin cells. Translocation of ARF6 stimulates a plasma membrane-associated phospholipase D. *J Biol Chem* 273, 1373-1379 (1998).
303. Kim SW, Hayashi M, Lo JF, Yang Y, Yoo JS, Lee JD: ADP-ribosylation factor 4 small GTPase mediates epidermal growth factor receptor-dependent phospholipase D2 activation. *J Biol Chem* 278, 2661-2668 (2003).

304. Honda A, Nogami M, Yokozeki T *et al.*: Phosphatidylinositol 4-phosphate 5-kinase alpha is a downstream effector of the small G protein ARF6 in membrane ruffle formation. *Cell* 99, 521-532 (1999).
305. Henage LG, Exton JH, Brown HA: Kinetic analysis of a mammalian phospholipase D: allosteric modulation by monomeric GTPases, protein kinase C, and polyphosphoinositides. *J Biol Chem* 281, 3408-3417 (2006).
306. Cai S, Exton JH: Determination of interaction sites of phospholipase D1 for RhoA. *Biochem J* 355, 779-785 (2001).
307. Jiang H, Luo JQ, Urano T *et al.*: Involvement of Ral GTPase in v-Src-induced phospholipase D activation. *Nature* 378, 409-412 (1995).
308. Kim L, Wong TW: Growth factor-dependent phosphorylation of the actin-binding protein cortactin is mediated by the cytoplasmic tyrosine kinase FER. *J Biol Chem* 273, 23542-23548 (1998).
309. Chen JS, Exton JH: Sites on phospholipase D2 phosphorylated by PKCalpha. *Biochem Biophys Res Commun* 333, 1322-1326 (2005).
310. Wu F, Wang P, Zhang J, Young LC, Lai R, Li L: Studies of phosphoproteomic changes induced by nucleophosmin-anaplastic lymphoma kinase (ALK) highlight deregulation of tumor necrosis factor (TNF)/Fas/TNF-related apoptosis-induced ligand signaling pathway in ALK-positive anaplastic large cell lymphoma. *Molecular & cellular proteomics : MCP* 9, 1616-1632 (2010).
311. Conricode KM, Brewer KA, Exton JH: Activation of phospholipase D by protein kinase C. Evidence for a phosphorylation-independent mechanism. *J Biol Chem* 267, 7199-7202 (1992).
312. Lopez I, Burns DJ, Lambeth JD: Regulation of phospholipase D by protein kinase C in human neutrophils. Conventional isoforms of protein kinase C phosphorylate a phospholipase D-related component in the plasma membrane. *J Biol Chem* 270, 19465-19472 (1995).
313. Han JM, Kim JH, Lee BD *et al.*: Phosphorylation-dependent regulation of phospholipase D2 by protein kinase C delta in rat Pheochromocytoma PC12 cells. *J Biol Chem* 277, 8290-8297 (2002).
314. Di Fulvio M, Lehman N, Lin X, Lopez I, Gomez-Cambronero J: The elucidation of novel SH2 binding sites on PLD2. *Oncogene* 25, 3032-3040 (2006).
315. Chardin P, Camonis JH, Gale NW *et al.*: Human Sos1: a guanine nucleotide exchange factor for Ras that binds to GRB2. *Science* 260, 1338-1343 (1993).
316. Simon MA, Bowtell DD, Dodson GS, Laverty TR, Rubin GM: Ras1 and a putative guanine nucleotide exchange factor perform crucial steps in signaling by the sevenless protein tyrosine kinase. *Cell* 67, 701-716 (1991).
317. Chen Y, Rodrik V, Foster DA: Alternative phospholipase D/mTOR survival signal in human breast cancer cells. *Oncogene* 24, 672-679 (2005).
318. Delon C, Manifava M, Wood E *et al.*: Sphingosine kinase 1 is an intracellular effector of phosphatidic acid. *J Biol Chem* 279, 44763-44774 (2004).

319. Ghosh S, Strum JC, Sciorra VA, Daniel L, Bell RM: Raf-1 kinase possesses distinct binding domains for phosphatidylserine and phosphatidic acid. Phosphatidic acid regulates the translocation of Raf-1 in 12-O-tetradecanoylphorbol-13-acetate-stimulated Madin-Darby canine kidney cells. *J Biol Chem* 271, 8472-8480 (1996).
320. Zhao C, Du G, Skowronek K, Frohman MA, Bar-Sagi D: Phospholipase D2-generated phosphatidic acid couples EGFR stimulation to Ras activation by Sos. *Nature cell biology* 9, 706-712 (2007).
321. Bruntz RC, Taylor HE, Lindsley CW, Brown HA: Phospholipase D2 mediates survival signaling through direct regulation of Akt in glioblastoma cells. *J Biol Chem* 289, 600-616 (2014).
322. Hanahan D, Weinberg RA: Hallmarks of cancer: the next generation. *Cell* 144, 646-674 (2011).
323. Song JG, Pfeffer LM, Foster DA: v-Src increases diacylglycerol levels via a type D phospholipase-mediated hydrolysis of phosphatidylcholine. *Mol Cell Biol* 11, 4903-4908 (1991).
324. Carnero A, Cuadrado A, del Peso L, Lacal JC: Activation of type D phospholipase by serum stimulation and ras-induced transformation in NIH3T3 cells. *Oncogene* 9, 1387-1395 (1994).
325. Frankel P, Ramos M, Flom J *et al.*: Ral and Rho-dependent activation of phospholipase D in v-Raf-transformed cells. *Biochem Biophys Res Commun* 255, 502-507 (1999).
326. Zhong M, Shen Y, Zheng Y, Joseph T, Jackson D, Foster DA: Phospholipase D prevents apoptosis in v-Src-transformed rat fibroblasts and MDA-MB-231 breast cancer cells. *Biochem Biophys Res Commun* 302, 615-619 (2003).
327. Uchida N, Okamura S, Nagamachi Y, Yamashita S: Increased phospholipase D activity in human breast cancer. *J Cancer Res Clin Oncol* 123, 280-285 (1997).
328. Noh DY, Ahn SJ, Lee RA *et al.*: Overexpression of phospholipase D1 in human breast cancer tissues. *Cancer Lett* 161, 207-214 (2000).
329. Imamura F, Horai T, Mukai M, Shinkai K, Sawada M, Akedo H: Induction of in vitro tumor cell invasion of cellular monolayers by lysophosphatidic acid or phospholipase D. *Biochem Biophys Res Commun* 193, 497-503 (1993).
330. Pilquil C, Dewald J, Cherney A *et al.*: Lipid phosphate phosphatase-1 regulates lysophosphatidate-induced fibroblast migration by controlling phospholipase D2-dependent phosphatidate generation. *J Biol Chem* 281, 38418-38429 (2006).
331. Gorshkova I, He D, Berdyshev E *et al.*: Protein kinase C-epsilon regulates sphingosine 1-phosphate-mediated migration of human lung endothelial cells through activation of phospholipase D2, protein kinase C-zeta, and Rac1. *J Biol Chem* 283, 11794-11806 (2008).
332. Heasman SJ, Ridley AJ: Mammalian Rho GTPases: new insights into their functions from in vivo studies. *Nat Rev Mol Cell Biol* 9, 690-701 (2008).

333. Matsuzaki T, Hanai S, Kishi H *et al.*: Regulation of endocytosis of activin type II receptors by a novel PDZ protein through Ral/Ral-binding protein 1-dependent pathway. *J Biol Chem* 277, 19008-19018 (2002).
334. Nakashima S, Morinaka K, Koyama S *et al.*: Small G protein Ral and its downstream molecules regulate endocytosis of EGF and insulin receptors. *EMBO J* 18, 3629-3642 (1999).
335. Awasthi S, Singhal SS, Sharma R, Zimniak P, Awasthi YC: Transport of glutathione conjugates and chemotherapeutic drugs by RLIP76 (RALBP1): a novel link between G-protein and tyrosine kinase signaling and drug resistance. *Int J Cancer* 106, 635-646 (2003).
336. Awasthi YC, Misra G, Rassin DK, Srivastava SK: Detoxification of xenobiotics by glutathione S-transferases in erythrocytes: the transport of the conjugate of glutathione and 1-chloro-2,4-dinitrobenzene. *Br J Haematol* 55, 419-425 (1983).
337. LaBelle EF, Singh SV, Srivastava SK, Awasthi YC: Dinitrophenyl glutathione efflux from human erythrocytes is primary active ATP-dependent transport. *Biochem J* 238, 443-449 (1986).
338. Sharma R, Gupta S, Singh SV *et al.*: Purification and characterization of dinitrophenylglutathione ATPase of human erythrocytes and its expression in other tissues. *Biochem Biophys Res Commun* 171, 155-161 (1990).
339. Awasthi S, Singhal SS, Srivastava SK *et al.*: Adenosine triphosphate-dependent transport of doxorubicin, daunomycin, and vinblastine in human tissues by a mechanism distinct from the P-glycoprotein. *J Clin Invest* 93, 958-965 (1994).
340. Awasthi S, Cheng J, Singhal SS *et al.*: Novel function of human RLIP76: ATP-dependent transport of glutathione conjugates and doxorubicin. *Biochemistry* 39, 9327-9334 (2000).
341. Paul EC, Quaroni A: Identification of a 102 kDa protein (cytocentrin) immunologically related to keratin 19, which is a cytoplasmically derived component of the mitotic spindle pole. *J Cell Sci* 106 (Pt 3), 967-981 (1993).
342. Quaroni A, Paul EC: Cytocentrin is a Ral-binding protein involved in the assembly and function of the mitotic apparatus. *J Cell Sci* 112 (Pt 5), 707-718 (1999).
343. Cantor SB, Urano T, Feig LA: Identification and characterization of Ral-binding protein 1, a potential downstream target of Ral GTPases. *Mol Cell Biol* 15, 4578-4584 (1995).
344. Park SH, Weinberg RA: A putative effector of Ral has homology to Rho/Rac GTPase activating proteins. *Oncogene* 11, 2349-2355 (1995).
345. Yamaguchi A, Urano T, Goi T, Feig LA: An Eps homology (EH) domain protein that binds to the Ral-GTPase target, RalBP1. *J Biol Chem* 272, 31230-31234 (1997).
346. Ikeda M, Ishida O, Hinoi T, Kishida S, Kikuchi A: Identification and characterization of a novel protein interacting with Ral-binding protein 1, a putative effector protein of Ral. *J Biol Chem* 273, 814-821 (1998).

347. Hu Y, Mivechi NF: HSF-1 interacts with Ral-binding protein 1 in a stress-responsive, multiprotein complex with HSP90 in vivo. *J Biol Chem* 278, 17299-17306 (2003).
348. Albright CF, Giddings BW, Liu J, Vito M, Weinberg RA: Characterization of a guanine nucleotide dissociation stimulator for a ras-related GTPase. *EMBO J* 12, 339-347 (1993).
349. Kikuchi A, Demo SD, Ye ZH, Chen YW, Williams LT: ralGDS family members interact with the effector loop of ras p21. *Mol Cell Biol* 14, 7483-7491 (1994).
350. Urano T, Emkey R, Feig LA: Ral-GTPases mediate a distinct downstream signaling pathway from Ras that facilitates cellular transformation. *EMBO J* 15, 810-816 (1996).
351. Jullien-Flores V, Dorseuil O, Romero F *et al.*: Bridging Ral GTPase to Rho pathways. RLIP76, a Ral effector with CDC42/Rac GTPase-activating protein activity. *J Biol Chem* 270, 22473-22477 (1995).
352. Diekmann D, Brill S, Garrett MD *et al.*: Bcr encodes a GTPase-activating protein for p21rac. *Nature* 351, 400-402 (1991).
353. Minden A, Lin A, Claret FX, Abo A, Karin M: Selective activation of the JNK signaling cascade and c-Jun transcriptional activity by the small GTPases Rac and Cdc42Hs. *Cell* 81, 1147-1157 (1995).
354. Cheng JZ, Sharma R, Yang Y *et al.*: Accelerated metabolism and exclusion of 4-hydroxynonenal through induction of RLIP76 and hGST5.8 is an early adaptive response of cells to heat and oxidative stress. *J Biol Chem* 276, 41213-41223 (2001).
355. Bos JL: ras oncogenes in human cancer: a review. *Cancer Res* 49, 4682-4689 (1989).
356. Wang XJ, Hayes JD, Wolf CR: Generation of a stable antioxidant response element-driven reporter gene cell line and its use to show redox-dependent activation of nrf2 by cancer chemotherapeutic agents. *Cancer Res* 66, 10983-10994 (2006).
357. Robinson SP, Langan-Fahey SM, Johnson DA, Jordan VC: Metabolites, pharmacodynamics, and pharmacokinetics of tamoxifen in rats and mice compared to the breast cancer patient. *Drug Metab Dispos* 19, 36-43 (1991).
358. Kisanga ER, Gjerde J, Guerrieri-Gonzaga A *et al.*: Tamoxifen and metabolite concentrations in serum and breast cancer tissue during three dose regimens in a randomized preoperative trial. *Clin Cancer Res* 10, 2336-2343 (2004).
359. Fromson JM, Pearson S, Bramah S: The metabolism of tamoxifen (I.C.I. 46,474). II. In female patients. *Xenobiotica* 3, 711-714 (1973).
360. Schreier SM, Muellner MK, Steinkellner H *et al.*: Hydrogen sulfide scavenges the cytotoxic lipid oxidation product 4-HNE. *Neurotoxicity research* 17, 249-256 (2010).
361. Nicholson DW, Ali A, Thornberry NA *et al.*: Identification and inhibition of the ICE/CED-3 protease necessary for mammalian apoptosis. *Nature* 376, 37-43 (1995).

362. Westwick JK, Bielawska AE, Dbaibo G, Hannun YA, Brenner DA: Ceramide activates the stress-activated protein kinases. *J Biol Chem* 270, 22689-22692 (1995).
363. Hetz CA, Hunn M, Rojas P, Torres V, Leyton L, Quest AF: Caspase-dependent initiation of apoptosis and necrosis by the Fas receptor in lymphoid cells: onset of necrosis is associated with delayed ceramide increase. *J Cell Sci* 115, 4671-4683 (2002).
364. Parra V, Eisner V, Chiong M *et al.*: Changes in mitochondrial dynamics during ceramide-induced cardiomyocyte early apoptosis. *Cardiovasc Res* 77, 387-397 (2008).
365. Gomez-Munoz A, Waggoner DW, O'Brien L, Brindley DN: Interaction of ceramides, sphingosine, and sphingosine 1-phosphate in regulating DNA synthesis and phospholipase D activity. *J Biol Chem* 270, 26318-26325 (1995).
366. Nishitoh H, Saitoh M, Mochida Y *et al.*: ASK1 is essential for JNK/SAPK activation by TRAF2. *Mol Cell* 2, 389-395 (1998).
367. Johnson JA, Johnson DA, Kraft AD *et al.*: The Nrf2-ARE pathway: an indicator and modulator of oxidative stress in neurodegeneration. *Ann N Y Acad Sci* 1147, 61-69 (2008).
368. Venugopal R, Jaiswal AK: Nrf1 and Nrf2 positively and c-Fos and Fra1 negatively regulate the human antioxidant response element-mediated expression of NAD(P)H:quinone oxidoreductase1 gene. *Proc Natl Acad Sci U S A* 93, 14960-14965 (1996).
369. Liu RZ, Graham K, Glubrecht DD, Germain DR, Mackey JR, Godbout R: Association of FABP5 expression with poor survival in triple-negative breast cancer: implication for retinoic acid therapy. *Am J Pathol* 178, 997-1008 (2011).
370. Taher MM, Mahgoub MA, Abd-Elfattah AS: Redox regulation of signal transduction in vascular smooth muscle cells: thiol oxidizing agents induced phospholipase D. *Biochemistry and molecular biology international* 46, 619-628 (1998).
371. Natarajan V, Vepa S, Verma RS, Scribner WM: Role of protein tyrosine phosphorylation in H2O2-induced activation of endothelial cell phospholipase D. *Am J Physiol* 271, L400-408 (1996).
372. den Hertog J, Groen A, van der Wijk T: Redox regulation of protein-tyrosine phosphatases. *Archives of biochemistry and biophysics* 434, 11-15 (2005).
373. Garcia-Morales P, Minami Y, Luong E, Klausner RD, Samelson LE: Tyrosine phosphorylation in T cells is regulated by phosphatase activity: studies with phenylarsine oxide. *Proc Natl Acad Sci U S A* 87, 9255-9259 (1990).
374. Sullivan SG, Chiu DT, Errasfa M, Wang JM, Qi JS, Stern A: Effects of H2O2 on protein tyrosine phosphatase activity in HER14 cells. *Free Radic Biol Med* 16, 399-403 (1994).
375. Hadari YR, Geiger B, Nadiv O *et al.*: Hepatic tyrosine-phosphorylated proteins identified and localized following in vivo inhibition of protein

tyrosine phosphatases: effects of H2O2 and vanadate administration into rat livers. *Mol Cell Endocrinol* 97, 9-17 (1993).
376. Meerson FZ, Kagan VE, Kozlov Yu P, Belkina LM, Arkhipenko Yu V: The role of lipid peroxidation in pathogenesis of ischemic damage and the antioxidant protection of the heart. *Basic research in cardiology* 77, 465-485 (1982).
377. Natarajan V, Scribner WM, Taher MM: 4-Hydroxynonenal, a metabolite of lipid peroxidation, activates phospholipase D in vascular endothelial cells. *Free Radic Biol Med* 15, 365-375 (1993).
378. Tappia PS, Dent MR, Dhalla NS: Oxidative stress and redox regulation of phospholipase D in myocardial disease. *Free Radic Biol Med* 41, 349-361 (2006).
379. Chen Y, Zheng Y, Foster DA: Phospholipase D confers rapamycin resistance in human breast cancer cells. *Oncogene* 22, 3937-3942 (2003).
380. Cho JH, Hong SK, Kim EY *et al.*: Overexpression of phospholipase D suppresses taxotere-induced cell death in stomach cancer cells. *Biochim Biophys Acta* 1783, 912-923 (2008).
381. Henkels KM, Boivin GP, Dudley ES, Berberich SJ, Gomez-Cambronero J: Phospholipase D (PLD) drives cell invasion, tumor growth and metastasis in a human breast cancer xenograph model. *Oncogene* 32, 5551-5562 (2013).
382. Riebeling C, Muller C, Geilen CC: Expression and regulation of phospholipase D isoenzymes in human melanoma cells and primary melanocytes. *Melanoma research* 13, 555-562 (2003).
383. Yamada Y, Hamajima N, Kato T *et al.*: Association of a polymorphism of the phospholipase D2 gene with the prevalence of colorectal cancer. *Journal of molecular medicine* 81, 126-131 (2003).
384. Zhao Y, Ehara H, Akao Y *et al.*: Increased activity and intranuclear expression of phospholipase D2 in human renal cancer. *Biochem Biophys Res Commun* 278, 140-143 (2000).
385. Shi M, Zheng Y, Garcia A, Xu L, Foster DA: Phospholipase D provides a survival signal in human cancer cells with activated H-Ras or K-Ras. *Cancer Lett* 258, 268-275 (2007).
386. Awasthi S, Singhal SS, Pandya U *et al.*: ATP-Dependent colchicine transport by human erythrocyte glutathione conjugate transporter. *Toxicol Appl Pharmacol* 155, 215-226 (1999).
387. Armstrong JS, Steinauer KK, Hornung B *et al.*: Role of glutathione depletion and reactive oxygen species generation in apoptotic signaling in a human B lymphoma cell line. *Cell Death Differ* 9, 252-263 (2002).
388. Awasthi S, Singhal SS, Awasthi YC *et al.*: RLIP76 and Cancer. *Clin Cancer Res* 14, 4372-4377 (2008).
389. Renes J, de Vries EE, Hooiveld GJ, Krikken I, Jansen PL, Muller M: Multidrug resistance protein MRP1 protects against the toxicity of the major lipid peroxidation product 4-hydroxynonenal. *Biochem J* 350 Pt 2, 555-561 (2000).

390. Benesch MG, Tang X, Dewald J *et al.*: Tumor-induced inflammation in mammary adipose tissue stimulates a vicious cycle of autotaxin expression and breast cancer progression. *FASEB J* 29, 3990-4000 (2015).
391. Bennani-Baiti B, Toegel S, Viernstein H, Urban E, Noe CR, Bennani-Baiti IM: Inflammation Modulates RLIP76/RALBP1 Electrophile-Glutathione Conjugate Transporter and Housekeeping Genes in Human Blood-Brain Barrier Endothelial Cells. *PLoS One* 10, e0139101 (2015).
392. Ye Q, Bodell WJ: Production of 8-hydroxy-2'-deoxguanosine in DNA by microsomal activation of tamoxifen and 4-hydroxytamoxifen. *Carcinogenesis* 17, 1747-1750 (1996).
393. Schiff R, Reddy P, Ahotupa M *et al.*: Oxidative stress and AP-1 activity in tamoxifen-resistant breast tumors in vivo. *J Natl Cancer Inst* 92, 1926-1934 (2000).
394. Lee YS, Kang YS, Lee SH, Kim JA: Role of NAD(P)H oxidase in the tamoxifen-induced generation of reactive oxygen species and apoptosis in HepG2 human hepatoblastoma cells. *Cell Death Differ* 7, 925-932 (2000).
395. Kim SK, Yang JW, Kim MR *et al.*: Increased expression of Nrf2/ARE-dependent anti-oxidant proteins in tamoxifen-resistant breast cancer cells. *Free Radic Biol Med* 45, 537-546 (2008).
396. Mandlekar S, Yu R, Tan TH, Kong AN: Activation of caspase-3 and c-Jun NH2-terminal kinase-1 signaling pathways in tamoxifen-induced apoptosis of human breast cancer cells. *Cancer Res* 60, 5995-6000 (2000).
397. Ferlini C, Scambia G, Marone M *et al.*: Tamoxifen induces oxidative stress and apoptosis in oestrogen receptor-negative human cancer cell lines. *Br J Cancer* 79, 257-263 (1999).
398. Katzenellenbogen BS, Miller MA, Mullick A, Sheen YY: Antiestrogen action in breast cancer cells: modulation of proliferation and protein synthesis, and interaction with estrogen receptors and additional antiestrogen binding sites. *Breast Cancer Res Treat* 5, 231-243 (1985).
399. Santana P, Pena LA, Haimovitz-Friedman A *et al.*: Acid sphingomyelinase-deficient human lymphoblasts and mice are defective in radiation-induced apoptosis. *Cell* 86, 189-199 (1996).
400. Zhang Y, Mattjus P, Schmid PC *et al.*: Involvement of the acid sphingomyelinase pathway in uva-induced apoptosis. *J Biol Chem* 276, 11775-11782 (2001).
401. Liu B, Hannun YA: Inhibition of the neutral magnesium-dependent sphingomyelinase by glutathione. *J Biol Chem* 272, 16281-16287 (1997).
402. Yang Y, Zhao S, Song J: Caspase-dependent apoptosis and -independent poly(ADP-ribose) polymerase cleavage induced by transforming growth factor beta1. *Int J Biochem Cell Biol* 36, 223-234 (2004).
403. Janicke RU, Sprengart ML, Wati MR, Porter AG: Caspase-3 is required for DNA fragmentation and morphological changes associated with apoptosis. *J Biol Chem* 273, 9357-9360 (1998).
404. Liu W, Akhand AA, Takeda K *et al.*: Protein phosphatase 2A-linked and -unlinked caspase-dependent pathways for downregulation of Akt kinase triggered by 4-hydroxynonenal. *Cell Death Differ* 10, 772-781 (2003).

405. Shibata T, Kokubu A, Gotoh M *et al.*: Genetic alteration of Keap1 confers constitutive Nrf2 activation and resistance to chemotherapy in gallbladder cancer. *Gastroenterology* 135, 1358-1368, 1368 e1351-1354 (2008).
406. Singh A, Boldin-Adamsky S, Thimmulappa RK *et al.*: RNAi-mediated silencing of nuclear factor erythroid-2-related factor 2 gene expression in non-small cell lung cancer inhibits tumor growth and increases efficacy of chemotherapy. *Cancer Res* 68, 7975-7984 (2008).
407. Zhang P, Singh A, Yegnasubramanian S *et al.*: Loss of Kelch-like ECH-associated protein 1 function in prostate cancer cells causes chemoresistance and radioresistance and promotes tumor growth. *Mol Cancer Ther* 9, 336-346 (2010).
408. Choi HK, Yang JW, Roh SH, Han CY, Kang KW: Induction of multidrug resistance associated protein 2 in tamoxifen-resistant breast cancer cells. *Endocr Relat Cancer* 14, 293-303 (2007).
409. Kiyotani K, Mushiroda T, Imamura CK *et al.*: Significant effect of polymorphisms in CYP2D6 and ABCC2 on clinical outcomes of adjuvant tamoxifen therapy for breast cancer patients. *J Clin Oncol* 28, 1287-1293 (2010).
410. Kunicka T, Vaclavikova R, Hlavac V *et al.*: Non-coding polymorphisms in nucleotide binding domain 1 in ABCC1 gene associate with transcript level and survival of patients with breast cancer. *PLoS One* 9, e101740 (2014).
411. Callaghan R, Higgins CF: Interaction of tamoxifen with the multidrug resistance P-glycoprotein. *Br J Cancer* 71, 294-299 (1995).
412. Beguerie JR, Xingzhong J, Valdez RP: Tamoxifen vs. non-tamoxifen treatment for advanced melanoma: a meta-analysis. *International Journal of Dermatology* 49, 1194-1202 (2010).
413. Sareddy GR, Nair BC, Gonugunta VK *et al.*: Therapeutic significance of estrogen receptor beta agonists in gliomas. *Mol Cancer Ther* 11, 1174-1182 (2012).
414. Montano MM, Jaiswal AK, Katzenellenbogen BS: Transcriptional regulation of the human quinone reductase gene by antiestrogen-liganded estrogen receptor-alpha and estrogen receptor-beta. *J Biol Chem* 273, 25443-25449 (1998).
415. Okabe K, Hayashi M, Kato K *et al.*: Lysophosphatidic acid receptor-3 increases tumorigenicity and aggressiveness of rat hepatoma RH7777 cells. *Molecular carcinogenesis* 52, 247-254 (2013).
416. Goldshmit Y, Matteo R, Sztal T *et al.*: Blockage of lysophosphatidic acid signaling improves spinal cord injury outcomes. *Am J Pathol* 181, 978-992 (2012).
417. Ren D, Villeneuve NF, Jiang T *et al.*: Brusatol enhances the efficacy of chemotherapy by inhibiting the Nrf2-mediated defense mechanism. *Proc Natl Acad Sci U S A* 108, 1433-1438 (2011).
418. Arlt A, Sebens S, Krebs S *et al.*: Inhibition of the Nrf2 transcription factor by the alkaloid trigonelline renders pancreatic cancer cells more

susceptible to apoptosis through decreased proteasomal gene expression and proteasome activity. *Oncogene* 32, 4825-4835 (2013).
419. Tang X, Wang H, Fan L *et al.*: Luteolin inhibits Nrf2 leading to negative regulation of the Nrf2/ARE pathway and sensitization of human lung carcinoma A549 cells to therapeutic drugs. *Free Radic Biol Med* 50, 1599-1609 (2011).
420. Gottesman MM: Mechanisms of cancer drug resistance. *Annual review of medicine* 53, 615-627 (2002).
421. Cabot MC, Zhang Z, Cao H *et al.*: Tamoxifen activates cellular phospholipase C and D and elicits protein kinase C translocation. *Int J Cancer* 70, 567-574 (1997).
422. Kiss Z: Tamoxifen stimulates phospholipase D activity by an estrogen receptor-independent mechanism. *FEBS Lett* 355, 173-177 (1994).
423. Gopalakrishna R, Jaken S: Protein kinase C signaling and oxidative stress. *Free Radic Biol Med* 28, 1349-1361 (2000).
424. Kazanietz MG, Wang S, Milne GW, Lewin NE, Liu HL, Blumberg PM: Residues in the second cysteine-rich region of protein kinase C delta relevant to phorbol ester binding as revealed by site-directed mutagenesis. *J Biol Chem* 270, 21852-21859 (1995).
425. Gozgit JM, Pentecost BT, Marconi SA, Ricketts-Loriaux RS, Otis CN, Arcaro KF: PLD1 is overexpressed in an ER-negative MCF-7 cell line variant and a subset of phospho-Akt-negative breast carcinomas. *Br J Cancer* 97, 809-817 (2007).
426. Goldfinger LE, Ptak C, Jeffery ED, Shabanowitz J, Hunt DF, Ginsberg MH: RLIP76 (RalBP1) is an R-Ras effector that mediates adhesion-dependent Rac activation and cell migration. *J Cell Biol* 174, 877-888 (2006).
427. Brown HA, Gutowski S, Moomaw CR, Slaughter C, Sternweis PC: ADP-ribosylation factor, a small GTP-dependent regulatory protein, stimulates phospholipase D activity. *Cell* 75, 1137-1144 (1993).
428. Cockcroft S, Thomas GM, Fensome A *et al.*: Phospholipase D: a downstream effector of ARF in granulocytes. *Science* 263, 523-526 (1994).
429. Schutze S, Wiegmann K, Machleidt T, Kronke M: TNF-induced activation of NF-kappa B. *Immunobiology* 193, 193-203 (1995).
430. Baeuerle PA, Henkel T: Function and activation of NF-kappa B in the immune system. *Annual review of immunology* 12, 141-179 (1994).
431. Sehrawat A, Yadav S, Awasthi YC, Basu A, Warden C, Awasthi S: P300 regulates the human RLIP76 promoter activity and gene expression. *Biochem Pharmacol* 85, 1203-1211 (2013).
432. Singhal SS, Singhal J, Yadav S *et al.*: Regression of lung and colon cancer xenografts by depleting or inhibiting RLIP76 (Ral-binding protein 1). *Cancer Res* 67, 4382-4389 (2007).
433. Singhal SS, Roth C, Leake K, Singhal J, Yadav S, Awasthi S: Regression of prostate cancer xenografts by RLIP76 depletion. *Biochem Pharmacol* 77, 1074-1083 (2009).

434. Singhal SS, Singhal J, Yadav S, Sahu M, Awasthi YC, Awasthi S: RLIP76: a target for kidney cancer therapy. *Cancer Res* 69, 4244-4251 (2009).

7 Appendix

Expression of PLD2 in MCF-7 WT versus MCF-7 TAM-R cells.

As shown from the Western blot (Fig. 7.1), the PLD2 protein expression level is same between MCF-7 WT and MCF-7 TAM-R cells. These results are in agreement with our qRT-PCR result (Fig 4.5), which showed no change in the expression level of PLD2 in these cells.

The PLD2 antibody was a kind gift from Dr. Sylvain Bourgoin (Université Laval, Québec Canada).

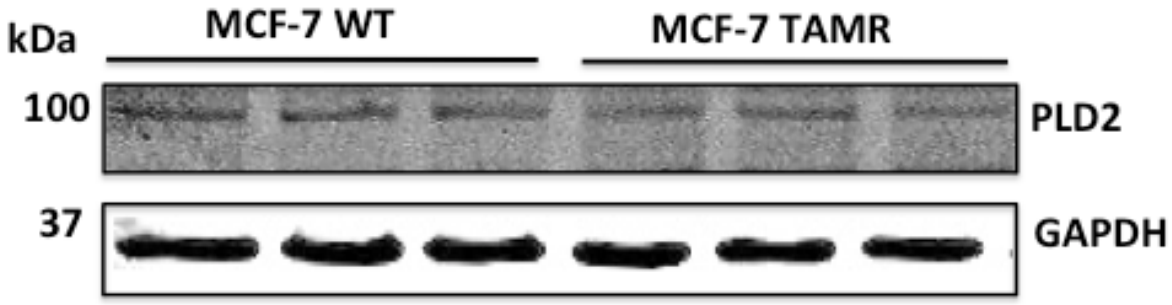

Figure 7.1: Tamoxifen resistant and the corresponding syngeneic wild-type cells have similar PLD2 levels.

Protein lysates from MCF-7 WT and MCF-7 TAM-R cells from n=3 were probed for PLD2 expression.

Time course for the action of PLD by different metabolites.

The time dependent effects of the different metabolites of tamoxifen were measured by treating MCF-7 TAM-R cells with 10 μM concentrations of TAM, 4HT and NTAM for time period of 6-60 min.

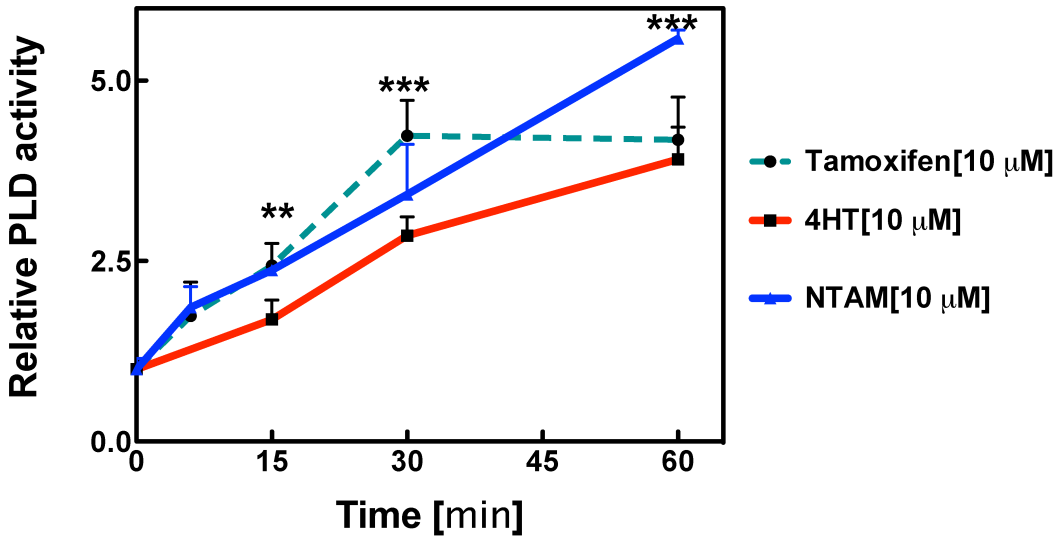

Figure 7.2: Activation of PLD at different time points by tamoxifen and metabolites.

Results are means ± SEM from for n=3 experiments. Significant differences were indicated with **= p<0.01 and ***= p<0.001.

The results show TAM activated PLD more rapidly than 4HT with maximal activation of PLD for TAM occurring after 30 min (Fig. 7.2) as opposed to 60 min by 4HT (Fig. 4.7). Moreover, NTAM had the highest PLD activation and did not reach maximal activation at 60 min and so more time course is necessary to find the maximal activation for NTAM. Overall, the result shows that tamoxifen and metabolites had a different kinetics for activating PLD and this may possibly linked to the generation of ROS. Hence, more studies are needed to study this phenomenon.

Expression of RALBP1 by lysophosphatidate.

The Autotaxin inhibitor, ONO-8430506, decreased RALBP1 expression in mouse tumors. Thus, to investigate if treatment of cells with LPA will induce the expression of RALBP1, we treated MCF-7 cells with 5 μM LPA and also with 10 μM of tamoxifen and metabolites as a positive control.

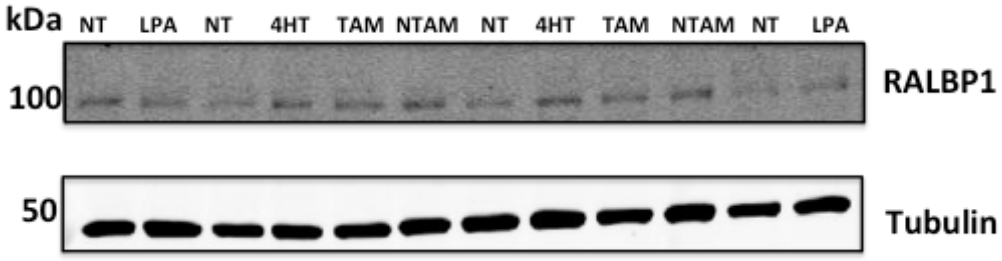

Figure 7.3: RALBP1 expression by lysophosphatidate.

MCF-7 cells were starved for 24 h prior to treatment and treated with 5 μM LPA and 10 μM 4HT, TAM and NTAM for 24 h. Protein lysates were then probed for RALBP1 from n=2 experiments.

Our preliminary results show that LPA does not induce the expression of RALBP1 as much as tamoxifen and metabolites (Fig 7.3). Since LPA could induce the expression of RALBP1 indirectly through the upregulation of TNF-α optimal conditions for such upregulation may be necessary to observe LPA-induced effect in RALBP1. Hence, the experiment needs further optimization using delipidated serum as well as different concentration and time of treatment for LPA. An additional future experiment is also suggested in Section 5.3, future directions, of Chapter 5.

The role of sphingosine-1-phosphate in tamoxifen-induced killing.

The enzyme Sphingosine kinase (SK1/2) phosphorylates sphingosine to sphingosine-1-phosphate (S1P). Moreover, overexpression of SK is observed in many cancers including cells developed to become resistant to tamoxifen [99]. Thus, to investigate the role S1P in tamoxifen-induced killing, MCF-7 cells were treated with 100-1000 nM S1P in the presence of 1-20 μM 4HT and compared relative to no treatment vehicle control.

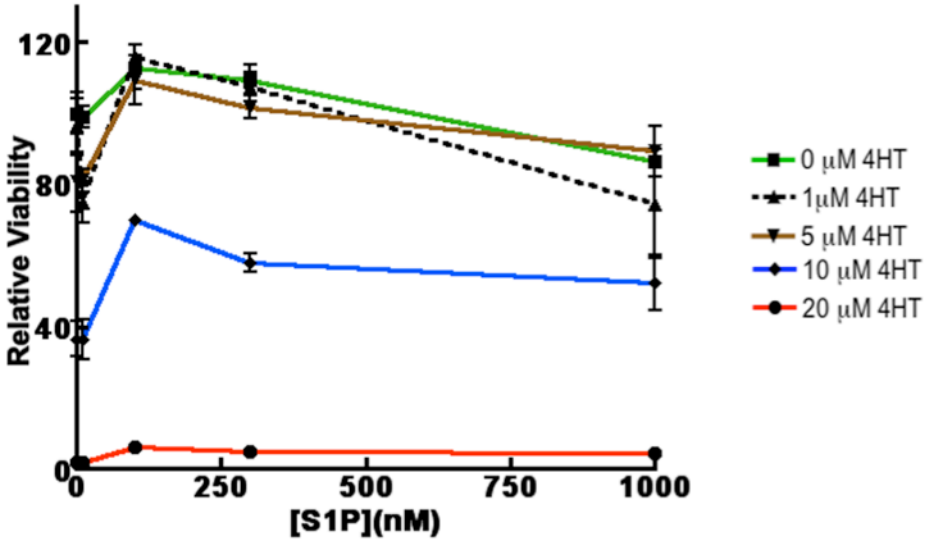

Figure 7.4: sphingosine-1-phosphate rescues cells from tamoxifen-induced killing.

Treatment of MCF-7 cells with 100-1000 nM S1P rescued cells from tamoxifen-induced cell killing. The viability of the cells was measured by MTT assay from for n=2 experiments.

Table 5: Clinical and pathological features of the breast cancer patients in the Breast Cancer Relapsing Early Determinants study.

Factors	Criterion	N	Relative %
ER α	Negative	64	36
	Positive	112	64
PR	Negative	82	47
	Positive	94	53
HER2	Negative	146	83
	Positive	30	17
Age	≤60	127	72
	>60	49	28
Gender	Female	176	100
	Male	0	0
Patient status	Alive	119	68
	Deceased	57	32
Cancer stage	I	75	43
	II-III	101	57
Nuclear grade	Low	44	25
	High	132	75
Mitotic grade	Low	78	44
	High	98	56
Arch grade	Low	29	16
	High	147	84
Overall grade	Low	56	32
	High	120	68

Breast cancer patient cases were selected for high cellularity (70% malignant cells in sample). Abbreviations for Progesterone Receptor: PR and Human Epidermal growth factor Receptor 2: HER2.

Table 6: The chromosomal location and functions of the different human ABC transporters

Symbol	Alias	Location	Function
ABCA1	ABC1	9q31.1	Cholesterol efflux onto HDL
ABCA2	ABC2	9q34	Drug resistance
ABCA3	ABC3	16p13.3	Phosphatidyl choline efflux
ABCA4	ABCR	1p22.1-p21	N-retinylidiene-PE efflux
ABCA5		17q24	
ABCA6		17q24	
ABCA7		19p13.3	
ABCA8		17q24	
ABCA9		17q24	
ABCA10		17q24	
ABCA12		2q34	
ABCA13		7p11-q11	
ABCB1	PGY1, MDR	7p21	Multidrug resistance
ABCB2	TAP1	6p21	Peptide transport
ABCB3	TAP2	6p21	Peptide transport
ABCB4	PGY3	7q21.1	PC transport
ABCB5		7p14	
ABCB6	MTABC3	2q36	Iron transport
ABCB7	ABC7	Xq12-q13	Fe/S cluster transport
ABCB8	MABC1	7q36	
ABCB9		12q24	
ABCB10	MTABC2	1q42	
ABCB11	SPGP	2q24	Bile salt transport
ABCC1	MRP1	16p13.1	Drug resistance
ABCC2	MRP2	10q24	Organic anion efflux
ABCC3	MRP3	17q21.3	Drug resistance
ABCC4	MRP4	13q32	Nucleoside transport
ABCC5	MRP5	3q27	Nucleoside transport
ABCC6	MRP6	16p13.1	
CFTR	ABCC7	7q31.2	Chloride ion channel
ABCC8	SUR	11p15.1	Sulfonylurea receptor
ABCC9	SUR2	12p12.1	Potassium channel regulation
ABCC10	MRP7	6p21	
ABCC11		16q11-q12	
ABCC12		16q11-q12	
ABCD1	ALD	Xq28	VLCFA transport regulation
ABCD2	ALDL1, ALDR	12q11-q12	
ABCD3	PXMP1, PMP70	1p22-p21	
ABCD4	PMP69, P70R	14q24.3	
ABCE1	OABP, RNS4I	4q31	Elongation factor complex
ABCF1	ABC50	6p21.33	
ABCF2		7q36	
ABCF3		3q25	
ABCG1	ABC8, White	21q22.3	Cholesterol transport
ABCG2	ABCP, MXR, BCRP	4q22	Toxin efflux, drug resistance
ABCG4	White2	11q23	Cholesterol transport
ABCG5	White3	2p21	Sterol transport
ABCG8		2p21	Sterol transport

*Table was taken from reference [154]